Nouvelles voies de synthèse sans métaux d'oligomères et de polymères π-conjugués pour l'électronique organique

Guillaume Garbay

université de BORDEAUX

THÈSE PRÉSENTÉE

POUR OBTENIR LE GRADE DE

DOCTEUR DE

L'UNIVERSITÉ DE BORDEAUX

ÉCOLE DOCTORALE DES SCIENCES CHIMIQUES

SPÉCIALITÉ POLYMÈRES

Par Guillaume GARBAY

Nouvelles voies de synthèse sans métaux d'oligomères et de polymères π-conjugués pour l'électronique organique

Original metal-free synthesis routes of semi-conducting oligomers and (co)polymers for organic electronics

---

Sous la direction de : Dr. Éric CLOUTET et Dr. Cyril BROCHON

Soutenue le 22/11/2016

Membres du jury :

Pr. HISSLER Muriel, Professeur, ISCR, Université de Rennes	Rapporteur
Dr. BLANCHARD Philippe, Directeur de recherche, MOLTECH ANJOU, Université d'Angers	Rapporteur
Pr. VIGNAU Laurence, Professeur, IMS, Université de Bordeaux	Examinateur
Pr. AUDEBERT Pierre, Professeur, PPSM, ENS Paris-Saclay	Examinateur
Pr. HADZIIOANNOU Georges, Professeur, LCPO, Université de Bordeaux	Invité
Dr. BROCHON Cyril, Maître de conférences, LCPO, Université de Bordeaux	Directeur de thèse
Dr. CLOUTET Éric, Directeur de recherche, LCPO, Université de Bordeaux	Directeur de thèse

“The most exciting phrase to hear in science, the one that heralds new discoveries, is not “Eureka!” (I found it!) but “That’s funny…””

— Isaac Asimov

BL

Remerciements

Voilà la partie qui est la toute première de cette thèse mais aussi celle qui clôt définitivement la rédaction et plus de 3 années passées au LCPO et 8 à l'Université de Bordeaux !

Je souhaite avant tout remercier les membres du jury, pour avoir accepter d'évaluer ces travaux de thèse, ainsi que pour les discussions qui en ont découlé, Pr. Muriel HISSLER, Dr. Philippe BLANCHARD, Pr. Laurence VIGNAU et Pr. Pierre AUDEBERT, que je tiens tout particulièrement à remercier, pour la semaine que nous avons passé ensemble à maniper au labo, j'ai appris énormément de chose, et surtout ce qu'on pourrait appeler un « savoir des anciens » qui m'a beaucoup aider par la suite.

Je remercie aussi Henry CRAMAIL et Sébastien LECOMMANDOUX, les deux directeurs du LCPO qui m'ont accueilli au sein du laboratoire. Je remercie également tout le personnel du LCPO, que cela soit le personnel administratif, les ingénieurs et techniciens m'ayant aidé durant ces années.

Je tiens aussi à remercier Georges, qui m'a accepté dans son équipe et qui m'a fait confiance, me laissant la liberté d'explorer de nouvelles synthèses, de nouvelles réactions et de nouveaux polymères, sans garanties que cela débouche sur des applications. Vous avez néanmoins su réorienter le sujet quand il le fallait, et c'est cet ensemble qui m'a permis de réaliser cette thèse et d'avoir obtenu cette première OLED.

Merci Cyril et Eric, pour tout, vous m'avez vous aussi fait confiance, me laissant tester de nombreuses choses, me permettant réellement de m'amuser et m'épanouir dans la chimie des polymères. Votre porte m'a toujours été ouverte pour des conseils, et merci pour le temps passé à corriger cette thèse et les papiers qui sont en cours de rédaction. Merci Cyril pour ton optimisme, qui compense avec le réalisme d'Eric, le tout nous poussant à toujours améliorer nos résultats. Encore merci à vous deux !

Merci aussi à Luca pour les calculs réalisés et les diverses discussions (scientifiques ou non) que nous avons eu, et Eleni, qui a toujours été prête à m'aider et me conseiller, et ce même si tu étais débordée par le travail ou en train de faire autre chose à ce moment là (comme travailler avec Laurie au hasard).

Merci aussi à Jules et Feifei, qui m'ont accueilli, jeune stagiaire que j'étais, dans leur labo, et m'ont appris les bases d'analyses des propriétés optiques des polymères.

Je souhaite aussi remercier mes amis et collègues qui m'ont côtoyé durant ces 3 années de thèse et plus largement durant toutes mes études (et ce par ordre vaguement chronologique).

Tout d'abord merci Mikael ! C'est en partie grâce à toi, la cuisine de tes parents et tes choix stratégiques d'options que j'en suis la ! Merci pour tout, que cela soit d'un point de vu boulot ou en dehors, tu as toujours été dispo en cas de besoin et c'est réciproque (et ce n'est pas prêt de changer).

Laura, merci pour m'avoir accordé ta confiance et ton amitié durant toutes ces années, et ce, malgré nos styles de vie très différents. Sache que tu as toute mon amitié et que je suis sûr que ça

durera, comme ça a duré malgré tout ce que nous avons pu surmonter. Bon courage pour cette dernière année de thèse et n'oublie pas, *Carpe Diem* !

Merci Romain, notamment pour m'avoir fait découvrir la vie à la dure, la recherche des cèpes, l'enduro, et la joie de perdre une épaule au ball-trap mais aussi pour tes conseils scientifiques.

Merci Laurie pour ces trois années de thèse, à m'avoir supporté dans ton labo et bureau de nombreuses heures, pour toutes les discussions sérieuses (ou non) que nous avons pu avoir, je pense que c'est en grande partie grâce à toi que ma thèse s'est passée dans de super conditions ! Merci aussi à toi Amélie, qui a pris le relai lorsque Laurie rédigeais sa thèse, et que son bureau était devenu une zone inaccessible pour un « perturbateur » comme moi. Merci pour vos macarons, les soirées jeux de société et tous les moments que nous avons passé ensemble, je vous considère vraiment comme deux amies. J'en profite aussi pour remercier Clément et Pierre qui ont aussi contribué à ces moments.

Je remercie aussi toutes les personnes du B8, notamment Alexis (bonne chance pour la suite vieux, et que les cacahuètes soient avec toi), Sylvain, Mickael (et merci pour ton investissement pour les OLED) Ioannis et Anna (bonne chance pour vos post-doc respectifs), Camille, Benjamin, Pierre, Efty, Dimitrios, Ségolène, … et je souhaite une bonne thèse aux nouveaux arrivants, notamment Geoffrey et Lauriane (fais bien le tri des (trop) nombreuses idées de tes (très) nombreux chefs et tu feras une super thèse, je n'en doute pas) ! Merci aussi aux différents stagiaires ayant travaillé avec moi, Alice, Amine, Antoine et surtout Tiphaine, surtout pour l'intérêt et l'implication que tu as portée à ce sujet pendant ces deux stages ! Merci aussi à tous les membres du LCPO « maison mère » que je n'ai pas cité et dont la liste serait bien trop longue à énumérer, (ils se reconnaîtront) mais merci pour toutes ces années, je me suis vraiment bien amusé avec vous tous ! Merci aussi à toutes les personnes rencontrées durant ces années dont certaines sont maintenant devenue plus que de simples collègues.

Je tiens aussi à remercier Matthieu et Olivier, ainsi que Maxime et Yohan !

Enfin un grand merci à toute ma famille, et surtout mes parents et ma sœur préférée, pour leur soutien durant toute ces années (dont un représentant reste au LCPO après mon départ, histoire que vous ne soyez pas trop déstabilisés) !

List of abbreviations

µ-wave	micro-wave
Ac_2O	Anhydride Acetic
Ada-TzCl	3-Adamantane-6-Chloro-1,2,4,5-tetrazine
ATR-FTIR	Attenuated Total Reflectance - Fourier Transform Infrared Spectroscopy
BLA	Bond length alternation
BOA	Bond order alternation
ButDiOl	1,4-Butanediol (Butane-1,4-diol)
Bz	Benzobisthiazole
Cbz	Carbazole
CCT	Correlated Color Temperature
CIE	Commission Internationale de l'Eclairage (International Comission on Illumination)
CRI	Color Rendering Index
Cro	Croconic acid
Đ	Dispersity
DiVani	Divanillin
DMAP	4-Dimethylaminopyridine
DMEDA	N,N-Dimethylethylenediamine
DMF	N,N-Dimethylformamide
DMSO	Dimethylsulfoxide
DodDiOl	1,12-dodecanediol (Dodecane-1,12-diol)
Dpn	Number-average Degree of Polymerization
dppe	1,2-Bis(diphenylphosphino)ethane
dppp	1,3-Bis(diphenylphosphino)propane
DSC	Differential Scanning Calorimetry
EDOT	3,4-Ethylenedioxythiophene
Eg	Band gap
eq	Equivalent
EQE	External Quantum Efficiency
Et_2O	Diethyl Ether (Ethoxyethane)
Et3N	Triethylamine (N,N-Diethylethan-1-amine)
EtOH	Ethanol
Gly	Glycerol (Propane-1,2,3-triol)
GRIM	Grignard Metathesis
HAc	Acetic Acid (Ethanoic acid)
HOMO	Highest Occupied Molecular Orbital
HSQC	Heteronuclear Single Quantum Coherence spectroscopy
HWE	Horner–Wadsworth–Emmons
ICT	Intramolecular Charge Transfer
IR	Infra-Red
ITO	Indium Tin Oxide
IUPAC	International Union of Pure and Applied Chemistry

LUMO	Lowest Unoccupied Molecular Orbital
MAOS	Micro-waved Assisted Organic Synthesis
$MeNO_2$	Nitromethane
MeOH	Methanol
Mn	Number Average Molecular Weight
Mw	Weight Average Molecular Weight
n-BuLi	Butyllithium
NMP	1-Methyl-2-pyrrolidone
NMR	Nuclear Magnetic Resonance
NOESY	Nuclear Overhauser effect spectroscopy
OLED	Organic Light-Emitting Diode
OPV	Organic PhotoVoltaic
Ox	Oxidation
PANI	Polyaniline
P3HT	Poly(3-hexylthiophene)
PBE0	Perdew, Burke and Ernzerhof gradient-corrected correlation functional
PBu_3	Tributylphosphine (Tributylphosphane)
PEDOT-PSS	Poly(3,4-ethylenedioxythiophene) Polystyrene Sulfonate
PEG	Polyethylene glycol
PentDiOl	1,5-pentanediol (Pentane-1,5-diol)
$POEt_3$	Triethyl phosphite
PPE	Poly(*p*-phenyleneethynylene)
PPP	Poly(*p*-phenylene)
PPX	Poly(*p*-xylylene)
PPh_3	Triethyl phosphite
ppm	Parts Per Million
PPV	Poly(*p*-phenylenevinylene)
Prop	1-propanol
PropDiOl	1,3-propanediol (Propane-1,5-diol)
Red	Reduction
RPM	Revolutions Per Minute
SEC	Size-Exclusion Chromatography
Sq	Squaric acid (dihydroxycyclobut-3-ene-1,2-dione)
SqCl	3,4-dichlorocyclobut-3-ene-1,2-dione
$TBAPF_6$	4 tetrabutylamonium hexafluorophosphate
Td	Degradation temperature
TDA	Tamm Dancoff Approximation
TD-DFT	Time-Dependant Density Functional Theory
TFA	Trifluoroacetic Acid
Tg	Glass transition temperature
TGA	Thermogravimetric Analysis
THF	Tetrahydrofurane (Oxolane)
Tm	Melting temperature
TPDA	TriPhenylDiAmine

Tz	Tetrazine
TzCl	3,6-Dichloro-1,2,4,5-tetrazine
TzHi	Hiskey tetrazine (((3,6-bis(3,5-dimethylpyrazol-1-yl)-1,2,4,5-tetrazine)
UV-Vis	Ultraviolet - Visible

General Table of Content

List of Abbreviations VII

General table of content XI

Introduction Générale 1

Chapter 1: Metal-free synthesis of conjugated polymers for organic electronics: state of the art 7

1.1. Introduction 11

1.2.1. Transition-metal catalyzed coupling 11

1.2.1.1. Aryl alkene and aryl alkyne coupling 11

1.2.1.2. Aryl - Aryl coupling 13

1.2.1.3. Summary 18

1.2.1.3. Purification and purity impact 19

1.2.2. Metal-free polymerization 20

1.2.2.1. Vapor deposition 20

1.2.2.2. Electrochemistry 21

1.2.2.3. Aryl-Aryl organocatalysis 22

1.2.2.4. Conjugated polymers synthesized *via* non conjugated precursors 24

1.2.2.5. Formation of PPV like derivatives (C=C bond) 26

1.2.2.6. Other original condensations 28

1.3. Conclusion 33

1.4. References 37

Chapter 2: Synthesis of carbazole-based π-conjugated polyazomethines: Influence of the linkage position and the insertion of a co-monomer on optoelectronic properties 43

Abstract Chapter 2 43

2.1. Literature overview 49

2.2. Carbazole-based polyazomethine 51

2.2.1. Synthesis 51

2.2.1.1. Monomer synthesis 51

2.2.1.2. Polymer synthesis 57

2.2.2. Characterization 58

2.2.2.1. Physical and optical features 58

2.2.2.1.1. Physical properties 58

2.2.2.1.2. Optical characterizations 60

2.2.2.2. Simulation 62

2.3. Synthesis of random copolymers with EDOT 64

2.3.1. Polymer Synthesis 64

2.3.2. EDOT and carbazole based polyazomethine characterization 64

2.3.2.1. Physical and optical properties 64

2.3.2.2. Electrochemical analysis 66

2.4. Conclusions 68

2.5. References 69

2.6. Experimental part 71

Chapter 3: Synthesis of polysquaraines and polycroconaines 113

Abstract Chapter 3 113

Structure and names of compounds synthesized in chapter 3 115

3.1. Literature overview 119

3.2. Polycroconaine based on bis(indolium)thiophene 122

3.3. Polycondensation with N,N'-didodecyldiphenyl-1,4-benzenediamine (TPDA) 124

3.3.1. Monomer synthesis 124

3.3.2. Polymer synthesis 126

3.3.3. Characterizations 127

3.3.4. Control of the linkage 128

3.3.4.1. Modification of the Squaric acid 128

3.3.4.2. Impact of the solvent 131

3.3.4.3. Investigation of various alcohol as comonomers and modification of alcohol ratio 138

3.3.4.3.1. Effect of the solvent used 139

3.3.4.3.2. Effect of the solvent ratio 141

3.4. Toward integration in OLED 143

3.4.1. Optical and electrochemical characterization 143

3.4.2. Integration into OLED 147

3.5. Conclusions 151

3.6. References 152

3.7. Experimental part 155

3.7.1. Syntheses 155

3.7.2. Characterizations 160

Chapter 4: Exploratory study of new « bricks » for original π-conjugated polymers 183

Abstract Chapter 4 183

4.1. π-conjugated polymers composed of Benzobisthiazole 189

4.1.1. State of the art 189

4.1.2. Synthesis and characterization 190

4.2. π-conjugated polymers composed of Tetrazine 192

4.2.1. State of the art 192

4.2.2. Preliminary results 195

4.3. π-conjugated polymers composed of Divanillin 198

4.3.1. State of the art 198

4.3.2. Synthesis 200

4.3.2.1. Monomer synthesis 200

4.3.2.2. Polymers syntheses 202

4.3.3. Optoelectronic properties 205

4.3.3.1. Optical characterizations 205

4.3.3.2. Electrochemical properties 207

4.4. Conclusion 209

4.5. References 210

4.6. Experimental Section 213

4.6.1. General procedure for the synthesis of Poly (Benzobisthiazole-*alt*-carbazole) 213

4.6.2. Tetrazine **213**

4.6.3. Divanillin **215**

Conclusion générale et perspectives **235**

Experimental (general) **237**

Introduction Générale

De nos jours, les polymères sont omniprésents dans notre vie quotidienne. Les progrès réalisés dans la synthèse de nouveaux composés permettent d'obtenir des polymères variés et utilisés dans de nombreux domaines. Parmi ces polymères, certains présentent une conductivité électrique. Même si ces semi-conducteurs organiques ont été décrits dès le vingtième siècle,[1] ces polymères originaux se sont largement développés grâce aux travaux réalisés par Hideki Shirakawa, Alan G. MacDiarmid et Alan J. Heeger en 1977 avec la découverte des propriétés de conductivité électrique du polyacétylène (Figure 1), ce qui leur valut le prix Nobel de chimie pour « la découverte et le développement des polymères conducteurs » en 2000.[2]

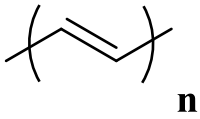

Figure 1 : Structure du polyacétylène

En plus de montrer la conductivité du polyacétylène, ils ont étudié l'impact de différents dopants sur sa conductivité. L'intégration de tels polymères dans des dispositifs électroniques a donné naissance à l'électronique organique.

L'électronique organique s'est développée en parallèle de l'essor technologique avec le début de la micro-informatique et de la miniaturisation dans les années 1970, avec notamment la commercialisation du premier micro-processeur Intel 4004. Depuis, l'électronique a inondé notre quotidien ; ordinateurs, téléphones, tablettes, télévision, voitures, électroménager, etc. Ces dispositifs sont majoritairement fabriqués à partir de matériaux inorganiques, en particulier le Silicium. Malgré ses avantages, il possède un inconvénient majeur qui est l'énergie nécessaire à le mettre en forme. Des études calculant le temps nécessaire pour rentabiliser énergétiquement les panneaux solaires (Energy Pay-Back Time) montrent que 80% de l'énergie nécessaire à leur fabrication vient de l'extraction et la mise en forme du Silicium.[3] En effet, ces matériaux doivent être très purs, et être fondus à plus de 1350K.[4]

C'est notamment sur ce point que les polymères peuvent être intéressants. Leur purification est en effet beaucoup plus économique énergétiquement, que cela soit par précipitation, extraction solide-liquide ou chromatographie par exemple. Les polymères π-conjugués ont été intégrés dans les premiers dispositifs par les équipes de A. VanSlyke et A. B. Homes en 1987 et 1990.[5,6] Ces polymères, consistant en l'enchainement de molécules ou de macromolécules π-conjuguées, intègrent la majeure partie du temps des hétéroéléments comme le Soufre, l'Azote ou l'Oxygène mais aussi d'autres éléments comme le Bore, le Fluor ou le Germanium. En plus de leur purification relativement simple, nécessitant toutefois l'utilisation de solvants dont les volumes doivent être contrôlés ou devant être recyclés (ce qui est le cas dans l'industrie de nos jours), il est plus aisé et économique d'un point de vue énergétique, de manipuler une solution ou une encre qu'un solide. En effet, les composés peuvent alors être déposés par des méthodes simples pouvant être appliquées à différentes échelles, du laboratoire à l'industrie. Parmi ces méthodes, nous pouvons mentionner la tournette (spin-coating),[7] le raclage (doctor-blade),[8] la pulvérisation (spray-coating), le rouleau à rouleau (roll to roll) [9,10] ou encore l'impression (printing).[11,12] Un autre avantage est la légèreté des dispositifs obtenus à partir de ces matériaux. De plus, en choisissant judicieusement l'architecture des dispositifs, il est possible de les rendre flexibles et de les intégrer dans des textiles ou encore de les rendre biocompatibles, comme par exemple en « nourrissant » une plante avec un solution aqueuse de PEDOT-PSS (Figure 2).[13–15]

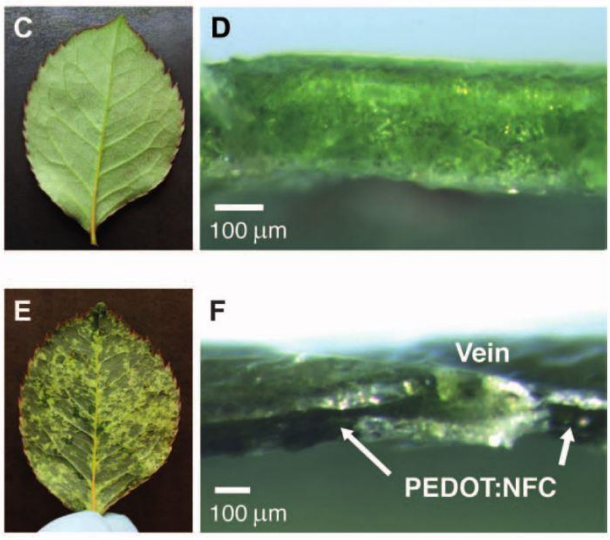

Figure 2 : Feuille (C) et coupe verticale (D) de la feuille (haut), feuille (E) et coupe verticale (F) (bas) après infiltration de PEDOT-PSS.[13]

Au-delà d'être une alternative aux dispositifs à base de Silicium, les polymères semi-conducteurs viennent donc étendre les champs d'applications des dispositifs électroniques.

Cependant, la majorité des polymères conjugués synthétisés de nos jours le sont *via* des méthodes utilisant des catalyseurs à base de métaux de transition. Ces métaux pouvant altérer les propriétés des dispositifs il est nécessaire de les supprimer.[16,17] Il est donc possible d'envisager la synthèse de polymères conjugués demandant encore moins d'étapes de purification en réalisant des synthèses de polymères sans ces catalyseurs. De plus, l'utilisation de voies de synthèse plus originales mène à l'obtention de nouveaux polymères présentant ainsi de nouvelles propriétés optoélectroniques.

L'objectif de cette thèse a donc été de synthétiser de nouveaux polymères conjugués sans catalyseur métallique et d'étudier leurs propriétés optoélectroniques en vue de leur intégration dans des dispositifs. Une première partie de ces travaux a été réalisée sur la synthèse de polyazomethines (ou polyimines) à base de carbazole. Ensuite, la polycondensation de l'acide squarique et de l'acide croconique, avec des dérivés du diphenyl-phénylènediamine, a été réalisée dans diverses conditions puis leurs propriétés ont été étudiées en vue de leur intégration dans des dispositifs de type OLED (Diode ElectroLuminescente Organique). Enfin, le dernier chapitre décriera la synthèse de polymères plus originaux, intégrant des monomères comme la tétrazine ou la divanilline, ou décrivant des méthodes de polymérisations plus originales, permettant par exemple de former des benzobisthiazole directement pendant la polymérisation.

[**1**] N. S. Hush, *Annals of the New York Academy of Sciences*, **2003**, *1006*, 1.

[**2**] C. K. Chiang, C. R. Fincher, Y. W. Park, A. J. Heeger, H. Shirakawa, E. J. Louis, S. C. Gau, A. G. MacDiarmid, *Physical Review Letters*, **1977**, *39*, 1098.

[**3**] V. Fthenakis, H. Kim, R. Frischknecht, *International Energy Agency*, **2011**, 63.

[**4**] S. Geng, *ENES489P: Hands-On Systems Engineering Project Report*, **2011**, 1.

[**5**] C. W. Tang, S. A. Vanslyke, *Applied Physics Letters*, **1987**, *51*, 913.

[**6**] J. H. Burroughes, D. D. C. Bradley, A. R. Brown, R. N. Marks, K. Mackay, R. H. H. Friend, P. L. Burns, A. B. Holmes, *Nature*, **1990**, *347*, 539.

[**7**] F. Aziz, A. F. Ismail, *Materials Science in Semiconductor Processing*, **2015**, *39*, 416.

[**8**] U. Siemann, *Progress in Colloid and Polymer Science*, **2005**, *130*, 1.

[**9**] E. Bundgaard, O. Hagemann, M. Jorgensen, F. C. Krebs, *Green*, **2011**, *1*, 55.

[**10**] Flexcellence Project, **2015**.

[**11**] F. C. Krebs, *Solar Energy Materials and Solar Cells*, **2009**, *93*, 394.

[**12**] S. R. Forrest, *Nature*, **2004**, *428*, 911.

[**13**] E. Stavrinidou, R. Gabrielsson, E. Gomez, X. Crispin, O. Nilsson, D. T. Simon, M. Berggren, *Science advances*, **2015**, *1*, e1501136.

[**14**] D. J. Lipomi, M. Vosgueritchian, B. C.-K. Tee, S. L. Hellstrom, J. a Lee, C. H. Fox, Z. Bao, *Nature nanotechnology*, **2011**, *6*, 788.

[**15**] B. C.-K. Tee, C. Wang, R. Allen, Z. Bao, *Nature nanotechnology*, **2012**, *7*, 825.

[**16**] Ö. Usluer, M. Abbas, G. Wantz, L. Vignau, L. Hirsch, E. Grana, C. Brochon, E. Cloutet, G. Hadziioannou, *ACS Macro Letters*, **2014**, *3*, 1134.

[**17**] M. Urien, G. Wantz, E. Cloutet, L. Hirsch, P. Tardy, L. Vignau, H. Cramail, J.-P. P. Parneix, *Organic Electronics: physics, materials, applications*, **2007**, *8*, 727.

Chapter 1: Metal-free synthesis of conjugated polymers for organic electronics: state of the art

1.1. Introduction 11

1.2.1. Transition-metal catalyzed coupling 11

1.2.1.1. Aryl alkene and aryl alkyne coupling 11

1.2.1.2. Aryl - Aryl coupling 13

1.2.1.3. Summary 18

1.2.1.3. Purification and purity impact 19

1.2.2. Metal-free polymerization 20

1.2.2.1. Vapor deposition 20

1.2.2.2. Electrochemistry 21

1.2.2.3. Aryl-Aryl organocatalysis 22

1.2.2.4. Conjugated polymers synthesized *via* non conjugated precursors 24

1.2.2.5. Formation of PPV like derivatives (formation of C=C bond) 26

1.2.2.6. Other original condensations 28

1.3. Conclusion 33

1.4. References 37

1.1. Introduction

Since 1977 and the accidental discovery made by H. Shirakawa on polyacetylene showing a metallic behavior, considerable efforts have been made to develop the family of π-conjugated polymers.[1] These materials are for instance characterized by their energy diagram, the relative position of their HOMO (Highest Occupied Molecular Orbital) and LUMO (Lowest Unoccupied Molecular Orbital) levels and thus their energetic gap. sp_2 hybridization of carbons, with the extent of alternation of single and double bonds within a polymer chain is among the more important key feature to control in order to achieve highly performing organic materials in optoelectronic devices. Any change in the polymer backbone, chain length, substituent, architecture, structure, etc. affects the energy gap of the material and thus its optoelectronic properties.

In view of the promising applications of such π-conjugated polymers in devices and flexible optoelectronics there has been a tremendous work on the synthesis routes to these polymers. As discussed in the following, mostly the methodologies are based on organometallic cross coupling polymerization reactions or electrochemical pathways while metal-free routes are less considered or exotic up to now.

1.2.1. Transition-metal catalyzed coupling

1.2.1.1. Aryl alkene and aryl alkyne coupling

The polymerization of acetylene (and other insaturated compounds) has been first evoked by M. Berthelot in 1866. Then, acetylene has been polymerized in 1953 using the Ziegler Natta polymerization (Scheme 1-1).[2]

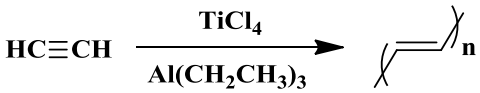

Scheme 1-1: Polyacetylene synthesis *via* Ziegler Natta polymerization.

The doped polyacetylene, studied by Hideki Shirakawa, Alan G. MacDiarmid and Alan J. Heeger in 1977, was synthesized *via* a Ziegler Natta polymerization of the acetylene and doped with chlorine, bromine or iodine.[1,3]

In 1972, Heck coupling consisting in reaction between compounds bearing respectively halogens and vinyl groups in the presence of a palladium catalyst.[4,5] Luping Yu and coll. have used such route for the synthesis of alkylated PPV (poly(*p*-phenylenevinylene)) in 1993 (Scheme 1-2).[6,7]

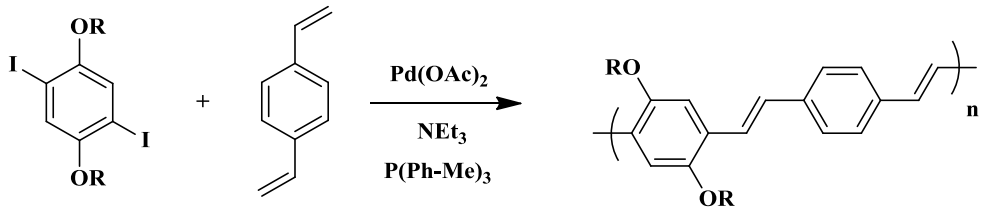

Scheme 1-2: Synthesis of PPV derivatives *via* Heck coupling (adapted from reference 6).

The Sonogashira coupling, developed in 1975, consists in a coupling between a di-halide aromatic compound and an aromatic di alkyne one. It has been, for example, used to synthesize a PPE (poly(*p*-phenyleneethynylene)) with a molar mass of 10 000 g.mol^{-1} in 1998 using a mixture of palladium, copper iodide and using trimethylamine as a ligand (Scheme 1-3).[8,9]

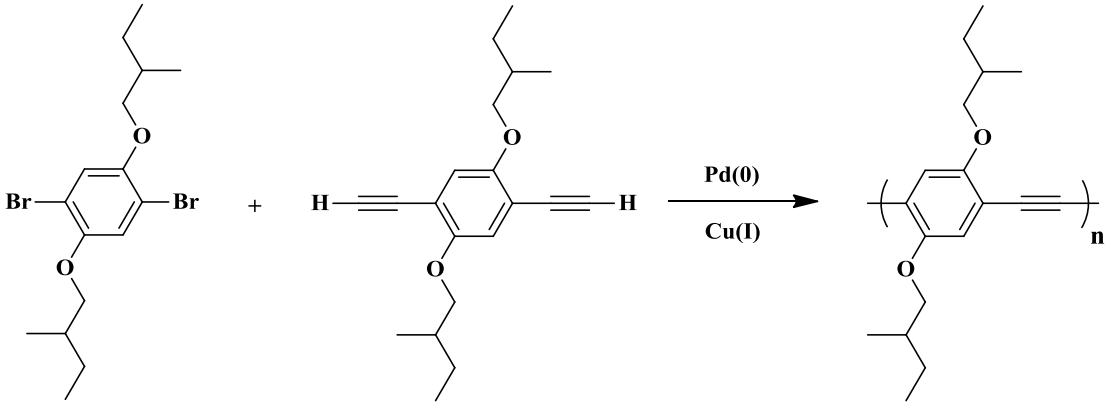

Scheme 1-3: Synthesis of PPE derivatives *via* Sonogashira coupling (adapted from reference 9).

In 1976, Collin Eaborn *et al.* used tin, germanium, silicon derivatives and palladium as transition-metal based catalyst to perform the coupling between a di-halide and a di-stannic derivative (Scheme 1-4).[10] J. K. Stille generalized this reaction using $Pd(PPh_3)_4$ as catalyst and by coupling numerous different aromatic compounds. However, this discovery didn't awarded him the Nobel price in 2010, earned by R. F. Heck A. Suzuki and E. Negishi for their work on palladium-catalyzed cross couplings in organic synthesis.[5]

The first polymers based on this method have been synthesized by Manfred Bochmann and Keith Kelly in 1989.[11] Later, this reaction has also been used to form aromatic-vinyl linkage (Scheme 1-4).[12–14]

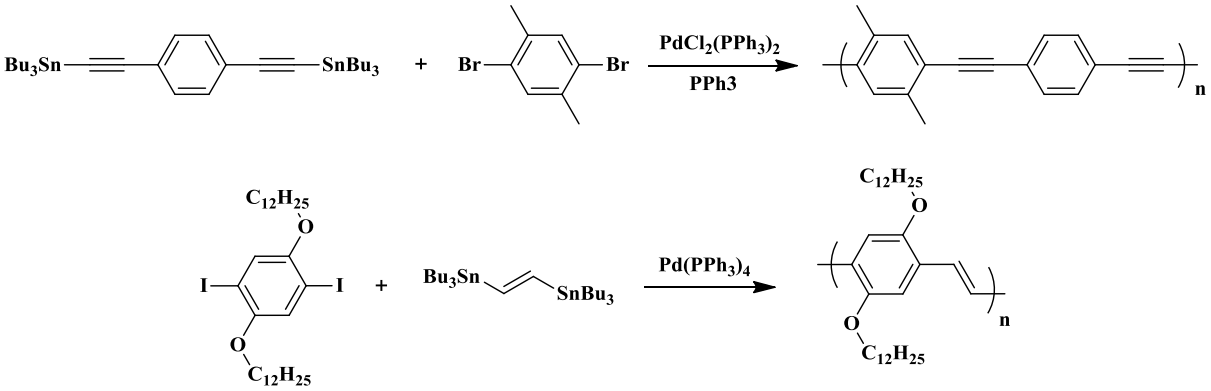

Scheme 1-4: PPV and PPE (polyparaphenylene ethynylene) derivatives, synthesized *via* Stille coupling.

This reaction has also been used to synthesized for example poly(phenylenethiophene) in 1995 as reported by Luping Yu and coll. (Scheme 1-5).[6,7]

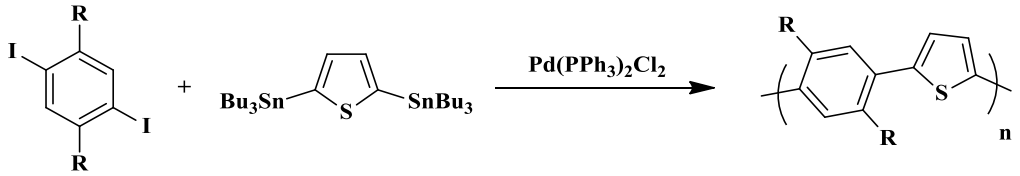

Scheme 1-5: Synthesis of Poly(phenylthiophene) *via* Stille coupling (adapted form reference 7).

In this case, linkage is formed directly between the two aromatic compounds.

1.2.1.2. Aryl - Aryl coupling

In 1980, the synthesis of PPP (poly(*p*-phenylene)) has been developed by the team of R. H. Baughman.[15] This polymer was obtained from benzene *via* a Friedel-Crafts mechanism using $AlCl_3$ and $CuCl_2$ as the oxidant mixture (Scheme 1-6).

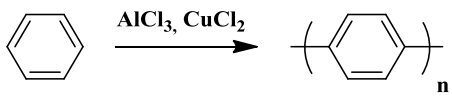

Scheme 1-6: PPP synthesis *via* Friedel-Crafts coupling (adapted from reference 15).

In 1979, A. Suzuki and N. Miyaura developed the cross–coupling reaction between a boronate and a dibromo derivative.[16] The first conjugated polymer made by this process was reported in 1989. It was a hexylated PPP, obtained using a difunctional monomer bearing a bromine

and a boronic acid (Scheme 1-7).[17] This methodology has been extensively described from there.[18–21]

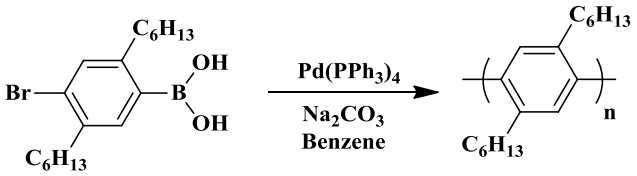

Scheme 1-7: Synthesis of PPP *via* Suzuki coupling (adapted from reference 17).

Another type of polymer received a particular attention, the poly(alkylthiophene). Three different couplings have been used to synthesize these polymers. The oldest reaction used is the Ullman coupling, developed in 1901 and brought up to date by Yamamoto in 1992 for polymers synthesis (Scheme 1-8).[22–24] In this case, a di-halogenated aromatic compound has been polymerized using nickel and PPh_3 (triphenylphosphine) or bdy X as a ligand (see figure 1-1 for ligand structure).

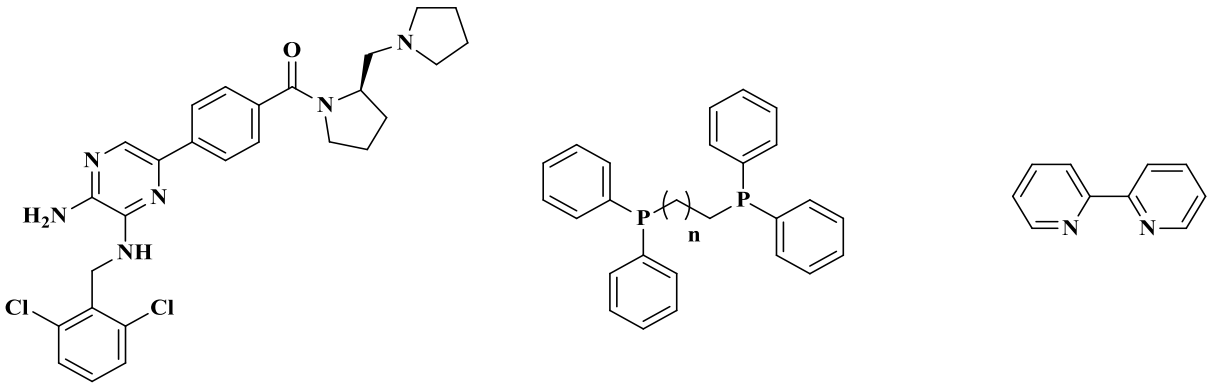

Figure 1-1: Structures of ligands used for Ullman coupling.
Left:
N~3~-(2,6-dichlorobenzyl)-5-(4-{[(2R)-2-(pyrrolidin-1-ylmethyl)pyrrolidin-1-yl]carbonyl}phenyl)pyrazine-2,3-diamine **(bdy)**
Middle: n = 1: 1,2-Bis(diphenylphosphino)ethane **(dppe);**
n = 2: 1,3-Bis(diphenylphosphino)propane **(dppp)**
Right: 2,2'-Bipyridine

An alternative to synthesize polythiophene consists in Kumada coupling between a Grignard reagent and an halide, as first discovered by teams of Corriu and Kumada, respectively in October 1971 and February 1972.[25,26] Extension to polymer was performed in 1992 by Mccullough and coll. The polymerization consists in the coupling between a Grignard reagent and a halide function (Scheme 1-8).[27]

Finally, a third reaction, the Negishi coupling, developed in 1976, consists in a coupling between a Zinc derivative and a halide one using either palladium or nickel as transition metal.[28] By synthesizing thiophene bearing both reactive functions, Rieke and coll. managed to polymerize different alkylthiophene in 1992 (Scheme 1-8).[29,30] It is interesting to note than these three methodologies have been developed in the same year, all using nickel as catalyst.

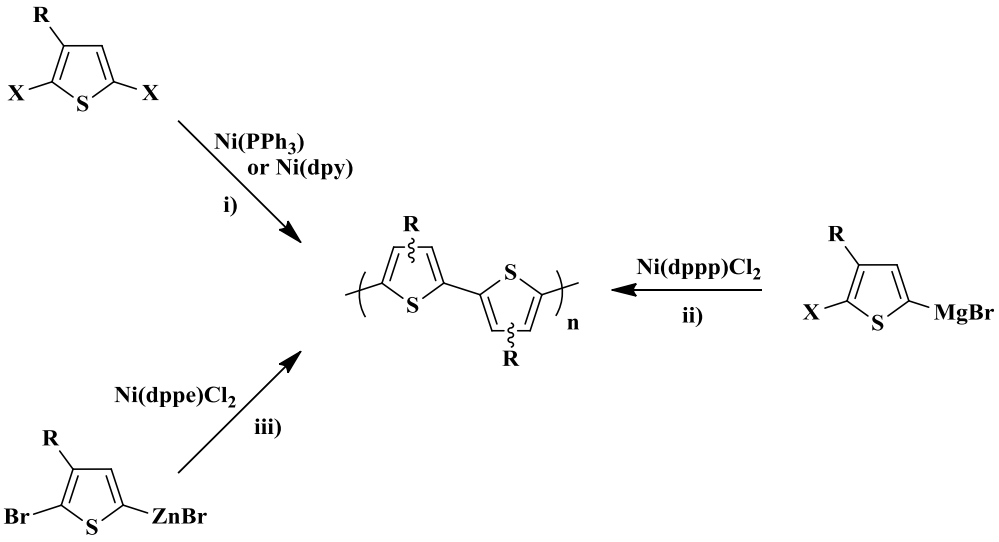

Scheme 1-8: Poly(thiophene) synthesized *via* respectively i) Ullman, ii) Kumada and iii) Negishi coupling.

Depending of the conditions used during the reaction (as the temperature for example), different linkages can be obtained, named “Head to Head”, “Head to Tail” or “Tail to Tail” corresponding to the position of the alkyl chain on one repeating unit compared to the next one. This has an impact on the regioregularity and the properties of the different polymers synthesized.

All these reactions creating a C-C single bond follow a quite similar general mechanism through a common catalytic cycle. As an example, the scheme below shows formation of a R^1-R^2 product through a palladium assisted catalysis following three steps: an oxidative addition, a transmetalation and a reductive elimination (Scheme 1-9).

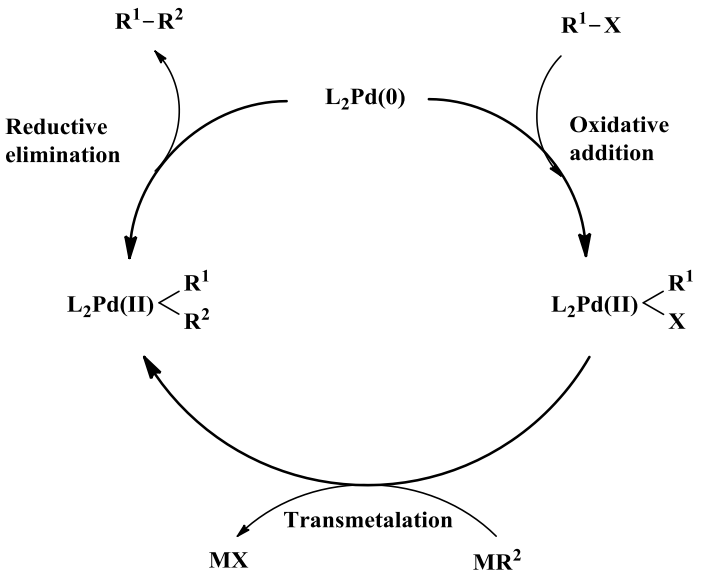

Scheme 1-9: Simplified mechanism scheme for organometallic catalyzed cross-coupling reaction (example of Pd).

The mechanism of transition-metal catalyzed coupling includes three main steps. At first, an oxidative addition of the aromatic moiety on the $L_2Pd(0)$ active catalyst forms the Pd(II) intermediate $[L_2Pd(II)R^1X]$ (L = ligand). Then, the transmetalation step takes place, in which the second monomer link on the catalyst (the Palladium in this example) to form the intermediate $L_2Pd(II)R^1R^2$. In the last step, the desired product (R^1-R^2) is achieved *via* reductive elimination and the $L_2Pd(0)$ catalyst is regenerated.

As previously mentioned, the key objective during the polymerization of such monomers is to control the regioregularity of the chain. To have this control with previously described coupling, a cryogenic reaction temperature was needed.[31] That's why in 1999, McCullough and his team developed a way to synthesize regioregular and low-dispersed poly(alkylthiophene) in milder conditions using GRIM metathesis.[32] Later, this polymerization has even been described as quasi-living by the team of R. D. McCullough and T. Yokosawa (Scheme 1-10).[33–35]

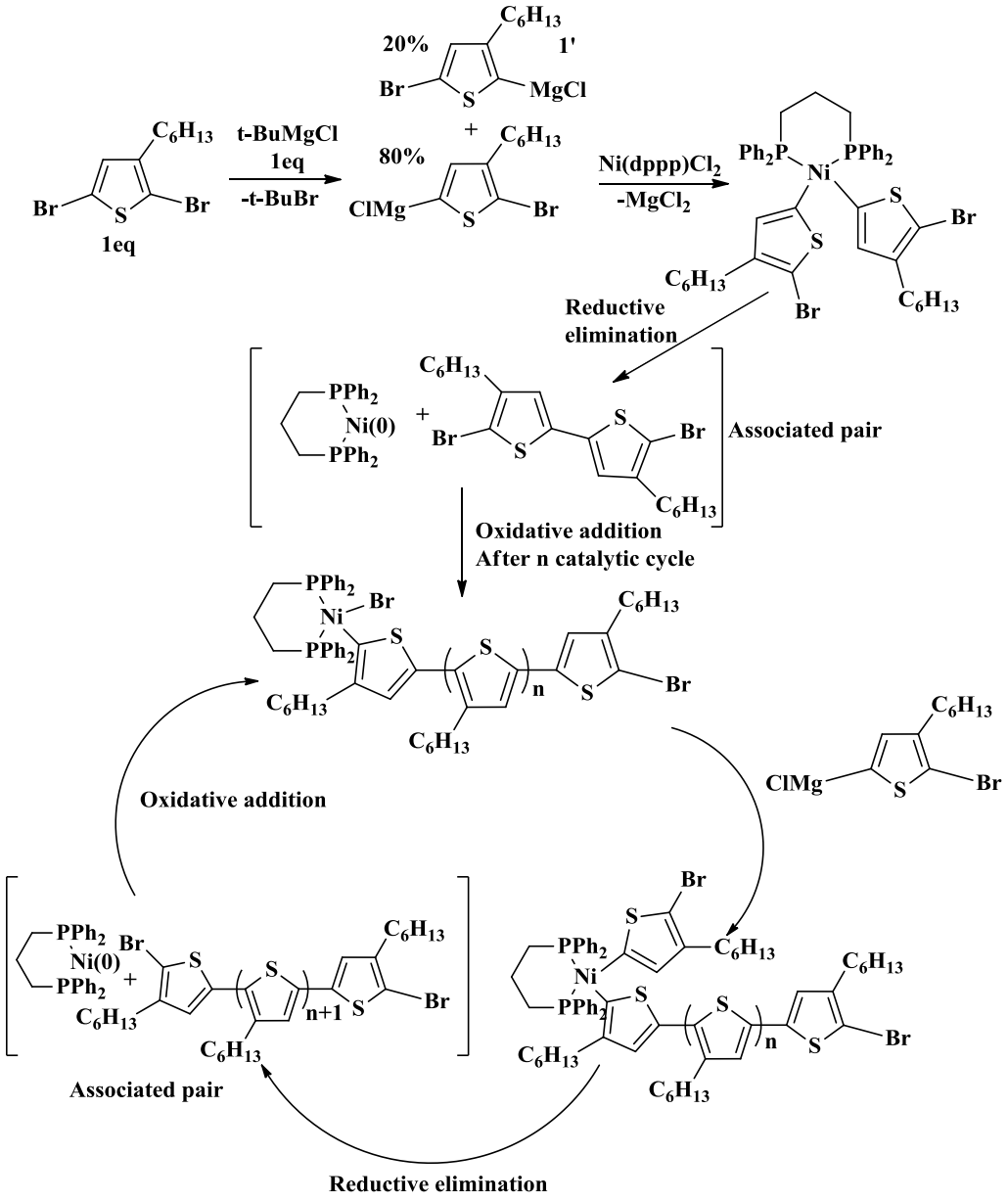

Scheme 1-10: Mechanism of poly(3-hexylthiophene) synthesis *via* GRIM metathesis.

This reaction is similar to the Kumada coupling previously described. However in this case, the Grignard reagent is synthesized *in situ*. This has the advantages of being faster and easier to perform. In the specific case where the aromatic monomer is an alkylated thiophene, the high regioregularity of the poly(3-hexylthiophene) synthesized is due to kinetic and thermodynamic effect thanks to the catalyst ($Ni(dppp)Cl_2$) selectivity.[33] This methodology has the advantage to prepare functional P3HT either mono or difunctional depending on the Grignard reagent used to quench the reaction.

In order to broaden the available monomer library and to simplify the preparation and purification of monomers, a recent trend consists in the polymerization of mono-halogenated monomers or of a di-halide monomer with a non-functionalized one (Scheme 1-11).[36,37]

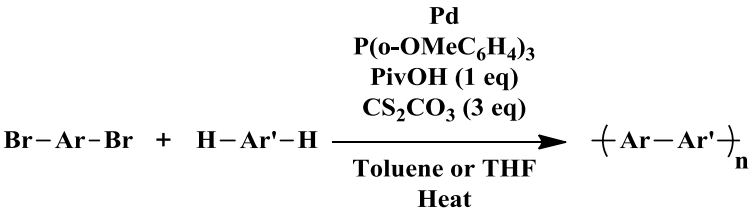

Scheme 1-11: General scheme of transition-metal based catalysed coupling via direct alkylation (adapted from reference [37])

This reaction has first been described in 1999 by M. Lemaire *et al.* on the synthesis of alkylthiophenes, corresponding to a Heck-like coupling.[38] However the reaction yield was very low and hasn't been developed for years, until recently.[36] This direct (hetero)arylation methodology emerged as a very promising route.[37] Indeed, there is no need for tin or boron moiety on monomers, the C-C formation directly involves C-H and C-X (X being a halogen) and results in polymers comparable to those obtained *via* classical methods.

1.2.1.3. Summary

Nowadays, thanks to their versatility and high yield, all the above mentioned cross-coupling reactions have been optimized and are broadly used to synthesize conjugated polymers (Table 1-1).

Linkage	Metal used	Reaction	First Monomer	Second Monomer	Remarks
	Ti or Zr	Ziegler-Natta	$HC\equiv CH$	/	×
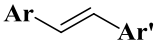	Pd	Heck		$Ar'-X$	Ligand Base
	Pd + Cu	Sonogashira	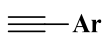	$Ar'-X$	×
$Ar-Ar'$	Pd	Stille	$Ar-SnR_3$	$Ar'-X$	Ligand
		Suzuki	$Ar-BR_2$	$Ar'-X$	Ligand Base
	Pd or Ni	Kumada	$Ar-MgX$	$Ar'-X$	Ligand Base
		Negishi	$Ar-ZnX$	$Ar'-X$	Ligand
	Cu or Ni	Ullmann	$Ar-X$	$Ar'-X$	Ligand
	Pd	Direct Arylation	$Ar-X$	$Ar'-H$	Ligand Base
$Ar-Ar$	Ni	GRIM	$Ar-MgX$	$Ar-MgX$	Ligand Base

Table 1-1: Examples of metal-catalyzed cross-couplings reactions used in conjugated polymers synthesis (Ar = aromatic).

1.2.1.4. Purification and purity impact

Among advantages linked to these routes, one can cite rather good control of dispersity and regioselectivity, high molar masses and even water-tolerance in the cases of Suzuki[39,40] or Sonogashira[41] cross-coupling. Moreover, the large panel of reactions offers a great diversity of linkages depending on monomers. Nevertheless, the main drawback is the use of transition-metal catalysts. In addition to their relative toxicity, metals show some issues regarding their impact on optoelectronic performances when there are considered as residues when π-conjugated polymers are integrated in the active layer. In fact their complete removal

needs number of tedious and lengthy purification steps. For instance, Urien *et al.* studied the effect of repetitive liquid-solid extraction on poly(3-hexylthiophene) (P3HT) and measured OFET characteristics: the purest fraction showed the lowest amount of Ni, Zn, Na and Mg, and exhibited the best performances.[42] Ashraf *et al.* enhanced the OPV performances of low band gap polymers using preparative chromatography.[43] The obtained benefit was attributed to the molecular weight increase as well as the elimination of low molecular weight impurities. In 2001, Heeger and coll. identified the trapping mechanism in bulk heterojunction solar cell made from low band-gap polymers, using $PC_{84}BM$ as a model impurity.[44] Two years later, Darling and coll., specifically studied the role of Pd traces in polymers synthesized *via* Stille coupling, and identified a threshold from where OPV performances are strongly affected.[45]

More recently, the effect on the opto-electronic properties of transition metals residues issued from metal-catalyzed polymerization, has been investigated by O. Usluer *et al*.[46] GRIM-derived P3HTs using a Ni-based catalyst was thoroughly purified by various drastic procedures involving the use of scavengers as well as chelating agents (such as various crown ether or ethylenediamine). Optimum device performances of organic field effect transistors and organic solar cells were obtained from a polymer containing the lowest level of metal impurities (measured by inductive coupled plasma spectrometry), evidencing that such impurities dramatically impact opto-electronic properties.

Although well purified metal-free π-conjugated polymers can be achieved, extensive purification processes are time consuming and utilize enormous amounts of electronic grade (ultra-pure) solvents. Purification issue is a strong limitation for the large-scale industrialization of π-conjugated polymer materials. That's one of the reasons why some research groups decided to work on transition metal-free polymerization. Another reason is that by changing the polymerization reaction, original materials can be obtained, with new linkages which couldn't be obtained *via* these transition-metals catalyzed reactions.

1.2.2. Metal-free polymerization

To overcome this problem, some metal-free reactions have been developed over time, from vapor deposition to different condensation reactions, through electrochemistry, non conjugated precursors or direct aryl-aryl coupling using basic conditions that will be discussed below.

1.2.2.1. Vapor deposition

The vapor deposition consists in heating the monomers at high temperature under vacuum and let them condensate on a cooler surface where will occur the polymerization.[47–49] This method has been broadly used and particularly to obtain graphene films.[50] It's a versatile method where a lot of different compounds and polymers can be obtained. The main drawback of this method is that monomers have to be volatile below their decomposition temperature in the experimental conditions. However, a method has been developed called Aerosol assisted chemical vapor deposition, lowering the temperature needed.[51] This method consists in vaporizing monomers previously solubilized in a good solvent. The solvent will evaporate, monomers will then be adsorbed on the surface and form the polymer film. A drawback of this method is the scalability due to the conditions needed to sublimate the precursors or vaporize the solvent.

1.2.2.2. Electrochemistry

Electrochemical polymerization is a widely used method for the preparation of conductive polymers because of its efficiency, high degree of process control, and low cost.[52] Moreover, it allows the preparation of films composed of non-soluble polymers which couldn't be synthesized otherwise.

The electrochemistry consists in applying a potential between two electrodes, the polymerization reaction occurring at one of them, depending on the monomer, some of them polymerizing thanks to an oxidation reaction (anodic) and others through a reduction (cathodic).[53,54] The proposed general mechanism for an oxidative electropolymerization is shown below on Scheme 1-12 with the example of a thiophene derivative.[55]

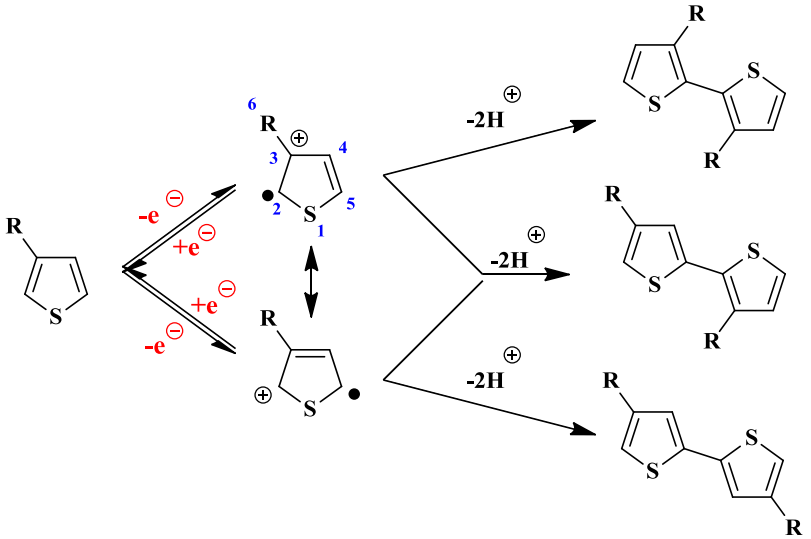

Scheme 1-12: General mechanism of electropolymerization illustrated on a 3-alkylthiophene monomer.

The first step consists in the formation of a radical cation, entity which then dimerizes. Then a loss of dihydrogen leads to a conjugated dimer by rearomatization . After a second oxidation, two dimers will be able to dimerize to form a tetramer and so on. Some studies showed that at low conversion, only dimers, tetramers or hexamers are obtained.[55,56] Some defects can also appear, depending on the position of the radical and cation formed, in carbon 2 or 5 (see Scheme 1-12). Finally, when the oligomer or polymer reaches a certain size it precipitates on the electrode.

As for the transition-metal catalyzed coupling, first polymers synthesized with this method are the PPP and PPV derivatives. For example, the PPV has first been electropolymerized in 1987 by Nishihara *et al.*.[57] For the reaction, different working electrodes have been tested, such as ITO (Indium Tin Oxide), glassy carbon, platinum, nickel or copper. *n*-Bu_4NBF_4 was used as the electrolyte in THF. Then the monomer (α, α, α', α', tetrabromo-*p*-xylene) has been solubilized to reach a concentration of 47 mM. Finally, a potential of -3V has been applied during 6 hours (using Ag/AgCl as reference electrode). This protocol can be generalized for all electropolymerization reactions, with a working, a reference and a counter electrode, an electrolyte solution and the monomer.

Some others polymers have been synthesized using this method, such as PPP[58–60], PPX (poly-paraxylylenes)[53,61], different PPV derivatives[62], polypyrroles[63] or some more originals polymers such as some carbazole based polymers (Figure 1-2).[64,65]

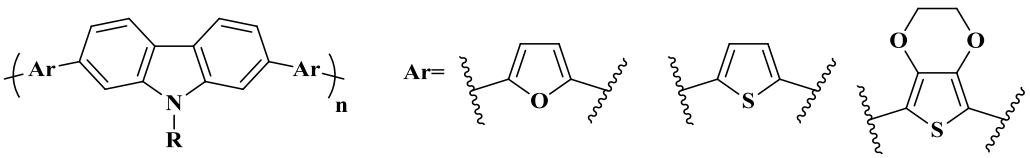

Figure 1-2: Carbazole based co-polymers synthesized *via* electropolymerization.

While electropolymerization is a convenient route to access π-conjugated polymer in the absence of any metal catalyst, it suffers from not well defined materials, difficult to handle and process.

1.2.2.3. Aryl-Aryl organocatalysis

A lot of metal-free reactions have been performed to link two aromatic moieties together.[66] Among clean processes, one could emphasize on electro-polymerization which is very convenient to access π-conjugated polymers free from any catalyst. However, this option is not viable as such electropolymerized materials are not well defined and difficult to handle and process.[67]

In the literature there are some examples (mostly for small molecules) of transition metal-free aryl-aryl coupling even through C-H/C-H[68] or C-H/C-X[69,70] couplings.[71] For instance, the team of A. Lei performed the coupling of a benzene on a iodobenzene in the DMEDA (N,N'-Dimethylethylenediamine) in presence of a base, the *t*-BuOK. Moreover, the authors managed to couple a benzene with different aromatic moieties (Scheme 1-13).

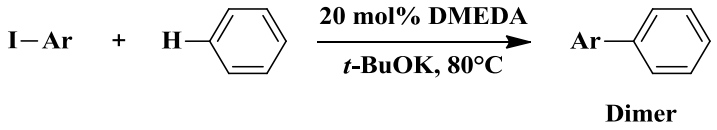

Aromatic cycle (Ar =)	
4-MeC_6H_4	3-$MeOC_6H_4$
C_6H_5	4-$iPrC_6H_4$
4-$MeOC_6H_4$	2-naphtalyl
3-MeC_6H_4	4-PhC_6H_4
2-MeC_6H_4	4-FC_6H_4
2-$MeOC_6H_4$	4-CNC_6H_4

Scheme 1-13: Metal-free direct aryl-aryl coupling.

The authors performed the addition of di-halobenzene on a non-functionalized benzene. Yields are 70 to 80% and reactions times a relatively long (3 days). These yields have then been improved by Y.Qiu *et al*. by introducing different ligands. They managed to obtain yields up to 88%.[72] More and more transition metal free C-C coupling have then been developed.[71] However, at this time, the yields are too low to extend these reactions to polymers, as well as the use of one moiety in excess. Indeed, according to the Carothers law, a yield of 99%, with an exces of one reactant (2 equivalents of one compared to the other for example), gives a theoretical DPn of 3.

In 2016 a reaction previously developed by Z. Chen *et al*. in 2010 has been used to synthesize polydiynes. The reaction consists in a condensation of two alkynes functions in presence of potassium iodide (Scheme 1-14).[73,74]

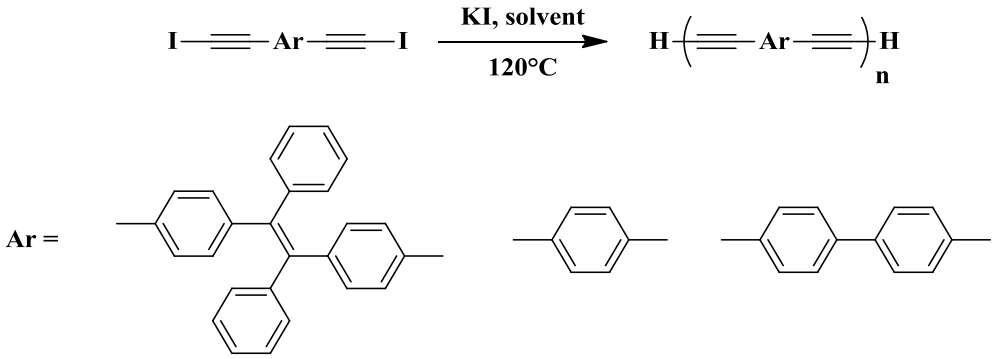

Scheme 1-14: Synthesis of conjugated polydiynes (adapted from reference [74]).

Nevertheless, the polymerization has been performed with aromatic cycles constituted only by carbon and hydrogen atoms, while the presence of heteroelements in the polymer chain would be prefered for optoelectronic applications.

1.2.2.4. Conjugated polymers synthesized *via* non conjugated precursors

In 1968, Wessling and Zimmerman developed a method, also based on elimination under heating. In this case, the reaction consists in a polyaddition with elimination of a thioester. The elimination of the second thioester leads to a conjugated PPV (Scheme 1-15).[75,76]

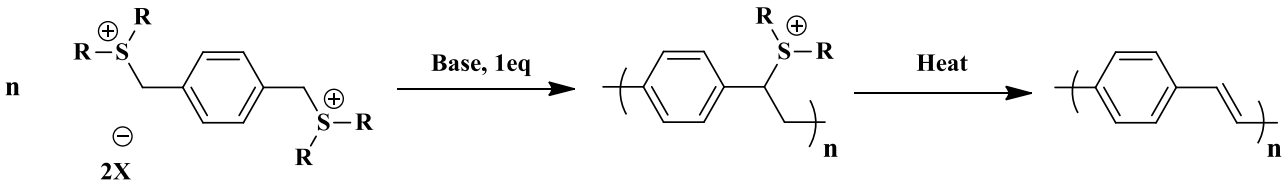

Scheme 1-15: Synthesis of PPV *via* Wessling route (adapted from reference [75]).

L. Ramberg and B. Bäcklund developed a method which has been used to synthesize PPV like oligomer in 1992 by the team of Ono and coll.[77] In this case, a poly(benzylsulfide) is first synthesized and the conjugation is obtained after oxidation of the sulfide into sulfone and elimination in presence of potassium and tetrachloromethane (CCl_4) in a mixture of THF and methanol (MeOH) (Scheme 1-16).

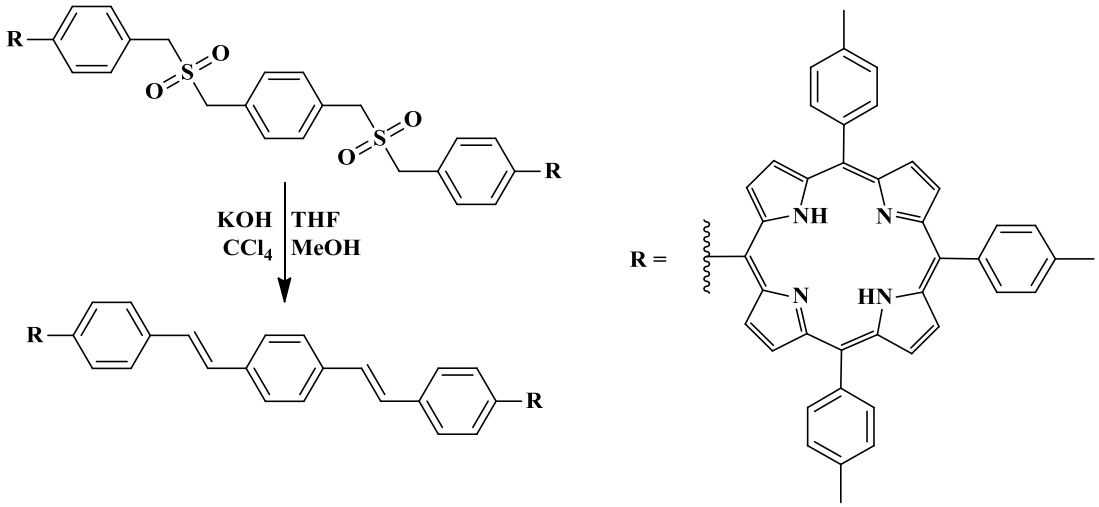

Scheme 1-16: Synthesis of PPV derivative *via* Ramberg-Bäcklund route (adapted from reference [77]).

A different reaction, developed in 1966, is the Gilch reaction. The reaction consists in the coupling of two halogenated compound to obtain PPV derivatives. The first mechanism

proposed in 1966 by Gilch and Wheelwright consists in an addition of two monomers after the deprotonation of one of them followed by the elimination of a hydrogen halide.[78]
Recently some new evidences seem to prove than in fact the reaction consists in a self-dimerization of the monomers followed by a radical polymerization and terminated by cascade elimination.[79,80] An advantage of this reaction, compared to the Wessling or Ramberg-Bäcklund routes is that the monomer only needs to be halogenated. However, due to the mechanism, the center of the polymer chain isn't conjugated (Scheme 1-18).

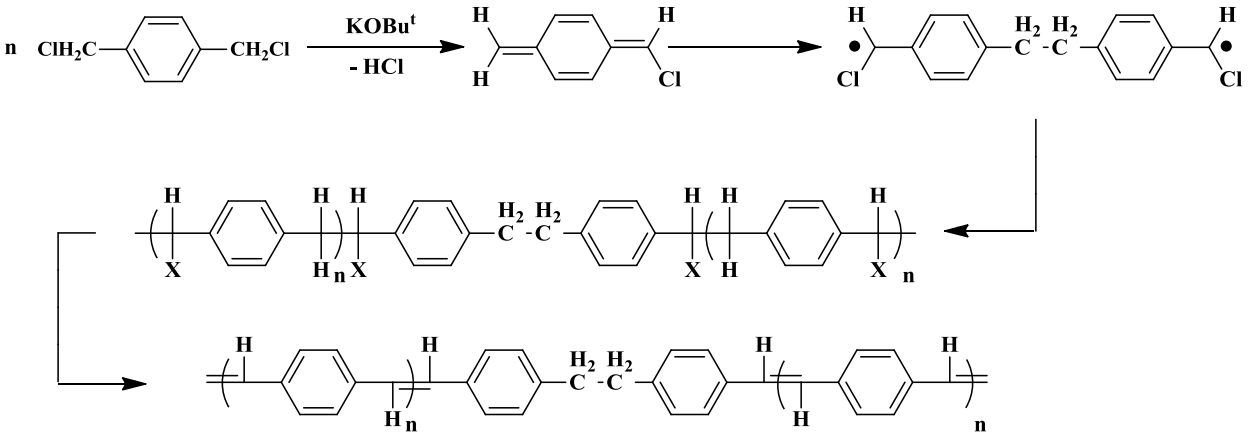

Scheme 1-18: Mechanism of the Gilch reaction to synthesize PPV derivatives (adapted form reference [78]).

This reaction has been particularly used to synthesize MeH-PPV with, for example, the work from Sandford *et al.* in 1999 (Scheme 1-19).[81]

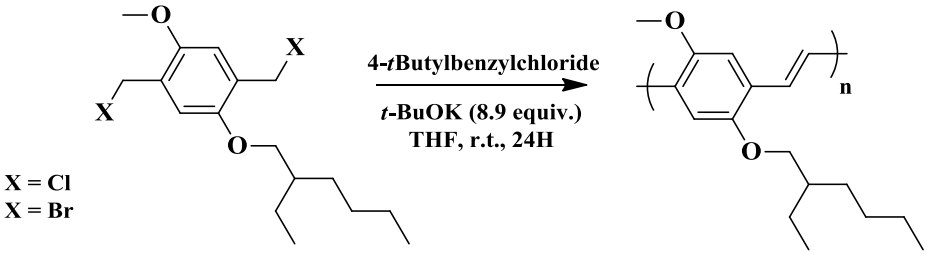

Scheme 1-19: Synthesis of MeH-PPV *via* Gilch reaction (adapted from reference [81]).

This electron donating (p-type) polymer has been for example used in solar cell forming p-n junction with C_{60} and PCBM.[82–84]
The main disadvantage of these methods is the risk of an incomplete elimination, leading to defect in the conjugation.

1.2.2.5. Formation of PPV like derivatives (formation of C=C bond)

Condensation reactions are another class of synthesis route to π-conjugated polymers that doesn't require the use of transition metals.

In 1969 the Siegrist reaction has been developed.[85] This reaction involves an amino and an aldehyde compound. The first step is the formation of an imine bond through a condensation reaction (Scheme 1-20).

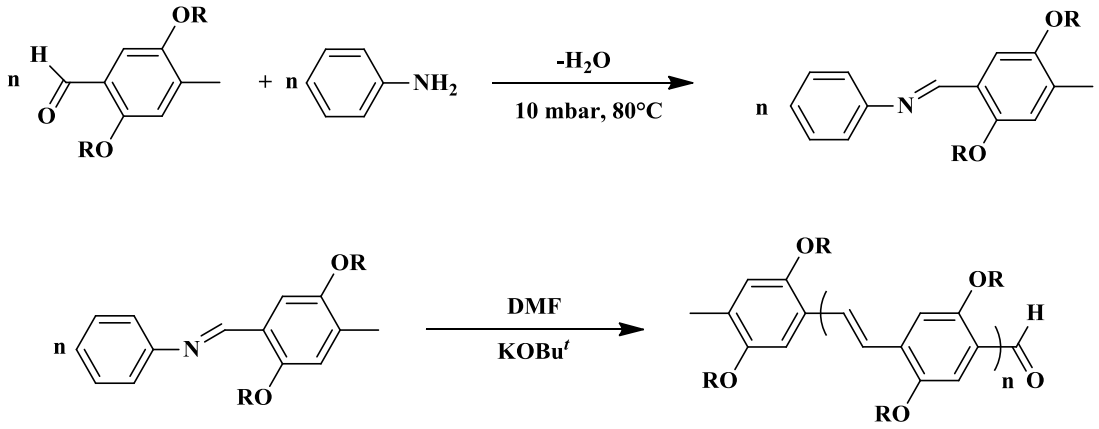

Scheme 1-20: Synthesis of MeH-PPV *via* Siegrist reaction (adapted from reference [85]).

The polymerization mechanism is based on the deprotonation of the methyl group with a strong base, followed by its addition on the imine function with the elimination of aniline. An advantage of this reaction is that the reactivity depends of the acidity of the proton on the methyl group. Since the acidity is due to the electron density on this group, and with the increase of the polymer size the delocalization becomes less important, the reactivity decreases, leading to relatively low molecular weight with a low dispersity. Moreover, the leaving group being bulky, the reaction is highly stereoselective and form mainly linkages with the trans-configuration.[85–87]

Synthesis of MeH-PPV has been also reported following different routes such as the Wittig [88] or Horner–Wadsworth–Emmons (or HWE)[89] reactions. These two pathways imply the condensation of an aldehyde compound with either a phosphonate or a phosphine derivatives respectively in the case of Wittig and HWE reactions. For instance, the first report of PPV synthesis via Wittig reaction was reported by R. N. McDonald and T. W. Campbell in 1960.[90] Anyway, the versatility of these two reactions was evidenced through the use of various monomers such as carbazole, oxadiazole, quinoline... (Scheme 1-21).[91–95]

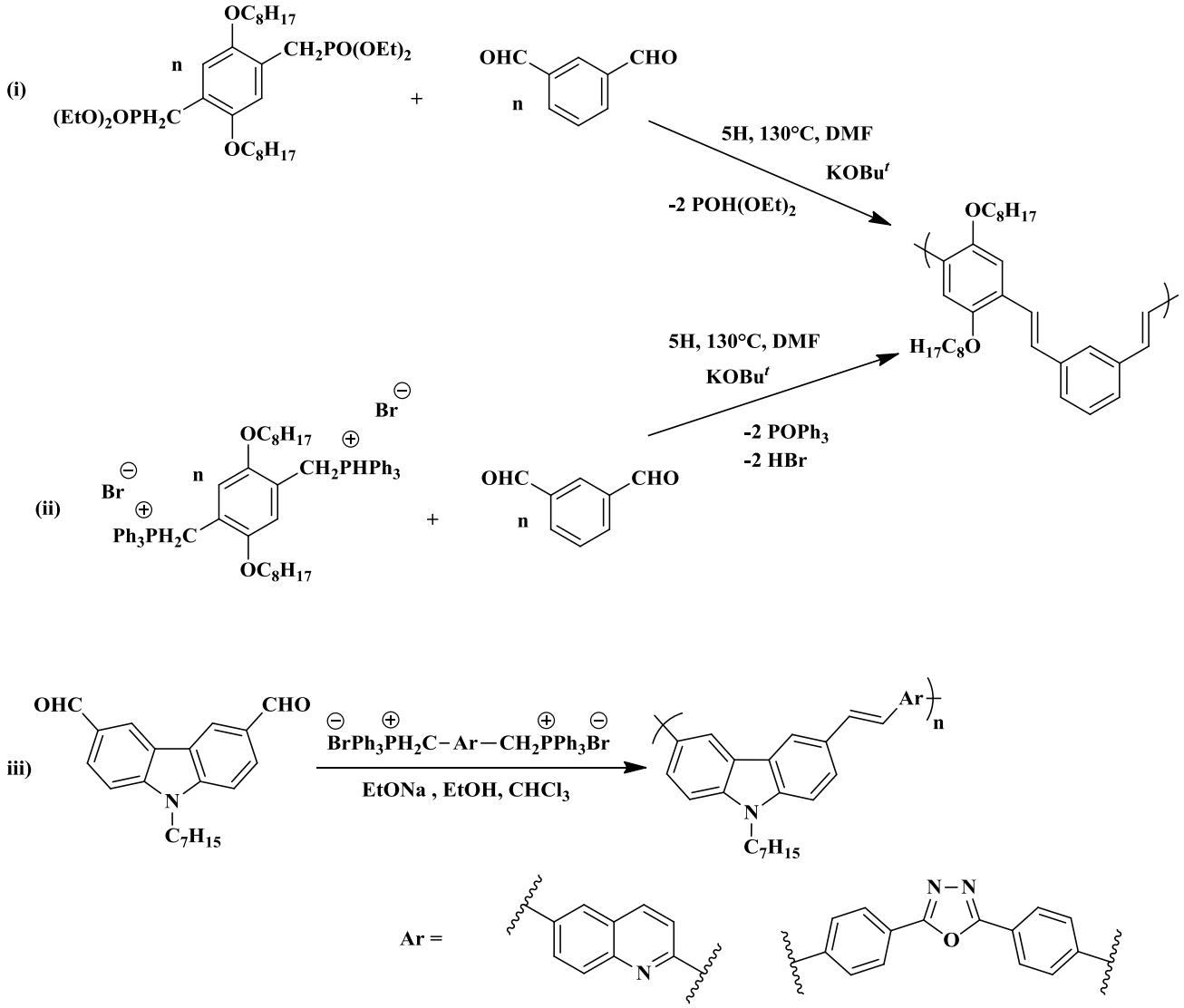

Scheme 1-21: Different polymers synthesized *via*: i) Horner ii), iii) Wittig reactions (adapted from references [91] and [94]).

Another advantage of these two reactions, compared to the Gilch and Siegrist reactions, is that two different monomers can be used during the polymerization, allowing for a better tuning of the polymer properties by inserting two different moieties.

PPV derivatives can also be synthesized *via* the Knoevenagel condensation (Scheme 1-22).[96]

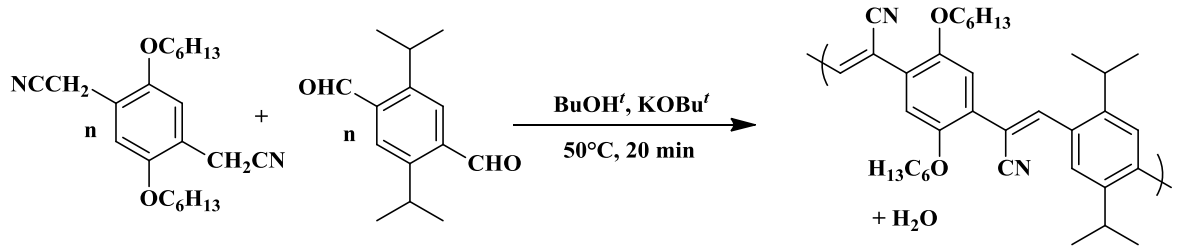

Scheme 1-22: Synthesis of cyano-PPV *via* the Knoevenagel condensation (adapted from reference [96]).

The reaction starts with a deprotonation of the carbon bearing the cyano functions which then will condensate on the aldehyde function. In this case, the reaction allows obtaining cyano-PPV derivatives. They are known for being electron acceptor (n-type material) when integrated in devices, thanks to the electron-attractive cyano groups. They have been broadly used in light emitting devices as OLED for example.[96,97]

1.2.2.6. Other original condensation reactions

Some more original, unusual and relatively specific reactions have also been used to synthesize conjugated polymers.

An extensively studied polymer is the polyaniline (PANI).[98–102] This polymer has been discovered in 1840 and can be synthesized *via* numerous methods including electropolymerization and some metal-free coupling, for example using *p*-toluenesulfonic acid.[103–105] The particularity of this polymer is a self-doping occurring during its polymerization (Figure 1-3).[102] Interestingly, doping levels can be tuned via acido-basic reactions.[106]

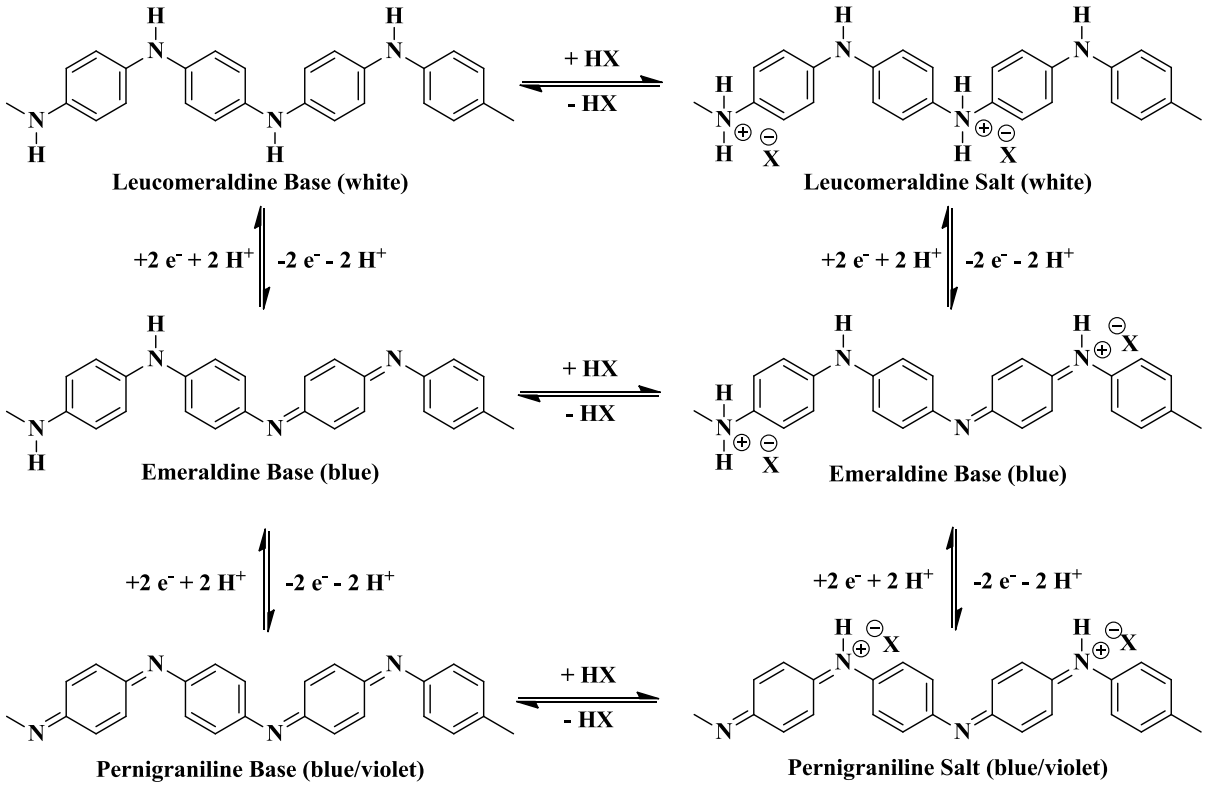

Figure 1-3: Different form of polyaniline (adapted from reference [106]).

Interestingly, PANI can be obtained as dispersions in water.[107–109]

In 1965, Y. Iwakura *et al*. developed an original reaction to synthesize a poly(1,3,4-oxadiazole-2,5-diyl-1,4-phenylene) (Scheme 1-23).[110]

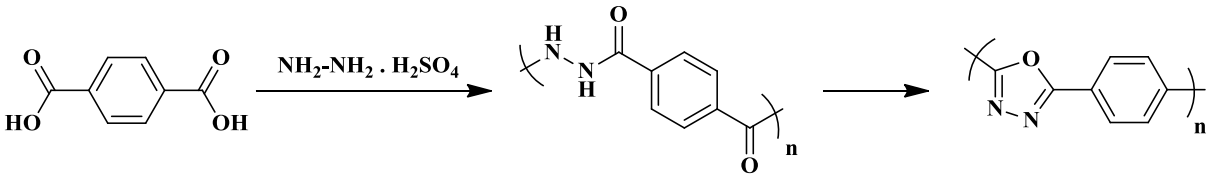

Scheme 1-23: Synthesis of poly(1,3,4-oxadiazole-2,5-diyl-1,4-phenylene) (adapted from reference [110]).

This polymerization consists in the condensation of an aromatic carboxylic acid (or amide) with hydrazine, followed by the self-condensation of the hydrazine on the newly formed hydrazide functions to form the 1,3,4-oxadiazole. Opto-electronic properties of this polymer haven't been studied in details.

There is also the example of a similar reaction developed in 1998 by Park et al involving the formation of benzoxazoles (Scheme 1-24).[111]

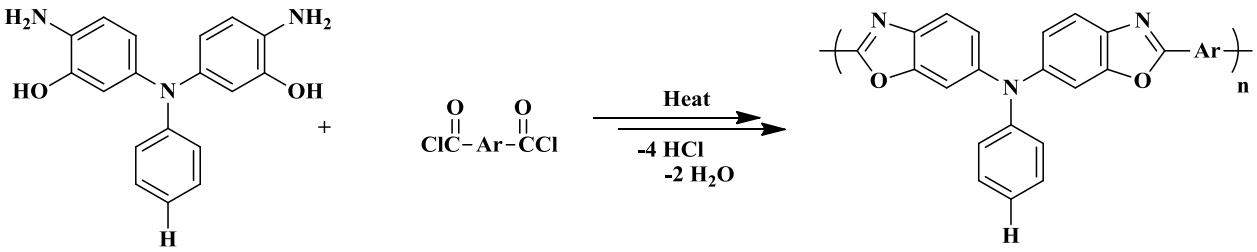

Scheme 1-24: Synthesis of polybenzoxazoles with the formation of the benzoxazole during the polymerization (adapted from reference [111]).

This reaction consists in a double addition of an alcohol and amine on an acyl chloride. This is an elegant method to obtain a polymer with in the same time the formation of a benzoxazoles function. However, the authors didn't investigate their electro-chemicals properties.

Another similar method has been used to synthesize benzobisthiazole compounds since 1964 where a thiol and an ammonium condensate on a carboxylic acid (Scheme 1-25).[112–115]

Scheme 1-25: Synthesis of polybenzobisthiazole (adapted from reference 105).

Polymers obtained *via* this method are insoluble and were used as high modulus and high strength organic fibers (Table 1-2).

Compound	Tenacity (cN/dtex)	Elongation (%)	Initial Young's modulus (cN/dtex)
Polyester	3.7-4.4	30-38	97
Kevlar® 956C K129	28.5	3.15	849
Polybenzobisthiazole[115]	23	1.5	2380

Table 1-2: Physical properties of polybenzobisthiazole compared to polyester and Kevlar®.[116]

Another way to obtain benzobisthiazole is to perform the condensation of an amine and thiol function on an aldehyde (Scheme 1-26).[117,118]

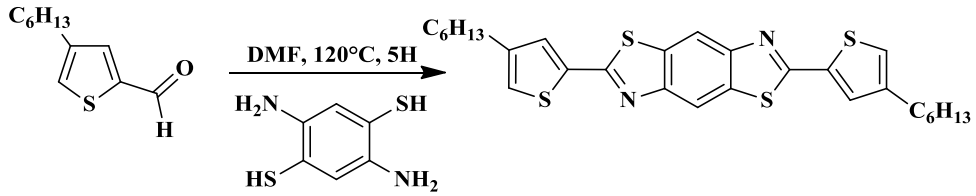

Scheme 1-26: Synthesis of benzobisthiazole dithiophene with the formation of the benzobisthiazole during the coupling reaction (adapted from reference [118])

As far as we know, this method has never allowed to obtain soluble polymers; this reaction will be further investigated in the fourth chapter of this manuscript.

Conjugated polyazomethine is a polymer family mainly studied by the teams of S. Jenekhe, W. G. Skene, A. Iwan and B. Jarzabek and J. M. Lehn (as a part of dynamer studies).[119–140] Different names are used in the literature to describe the linkage formed during the polymerization. It has been called an imine, an azomethine or a Schiff base. In term of nomenclature, the name theoretically depends of the functions linked to both the carbon and nitrogen on the imine bound, imine being the most general name and Schiff base the most specific (Figure 1-4).

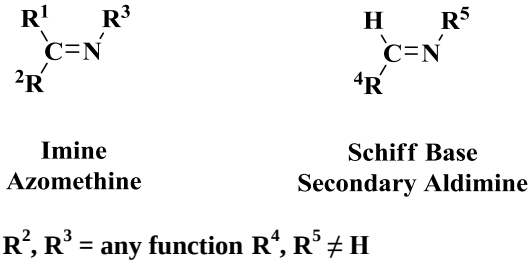

Figure 1-4: General structures of an imine (azomethine) and a Schiff base (secondary aldimine).

Imine and azomethine are synonym, while Schiff base is synonym of the secondary aldimine. Different ways to synthesize them, *via* metal-free polymerization, have been studied. A first route is an alternative version of the Wittig reaction described previously. In this case, a dialdehyde compound is polymerized with a diazido compound, also known as the Aza-Wittig reaction (Scheme 1-27).[141–143]

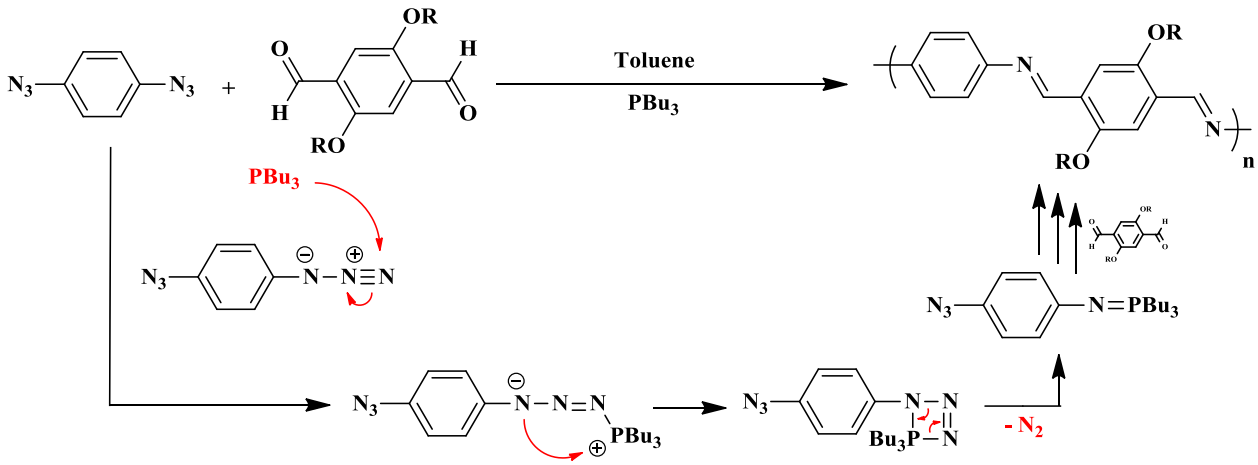

Scheme 1-27: Mechanism of the polyazomethine synthesis *via* Aza-Wittig polycondensation (adapted from reference [143]).

Actually, this reaction occurs in two steps, the first being a Staudinger reaction which consists in a coupling between azido and aldehyde monomers, reaction usually used to reduce azide in amine.[144] If the iminophosphorane formed during this reaction is put in presence of an aldehyde function instead of water, an imine is formed between the two moieties, forming an azomethine function.[142]

Another method to synthesize polyazomethines has been developed in 1999 by the team of F. R. Diaz (Scheme 1-28).[145]

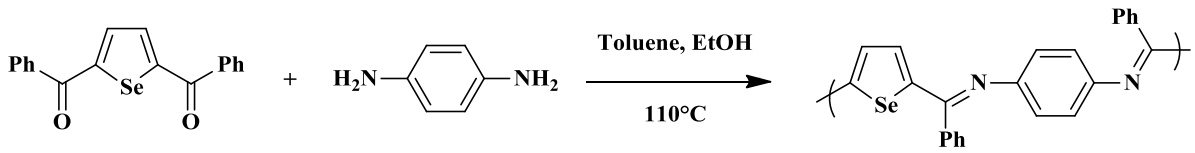

Scheme 1-28: Synthesis of polyazomethine *via* a condensation reaction between a diamino and a diketo compound (adapted from reference [145]).

It consists in a condensation between an amine and a ketone leading to a polyazomethine. In this case, an aromatic moiety is present on the carbon of the azomethine function, hence the azomethine formed is a secondary ketamine and not a Schiff base.

However, the most conventional method to synthesize polyazomethine is the condensation between a diamino and a dialdehyde compound (arylimino-de-oxo-bisubstitution). This reaction, has first been used to obtain (insoluble and infusible) polymers in 1923 by Adams and co-workers from terephthalaldehyde and benzidine or dianisidine.[146] This polymer has

been synthesized by performing the condensation of benzidine (4,4'-diaminobiphenyl) and *p*-Phthalaldehyde (Figure 1-5).

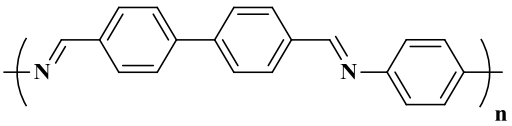

Figure 1-5: Synthesis of polyazomethine *via* a condensation reaction between a diamino and a dialdehyde compound (adapted from reference [146]).

The bibliography study on this reaction will be described and explored more in details in the second chapter of this manuscript.

Another type of polymer can be synthesized with metal-free polymerization, the polysquaraine. These molecules, first synthesized in 1959 by S. Cohen, J. R. Lacher and J. D. Park and polymerized in 1965 by A. Treibs and A. Jacob have been, for example, developed in 1992 by Havinga *et al.* (Scheme 1-29). They are nowadays broadly used for their near IR absorption and emission features.[147–149]

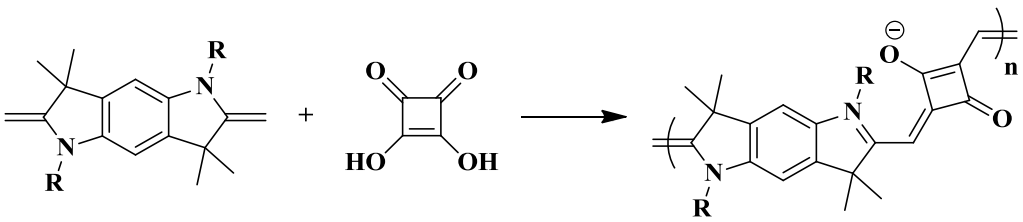

Schema 1-29: Synthesis of a benzobisazole polysquaraine in 1992.

A specific literature survey is dedicated to this family in the third chapter of this manuscript. The (non-exhaustive) table below summarizes polymerization pathways that have been discussed in this part concerning metal-free process for π-conjugated polymers.

1.3. Conclusion

To sum-up, it is clear from this literature survey that there are plenty of original ways to design π-conjugated polymer in the absence of any transition metal catalyst. Interestingly, original π-conjugated polymers constituted of azomethines, squaraines, cyanovinylene or, for example, benzoxazoles subunits have been reported so far (Table 1-3).

Type of reaction	Linkage formed	Reaction	First Monomer	Second Monomer	Ref
Elimination	**Vinylene** 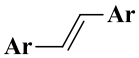	Wessling	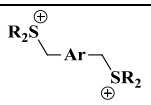	×	75
		Ramberg Bäcklund	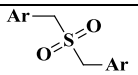	×	77
		Gilch	$XH_2C\text{-}Ar\text{-}CH_2X$	×	78 81
"Well-known" Condensation reactions		Siegrist		×	85–87
	Vinylene 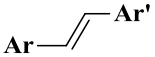	Wittig	$(RO)_3OPH_2C\ Ar\ CH_2PO(OR)_3$	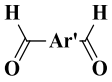	88 90
		Horner	$R_3H_2\overset{\oplus}{P}H_2C\ Ar\ CH_2\overset{\oplus}{P}H_2R_3$	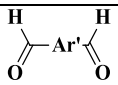	89
	Cyano-vinylene 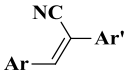	Knoevenagel	$NCH_2C\ Ar\ CH_2CN$	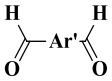	96 97
	Azomethines 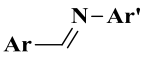	Aza-Wittig	$N_3-Ar'-N_3$	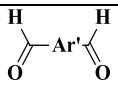	144
		Azomethine	$H_2N-Ar'-NH_2$	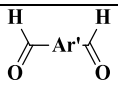	150
		Secondary Ketamine	$H_2N-Ar'-NH_2$	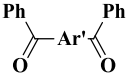	145
	Squaraïne	Squaraine			147
Original reactions	**Benzoxazole and benzothiazole** 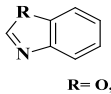 R= O, S	Benzoxazole and Benzothiazole	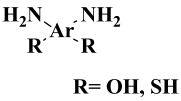 R= OH, SH	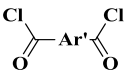	111 118
	1,3,4-oxazole 	1,3,4-oxazole	$NH_2\text{-}NH_2$	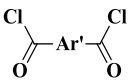	110
	Acetylene	Polydiynes		×	73 74

Table 1-3: Examples of metal-free polymerization routes to π-conjugated polymers.

However, it should be noted that such pathways usually require the use of basic reagents including potassium, sodium or lithium species that need to be eliminated in order to make sure of the absence of metal residues in final devices integrating such polymers materials.

For further development and widespread use of such methodology, *i.e.* metal-free process, it has to be taken into account by the whole community in particular people in charge of the integration of materials in devices. As an example we have shown how metals residues affect the working of devices and efficiency.[46] We have also shown previously that comparable results in terms of structure and optical behavior could be obtained for polysquaraines prepared via classical Suzuki or Stille coupling and a transition metal-free process.[151]

In the continuation of this study, further work was performed on polysquaraines and will be disclosed in chapter three. Besides, chapter two describes the work that has been carried out on polyazomethine type π-conjugated polymers. Finally in chapter four, I will discuss various adventurous pathways integrating original subunits such as tetrazine, a bio-sourced vanillin or benzobisthiazole in the π-conjugated polymer structures, paving the way for further developments in the field.

1.4. References

[**1**] C. K. Chiang, C. R. Fincher, Y. W. Park, A. J. Heeger, H. Shirakawa, E. J. Louis, S. C. Gau, A. G. MacDiarmid, *Physical Review Letters*, **1977**, *39*, 1098.

[**2**] A. M. Saxman, R. Liepins, M. Aldissi, *Progress in Polymer Science*, **1985**, *11*, 57.

[**3**] T. Ito, H. Shirakawa, S. Ikeda, *Journal of Polymer Science - Polymer Chemistry Edition*, **1974**, *12*, 11.

[**4**] R. F. Heck, J. P. Nolley, *The Journal of Organic Chemistry*, **1972**, *37*, 2320.

[**5**] D. Milstein, J. K. Stille, *Journal of the American Chemical Society*, **1978**, *100*, 3636.

[**6**] Z. Bao, Y. Chen, R. Caij, L. Yu, *Macromolecules*, **1993**, 5281.

[**7**] Z. Bao, W. K. Chan, L. Yu, *Journal of the American Chemical Society*, **1995**, *117*, 12426.

[**8**] K. Sonogashira, Y. Tohda, N. Hagihara, *Tetrahedron Letters*, **1975**, *16*, 4467.

[**9**] R. Fiesel, U. Scherf, *Macromolecular Rapid Communications*, **1998**, *19*, 427.

[**10**] D. Azarian, S. S. Dua, C. Eaborn, D. R. M. Walton, *Journal of Organometallic Chemistry*, **1976**, *117*, 55.

[**11**] M. Bochmann, K. Kelly, *Journal of the Chemical Society, Chemical Communications*, **1989**, 532.

[**12**] C. Cordovilla, C. Bartolomé, J. M. Martínez-Ilarduya, P. Espinet, *ACS Catalysis*, **2015**, *5*, 3040.

[**13**] F. Babudri, A. Cardone, G. Ciccarella, G. M. Farinola, F. Naso, L. Chiavarone, G. Scamarcio, *Chemical Communications*, **2001**, 1940.

[**14**] F. Babudri, S. R. Cicco, L. Chiavarone, G. M. Farinola, L. C. Lopez, F. Naso, G. Scamarcio, *Journal of Materials Chemistry*, **2000**, *10*, 1573.

[**15**] L. W. Shacklette, R. R. Chance, D. M. Ivory, G. G. Miller, R. H. Baughman, *Synthetic Metals*, **1980**, *1*, 307.

[**16**] N. Miyaura, K. Yamada, A. Suzuki, *Tetrahedron Letters*, **1979**, *20*, 3437.

[**17**] M. Rehahn, A. D. Schlüter, G. Wegner, W. J. Feast, *Polymer*, **1989**, *30*, 1060.

[**18**] A. Suzuki, *Journal of Organometallic Chemistry*, **1999**, *576*, 147.

[**19**] C. C. C. Johansson Seechurn, M. O. Kitching, T. J. Colacot, V. Snieckus, *Angewandte Chemie - International Edition*, **2012**, *51*, 5062.

[**20**] R. Martin, S. L. Buchwald, *Accounts of chemical research*, **2008**, *41*, 1461.

[**21**] P. Das, W. Linert, *Coordination Chemistry Reviews*, **2015**, *311*, 1.

[**22**] F. Ullmann, J. Bielecki, *Ber. Dtsch. Chem. Ges.*, **1901**, *34*, 2174.

[**23**] Q. T. Zhang, J. M. Tour, *Journal of the American Chemical Society*, **1998**, *120*, 5355.

[**24**] T. Yamamoto, A. Morita, Y. Miyazaki, T. Maruyama, H. Wakayama, Z.-H. Zhou, Y. Nakamura, T. Kanbara, S. Sasaki, K. Kubota, *Macromolecules*, **1992**, *25*, 1214.

[**25**] Y. Kiso, K. Yamamoto, K. Tamao, M. Kumada, *Journal of the American Chemical Society*, **1972**, *94*, 4373.

[**26**] R. J. P. Corriou, J. P. Masse, *Journal of Chemical Information and Modeling*, **1972**, *53*, 1689.

[**27**] R. D. Mc Cullough, R. D. Lowe, *Journal of the Chemical Society, Chemical Communications*, **1992**, 70.

[**28**] S. Baba, E. Negishi, *Journal of the American Chemical Society*, **1976**, *98*, 6729.

[**29**] T. Chen, R. D. Rieke, *Journal of the American Chemical Society*, **1992**, 10087.

[**30**] T. Chen, T. Lee, M. Lin, S. M. A. Sohel, E. W. Diau, S. Lush, R. Liu, *Chemistry - A European Journal*, **1995**, *16*, 1826.

[**31**] M. P. Bhatt, H. D. Magurudeniya, P. Sista, E. E. Sheina, M. Jeffries-EL, B. G. Janesko, R. D. McCullough, M. C. Stefan, *Journal of Materials Chemistry A*, **2013**, *1*, 12841.

[**32**] R. S. Loewe, S. M. Khersonsky, R. D. McCullough, *Advanced Materials*, **1999**, *11*, 250.

[**33**] R. S. Loewe, P. C. Ewbank, J. Liu, L. Zhai, R. D. McCullough, *Macromolecules*, **2001**, *34*, 4324.

[**34**] M. C. Iovu, E. E. Sheina, R. R. Gil, R. D. McCullough, *Macromolecules*, **2005**, *38*, 8649.

[**35**] A. Yokoyama, R. Miyakoshi, T. Yokozawa, *Macromolecules*, **2004**, *37*, 1169.

[**36**] T. Bura, J. T. Blaskovits, M. Leclerc, *Journal of the American Chemical Society*, **2016**, *138*, 10056.

[**37**] L. G. Mercier, M. Leclerc, *Acc. Chem. Res.*, **2013**, *46*, 1597.

[**38**] M. Sévignon, J. Papillon, E. Schulz, M. Lemaire, *Tetrahedron Letters*, **1999**, *40*, 5873.

[**39**] N. Anwar, T. Willms, B. Grimme, A. J. C. Kuehne, *ACS Macro Letters*, **2013**, *2*, 766.

[**40**] L. Parrenin, C. Brochon, G. Hadziiannou, E. Cloutet, G. Hadziioannou, E. Cloutet, *Macromolecular Rapid Communications*, **2015**, *36*, 1816.

[**41**] E. Hittinger, A. Kokil, C. Weder, *Angewandte Chemie - International Edition*, **2004**, *43*, 1808.

[**42**] M. Urien, G. Wantz, E. Cloutet, L. Hirsch, P. Tardy, L. Vignau, H. Cramail, J.-P. P. Parneix, *Organic Electronics: physics, materials, applications*, **2007**, *8*, 727.

[**43**] R. S. Ashraf, B. C. Schroeder, H. A. Bronstein, Z. Huang, S. Thomas, R. J. Kline, C. J. Brabec, P. Rannou, T. D. Anthopoulos, J. R. Durrant, I. McCulloch, *Advanced Materials*, **2013**, *25*, 2029.

[**44**] S. R. Cowan, W. L. Leong, N. Banerji, G. Dennler, A. J. Heeger, *Advanced Functional Materials*, **2011**, *21*, 3083.

[**45**] M. P. Nikiforov, B. Lai, W. Chen, S. Chen, R. D. Schaller, J. Strzalka, J. Maser, S. B. Darling, *Energy & Environmental Science*, **2013**, *6*, 1513.

[**46**] Ö. Usluer, M. Abbas, G. Wantz, L. Vignau, L. Hirsch, E. Grana, C. Brochon, E. Cloutet, G. Hadziioannou, *ACS Macro Letters*, **2014**, *3*, 1134.

[**47**] W. F. Gorham, *Journal of Polymer Science Part A-1: Polymer Chemistry*, **1966**, *4*, 3027.

[**48**] E. G. J. Staring, D. Braun, G. L. J. A. Rikken, R. J. C. E. Demandt, Y. A. R. R. Kessener, M. Bouwmans, D. Broer, *Synthetic Metals*, **1994**, *67*, 71.

[**49**] O. Schäfer, A. Greiner, J. Pommerehne, W. Guss, H. Vestweber, H. Y. Tak, H. Bässler, C. Schmidt, G. Lüssem, B. Schartel, V. Stümpflen, J. H. Wendorff, S. Spiegel, C. Möller, H. W. Spiess, *Synthetic Metals*, **1996**, *82*, 1.

[**50**] K. S. Novoselov, V. I. Fal'ko, L. Colombo, P. R. Gellert, M. G. Schwab, K. Kim, *Nature*, **2012**, *490*, 192.

[**51**] C. E. Knapp, C. J. Carmalt, *Chemical Society Reviews*, **2016**, *45*, 1036.

[**52**] J. Heinze, B. A. Frontana-Uribe, S. Ludwigs, *Chemical Reviews*, **2010**, *110*, 4724.

[**53**] J. H. P. Utley, J. Gruber, *Journal of Materials Chemistry*, **2002**, *12*, 1613.

[**54**] N. Baute, L. Martinot, R. Jerome, *Journal of Electroanalytical Chemistry*, **1999**, *472*, 83.

[**55**] A. Smie, A. Synowczyk, J. Heinze, R. Alle, P. Tschuncky, G. Götz, P. Bäuerle, *Journal of Electroanalytical Chemistry*, **1998**, *452*, 87.

[**56**] J. Heinze, H. John, M. Dietrich, P. Tschuncky, *Synthetic Metals*, **2001**, *119*, 49.

[**57**] H. Nishihara, T. M. Ohsawa, R. Y. Tateishi, Y. Company, K. Kimura, *Chemistry Letters*, **1987**, 539.

[**58**] S. Aeiyach, P. C. Lacaze, *Journal of Polymer Science, Part A: Polymer Chemistry*, **1989**, *27*, 515.

[**59**] A. Shepard, B. F. Dannels, *Journal of Polymer Science Part A - Polymer Chemistry*, **1966**, *4*, 511.

[**60**] S. Descroix, G. Hallais, C. Lagrost, J. Pinson, *Electrochimica Acta*, **2013**, *106*, 172.

[**61**] F. H. Covitz, *Journal of the American Chemical Society*, **1966**, 5403.

[**62**] J. H. P. Utley, Y. Gao, J. Gruber, Y. Zhang, A. Munoz-Escalona, *Journal of Materials Chemistry*, **1995**, *5*, 1837.

[**63**] T. Benincori, E. Brenna, F. Sannicolo, G. Zotti, S. Zecchin, G. Schiavon, C. Gatti, G. Frigerio, *Society*, **2000**, 1480.

[**64**] K. Kawabata, H. Goto, *Synthetic Metals*, **2010**, *160*, 2290.

[**65**] J. A. Aristizabal, J. P. Soto, L. Ballesteros, E. Muñoz, J. C. Ahumada, *Polymer Bulletin*, **2013**, *70*, 35.

[**66**] C. L. Sun, Z. J. Shi, *Chemical Reviews*, **2014**, *114*, 9219.

[**67**] Handbook of conducting polymers.

[**68**] M. Ito, H. Kubo, I. Itani, K. Morimoto, T. Dohi, Y. Kita, *Journal of the American Chemical Society*, **2013**, *135*, 14078.

[**69**] W. Liu, H. Cao, H. Zhang, H. Zhang, K. H. Chung, C. He, H. Wang, F. Y. Kwong, A. Lei, *Journal of the American Chemical Society*, **2010**, *132*, 16737.

[**70**] E. Shirakawa, K. I. Itoh, T. Higashino, T. Hayashi, *Journal of the American Chemical Society*, **2010**, *132*, 15537.

[**71**] V. P. Mehta, B. Punji, *RSC Advances*, **2013**, *3*, 11957.

[**72**] Y. Qiu, Y. Liu, K. Yang, W. Hong, Z. Li, Z. Wang, Z. Yao, S. Jiang, *Organic Letters*, **2011**, *13*, 3556.

[**73**] Z. Chen, H. Jiang, A. Wang, S. Yang, *Journal of Organic Chemistry*, **2010**, *75*, 6700.

[**74**] Y. Zhang, E. Zhao, H. Deng, J. W. Y. Lam, B. Z. Tang, *Polymer Chemistry*, **2016**, 2492.

[**75**] R. A. Wessling, *Journal of Polymer Science: Polymer Symposium*, **1985**, *72*, 55.

[**76**] R. A. Wessling and R. G. Zimmerman, U. S. Pats. 3,401,152 (1968); 3,404,132 (1968) 3,532,643.

[**77**] N. Ono, H. Tomitab, K. Maruyamab, *Journal of the Chemical Society, Perkin Transactions 1*, **1992**, 2453.

[**78**] H. G. Gilch, W. L. Wheelwright, *Journal of Polymer Science Part A - Polymer Chemistry*, **1966**, *4*, 1337.

[**79**] J.-C. Chen, C.-J. Chiang, J.-C. Chiu, J.-J. Ju, *Chemical Communications*, **2012**, *48*, 7756.

[**80**] T. Schwalm, J. Wiesecke, S. Immel, M. Rehahn, *Macromolecular Rapid Communications*, **2009**, *30*, 1295.

[**81**] E. M. Sanford, A. L. Perkins, B. Tang, A. M. Kubasiak, J. T. Reeves, K. W. Paulisse, *Chemical Communications*, **1999**, *1*, 2347.

[**82**] C. H. Lee, G. Yu, D. Moses, K. Pakbaz, C. Zhang, N. S. Sariciftci, a J. Heeger, F. Wudl, *Physical Review B*, **1993**, *48*, 15425.

[**83**] N. Spitsina, I. Romanova, A. Lobach, I. Yakuschenko, M. Kapunov, I. Tolstov, M. Triebel, E. Frankevich, *Journal of Low Temperature Physics*, **2006**, *142*, 201.

[**84**] X. Deng, L. Zheng, C. Yang, Y. Li, G. Yu, Y. Cao, *The Journal of Physical Chemistry B*, **2004**, *108*, 3451.

[**85**] E. Siegrist, P. Liechti, H. R. Meyer, K. Weber, *Helvetica Chimica Acta*, **1969**, *52*, 2521.

[**86**] V. Der Veen, V. De Wetering, *Macromolecules*, **2006**, *37*, 3673.

[**87**] H. Kretzschmann, H. Meier, *Tetrahedron letters*, **1991**, *32*, 5059.

[**88**] G. Wittig, U. Schollkopf, *Chemische Berichte*, **1954**, *87*, 1318.

[**89**] L. Horner, H. Hoffmann, H. G. Wippel, G. Klahre, *Chemische Berichte*, **1959**, *92*, 2499.

[**90**] R. McDonald, T. Campbell, *Journal of the American Chemical Society*, **1960**, *82*, 4669.

[**91**] A. P. Davey, A. Drury, S. Maier, H. J. Byrne, W. J. Blau, *Synthetic Metals*, **1999**, *103*, 2478.

[**92**] S. Wang, W. Hua, F. Zhang, Y. Wang, *Synthetic Metals*, **1999**, *99*, 249.

[**93**] Y. Liu, S. Xu, J. Li, Y. Xin, G. Zhao, B. Ye, S. Cao, *Polymers for Advanced Technologies*, **2008**, *19*, 793.

[**94**] A. Upadhyay, S. Karpagam, *Journal of Fluorescence*, **2016**, *26*, 439.

[**95**] K. Van De Wetering, C. Brochon, C. Ngov, G. Hadziioannou, *Macromolecules*, **2006**, *39*, 4289.

[**96**] N. C. Greenham, N. C. Greenham, S. C. Moratti, S. C. Moratti, D. D. C. Bradley, D. D. C. Bradley, R. H. Friend, R. H. Friend, A. B. Holmes, A. B. Holmes, *Nature*, **1993**, *365*, 628.

[**97**] S. C. Moratti, R. Cervini, A. B. Holmes, D. R. Baigent, R. H. Friend, N. C. Greenham, J. Grüner, P. J. Hamer, *Synthetic Metals*, **1995**, *71*, 2117.

[**98**] E. M. Geniès, A. Boyle, M. Lapkowski, C. Tsintavis, *Synthetic Metals*, **1990**, *36*, 139.

[**99**] Z. Tian, H. Yu, L. Wang, M. Saleem, F. Ren, P. Ren, Y. Chen, R. Sun, Y. Sun, L. Huang, *RSC Advances*, **2014**, *4*, 28195.

[**100**] K. Saranya, M. Rameez, A. Subramania, *European Polymer Journal*, **2015**, *66*, 207.

[**101**] G. Ciric-Marjanovic, *Synthetic Metals*, **2013**, *177*, 1.

[**102**] S. Bhadra, D. Khastgir, N. K. Singha, J. H. Lee, *Progress in Polymer Science (Oxford)*, **2009**, *34*, 783.

[**103**] P. Marcasuzaa, S. Reynaud, F. Ehrenfeld, A. Khoukh, J. Desbrieres, *Biomacromolecules*, **2010**, *11*, 1684.

[**104**] C. Sie, D. Kartoffel, *Bull. scient. de Pétersb*, **1840**, *20*, 453.

[**105**] R. Nietzki, *Chem. Ber.*, **1878**, *11*, 1093.

[**106**] J. Anthony Smith, M. Josowicz, J. Janata, *Physical Chemistry Chemical Physics*, **2005**, *7*, 3614.

[**107**] J. Stejskal, P. Kratochvil, N. Gospodinova, L. Terlemezyan, P. Mokreva, **1992**, *33*, 4857.

[**108**] S. H. Lee, D. H. Lee, K. Lee, C. W. Lee, *Advanced Functional Materials*, **2005**, *15*, 1495.

[**109**] S. P. Armes, M. Aldissi, *Journal of the Chemical Society, Chemical Communications*, **1989**, *1*, 88.

[**110**] Y. Iwakura, K. Uno, S. Hara, *Journal of Polymer Science Part A - Polymer Chemistry*, **1965**, *3*, 45.

[**111**] K. H. Park, M. A. Kakimoto, Y. Imai, *Journal of Polymer Science Part A - Polymer Chemistry-Polymer Chemistry*, **1998**, *36*, 1987.

[**112**] T. Hattori, H. Akita, M. Kakimoto, Y. Imai, *Macromolecules*, **1992**, *25*, 3351.

[**113**] Y. I. Yoshio Imai, Isao Taoka, Keikichi Uno, *Die Makromolekulare Chemie*, **1964**, *83*, 167.

[**114**] J. F. Wolfe, B. H. Loo, *Macromolecules*, **1981**, *14*, 915.

[**115**] S. R. Allen, A. G. Filippov, R. J. Farris, E. L. Thomas, *Macromolecules*, **1981**, *14*, 1135.

[**116**] http://www2.dupont.com.

[**117**] E. Ahmed, F. S. Kim, H. Xin, S. A. Jenekhe, *Macromolecules*, **2009**, *42*, 8615.

[**118**] A. Dessì, G. Barozzino Consiglio, M. Calamante, G. Reginato, A. Mordini, M. Peruzzini, M. Taddei, A. Sinicropi, M. L. Parisi, F. Fabrizi de Biani, R. Basosi, R. Mori, M. Spatola, M. Bruzzi, L. Zani, *European Journal of Organic Chemistry*, **2013**, *2013*, 5961.

[**119**] B. Jarzabek, B. Kaczmarczyk, J. Jurusik, M. Siwy, J. Weszka, *Journal of Non-Crystalline Solids*, **2013**, *375*, 13.

[**120**] B. Jarzabek, J. Weszka, M. Domański, J. Jurusik, J. Cisowski, *Journal of Non-Crystalline Solids*, **2008**, *354*, 856.

[**121**] H. Bednarski, J. Gasiorowski, M. Domanski, B. Hajduk, J. Jurusik, B. Jarzabek, J. Weszka, *Acta Physica Polonica A*, **2012**, *122*, 1083.

[**122**] J. Cisowski, Z. Mazurak, J. Weszka, B. Hajduk, *Journal of Luminescence*, **2012**, *132*, 2098.

[**123**] S. G. Ciechanowicz, K. P. Korona, A. Wolos, A. Drabinska, A. Iwan, I. Tazbir, J. Wojtkiewicz, M. Kaminska, *The Journal of Physical Chemistry C*, **2016**, *120*, 11415.

[**124**] A. Iwan, B. Boharewicz, I. Tazbir, M. Malinowski, M. Filapek, T. Kłab, B. Luszczynska, I. Glowacki, K. P. Korona, M. Kaminska, J. Wojtkiewicz, M. Lewandowska, A. Hreniak, *Solar Energy*, **2015**, *117*, 246.

[**125**] F. Tsai, C. Chang, C. Liu, W. Chen, S. A. Jenekhe, *Synthesis*, **2005**, 1958.

[**126**] C.-J. Yang, S. A. Jenekhe, *Macromolecules*, **1995**, *28*, 1180.

[**127**] A. Bolduc, C. Mallet, W. G. Skene, *Science China Chemistry*, **2013**, *56*, 3.

[**128**] M. Bourgeaux, W. G. Skene, *Journal of Organic Chemistry*, **2007**, *72*, 8882.

[**129**] D. Tsang, M. Bourgeaux, W. G. Skene, *Journal of Photochemistry and Photobiology A: Chemistry*, **2007**, *192*, 122.

[**130**] S. Barik, W. G. Skene, *Polymer Chemistry*, **2011**, *2*, 1091.

[**131**] ufresne, S. A. Pérez Guarìn, A. Bolduc, A. N. Bourque, W. G. Skene, *Photochemical & photobiological sciences : Official journal of the European Photochemistry Association and the European Society for Photobiology*, **2009**, *8*, 796.

[**132**] S. Barik, T. Bletzacker, W. G. Skene, *Macromolecules*, **2012**, *45*, 1165.

[**133**] D. Işık, C. Santato, S. Barik, W. G. Skene, *Organic Electronics*, **2012**, *13*, 3022.

[**134**] S. Barik, S. Friedland, W. G. Skene, *Canadian Journal of Chemistry*, **2010**, *88*, 945.

[**135**] S. Barik, D. Navarathne, M. LeBorgne, W. G. Skene, *Journal of Materials Chemistry C*, **2013**, *1*, 5508.

[**136**] M.-H. Tremblay, T. Skalski, Y. Gautier, G. Pianezzola, W. G. Skene, *The Journal of Physical Chemistry C*, **2016**, *120*, 9081.

[**137**] S. Barik, W. G. Skene, *European Journal of Organic Chemistry*, **2013**, *2013*, 2563.

[**138**] N. Giuseppone, G. Fuks, J. M. Lehn, *Chemistry - A European Journal*, **2006**, *12*, 1723.

[**139**] J.-M. Lehn, J.-M. Lehn, *Chemical Society Reviews*, **2007**, *36*, 151.

[**140**] C. Yang, S. A. Jenekhe, *Chemistry of Materials*, **1991**, *3*, 878.

[**141**] S. Bräse, C. Gil, K. Knepper, V. Zimmermann, *Angewandte Chemie - International Edition*, **2005**, *44*, 5188.

[**142**] F. Palacios, C. Alonso, D. Aparicio, G. Rubiales, J. M. de los Santos, *Tetrahedron*, **2007**, *63*, 523.

[**143**] J. Miyake, Y. Chujo, *Macromolecules*, **2008**, *41*, 5671.

[**144**] H. Staudinger, J. Meyer, *Helvetica Chimica Acta*, **1919**, *2*, 612.

[**145**] F. R. Diaz, J. Moreno, L. H. Tagle, G. A. East, D. Radic, *Synthetic Metals*, **1999**, *100*, 187.

[**146**] R. Adams, J. E. Bullock, W. C. Wilson, *Journal of the American Chemical Society*, **1923**, *45*, 521.

[**147**] E. E. Havinga, W. ten Hoeve, H. Wynberg, *Polymer Bulletin*, **1992**, *29*, 119.

[**148**] E. E. Havinga, A. Pomp, W. ten Hoeve, H. Wynberg, *Synthetic Metals*, **1995**, *69*, 581.

[**149**] J. D. Park, J. R. Lacher, J. D. Park, *Journal of the American Chemical Society*, **1959**, *81*, 3480.

[**150**] C. S. Marvel, H. W. Hill, *Journal of the American Chemical Society*, **1950**, *72*, 4819.

[**151**] J. Oriou, F. Ng, G. Hadziioannou, G. Garbay, M. Bousquet, L. Vignau, E. Cloutet, C. Brochon, *Polymer Chemistry*, **2014**, *5*, 7100.

Chapter 2: Synthesis of carbazole-based π-conjugated polyazomethines: Influence of the linkage position and the insertion of a comonomer on optoelectronic properties.

Résumé en français.

Les polyazomethines représentés ci-dessous ont été synthétisées pour la première fois en 1923 par Adams *et al.* (Schéma 1).[1]

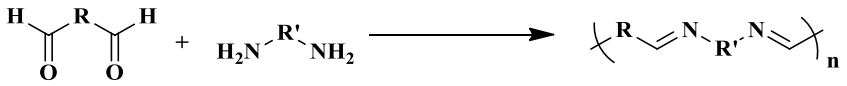

Schéma 1 : Schéma de synthèse général d'un polyazomethine.

Compte tenu de leur insolubilité dans de nombreux solvants, ils ont d'abord été développés en tant que fibres présentant une grande ténacité. Les premiers polyazomethines solubles dans les solvants organiques « communs » ont été synthétisés en 1989 par Lee *et al.* (Figure 1).[2]

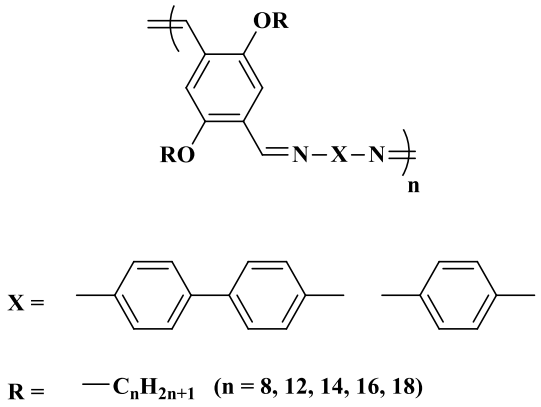

Figure 1 : Polyazomethines conjugués solubles dans des solvants organiques communs.

Il faut noter que le seul produit secondaire formé est l'eau, résultant de la condensation entre deux fonctions amine et aldéhyde. De plus, ce type de réaction peut être réalisé en l'absence de catalyseur métallique, sous irradiation micro-ondes notamment. Dans le cadre de ce travail, je me suis attaché à préparer des polyazomethines à base de carbazole, ces dérivés présentant des fonctions amine et aldéhyde en positions 2,7 ou 3,6 (Schéma 2).

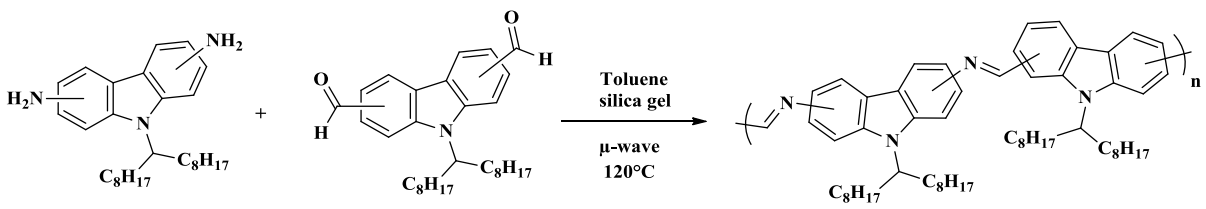

Schéma 2 : Carbazoles et polyazomethines synthétisés au cours de ce travail de thèse.

Les synthèses ont été réalisées sous irradiation micro-ondes en présence de silice comme desséchant. L'impact de l'enchainement (2,7 et 3,6) ainsi que l'addition d'un comonomère dérivé de l'éthylènedioxythiophene (EDOT) ont été étudiés, notamment sur les caractéristiques optiques et électroniques des matériaux obtenus. Ainsi, des résultats très prometteurs ont été obtenus lorsque l'EDOT est inséré dans la chaine de polycarbazole azomethine. Ces résultats ont par exemple été corroborés par des calculs basés sur la théorie de la fonctionnelle de la densité dépendante du temps (TD-DFT).

[**1**] R. Adams, J. E. Bullock, W. C. Wilson, *Journal of the American Chemical Society*, **1923**, *45*, 521.

[**2**] K. S. Lee, J. C. Won, J. C. Jung, *Makromolekulare Chemie-Macromolecular Chemistry and Physics*, **1989**, *190*, 1547.

Chapter 2: Synthesis of carbazole-based π-conjugated polyazomethines: Influence of the linkage position and the insertion of a co-monomer on optoelectronic properties

2.1. Literature overview 49

2.2. Carbazole-based polyazomethine 51

2.2.1. Synthesis 51

2.2.1.1. Monomer synthesis 51

2.2.1.2. Polymer synthesis 57

2.2.2. Characterization 58

2.2.2.1. Physical and optical features 58

2.2.2.1.1. Physical properties 58

2.2.2.1.2. Optical characterizations 60

2.2.2.2. Theoretical modelisation 62

2.3. Synthesis of random poly(azomethine carbazole-*co*-EDOT) 64

2.3.1. Polymer Synthesis 64

2.3.2. Characterization of random poly(azomethine carbazole-*co*-EDOT) 64

2.3.2.1. Physical and optical properties 64

2.3.2.2. Electrochemical analysis 66

2.4. Conclusions 68

2.5. References 69

2.6. Experimental part 71

2.1. Literature overview

As mentioned in the previous chapter, the most conventional method to synthesize polyazomethine is the condensation between a diamino and a dialdehyde compound. This coupling is also named arylimino-de-oxo-bisubstitution. It was first reported in 1923 by Adams *et al.*, by synthesizing an insoluble and infusible polyazomethine from terephthalaldehyde and benzidine or dianisidine.[1] Similarly, in 1950, Marvel *et al*. described the condensation of either the terephthaldehyde or the iso-phthalaldehyde with hydrazine (Scheme 2-1).[2]

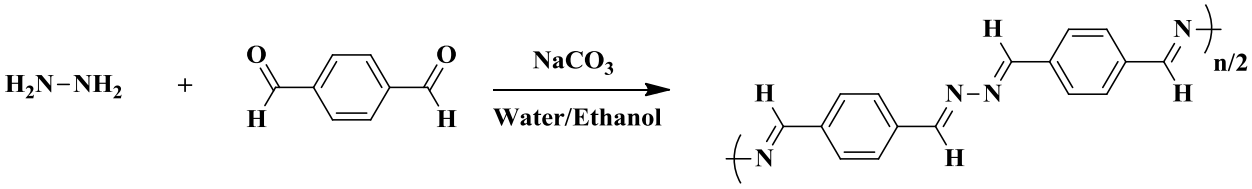

Scheme 2-1: Polyazomethine synthesized in 1950 by Marvel *et al.* [2]

Interests in polyazomethine lie in easy process and release of water as the only by-product. Such reaction doesn't need stringent experimental conditions and works in absence of metallic catalyst.[3] It can also be carried out under micro-wave irradiation in order to reduce reaction time and energy consumption, and is generally referred as microwave-assisted organic synthesis (MAOS).[4,5]

Nevertheless, their low solubility has impeded a large development up to mid 80's where such materials were used as high stretch fibers and liquid crystals.[6–9] Indeed, they show interesting properties in terms of tenacity, elongation and Young's modulus, comparable to Kevlar® (Table 2-1).

Compound	Tenacity (cN/dtex)	Elongation	Initial Young's modulus (cN/dtex)
Polyester	3.7-4.4	30-38	97
Kevlar® 956C K129[a]	28.5	3.15	849
Polybenzobisthiazole[10]	23	1.5	2380
Polyazomethine[7]	8.3 (43)	1.1 (4.4)	1030 (1150)

Table 2-1: Physical properties of polyazomethines compared to polyester and Kevlar®
[a]From DuPont Company®

Interestingly, a patent on such fibers has been issued back in 1975 by DuPont who already patented the Kevlar® in 1965 (Table 2-1).[11]

A major breakthrough in the development of polyazomethines for organic electronics occurs in 1989 with the insertion of alkyl chain in the polymer chain in order to facilitate their solubility (Scheme 2-2).[12]

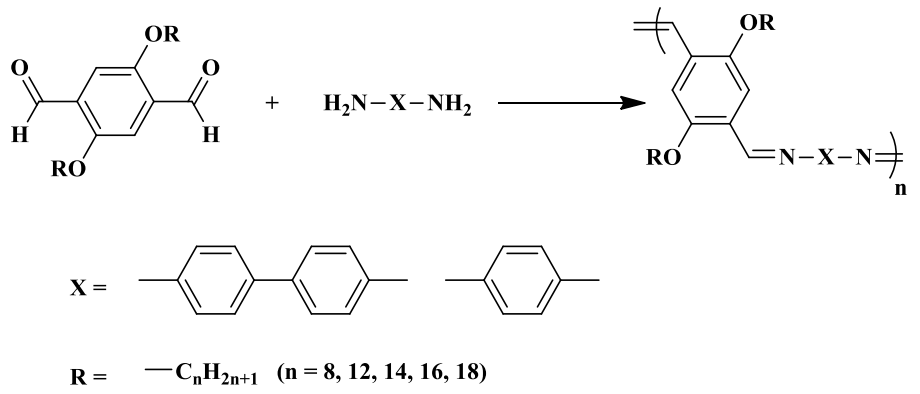

Scheme 2-2: Polyazomethine with pendant alkyl chain (adapted from reference [12]).

Such methodology allowed more precise characterization and paved the way to substituted polyazomethines and the development of many originals polymers with the insertion of different alkyl chains or the insertion of hetero-elements in the polymer backbone.[12–16] The study of their opto-electronic properties showed similar electronic structures as PPV (poly(*p*-phenylenevinylene)).[16]

Since 2008, plethora of different polyazomethines have then been synthesized, using new aromatic moieties such as thiophene, fluorene, carbazole, triphenylamine or even porphyrin.[17–27] All these polymers have been synthesized after 2008 because before that, polyazomethines were considered non-fluorescent. However, H. J. Kim *et al.* showed than pendant azomethine moieties could be protonated, switching the emission properties of the polymer.[28] Based on this work, S. Barik and W. Skene showed that by doping fluorene-based polyazomethine with TFA (trifluoroacetic acid) or $FeCl_3$ (Iron(III) chloride), the fluorescence quantum yield could go from 0.19 in neutral state, up to 0.75 when protonated. The same effect has been observed with a lowered temperature (down to 77K) demonstrating that azomethine fluorescence quenching mainly occurs by bond rotation and/or vibration processes.[21] The same doping work has then been performed on polyazomethines based on EDOT or different thiophene moieties.[23] Some work has also been performed on the study of charge transport through azomethine based single molecule which exhibit a quantum conductance of 1.3×10^{-4} G_0.[29] Polyazomethines have also been integrated into OPV (Organic PhotoVoltaics) devices (Figure 2-1).[26]

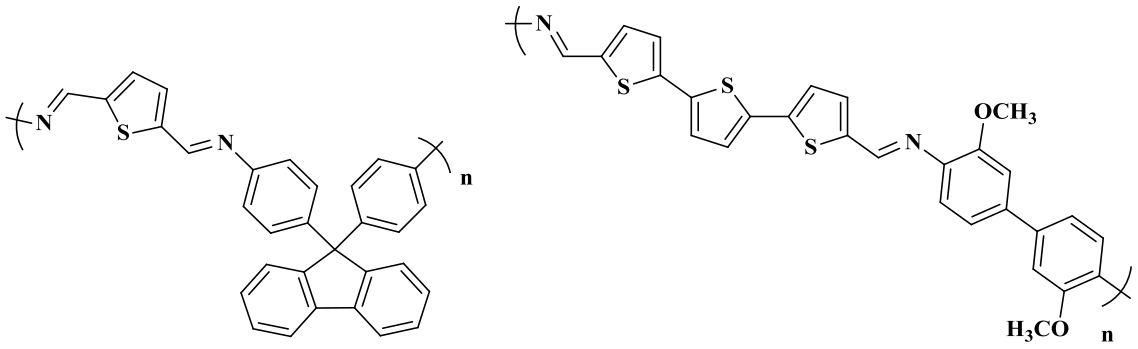

Figure 2-1: Example of polyazomethines integrated into OPV.[26]

Despite the broad polymer absorption and an efficient recombination process, the best solar cell obtained exhibited an EQE (External Quantum Efficiency) of only 3% (for comparison, cells built on P3HT (Poly(3-HexylThiophene) reaches 46%).[26]

In this context, the main objective of this work was to take advantage of the efficient and metal-free process for the design and synthesis of original carbazole-based polyazomethines. In fact, literature is quite scarce regarding such materials.[30–33] Particular emphasis was placed on the influence of linkage position on carbazole sub-unit, either 2,7 or 3,6, and on the addition of a co-monomer such as EDOT derivative, particularly on optoelectronic properties.

2.2. Carbazole-based polyazomethine

2.2.1. Synthesis

2.2.1.1. Monomer synthesis

Four carbazoles precursors have successfully been synthesized at gram scale. Two di-amino carbazole (**8,12**) and two di-formaldehyde (**6,10**), substituted in positions 3,6 and 2,7. The general procedure is shown in Scheme 2-3.

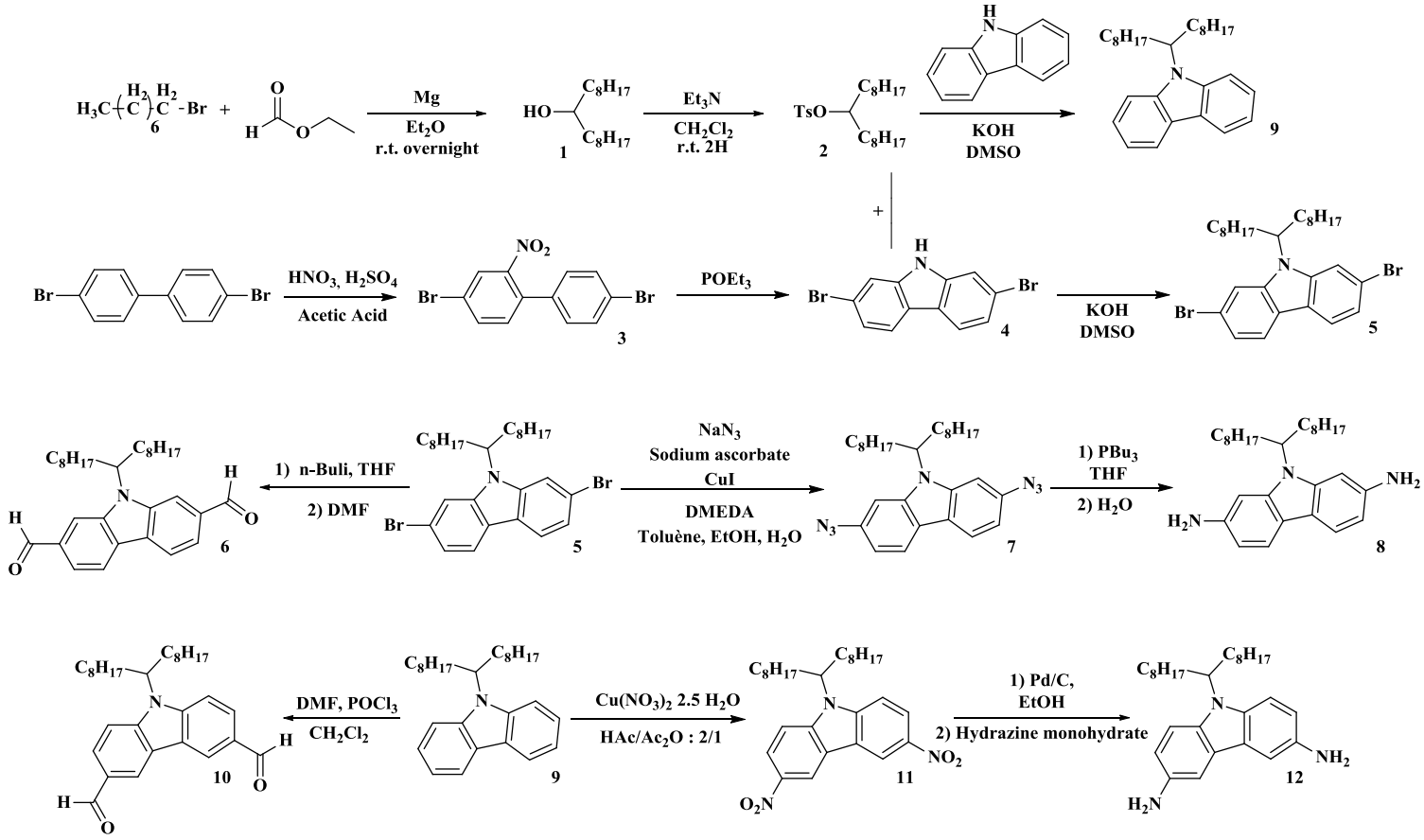

Scheme 2-3: Synthesis of carbazole precursors; the 2,7-diformylcarbazole (6), the 2,7-diaminocarbazole (8), the 3,6-diformylcarbazole (10) and the 3,6-diaminocarbazole (12).

Note that all carbazole monomers bear a branched C_{17} alkyl chain on the nitrogen for solubility reason. The two 2,7 substituted carbazole derivatives **6** and **8**, the diformyl and diaminocarbazole respectively, have been synthesized from the 2,7-dibromo-9H-carbazole **4**. That compound has been synthesized in two steps, starting with the nitration of the dibromo-biphenyl in presence of nitric acid in acetic acid to give the nitrated compound **3** followed by a Cadogan cyclization.[34,35] The compound has then been alkylated using the alkyl chain **2** in presence of potassium hydroxide. This alkylation step ensured the solubility of the final polymer. The alkylation has been confirmed by ^{1}H NMR where the disappearance of the aromatic proton on the carbazole nitrogen at 10.59 ppm and the appearance of all protons from the alkyl chain could be observed (Figure 2-2).

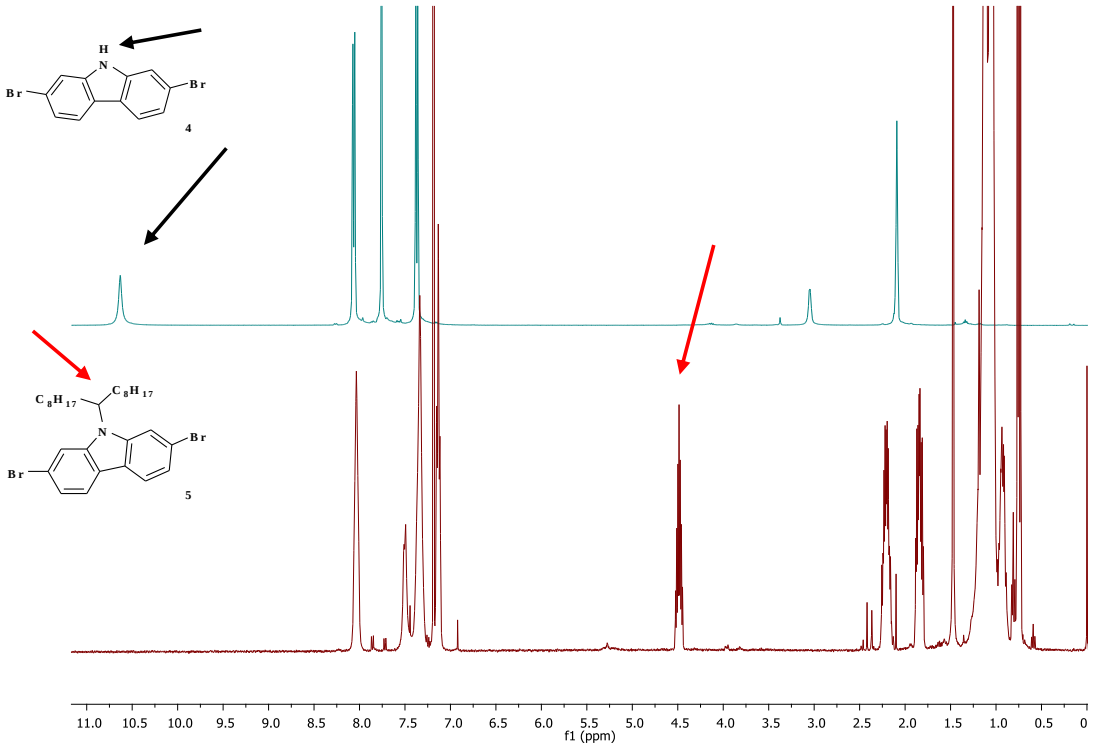

Figure 2-2: ^{1}H NMR (400 MHz, $CDCl_3$) spectra of non-alkylated (top) and alkylated (bottom) 2,7-dibromocarbazole derivatives.

The alkyl moiety **2** used for this purpose had to be synthesized in two steps via a Grignard reagent, through the synthesis of the alcohol derivative **1**. Regarding the alkylation of the carbazole it can be noticed a broadening of aromatic signals which is not happening when the alkylation of carbazole is performed with a linear alkyl chain. This has been confirmed by a comparison of ^{1}H NMR of carbazole presenting two different alkyl chains, and on the 2,7 diformylcarbazole **6** thanks to a NOESY NMR (Nuclear Overhauser Effect Spectroscopy - Nuclear Magnetic Resonance) spectroscopy where spatial interaction between aromatic protons at 8 ppm and those on the alkyl chain around 1 and 2 ppm can be observed (Figure 2-3).

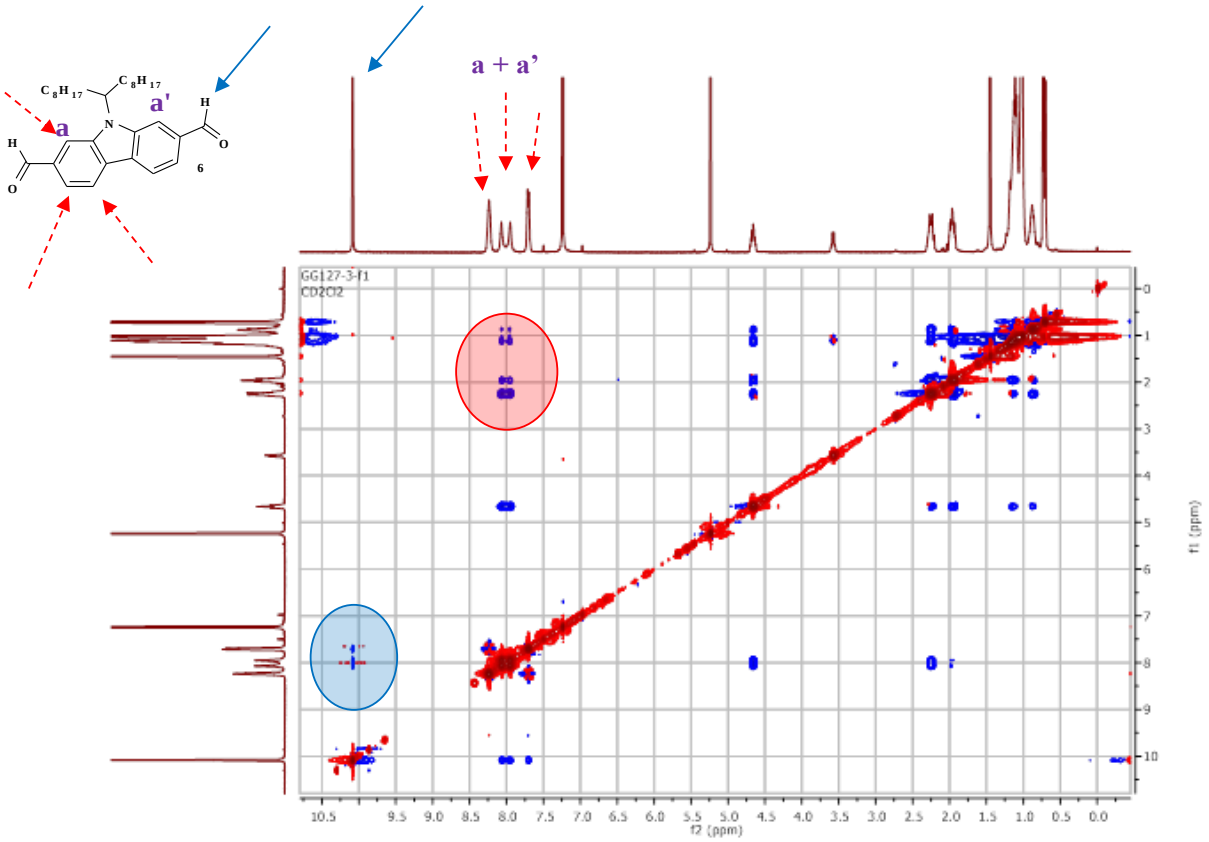

Figure 2-3: ^{1}H-^{1}H NOESY NMR of the 2,7 diformylcarbazole 9 (in CD_2Cl_2).

All the signals on the horizontal line at 10.17 ppm show the interactions between the aldehyde proton and aromatic ones. This atropoisomeric behaviour has already been described in the literature.[36,37] Interactions between alkyl chain, aldehyde proton and aromatic protons leads to a un-symmetrical compound which explain the presence of two signals at 7.9 and 8.1 ppm corresponding to **a** and **a'** protons (Figure 2-3).

Then, the 2,7 diformylcarbazole **6** has been obtained after an electrophilic substitution with butyl lithium and DMF. The 2,7 diaminocarbazole **8** has been synthesized in two uncommon steps, 2,7 diamino carbazole being usually synthesized *via* the 2,7-diaminocarbazole.[38] In our case, the 2,7 dibromocarbazole **5** (previously synthesized) was used and an azidation reaction using sodium azide and copper iodide (Ullman reaction) was first performed to give the diazido compound **7**.[39] In this reaction, the dimethylethylenediamine is used as a ligand and sodium ascorbate is used to stabilize the copper.[40] The presence of the azide functions has been confirmed with ATR-FTIR, where a strong band at 2120 cm^{-1} corresponding to the azide stretching deformation is observed (Figure 2-4).

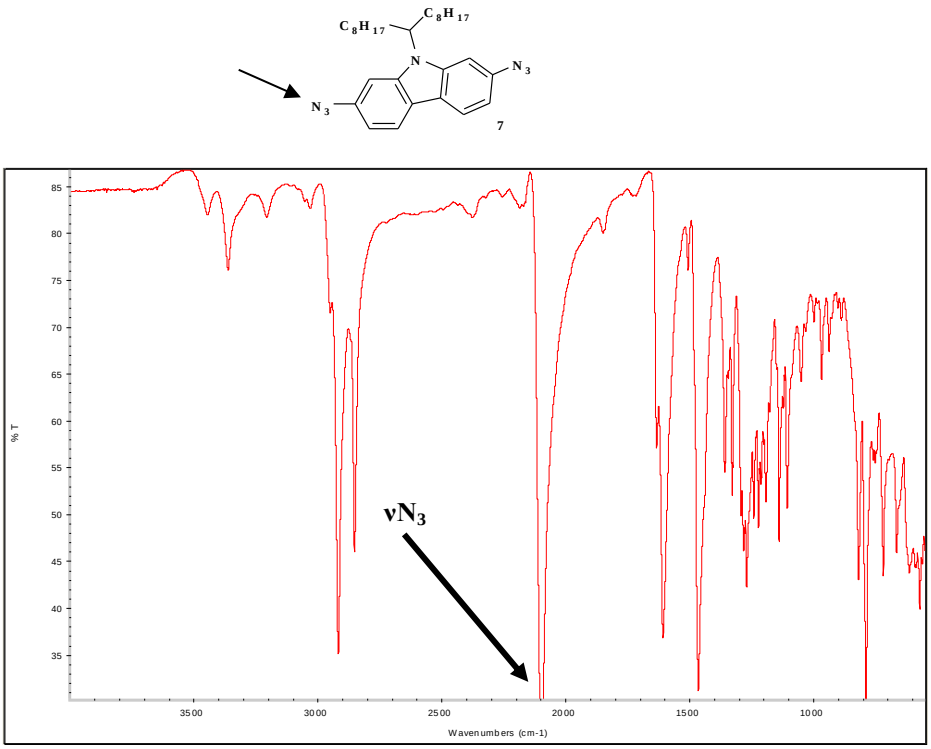

Figure 2-4: ATR-FTIR spectrum of the 2,7 diazidocarbazole 7.

The polymerization could have directly been performed between the 2,7 diazidocarbazole **7** and the two diformylcarbazol (**6** and **10**) thanks to an Aza-Wittig reaction.[41] However, in order to compare all the polymers as accurately as possible, the azido functions have been reduced thanks to a Staudinger reaction in presence of tributylphosphine.[42] This is not the classical way used to synthesize 2,7 diaminocarbazole; indeed the most common method consists in synthesizing the diaminocarbazole following a nitro reduction using Tin(II) chloride.[43–45] Once again, the purity and structure has been assessed by NMR amongst other analyses (see experimental part). For both monomers the NMR showed a shift of aromatic protons due to the substitution of bromine with amino and formyl moieties. Moreover, the appearance of the formyl signal at 10.11 ppm and the broad signal corresponding to the amino groups at 3.79 ppm for the diformyl and diaminocarbazole respectively confirmed the expected structure (Figure 2-5).

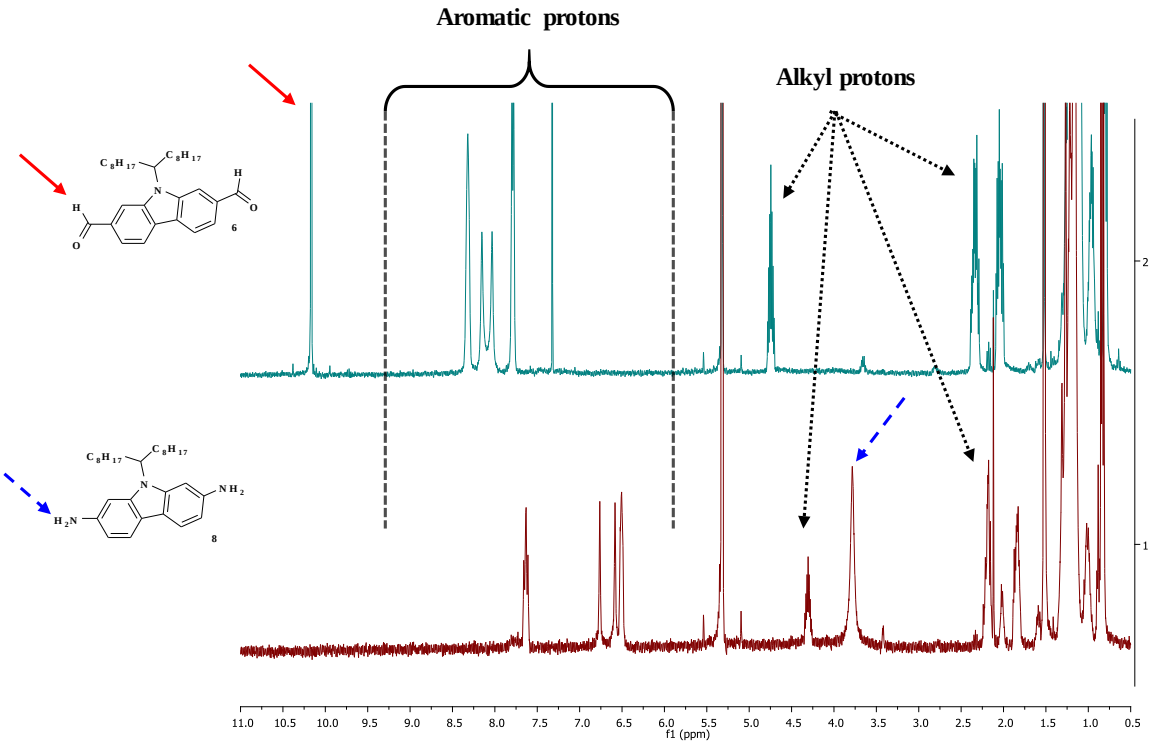

Figure 2-5: ^{1}H NMR spectra of the 2,7diformyl carbazole 6 (top) and the 2,7 diaminocarbazole 8 (bottom) (in CD_2Cl_2).

Both 3,6-disubstituted carbazole were synthesized from the alkylated carbazole **9** which has been obtained in one alkylation step from the commercial carbazole. The alkylated carbazole **9** can either be involved in a Vilsmeier-Haack reaction in presence of DMF and $POCl_3$ to afford the 3,6-diformylcarbazole **10** with a yield of 65% or a nitration in the so called Menke conditions in presence of copper nitrate in order to give the 3,6-dinitrocarbazole **11**.[46] Its reduction, using palladium on charcoal and hydrazine, gave the 3,6-diaminocarbazole **12** via the formation of an hydroxylamine during the reaction.[47,48] The purity and structure of these two monomers have been proven with ^{1}H-^{13}C HSQC (Heteronuclear Single-Quantum Correlation) NMR, ATR-FTIR and mass spectrometry experiments (see experimental part).

Finally, the EDOT dialdehyde co-monomer **13** was synthesized using butyl lithium and DMF in one step using commercial EDOT following the same protocol as for the 2,7-diformylcarbazole **6** (Scheme 2-3). Once again the structure of the product has been confirmed via different methods (see experimental part).

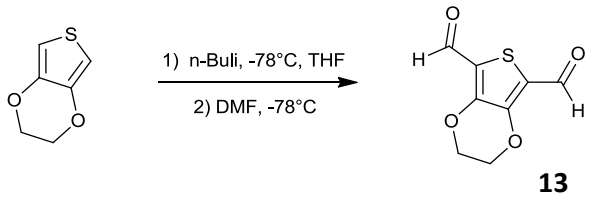

Scheme 2-4: Synthesis of the EDOT dialdehyde derivative 13.

2.2.1.2. Polymer synthesis

All the polymers have been synthesized following the same method (Scheme 2-5).

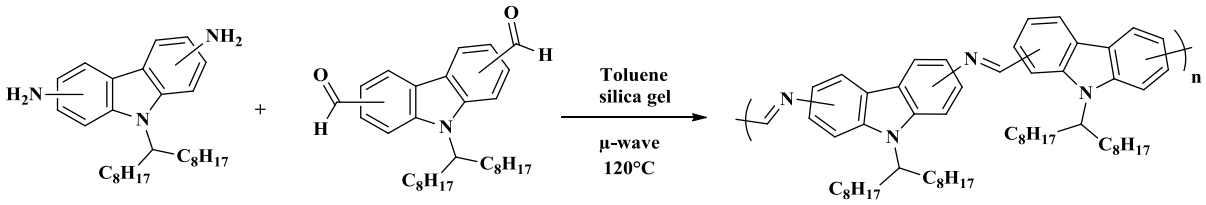

Scheme 2-5: Synthesis of carbazole-based polyazomethines.

One equivalent of diamino-carbazole was added to one equivalent of diformyl-carbazole in solution in toluene. The reaction was performed both in a micro-wave reactor and in a conventional oil-bath. The two methods allow obtaining similar polyazomehines in terms of size and optical properties, the advantages of using a micro-wave reactor being an easier manipulation (less glassware needed) and a shorter reaction time (from days to hours). Furthermore, in a micro-wave reactor, a conventional dean-stark apparatus couldn't be used to remove the water produced during the reaction. To overcome this issue, silica gel was added in the medium to move the equilibrium toward the formation of the polymer. Moreover, the water being removed with silica gel, there is no need of solvent forming azeotrope with water. Thus, reaction could be performed in chloroform for example. For the sake of comparison, polymerizations with more common desiccant (magnesium sulfate and lithium chloride) have been performed. They are known to increase the molar mass of polyazomethines during the synthesis.[49] The different polyazomethines synthesized have all a similar size regardless the desiccant used. This means that the silica is efficient enough to move the equilibrium toward the polymerization. Moreover, the silica being acidic it may help to catalyze the polymerization. The reaction mixture was then put under micro-wave irradiation for four hours at 130°C. The formation of the azomethines linkage has been especially confirmed *via* ATR-FTIR spectroscopy. In

both cases, the disappearance of amino and formyl signals has been observed, in particular those at 1600 cm^{-1} and 1700 cm^{-1} respectively in addition to the appearance of a signal at 1650 cm^{-1} corresponding to the azomethine C=N stretching. In ^{1}H NMR, the signal corresponding at the CH=N bond can be observed around 8.8 ppm, depending on the polymer (Figure 2-6).

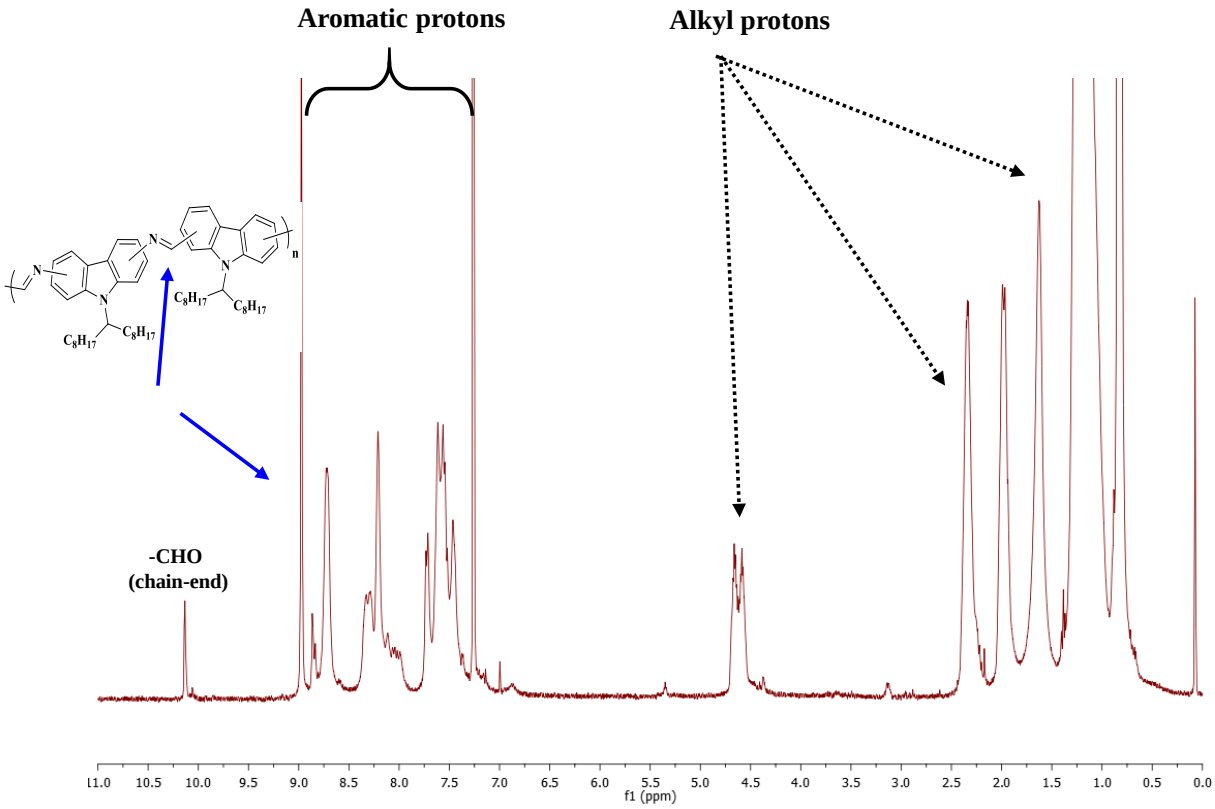

Figure 2-6: Typical ^{1}H NMR (400 MHz, $CDCl_3$) spectrum of carbazole based polyazomethines synthesized.

On this spectrum, the signal at 10.3 ppm corresponds to the chain-end aldehyde functions which can be useful to approximate the polymer molar mass. The terminal amine functions can't be observed because they are hidden by the alkyl signals at 4.5 ppm.

2.2.2. Characterization

2.2.2.1. Physical and optical features

2.2.2.1.1. Physical properties

Molar mass of compounds have been measured by SEC in chloroform using PS standards. A typical trace is shown, which is clearly representative of a

polycondensation reaction. Indeed, a multimodal distribution can be observed with a series of oligomers at higher elution time. Since monomers have a relatively high molar mass, a signal can be observed for each oligomer present in the mixture (Figure 2-7).

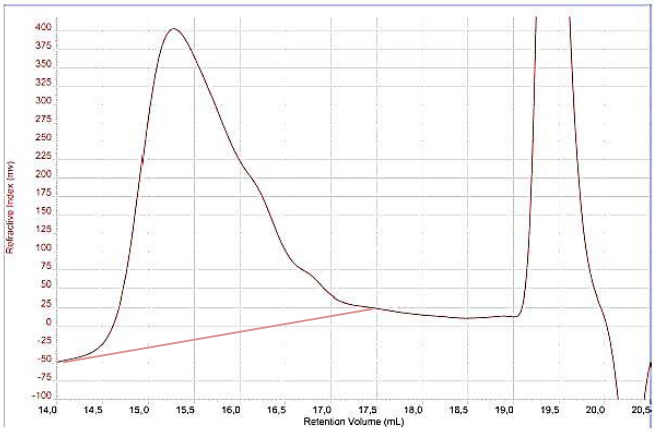

Figure 2-7: Typical SEC trace of the carbazole-based polyazomethines (in $CHCl_3$, polystyrene calibration)

Main features along with optical properties of carbazole-based polyazomethines synthesized using micro-waves irradiation are gathered in Table 2-2.

Polymer	$\overline{M_n}$[a] g.mol^{-1}	$\overline{M_w}$[a] g.mol^{-1}	Đ[a]	$\overline{DP}_n$[a] (Mass spectrometry)	T_d[b] °C	T_g[c] °C	Absorption[d]		Emission[d]	
							λ_{max}^{sol} nm	λ_{max}^{film} nm	λ_{max}^{sol} nm	Φ_f[e]
2,7-2,7 Cbz	3600	10500	2.9	4 (6)	451	98	272-428	270-436	405-540	0.03
2,7-3,6 Cbz	3650	13700	3.7	4 (6)	430	91	270-400	267-402	405-570	0.02
3,6-3,6 Cbz	3700	11700	3.2	4 (6)	436	93	264-310-360	263-315-362	405-455-565	0.04
3,6-2,7 Cbz	3500	10050	2.9	4 (6)	430	112	267-416	265-420	405-580	0.03

Table 2-2: Molar mass, thermal and optical properties of carbazole-based polyazomethines synthesized through micro-waves irradiation.

[a]Measured by SEC in $CHCl_3$ at 30 °C, relative to PS standards and by mass spectrometry MALDI-TOF. [b]Obtained by TGA under N_2 at 10 °C min^{-1}. [c]Obtained by DSC under He at 20 °C min−1. [d]Measured in $CHCl_3$ solutions (5.10^{-4} g l^{-1}) and spin-coated on quartz. [e]Measured in solution using an integration sphere.

All the four polycarbazoles have a similar size (confirmed with mass spectrometry MALDI-TOF and NMR, see experimental part), from 3500 to 3700 g.mol^{-1}. Their

dispersity between 2.0 and 3.0 is coherent with a condensation reaction. On each of these chromatograms the peaks corresponding to different oligomers sizes are observed. Besides, as previously mentioned, the relatively low molar mass and moderate impact of the desiccant, unveil the major impact of stoichiometry between reactants. Indeed, small deviation from stoichiometry caused by weighing error for instance can drastically affect molar mass of polymers. Moreover, a limited solubility can reduce the size of synthesized oligomers. The thermogravimetric analyses (TGA) and differential scanning calorimetry (DSC) performed afterwards showed good thermal stability with decomposition temperatures ranging from 376 to 395 °C, as well as glass transition temperatures ranging from 101 to 116 °C (see experimental part). As commonly observed in the case of alternated π-conjugated polymers, such materials are amorphous.

2.2.2.1.2. Optical characterizations

The absorption and emission spectra of the four polymers have been measured (Figure 2-8).

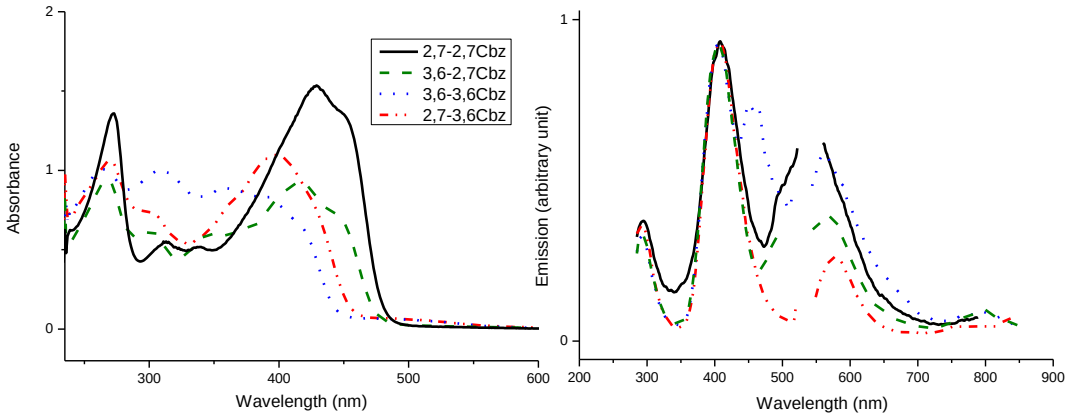

Figure 2-8: Absorbance (left) and emission (right) spectrum of the four polycarbazoles in chloroform at a concentration of 5.10^{-4} g.L^{-1}.

Two main signals are observed for the absorption of polymers. The low wavelength peak is assigned to the carbazole moiety while the highest wavelength one corresponds to the Intramolecular Charge Transfer (ICT) between the carbazole units.[50] The absorption is more intense for the polyazomethine with 2,7-2,7 linkage, the lowest absorption being for the 3,6-3,6 polycarbazole which can be due to a loss of the aromatic character. For a same concentration, the maximum of absorption is 1.5 times

higher for the polymer with azomethines functions in positions 2,7 than 3,6. A red-shift in the absorption can be observed as the conjugation increases thanks to the increase of the electronic delocalization (Figure 2-8). Indeed, the maximum of absorption of the four polymers increases with a maximum of absorption of 359 nm, 400 nm, 416 nm and 426 nm respectively for the 3,6-3,6, 2,7-3,6, 3,6-2,7 and 2,7-2,7 linkages.
Their emission spectra show broad signals on a large range of wavelength. This broad emission can be interesting in view of their future integration into devices. To compare polymers efficiencies, in term of fluorescence, with polyazomethine described in the literature, their absolute fluorescence quantum efficiency has been measured. In accord with the literature, the values are relatively low and could be increased by lowering the temperature or doping, for instance in the presence 2,2,2-Trifluoroethanoic acid (trifluoroacetic acid).[21,23,51] In some cases, the authors managed to obtain an absolute fluorescence quantum efficiency up to 0.66 (with an initial value of 0.13) or even 0.85 (with an initial value of 0.26).

In the case of carbazole directly linked with a carbon-carbon bond, a red-shift in absorptions of 2,7-linked polymers is expected because of longer conjugation length. Indeed, it was reported that the 3,6-linkage induces conjugation breaks on the nitrogen atom, thus limiting the conjugation length and lowering the absorption wavelength (Figure 2-9).[50]

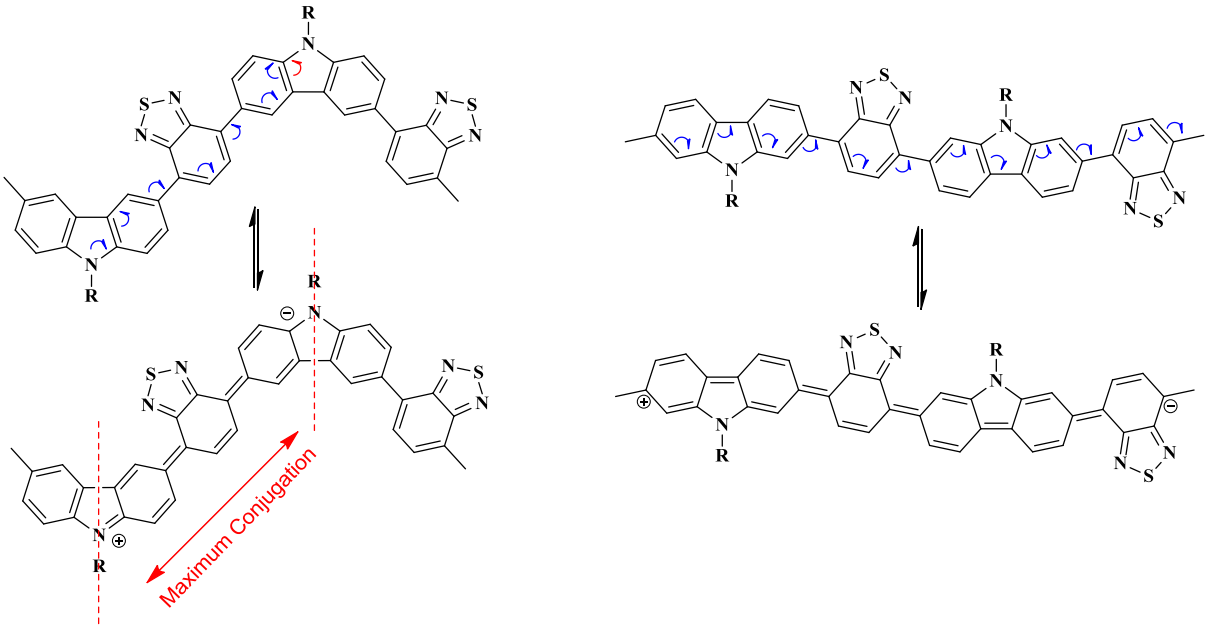

Figure 2-9: Representation of conjugation extent in 3,6- (left) and 2,7-linked (right) polycarbazoles.

It turns out that with the insertion of azomethine linkage, this delocalization pathway isn't different, the quinoid form of carbazoles being the same.

2.2.2.2. Theoretical modelisation

TD-DFT calculations where performed in order to corroborate the optical data. For the sake of comparison, TD-DFT calculations were carried out on carbazole or diphenylamine-based azomethines in the case of monomers and dimers. (Figure 2-10 and Table 2-3).

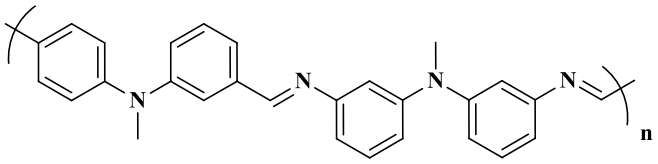

Figure 2-10: Structure of 2,7-Ph (n=1) and $(2,7\text{-Ph})_2$ (n=2).

Carbazole and phenyl based monomer and dimer (azomethine linkage)	HOMO level (eV)	LUMO level (eV)	GAP (eV)	S_0-S_1 *
2,7-2,7	- 5.67	- 1.92	3.75	3.37
$(2,7\text{-}2,7)_2$	- 5.47	- 2.11	3.36	2.87
2,7-3,6	- 5.53	- 1.70	3.82	3.41
$(2,7\text{-}3,6)_2$	- 5.32	- 1.81	3.51	3.00
3,6-2,7	- 5.56	- 1.74	3.82	3.38
$(3,6\text{-}2,7)_2$	- 5.25	- 1.57	3.68	2.93
3,6-3,6	- 5.42	- 1.46	3.97	3.48
$(3,6\text{-}3,6)_2$	- 5.37	- 1.97	3.40	3.12
2,7-phe	- 5.48	- 1.76	3.72	3.12
$(2,7\text{-phe})_2$	- 5.37	- 1.85	3.52	3.09

Table 2-3: TD-DFT calculations for carbazole and phenyl based azomethines monomers and dimers.

With the diphenylamine based polymer there is no significant differences in energetic levels or transitions between monomer and dimer, indicating that the HOMO level is localized, (no long range aromaticity). This also proves that the delocalization is higher in the case of carbazole-based polyazomethines and that the lone pairs of the different nitrogen atoms in the chain don't participate to the delocalization. Moreover, these results show that the carbazole with the azomethine linkage in positions 2,7 presents better delocalization than the alternated one or the one linked in positions 3,6. This imply that the polycarbazoles consisting in 2,7 azomethine linkages have smaller bandgaps. The impact of this gap reduction can be seen on the absorption spectra prediction (see experimental part, Figure 2-72). Moreover, the absorption is more intense for the 2,7-2,7 linkage. These results confirmed the previous experimental observations with the polymer presenting the 2,7-2,7 linkage showing a more intense and a red-shift absorption due to an increase of the conjugation thanks to the increase of the aromatic character.

Some more TD-DFT calculations have been performed (Table 2-4).

Carbazole based dimer (azomethine linkage)	**N=C (Å)**	**C-N (Å)**	**BLA**	**BOA**
(2,7-2,7)$_2$	1.274	1.397	0.0495	0.3153
(2,7-3,6)$_2$	1.275	1.399	0.0531	0.3372
(3,6-2,7)$_2$	1.275	1.396	0.0511	0.3429
(3,6-3,6)$_2$	1.274	1.398	0.0559	0.3691
(2,7-edot)$_2$	1.276	1.395	0.0558	0.3487
(2,7phe)$_2$	1.272	1.397	0.0418	0.2864

Table 2-4 : Results of calculations on phenyl and carbazole-based azomethines.

These results show that for all polymers, the N=C and C-N distance are similar in the different polyazomethines synthesized. However, the bond length alternation (BLA) and bond order alternation (BOA) have been calculated (Table 2-4). They are two

indicators of polymer aromaticity. The closer the C-N and N=C bond are, the more conjugated the polymer is. Once again, the theoretical results are consistent with the experimental ones.

2.3. Synthesis of random poly(azomethine carbazole-*co*-EDOT)

2.3.1. Polymer Synthesis

As PEDOT materials show great potential in the field of organic electronics,[52] EDOT was chosen as co-monomer in order to study its effect on 2,7 polycarbazole structures which was the best in term of opto-electronic features, as discussed previously. Dialdehyde EDOT **13** was thus introduced at different ratio (from 25% to 100%) in order to alternate with 2,7 carbazole subunits (Scheme 2-6).

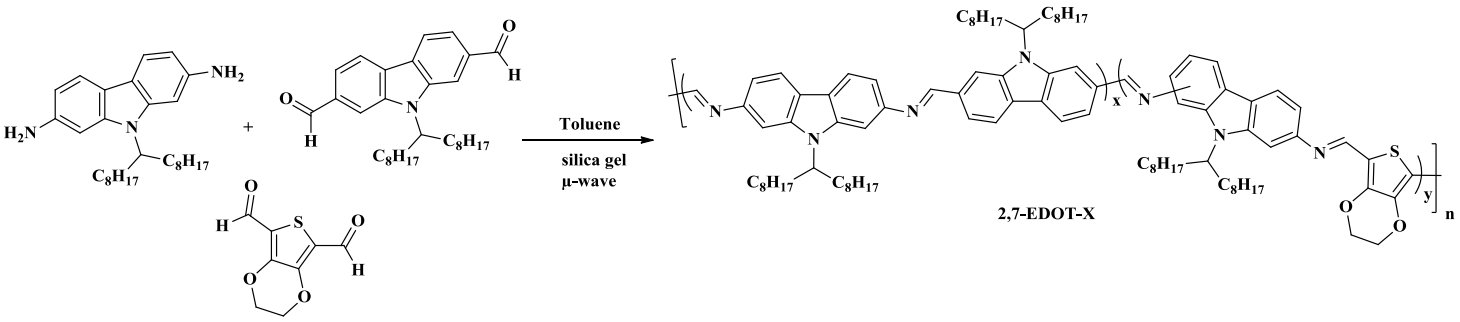

Scheme 2-6 : Polyazomethine copolymer between EDOT and carbazole.

As an example 0.75 equivalent of 2,7 dialdehyde carbazole **10** plus 0.25 equivalent of dialdehyde EDOT **13** were reacted with on equivalent of 2,7 diaminocarbazole in toluene for the synthesis of **2,7-EDOT-25** co-polymer.

2.3.2. Characterization of random poly(azomethine carbazole-*co*-EDOT)

2.3.2.1. Physical and optical properties

Molar mass, thermal and optical properties of the different copolymers with various ratio of EDOT are gathered in Table 2-5.

Polymer (Theoretical dialdehyde EDOT percentage)	$\overline{M_n}$ [a] g.mol^{-1}	$\overline{M_w}$ [a] g.mol^{-1}	Đ [a]	$\overline{DP}_n$ [a]	T_d [b] /°C	T_g [c] /°C	Absorption [d]	Emission [d]	
							λ_{max}^{sol} /nm	λ_{max}^{sol} /nm	Φ_f [e] film
2,7-2,7Cbz (0%)	3600	10500	2.9	4 (n = 4)	451	101	272-425	365	0.03
2,7-EDOT-25 (25%)	3150	9600	3.0	4 (y = 0.25)	393	114	272-439	367	0.04
2,7-EDOT-50 (50%)	4200	10100	2.4	6 (y = 0.5)	371	89	272-452	367	0.06
2,7-EDOT-75 (75%)	2500	7950	3.2	4 (y = 0.75)	391	/	265-482	370	0.08
2,7-EDOT-100 (100%)	2400	4900	2.0	4 (y = 1)	382	/	262-483	380	0.06

Table 2-5: Molar mass, thermal and optical properties of polyazomethines carbazole containing EDOT comonomer subunits at different ratio.

[a]Measured by SEC in $CHCl_3$ at 30 °C, relative to PS standards and by mass spectrometry MALDI-TOF. [b]Obtained by TGA under N_2 at 10 °C min^{-1}. [c]Obtained by DSC under He at 20 °C min^{-1}. [d]Measured in $CHCl_3$ solutions (5.10^{-4} g l^{-1}) and spin-coated on quartz. [e]Measured in solution in an integration sphere.

The EDOT insertion doesn't seem to have an impact on the decomposition temperature but with the increase of the EDOT insertion the glass transition becomes difficult to observe. Importantly, molar mass of co-polymers were found higher than in previous case, probably du to an increase of its solubility. In addition, a red-shift of the absorption peak is observed (Figure 2-11).

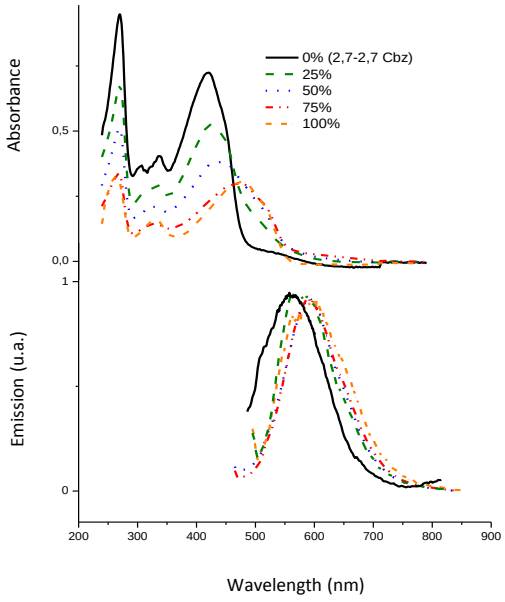

Figure 2-11 : Absorbance (top) and emission (bottom) spectra of polyazomethines containing different ratio of EDOT moiety (in solution in $CHCl_3$)

As fully 2,7 carbazole polyazomethine (**2,7-2,7Cbz**) and **2,7-EDOT-100** alternated copolymer have roughly the same degree of polymerization, the absorbance red-shift could be attributed to π-π interactions and/or formation of low band-gap copolymers. The relative difference in terms of absorbance between these polymers comes from molar attenuation coefficient difference between EDOT and carbazole, with a value of 7050 L.mol-1 for EDOT and 32000 L.mol^{-1} for the carbazole at 255 nm.[53,54]

2.3.2.2. Electrochemical analysis

Electrochemical characteristics were estimated by cyclic voltammetry using dichloromethane solutions of 4-tetrabutylammonium hexafluorophosphate ($TBAPF_6$) as electrolyte, with platinum wires as working and counter electrodes and silver wire as reference electrode. The oxidation and reduction potentials for the eight polycarbazoles could be evaluated from the voltammograms by taking the onset of the oxidation and reduction peaks (Figure 2-12).

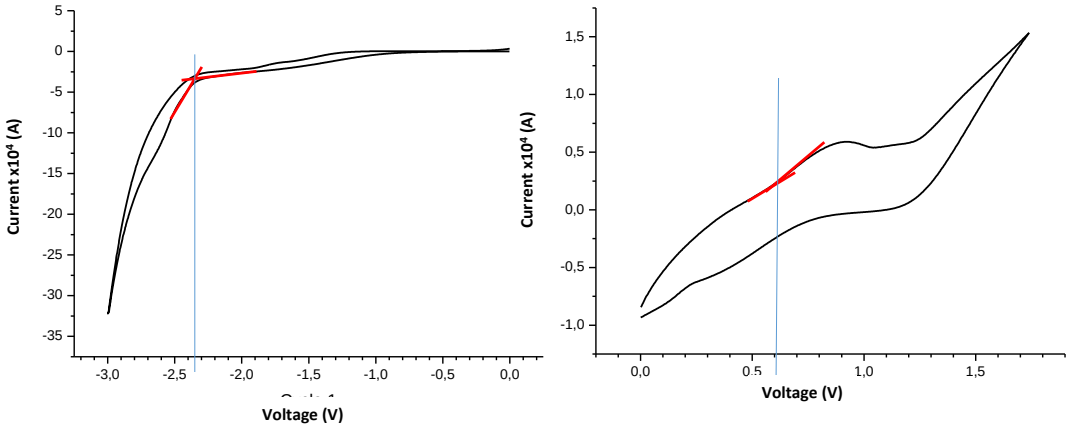

Figure 2-12: Cyclic voltammograms (left-reduction, right-oxidation) of 2,7-2,7Cbz in CH_2Cl_2 solution (0.1 g.l^{-1}), with $TBAPF_6$ as electrolyte (0.2 V.s^{-1})

In this example, the 2,7-2,7Cbz presents the onset of its oxidation peak at 0.6 V and the onset of the reduction at -2.32 V. HOMO and LUMO levels have been determined using the following equations:

$$E_{HOMO}(eV) = -(E_{Ox}\ (V) + 4.4 + 0.22)$$
$$E_{LUMO}(eV) = -(E_{Red}\ (V) + 4.4 + 0.22)$$

Where 4.4 + 0.22 eV corresponds to the energetic position of the potential $E_{1/2}$ for the ferrocene/ferrocene$^+$ (Fc/Fc^+) redox couple, estimated from a ferrocene solution in

chloroform using saturated calomel electrode as reference.[55,56] The HOMO and LUMO levels for this polymer are respectively at -5.22 eV and -2.30 eV which give an electronic gap of 2.92 eV.
The HOMO, LUMO and GAP values are reported in the table 2-6 below.

Polymer	HOMO (eV)[a]	LUMO (eV)[a]	GAP (eV)[b]	Optical GAP (eV)
2.7-2.7 Cbz	- 5.22	- 2.30	2.92	2.63
2.7-3.6 Cbz	- 5.40	- 2.22	3.18	2.75
3.6-3.6 Cbz	- 5.41	- 2.21	3.20	2.84
3.6-2.7 Cbz	- 5.50	- 2.45	3.05	2.68
2.7-Edot-25	- 5.31	- 2.70	2.61	2.55
2.7-Edot-50	- 5.52	- 3.09	2.45	2.28
2.7-Edot-75	- 5.35	- 3.05	2.30	2.25
2.7-Edot-100	- 5.20	- 3.09	2.11	2.24

Table 2-6: Electrochemical properties of the polyazomethines

[a]Calculated from the onset of the oxidation peak ($E_{onsetox}$) and reduction peak ($E_{onsetred}$) and adjusted with ferrocene.
[b]Calculated by difference between oxidation and reduction potentials

For carbazole-based polyazomethines, electrochemical GAP measured are between 2.9 and 3.2 eV. The impact of the azomethine linkage could be clearly seen, with a lower gap when the azomethine linkage is in 2,7 positions. With the insertion of EDOT moieties in the main chain a lowering of the electrochemical gap, from 2.96 to 2.05 eV is observed. This diminution is coherent with the apparition of the alternation between a donating unit and a less donating one. Finally, the calculated values reported in Table 2-3 and 2-4 have been compared with the theoretical ones and are coherent with the GAP diminution observed with replacement of 2,7-diformylcarbazole with the EDOT moiety.

2.4. Conclusions

In this work, we successfully synthesized new conjugated carbazole-based polyazomethines. An effort has been made in regards to the synthesis route by avoiding the use of metal-based catalysts and by working under microwave irradiation. Two series of aromatic polyazomethines were synthesized, the first one aiming to study the effect of carbazole linkage, either 2,7 or 3,6, and the second one intended to alternate EDOT subunit with carbazole. Interestingly, the introduction of EDOT subunits within the polycarbazole azomethine backbone allowed us to increase molar masses and lower the band gap of final polymer materials. Experimental data were found in accord with simulation data performed by TD-DFT. These results pave the way to new classes of π-conjugated organic polymers showing promise in the field of optoelectronics. Integration of such material into devices (OFET and OLED) is currently in progress.

2.5. References

[1] R. Adams, J. E. Bullock, W. C. Wilson, *Journal of the American Chemical Society*, **1923**, *45*, 521.

[2] C. S. Marvel, H. W. Hill, *Journal of the American Chemical Society*, **1950**, *72*, 4819.

[3] S. A. P. Guarin, M. Bourgeaux, S. Dufresne, W. G. Skene, *Journal of Organic Chemistry*, **2007**, *72*, 2631.

[4] C. O. Kappe, *Angewandte Chemie-International Edition*, **2004**, *43*, 6250.

[5] P. Lidström, J. Tierney, B. Wathey, J. Westman, *Tetrahedron*, **2001**, *57*, 9225.

[6] P. W. Wojtkowski, *Macromolecules*, **1987**, *20*, 740.

[**7**] P. W. Morgan, S. L. Kwolek, T. C. Pletcher, *Macromolecules*, **1987**, *20*, 729.

[**8**] C. K. Ober, R. W. Lenz, *Advances in Polymer Science*, **1984**, 1984.

[**9**] M. G. Dobb, J. E. Mclntyre, *Advances in Polymer Science*, **1984**, *60*, 61.

[**10**] S. R. Allen, A. G. Filippov, R. J. Farris, E. L. Thomas, *Macromolecules*, **1981**, *14*, 1135.

[**11**] Patent DuPont (Morgan, P. W.): U.S.P. 4,048,148 and 4,122,070 (priority 9 May **1975**),.

[**12**] K. S. Lee, J. C. Won, J. C. Jung, *Makromolekulare Chemie-Macromolecular Chemistry and Physics*, **1989**, *190*, 1547.

[**13**] S. B. Park, H. Kim, W. C. Zin, J. C. Jung, *Macromolecules*, **1993**, *26*, 1627.

[**14**] B. A. Reinhardt, M. R. Unroe, M. Prazak, R. C. Evers, J. Kane, C. Jariwala, M. Sinsky, *Materials Research*, **1990**, *109*, 670.

[**15**] H. Kretzschmann, H. Meier, *Tetrahedron letters*, **1991**, *32*, 5059.

[**16**] S. A. Jenekhe, C. J. Yang, H. Vanherzeele, J. S. Meth, *Chemistry of Materials*, **1991**, *3*, 987.

[**17**] J. C. Hindson, B. Ulgut, R. H. Friend, N. C. Greenham, B. Norder, A. Kotlewski, T. J. Dingemans, *Journal of Materials Chemistry*, **2010**, *20*, 937.

[**18**] Y. Takihana, M. Shiotsuki, F. Sanda, T. Masuda, *Macromolecules*, **2004**, *37*, 7578.

[**19**] H. Kim, J.-S. Kim, K. Kim, H. Park, S. Baek, M. Ree, *Journal of Polymer Science Part A: Polymer Chemistry*, **2004**, *42*, 825.

[**20**] Y. Takihana, M. Shiotsuki, F. Sanda, T. Masuda, *Macromolecules*, **2004**, *37*, 7578.

[**21**] S. Barik, W. G. Skene, *Polymer Chemistry*, **2011**, *2*, 1091.

[**22**] D. Işık, C. Santato, S. Barik, W. G. Skene, *Organic Electronics*, **2012**, *13*, 3022.

[**23**] S. Barik, T. Bletzacker, W. G. Skene, *Macromolecules*, **2012**, *45*, 1165.

[**24**] B. Jarzabek, B. Kaczmarczyk, J. Jurusik, M. Siwy, J. Weszka, *Journal of Non-Crystalline Solids*, **2013**, *375*, 13.

[**25**] A. Iwan, B. Boharewicz, I. Tazbir, M. Malinowski, M. Filapek, T. Kłab, B. Luszczynska, I. Glowacki, K. P. Korona, M. Kaminska, J. Wojtkiewicz, M. Lewandowska, A. Hreniak, *Solar Energy*, **2015**, *117*, 246.

[**26**] S. G. Ciechanowicz, K. P. Korona, A. Wolos, A. Drabinska, A. Iwan, I. Tazbir, J. Wojtkiewicz, M. Kaminska, *The Journal of Physical Chemistry C*, **2016**, *120*, 11415.

[**27**] Y.-H. Yao, J. Li, L.-F. Yuan, Z.-Q. Zhang, F.-X. Zhang, *RSC Advances*, **2016**, *6*, 45681.

[**28**] H. J. Kim, J. H. Lee, M. Lee, T. S. Lee, *Reactive and Functional Polymers*, **2008**, *68*, 1694.

[**29**] M. Koole, R. Frisenda, M. L. Petrus, M. L. Perrin, H. S. J. van der Zant, T. J. Dingemans, *Organic Electronics*, **2016**, *34*, 38.

[**30**] F. Tsai, C. Chang, C. Liu, W. Chen, S. A. Jenekhe, *Synthesis*, **2005**, 1958.

[**31**] J. Oriou, F. Ng, G. Hadziioannou, C. Brochon, E. Cloutet, *Journal of Polymer Science Part A: Polymer Chemistry*, **2015**, *53*, 2059.

[**32**] G. Sathiyan, E. K. T. Sivakumar, R. Ganesamoorthy, R. Thangamuthu, P. Sakthivel, *Tetrahedron Letters*, **2015**, *57*, 243.

[**33**] H. Xie, K. Zhang, C. Duan, S. Liu, F. Huang, Y. Cao, *Polymer (United Kingdom)*, **2012**, *53*, 5675.

[**34**] P. A. S. Smith, B. B. Brown, *Journal of the American Chemical Society*, **1951**, *73*, 2435.

[**35**] J.-F. Morin, M. Leclerc, *Macromolecules*, **2001**, *34*, 4680.

[**36**] N. Blouin, A. Michaud, M. Leclerc, *Advanced Materials*, **2007**, *19*, 2295.

[**37**] J. Clayden, *Tetrahedron*, **2004**, *60*, 4335.

[**38**] T. Michinobu, H. Kumazawa, E. Otsuki, H. Usui, K. Shigehara, *Journal of Polymer Science Part A: Polymer Chemistry*, **2009**, *47*, 3880.

[**39**] J. Andersen, U. Madsen, F. Björkling, X. Liang, *Synlett*, **2005**, *2005*, 2209.

[**40**] A. Kiyomori, J.-F. Marcoux, S. L. Buchwald, *Tetrahedron Letters*, **1999**, *40*, 2657.

[**41**] J. Miyake, Y. Chujo, *Macromolecules*, **2008**, *41*, 5671.

[**42**] K. Hemming, M. N. Khan, P. A. O'Gorman, A. Pitard, *Tetrahedron*, **2013**, *69*, 1279.

[**43**] A. Albert, W. H. Linnell, *Journal of the Chemical Society (Resumed)*, **1936**, 1614.

[**44**] Y. Tokunaga, S. Ikezaki, M. Kimura, K. Hisada, T. Kawasaki, *Chemical communications (Cambridge, England)*, **2013**, *49*, 11749.

[**45**] S. F. Nelsen, Y. Luo, M. N. Weaver, J. V. Lockard, J. I. Zink, *Journal of Organic Chemistry*, **2006**, *71*, 4286.

[**46**] M. Grigoras, N. C. Antonoaia, *European Polymer Journal*, **2005**, *41*, 1079.

[**47**] P. M. G. Bavin, *Canadian Journal of Chemistry*, **1958**, *36*, 238.

[**48**] S. Koyuncu, İ. Kaya, F. B. Koyuncu, E. Ozdemir, *Synthetic Metals*, **2009**, *159*, 1034.

[**49**] C.-J. Yang, S. A. Jenekhe, *Macromolecules*, **1995**, *28*, 1180.

[**50**] J. Kim, Y. S. Kwon, W. S. Shin, S.-J. Moon, T. Park, *Macromolecules*, **2011**, *44*, 1909.

[**51**] J. Cisowski, Z. Mazurak, J. Weszka, B. Hajduk, *Journal of Luminescence*, **2012**, *132*, 2098.

[**52**] J. Roncali, P. Blanchard, P. Frère, *Journal of Materials Chemistry*, **2005**, *15*, 1589.

[**53**] H. Walba, G. E. B. K., *Journal of the American Chemical Society*, **1951**, *1083*, 3341.

[**54**] Y. Lattach, A. Deniset-Besseau, J. M. Guigner, S. Remita, *Radiation Physics and Chemistry*, **2013**, *82*, 44.

[**55**] N. G. Tsierkezos, *Journal of Solution Chemistry*, **2007**, *36*, 289.

[**56**] C. M. Cardona, W. Li, A. E. Kaifer, D. Stockdale, G. C. Bazan, *Advanced Materials*, **2011**, *23*, 2367.

[**57**] C. Adamo, V. Barone, *The Journal of Chemical Physics*, **1999**, *110*, 6158.

[**58**] F. Neese, *Wiley Interdisciplinary Reviews: Computational Molecular Science*, **2012**, *2*, 73.

2.6. Experimental part

For general experimental informations, see the corresponding section page 235.

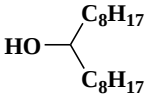

Heptadecan-9-ol (1):

In a 250 mL three neck flame-dried, magnesium turnings (2.21 g, 91 mmol) was put into dry diethylether (60 mL). After 30 min a solution of bromooctane (15 mL, 87 mmol) in diethylether (45 mL) was then added dropwise and the reaction mixture was allowed to stir for 1 more hour. Finally, a solution of ethyl formate (3 mL, 37.1 mmol) was added dropwise and stirred at room temperature overnight. The reaction was poured in water (300 mL) and extracted 3 times with 150 mL of ethyl acetate, dried over magnesium sulfate and the solvent was removed under vacuum to give a white solid which is used for the next step without further purification.

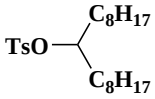

9-Heptadecane *p*-Toluenesulfonate (2):

p-toluenesulfonyl chloride (14.7 g, 77 mmol) in CH_2Cl_2 (60 mL) was added dropwise to a solution of heptadecan-9-ol (2) (18.00 g, 70 mmol) and trimethylamine (Et_3N) (24.4 mL, 181 mmol) in CH_2Cl_2 (90 mL) in a dry 250 mL flask. The mixture was stirred for 2 hours, 250 mL of water was added, and the mixture was extracted three times with CH_2Cl_2 (3x150 mL). The organic phase was washed with water, dried (Na_2SO_4), and concentrated under reduced pressure. The crude product was purified by silica-gel flash chromatography (cyclohexane-ethyl acetate, 95-5 as eluent) to give 22.5 g of colorless oil, which crystallized overtime as the title product (yield: 78 %).

^{1}H NMR (400 MHz, $CDCl_3$): δ (ppm) 7.78 (d, J = 8.3 Hz, 2H), 7.31 (d, J = 8.0 Hz, 2H), 4.54 (p, J = 6.0 Hz, 1H), 2.43 (s, 3H), 1.55 (m, 4H), 1.21 (m, 24H), 0.88 (t, 6H).

^{13}C NMR (101 MHz, $CDCl_3$): δ (ppm) 144.38, 134.97, 129.74, 127.85, 84.78, 70.82, 34.26, 31.97, 29.48, 29.42, 29.28, 24.81, 22.78, 21.71, 14.23.

FT-IR (ATR): ν= 2954, 2923, 2852, 1598, 1521, 1495, 1465, 1354, 1305, 1173, 1097, 1020, 895, 816, 766, 720, 662, 575, 554 $cm^{-1.}$

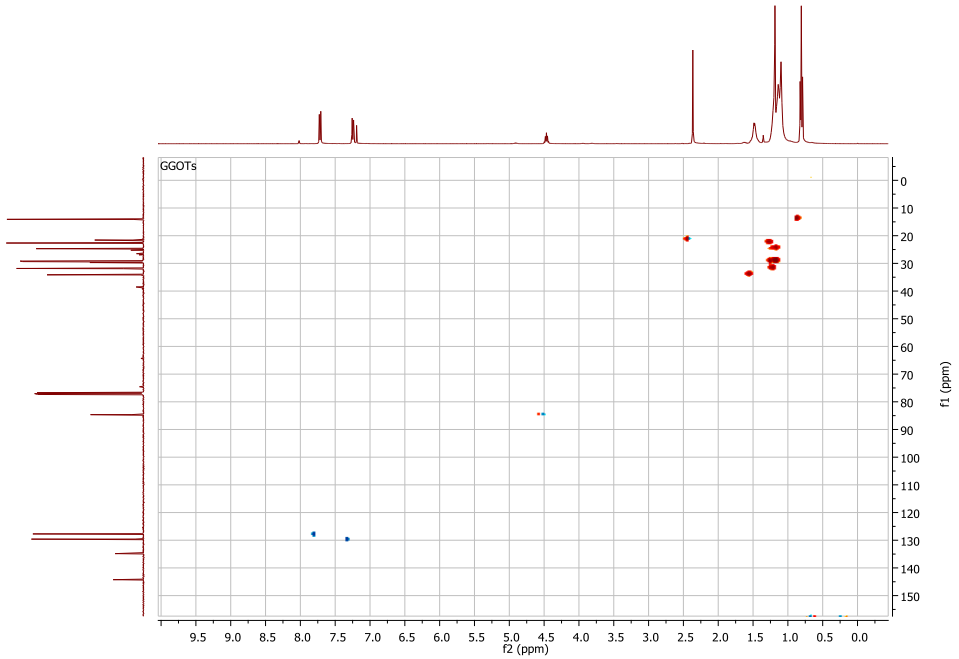

Figure 2-13: ^{1}H-^{13}C HSQC NMR spectrum of the 9-heptadecan alkyl chain 2 (in deuterated ethanol).

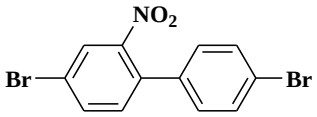

4,4'-Dibromo-2-nitrobiphenyl (3):

In a 500 mL flask, 4,4′-Dibromobiphenyl (10 g, 32 mmol) was mixed with acetic acid (200 mL). A mixture of sulphuric acid and nitric acid (respectively 16 mL and 8 mL) was then added dropwise. The reaction mixture was heated at 110°C for 1 hour, allowed to cool down at room temperature, poured into 300 mL of water and filtered. The yellow solid is purified by a recrystallization in methanol to obtain a pale yellow solid which is used in the next step without further purification.

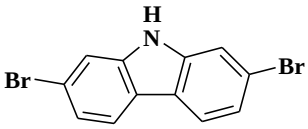

2,7-dibromo-9-H-carbazole (4):

In a 100 mL flame-dried flask, 4,4'-Dibromo-2-nitrobiphenyl (10 g, 28 mmol) was solubilized in 35 mL of triethyl phosphite ($P(OEt)_3$). The reaction was mixed overnight at 160°C. The reaction mixture was then allowed to cool down at room temperature and $POEt_3$ was distilled off under vacuum, followed by a flash chromatography in cyclohexane to obtain the final product as white crystals (yield: 65%).

^{1}H NMR (400 MHz, CD_2Cl_2): δ (ppm) 8.02 (d, J = 8.3 Hz, 2H); 7.72 (s, 2H); 7.33 (d, J = 8.3 Hz, 2H).

^{13}C NMR (101 MHz, CD_2Cl_2): δ (ppm) 141.96, 123.26, 122.55, 122.45, 119.94, 114.84.

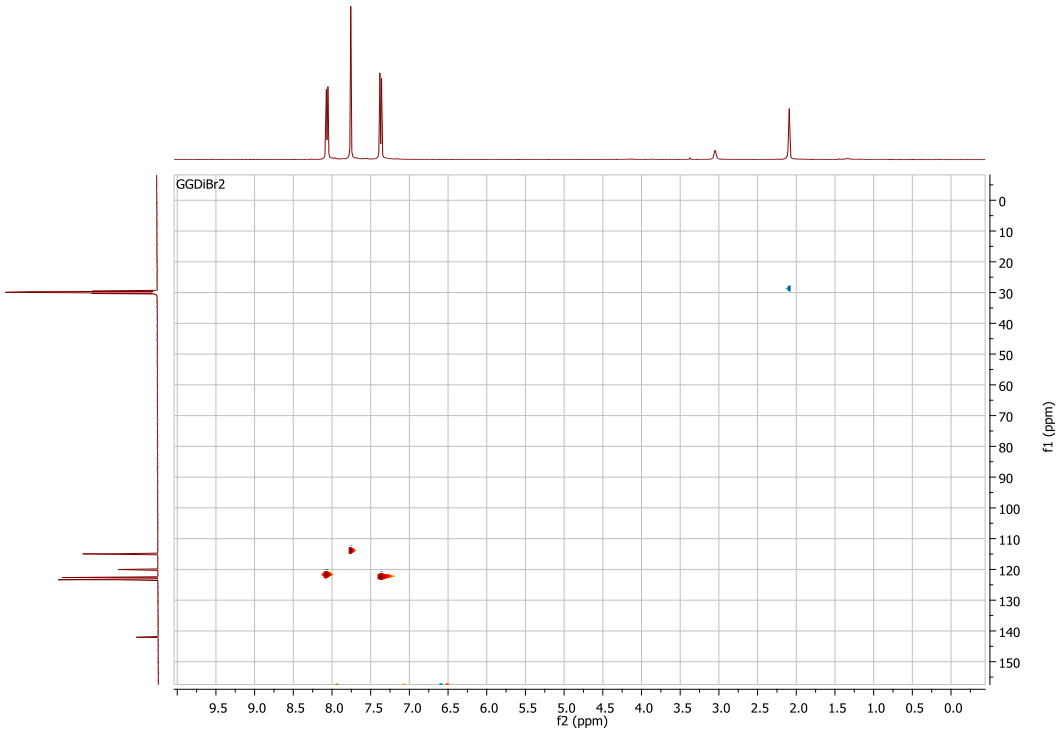

Figure 2-14: ^{1}H-^{13}C HSQC NMR spectrum of the 2,7-dibromocarbazole 4 (in CD_2Cl_2).

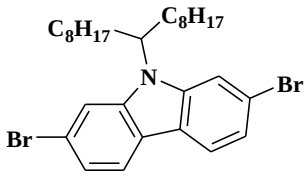

9-Heptadecanyl-2,7-dibromocarbazole (5):

This alkylation was performed in the same conditions than for the synthesis of the 9-Heptadecanylcarbazole (1) with 4 g of 2,7-dibromo-9-H-carbazole (8) (12 mmol), 40 mL of DMSO, 0.84 g (46.5 mmol) of potassium hydroxide and 6.4 g (15.6 mmol) of 9-Heptadecane *p*-Toluenesulfonate (3) to afford white crystals (yield: 90%).

^{1}H NMR (400 MHz, $CDCl_3$): δ (ppm) 7.5 (s, 2H); 7.27 (s, 2H); 7.12 (m, 2H), 4.48 (tt, J = 10.1, 5.1 Hz, 1H); 2.20 (m, 2H); 1.83 (m, 2H) 1.32 – 1.02 (m, 28H); 0.83 (t, J = 7.0 Hz, 6H).

^{13}C NMR (100 MHz, $CDCl_3$): δ (ppm) 125.61; 125.23; 120.43; 118.54; 111.70, 108.87, 56.43; 33.85; 31.89; 29.53; 29.43; 29.30; 26.94; 22.73; 14.20.

HRMS (EI+, m/z) [M]+ calculated (%) for $C_{29}H_{41}Br_2N$: 561.16057, found 561.16261

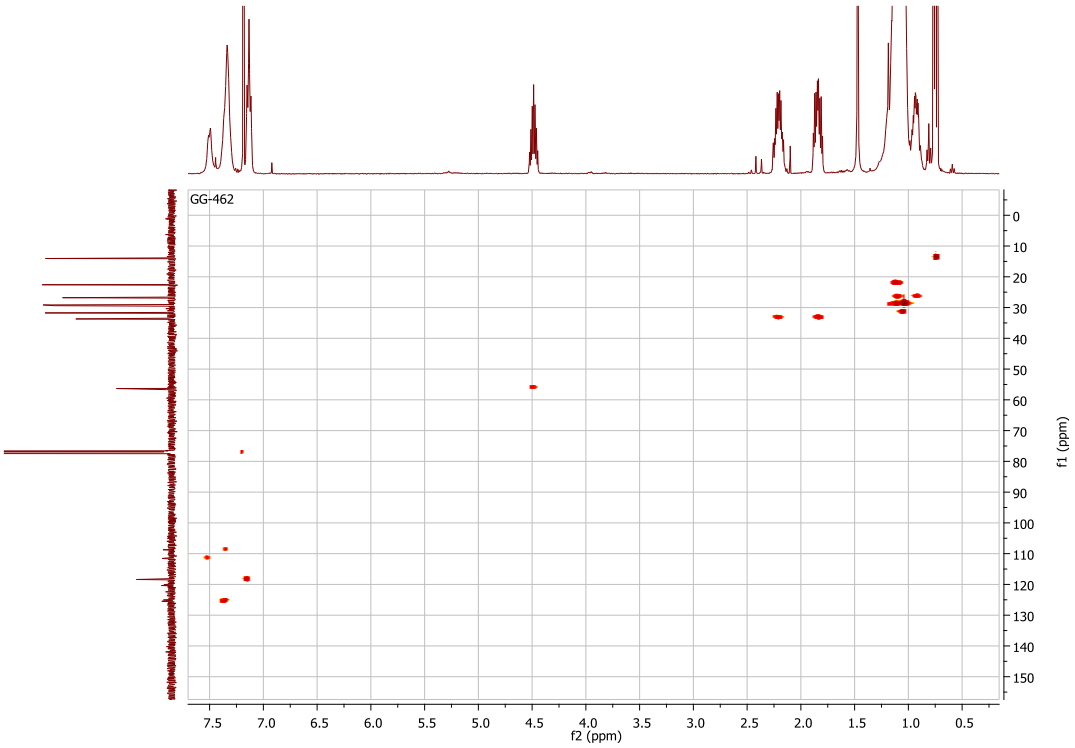

Figure 2-15: ^{1}H-^{13}C HSQC NMR spectrum of the alkylated 2,7-dibromocarbazole 5 (in $CDCl_3$).

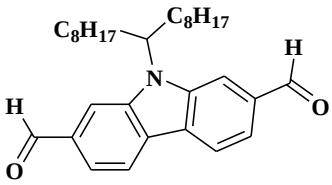

9-Heptadecanyl-2,7-diformylcarbazole (6):

9-Heptadecanyl-2,7-dibromocarbazole (3 g, 5.3 mmol) was solubilized in 130 mL of dry THF and was cooled at -78 °C. Then 16 mL (25.6 mmol) of a solution of n-butyl lithium was added dropwise. The reaction mixture was then heated up at 0°C for 1 hour and cooled down again at -78°C. Then 6 mL of DMF was added and the reaction was allowed to mix during 4 hours at room temperature. The reaction mixture was then poured into 100 mL of cold and lightly acid water, filtered and washed with water. The crude yellow solid was then firstly purified by flash chromatography in toluene and secondly in a mixture of heptane and ethyl acetate (80/20) to afford a yellow powder (yield: 82 %).

^{1}H NMR (400 MHz, $CDCl_3$): δ (ppm) 10.17 (s, 2H); 8.25 (s, 2H); 8.00 (d, J = 48.1 Hz, 2H); 7.72 (d, J = 8.0 Hz, 2H), 4.68 (tt, J = 10.2, 5.1 Hz, 1H); 2.25 (m, 2H); 1.92 (m, 2H) 1.26-1.09 (m, 28H); 0.80 (t, J = 7.0 Hz, 6H).

^{13}C NMR (101 MHz, $CDCl_3$): δ (ppm) 192.56; 121.28; 113.32; 112.66; 103.47; 57.28; 33.94; 31.83; 29.40; 29.38; 29.19; 26.94; 22.69; 14.16.

FT-IR (ATR): ν= 2916, 2844, 1689, 1570, 1460, 1444, 1223, 1166, 992, 856, 803, 731 cm^{-1}.

HRMS (EI+, m/z) [M]+ calculated (%) for $C_{31}H_{43}NO_2$: 461.32938, found 461.32967

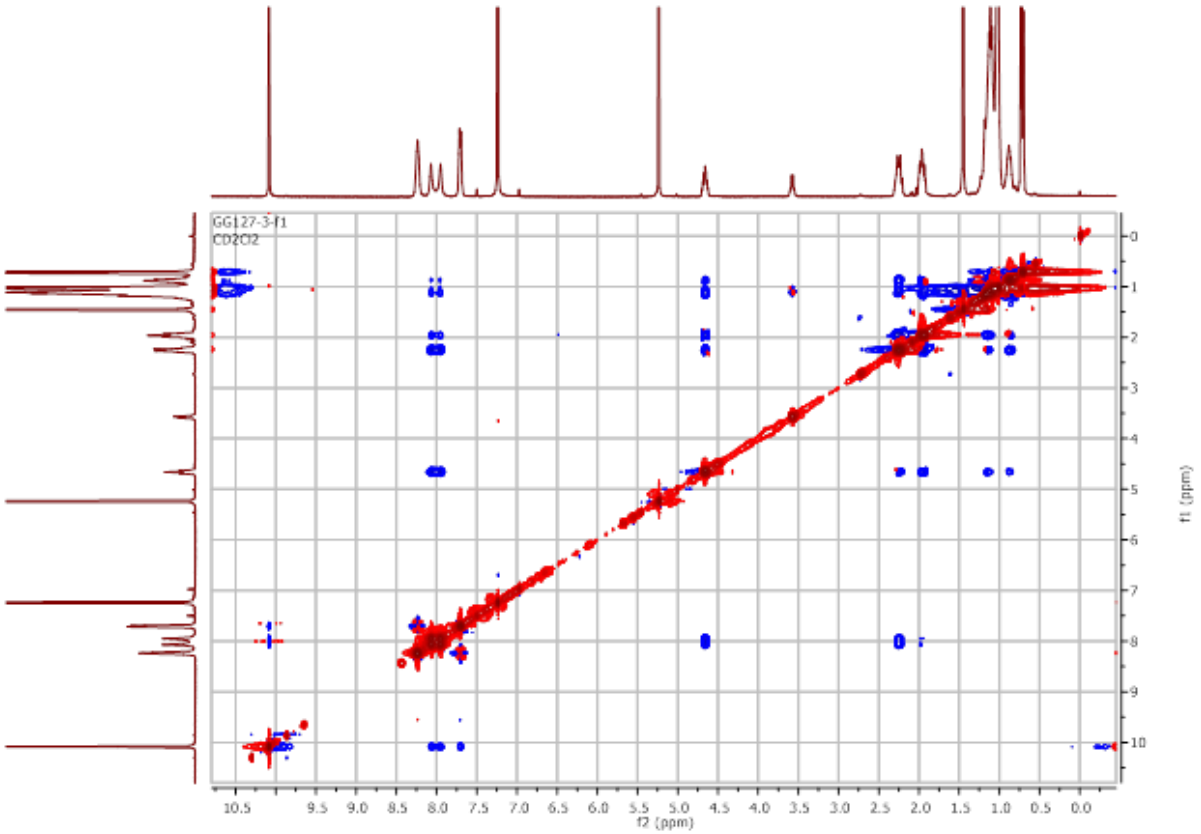

Figure 2-16: ^{1}H-^{1}H NOESY NMR spectrum of the 2,7-diformylcarbazole 6 (in $CDCl_3$).

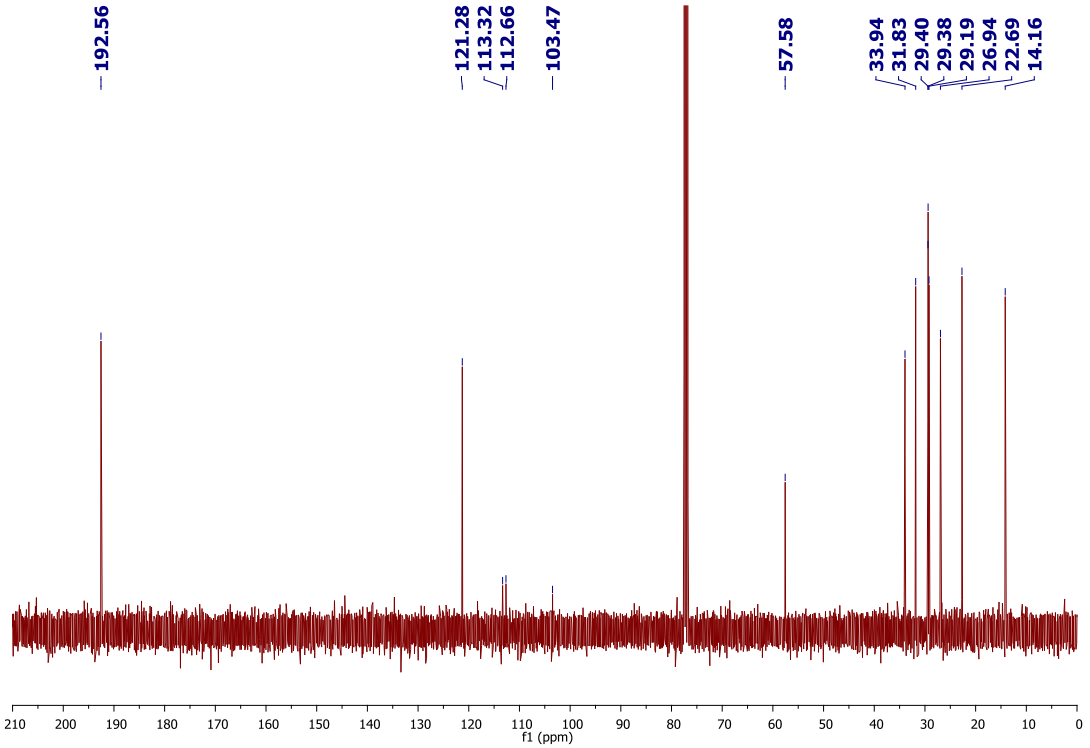

Figure 2-16bis: ^{13}C NMR spectrum of the 2,7-diformylcarbazole 6 (in $CDCl_3$).

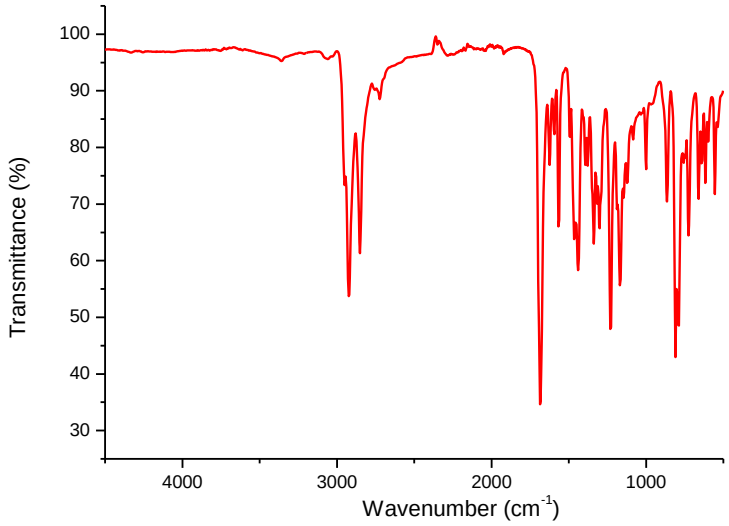

Figure 2-17: ATR-FTIR spectrum of the 2,7-diformylcarbazole 6.

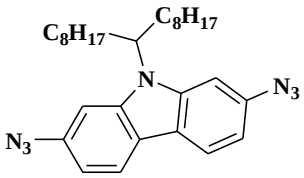

9-Heptadecanyl-2,7-diazidocarbazole (7):

9-Heptadecanyl-2,7-dibromocarbazole (4.00 g, 7.1 mmol), sodium azide (1.85 g, 28.5 mmol), copper iodide (0.28 g, 1.47 mmol), and sodium ascorbate (0.144 g, 0.77 mmol) were solubilized in 40 mL of toluene. DMF (0.240 mL, 2.23 mmol) is added with 12 mL of a mixture ethanol (8.5 mL) with water (3.5 mL) and was heated at 110°C for 20 hours. The reaction was then allowed to cool down at room temperature, poured into 50 mL of water and extracted three times with 50 mL of ethyl acetate, dried over magnesium sulfate and the residual solvent was removed under vacuum. The orange powder was purified by flash chromatography (cyclohexane/ethyl acetate 9:1) to afford an orange solid (yield: 65 %).

^{1}H NMR (400 MHz, $CDCl_3$): δ (ppm) 7.98 (t, J = 9.1 Hz, 2H); 7.12 (s, 2H), 6.95 (b, 2H); 4.41 (tt, J = 10.0, 4.9 Hz, 1H); 2.20 (m, 2H); 1.89 (m, 2H); 1.13 (m, 24H); 0.75 (t, J = 7.0 Hz, 6H).

^{13}C NMR (101 MHz, $CDCl_3$): δ (ppm) 143.47; 139.95; 137.86; 137.22; 130.52; 130.06; 121.24; 121.05; 119.90; 110.67; 102.20; 99.58; 56.95; 33.60; 31.87; 29.44; 29.41; 29.26; 26.86; 22.73; 14.18.

FT-IR (ATR): ν= 2100 cm^{-1} (C-N3 asymetric stretch)

HRMS (EI+, m/z) [M]+ calculated (%) for $C_{29}H_{41}N_7$: 487.34234, found 487.34247

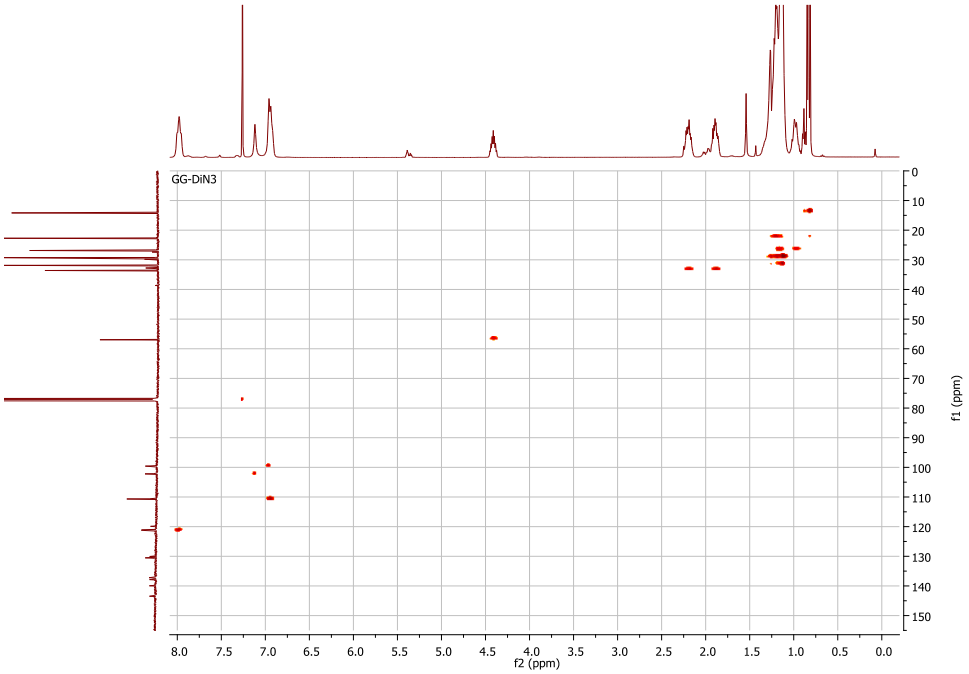

Figure 2-18: ^{1}H-^{13}C HSQC NMR spectrum of the 2,7-diazidocarbazole 7 (in $CDCl_3$).

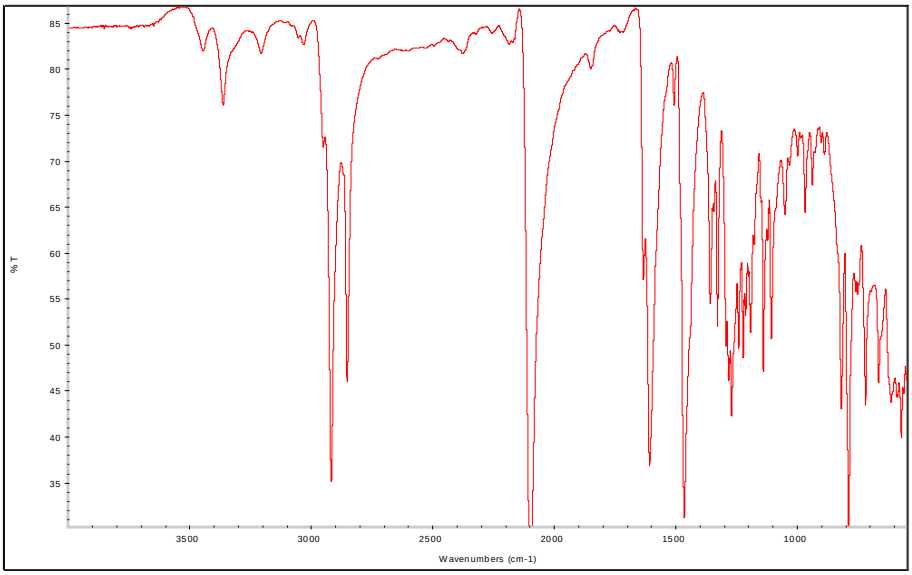

Figure 2-19: ATR-FTIR spectrum of the 2,7-diazidocarbazole 7.

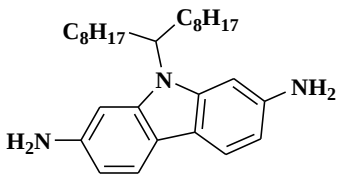

9-Heptadecanyl-2,7-diaminocarbazole (8):

In a 100 mL flame dried flask, 9-Heptadecanyl-2,7-diazidocarbazole (3 g, 6.15 mmol) was solubilized in 40 mL of THF. Then 3.88 mL (15.7 mmol) of tributylphosphine was added and the reaction mixture was mixed for 3 hours at room temperature. Then 15 mL of water were added and the reaction was mixed for 20 more hours. The reaction was then directly dried under vacuum and the orange oil purified by flash chromatography in toluene to give a pink powder (yield: 85%).

^{1}H NMR (400 MHz, CD_2Cl_2): δ (ppm) 7.63 (m 2H); 6.67 (d, *J* = 71.8 Hz, 2H); 6.48 (s, 2H); 4.31 (m, 1H); 3.72 (s, 4H); 2.18 (m, 2H); 1.86 (m, 2H); 1.41-0.92 (m, 24H); 0.85 (t, J = 7.0 Hz, 6H).

^{13}C NMR (101 MHz, CD_2Cl_2): δ (ppm) 144.68; 144.07; 143.89; 140.93; 119.87; 119.66; 108.08; 97.75; 94.97; 56.48; 33.72; 32.19; 29.87; 29.79; 29.61; 27.30; 23.00; 14.22.

FT-IR (ATR): ν= 2954, 2923, 2852, 1598, 1521, 1495, 1465, 1354, 1305, 1173, 1097, 1020, 895, 816, 766, 720, 662, 575, 554 cm^{-1}.

HRMS (EI+, m/z) [M]+ calculated (%) for $C_{29}H_{45}N_3$: 435.36135, found 435.36093

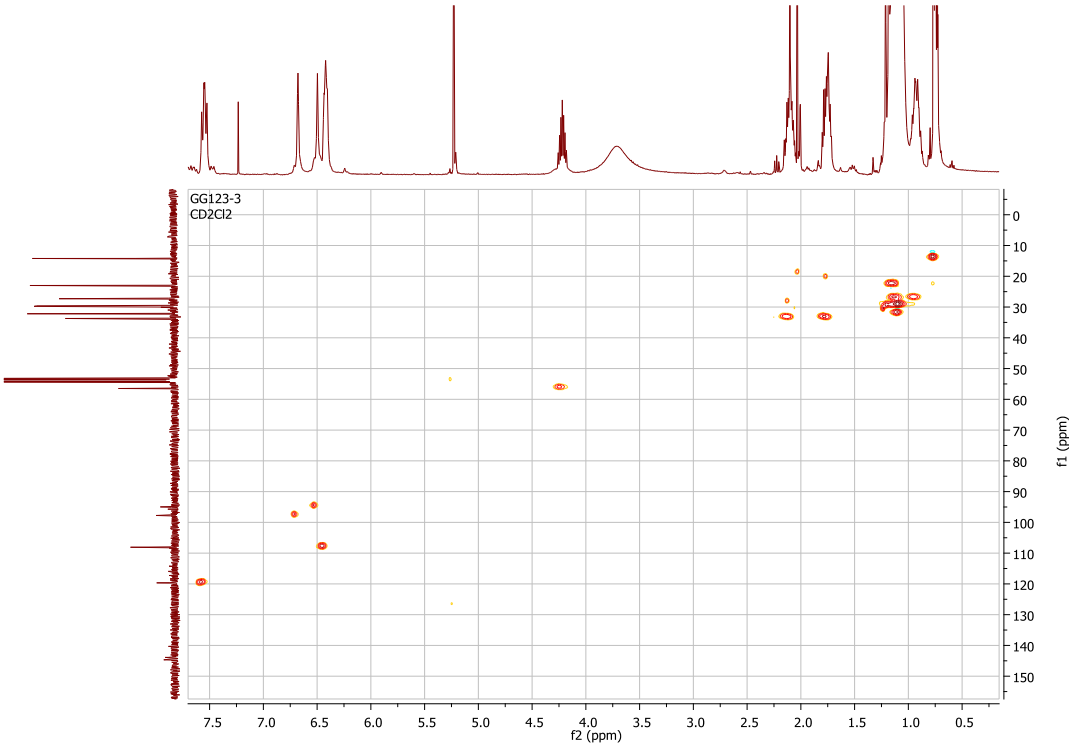

Figure 2-20: ^{1}H-^{13}C HSQC NMR spectrum of the 2,7-diaminocarbazole 8 (in CD_2Cl_2).

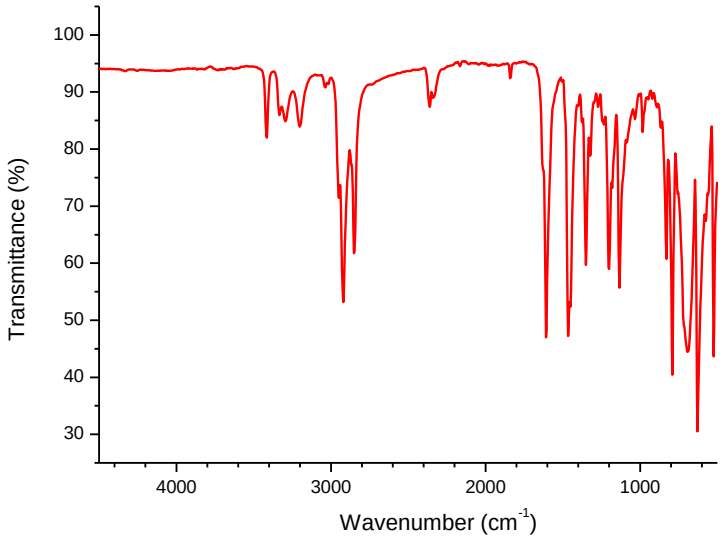

Figure 2-21: ATR-FTIR spectrum of the 2,7-diaminocarbazole 8.

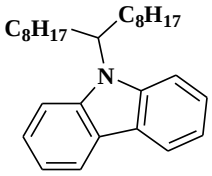

9-Heptadecanylcarbazole (9):

Carbazole (5g, 31 mmol) and potassium hydroxide (2.61 g, 46.5 mmol) were solubilized in dry DMSO (30 mL). The reaction mixture was heated at 80°C for one hour before adding dropwise a solution of 9-Heptadecane *p*-Toluenesulfonate (15.3 g, 37.2 mmol) in 60 mL of dry DMSO. After being allowed to cool down at room temperature, the reaction was poured into 300 mL of water and extracted three times with 100 mL of diethylether, dried over magnesium sulfate and the solvent was removed under vacuum. The white powder was purified by flash chromatography in cyclohexane to afford white crystals (yield: 85 %).
^{1}H NMR (400 MHz, CD_2Cl_2): δ (ppm) 8.10 (s, 2H); 7.59 (s, 1H); 7.43 (s, 3H); 7.20 (s, 2H), 4.59 (tt, J = 10.1, 5.0 Hz, 1H); 2.28 (m, 2H); 1.96 (m, 2H) 1.30-0.90 (m, 28H); 0.82 (t, J = 7.0 Hz, 6H).

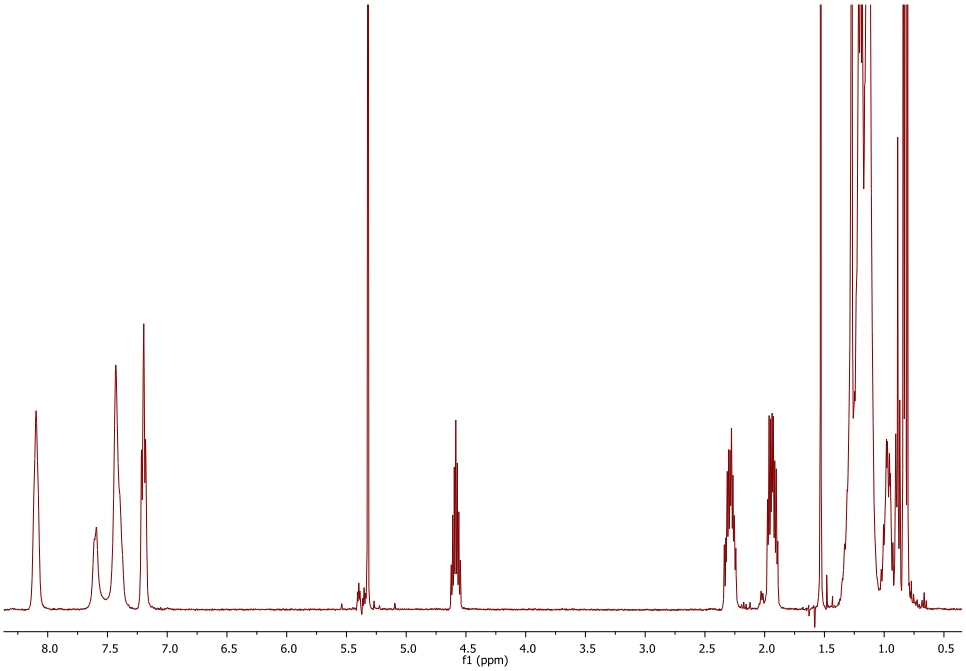

Figure 2-22: ^{1}H NMR (400 MHz) spectrum of the Heptadecanylcarbazole 9 (in CD_2Cl_2).

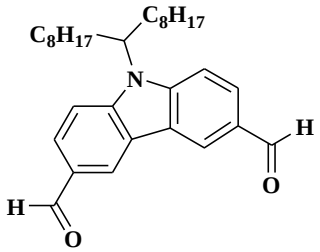

9-Heptadecanyl-3,6-diformylcarbazole (10):

In a 100 mL flask, 10 mL of DMF (130 mmol) was mixed with 12 mL of phosphoryl trichloride (125 mmol) at 0°C. In the same time, previously alkylated carbazole 1 (2 g, 4.9 mmol) was solubilized in 20 mL of methylene chloride. After warming up at room temperature, the carbazole solution was added to the mixture and the reaction has been heated at reflux temperature. After 65 hours the reaction mixture was allowed to cool down at room temperature, poured into water and extracted with methylene chloride. The crude product has then been purified with silica column chromatography in a mixture of cyclohexane/ethyl acetate (90/10) to afford a yellow powder (yield: 45 %).

^{1}H NMR (400 MHz, CD_2Cl_2, ppm): δ (ppm) 10.12 (s, 2H), 8.70 (d, J = 5.6 Hz, 2H), 8.03 (dd, *J* = 17.9, 8.4 Hz, 2H), 7.69 (dd, *J* = 68.2, 8.2 Hz, 1H), 4.68 (tt, *J* = 10.2, 5.1 Hz, 1H), 2.30 (m, 2H); 2.01 (m, 2H) 1.32-0.89 (m, 28H); 0.81 (t, J = 7.0 Hz, 6H).

^{13}C NMR (101 MHz, $CDCl_3$, ppm): δ (ppm) 192.41, 121.13, 113.17, 112.51, 110.54, 107.08, 103.32, 57.42, 33.78, 31.68, 29.25, 29.23, 29.04, 26.79, 22.54, 14.01.

FT-IR (ATR): ν= 2923, 2860, 1700, 1442, 1319, 1305, 1220, 1154, 1075, 945, 753, 620, 587 cm^{-1}.

HRMS (EI+, m/z) [M]+ calculated (%) for $C_{58}H_{86}Br_2N_2O_2$: 1000.5056, found 1000.5031

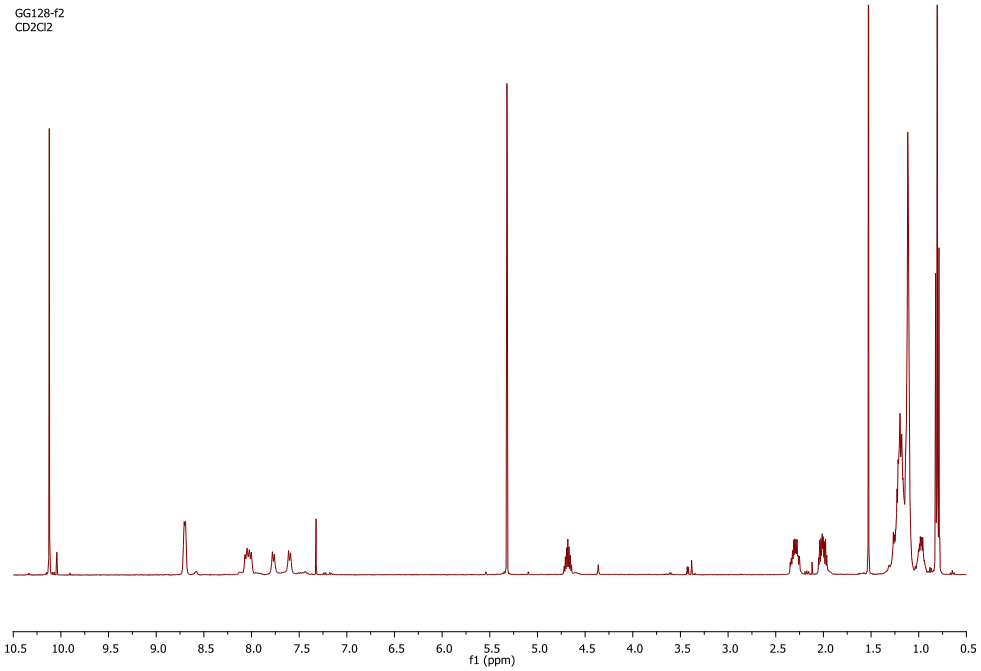

Figure 2-23: ^{1}H NMR (400 MHz) spectrum of the 9-Heptadecanyl-3,6-diformylcarbazole 10 (in CD_2Cl).

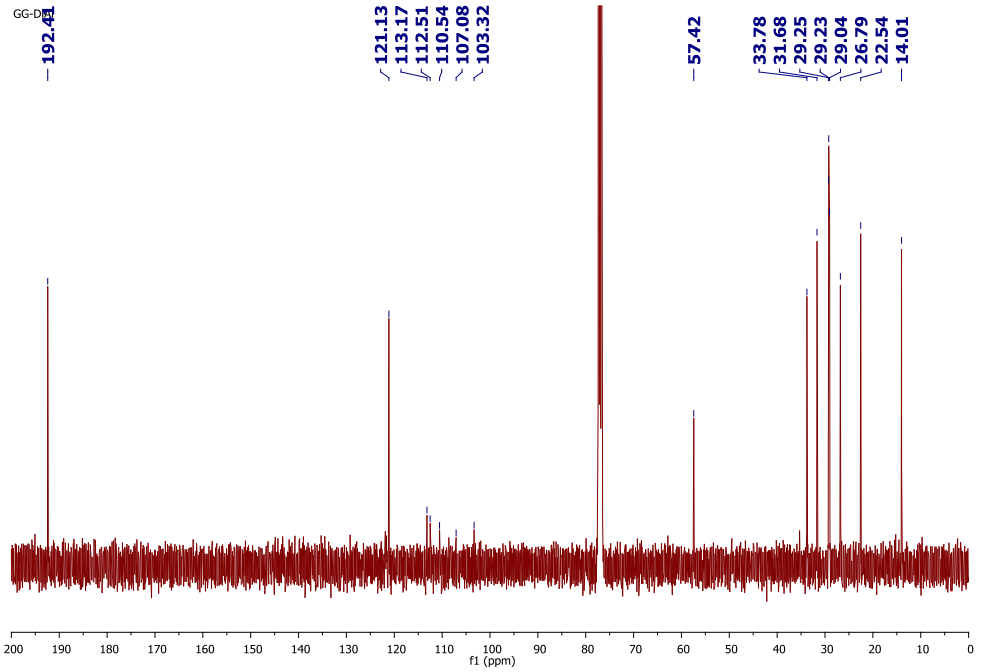

Figure 2-23bis: ^{13}C NMR (101 MHz) spectrum of the 9-Heptadecanyl-3,6-diformylcarbazole 10 (in $CDCl_3$).

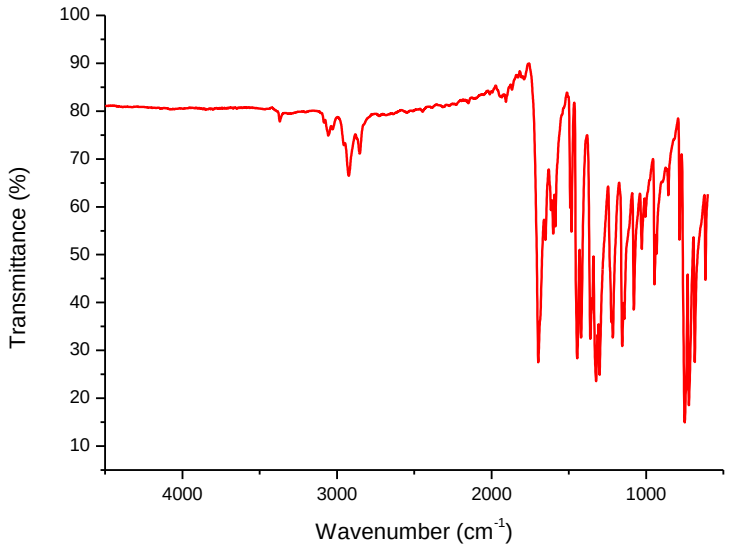

Figure 2-24: ATR-FTIR spectrum of the 3,6-diformylcarbazole 10.

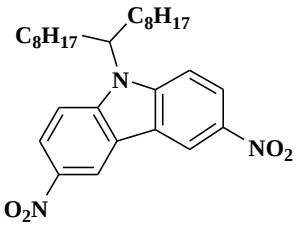

9-Heptadecanyl-3,6-dinitrocarbazole (11):

In a 50 mL flask, copper nitrate hemipentahydrate ($CuNO_3.H_2O$) (6.3 g, 27.1 mmol) was solubilised in a mixture of acetate anhydride (30 mL) and acetic acid (15 mL). Then 9-Heptadecanylcarbazole 1 (5 g, 12.3 mmol) was slowly added under vigorous stirring and was mixed during 3 hours at room temperature. The reaction mixture was then poured into 100 mL of cold water, filtered and washed with water. The powder was then purified by column chromatography in (cyclohexane/ethyl acetate - 9/1) to afford a yellow powder (yield: 62 %).

^{1}H NMR (400 MHz, CD_2Cl_2): δ (ppm) 9.10 (s, 2H); 8.42 (dd, *J* = 15.9, 8.6 Hz, 2H); 7.75 (d, J = 8.0 Hz, 2H), 7.62 (dd, *J* = 67.9, 9.2 Hz, 2H); 4.67 (tt, *J* = 10.2, 5.1 Hz, 1H); 2.26 (m, 2H); 2.02 (m, 2H) 1.32-0.91 (m, 28H); 0.79 (t, J = 7.0 Hz, 6H).

^{13}C NMR (101 MHz, CD_2Cl_2): δ (ppm) 146.91; 142.22; 123.38; 122.80; 118.09; 112.86; 110.48; 58.79; 34.09; 32.25; 29.75; 29.70; 29.58; 27.18; 23.12; 14.34.

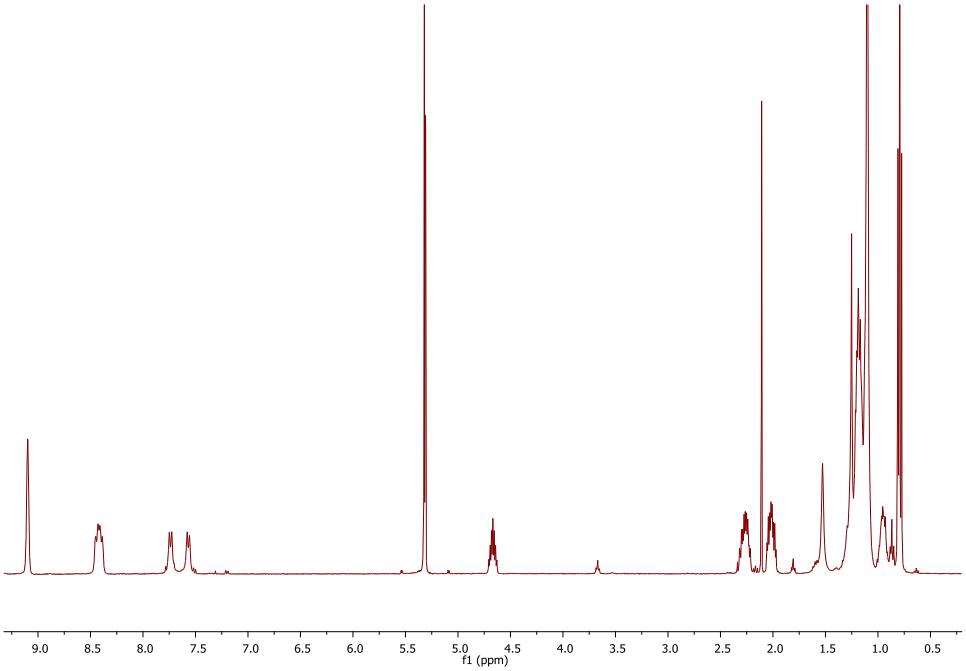

Figure 2-25: ^{1}H NMR (400 MHz) spectrum of the 9-Heptadecanyl-3,6-dinitrocarbazole 11 (in CD_2Cl_2).

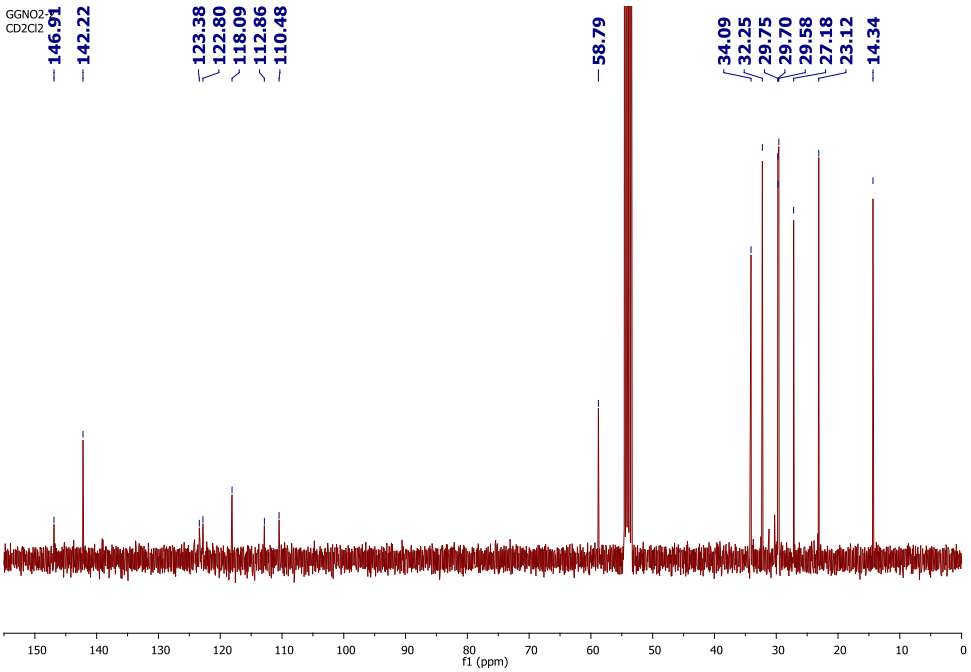

Figure 2-25bis: ^{13}C NMR (101 MHz) spectrum of the 9-Heptadecanyl-3,6-dinitrocarbazole 11 (in CD_2Cl_2).

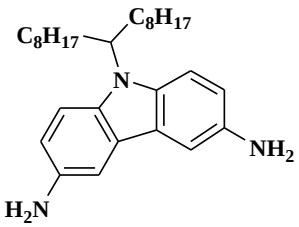

9-Heptadecanyl-3,6-diaminocarbazole (12):

In a 50 mL flask, 2.5 g of previously synthesized dinitrocarbazole 5 have been mixed with 107 mg of palladium on charcoal (1.0 mmol). Then 12 mL of ethanol was added and the reaction was heated at reflux temperature during one hour. 3.5 mL of hydrazine monohydrate (N_2H_4-H_2O) were then added to the reaction and heated at 55°C during 36 hours. After cooling down the reaction, the crude mixture was filtered and washed with ethanol. Finally, the filtrates have been dried and purified two times with silica column chromatography, first in toluene and then in a mixture of cyclohexane/ethyl acetate (95/5) to give a light brown compound (yield: 58 %).

^{1}H NMR (400 MHz, $CDCl_3$): δ (ppm) 7.29 (s, 3H), 7.16 (s, 1H), 6.87 (s, 2H), 4.37 (tt, J = 10.2, 5.1 Hz, 1H), 3.58 (s, 4H), 2.18 (m, 2H), 1.83 (m, 2H), 1.30-0.89 (m, 28H), 0.83 (t, J = 7.0 Hz 6H).

^{13}C NMR (101 MHz, $CDCl_3$, ppm): δ (ppm) 137.97, 129.18, 128.37, 115.77, 115.32, 109.45, 106.20, 56.26, 34.01, 31.91, 31.07, 29.57, 29.46, 29.32, 26.91, 22.73, 14.21.

FT-IR (ATR): ν= 3207, 2923, 2850, 1786, 1736, 1603, 1577, 1465, 1335, 1127, 807 cm^{-1}

HRMS (EI+, m/z) [M]+ calculated (%) for $C_{29}H_{45}N_3$: 435.36135, found 435.36181

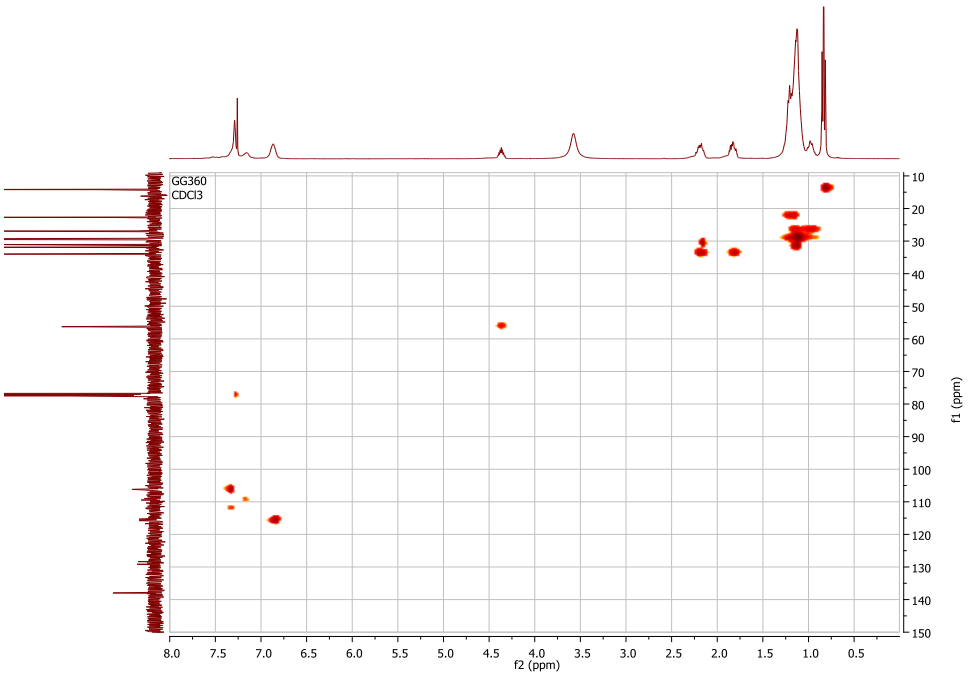

Figure 2-26: ^{1}H-^{13}C HSQC NMR spectrum of 9-Heptadecanyl-3,6-diaminocarbazole 12 (in $CDCl_3$).

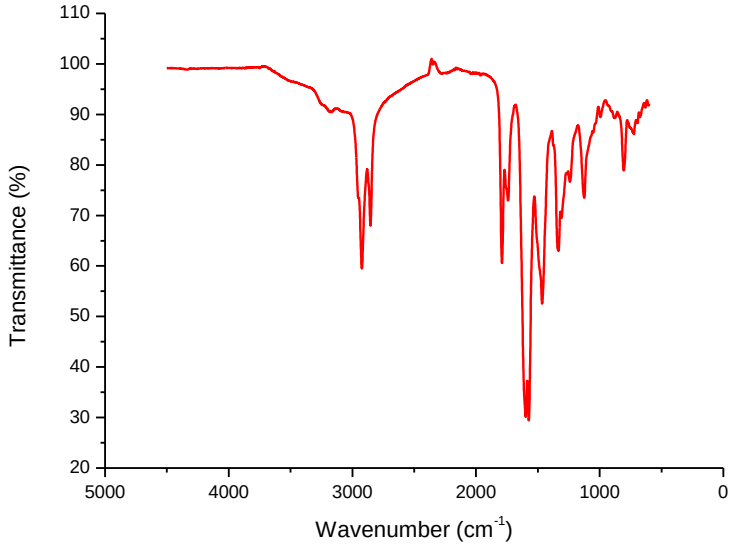

Figure 2-27: ATR-FTIR spectrum of the 3,6-diaminocarbazole 12.

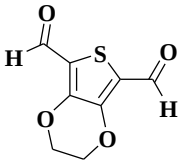

2,3-dihydrothieno[3,4-b][1,4]dioxine-5,7-dicarbaldehyde (13):

A solution of 3,4-ethylenedioxythiophene (1 g, 6.89 mmol) in dry THF (30 mL) was cooled to -78°C under argon and treated with 1.6 M solution of *n*-BuLi (9.5 mL). The temperature was slowly raised to 0 °C and the mixture was stirred at the same temperature for 20 minutes. The reaction mixture was cooled again to -78°C and treated with dry DMF (2 mL, 26 mmol). The resulting mixture was then stirred at r.t. for 2 hours and poured into crushed ice containing HCl. The white precipitate was filtered, washed with water, and dried (yield: 72 %).
^{1}H NMR (400 MHz, $CDCl_3$): δ (ppm) 10.04 (s, 2H), 4.44 (s, 4H);
^{13}C NMR (101 MHz, $CDCl_3$): δ (ppm) 181.09, 147.31, 124.30, 65.30.
HRMS (EI+, m/z) [M]+ calculated (%) for $C_8H_7O_4S$: 199.00650, found 199.00686

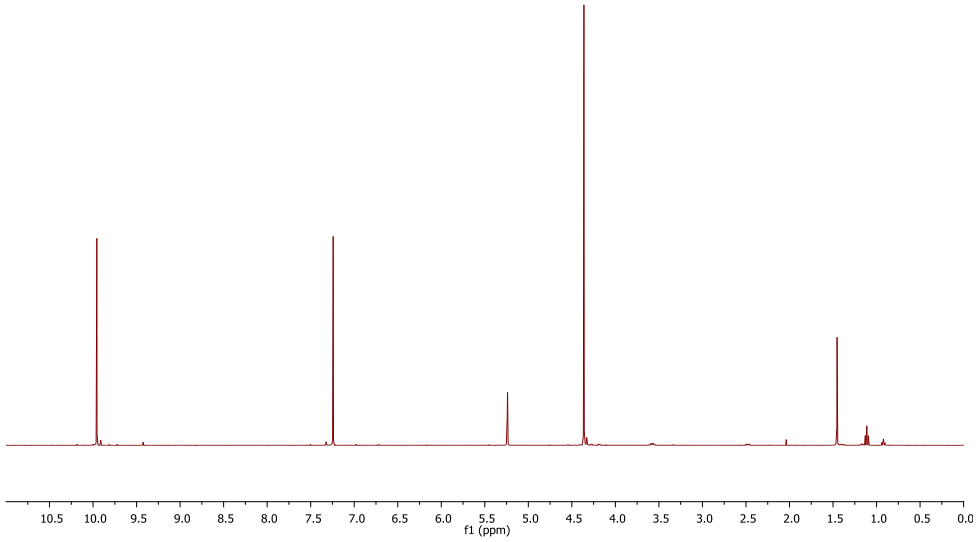

Figure 2-28: ^{1}H NMR (400 MHz) spectrum of the EDOT dialdehyde 13 (in $CDCl_3$, with CH_2Cl_2 and THF traces).

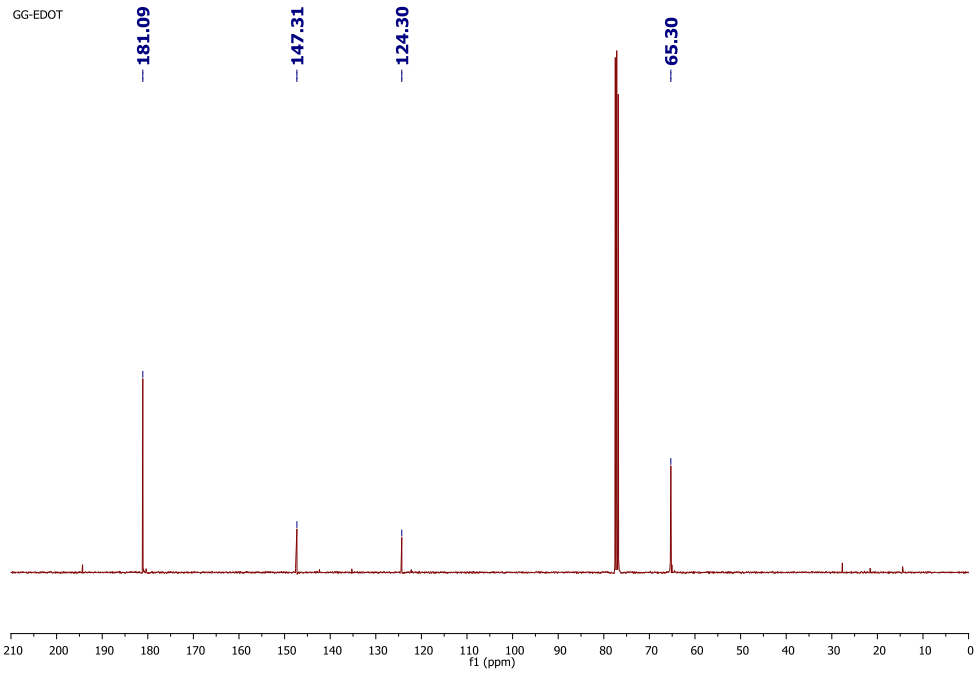

Figure 2-28bis: ^{13}C NMR (101 MHz) spectrum of the EDOT dialdehyde 13 (in $CDCl_3$, with ethyl acetate and heptane traces).

General procedure for polyazomethines synthesis

Diformylcarbazole and diaminocarbazole derivatives were dissolved in toluene (2 mL) in stoichiometric amounts. Silica (3 mg) was then added and the reaction mixture has been heated at 130°C under µ-wave radiation during 4 hours. The crude product was filtered and silica was washed with chloroform to recover the polymer. The crude polymer was then purified on Soxhlet apparatus with methanol and then chloroform. All four polymers are named depending of the position of the linkage on the carbazole moieties starting with the carbazole bearing the two nitrogen of the azomethine linkage. For example, the **(2,7-3,6Cbz)** has been synthesized in presence of the 2,7 diaminocarbazole **8** with the 3,6 diformylcarbazole **10**.

For the statistic co-polymers, the 2,7 diaminocarbazole **12** (1 equivalent) was dissolved in toluene in presence of 2,7 diformylcarbazole **6** and EDOT dialdehyde **13** in different proportions. However, the total amount of aldehyde functions was kept equal to the amount of amino functions (for example for the polymer **2,7-EDOT-75**, 1 eq of diamino carbazole **12** was reacted in presence of 0.25 equivalent of **6** and 0.75 equivalent of the EDOT derivative **13**). In this case for all of them their name is "**2,7-EDOT-EDOT percentage**". In the previous example, the polymer synthesized is called **2,7-EDOT-75**.

Poly(2,7-diimino-N-dodecylcarbazole-*alt*-2,7-N-dodecylcarbazole) (2,7-2,7Cbz)

^{1}H NMR (400 MHz, $CDCl_3$): δ (ppm) 9.00 – 6.55 (m, 14H), 4.75 (s, 1H), 4.59 (s, 1H), 2.36 (s, 4H), 1.98 (s, 4H), 1.48-0.91 (m, 48H), 0.81 (m, 12H).

FT-IR (ATR): ν= 3411 (N-H stretch), 2913 (CH_2 asymmetric stretch), 2858 (CH_2 symmetric stretch), 1691 (CH=O stretch), 1590 (CH=N stretch), 1458 (C=C stretch) cm^{-1}

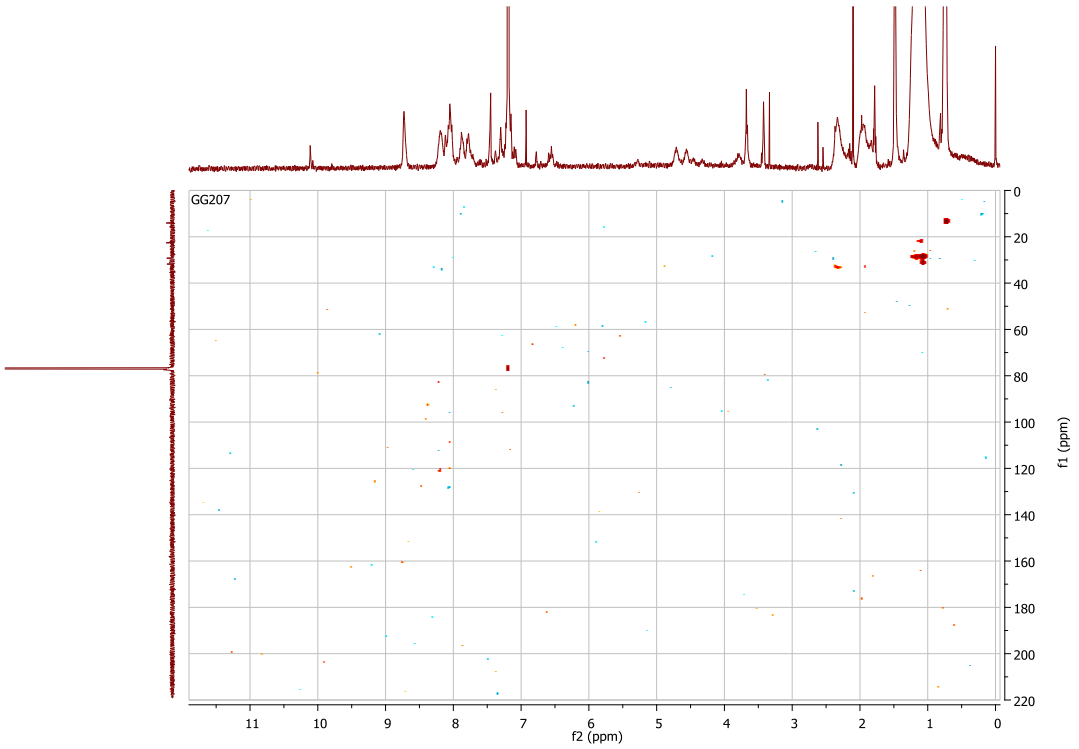

Figure 2-29: ^{1}H-^{13}C HSQC NMR spectrum of the 2,7-2,7Cbz (in $CDCl_3$).

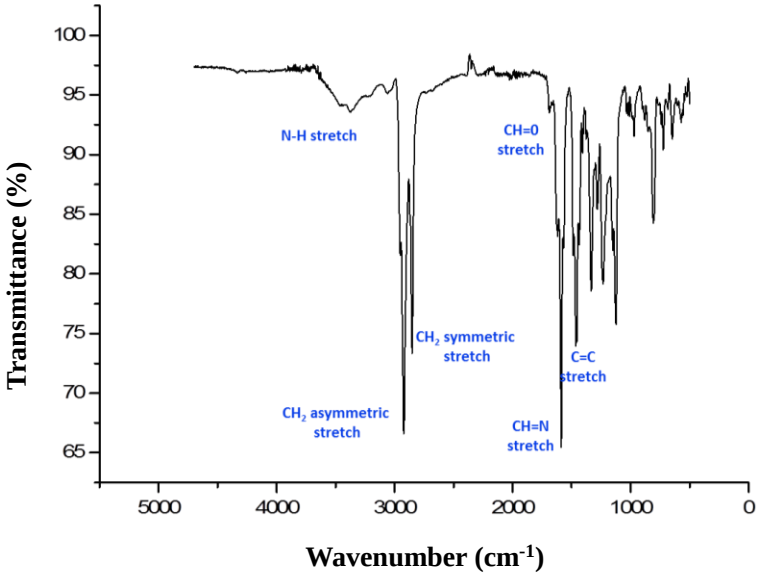

Figure 2-30: ATR-FTIR spectrum of the 2,7-2,7Cbz.

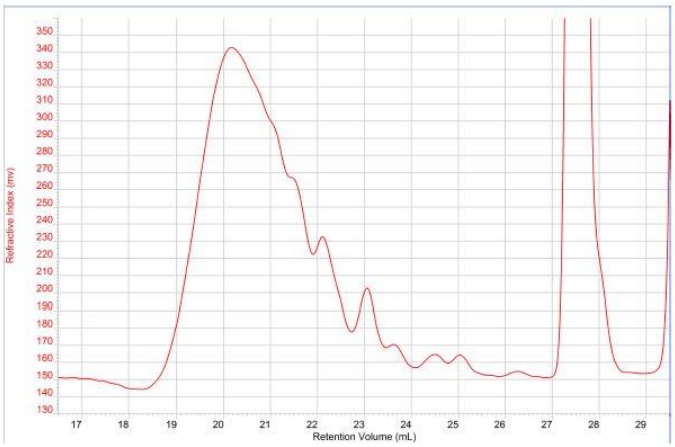

Peak	Mn	Mw	Mz	Mp	Mw/Mn	Ret Vol
1	3 602	10 479	18 218	13 002	2.909	20.153

Figure 2-31: SEC trace of the 2,7-2,7Cbz (in $CHCl_3$, polystyrene standard).

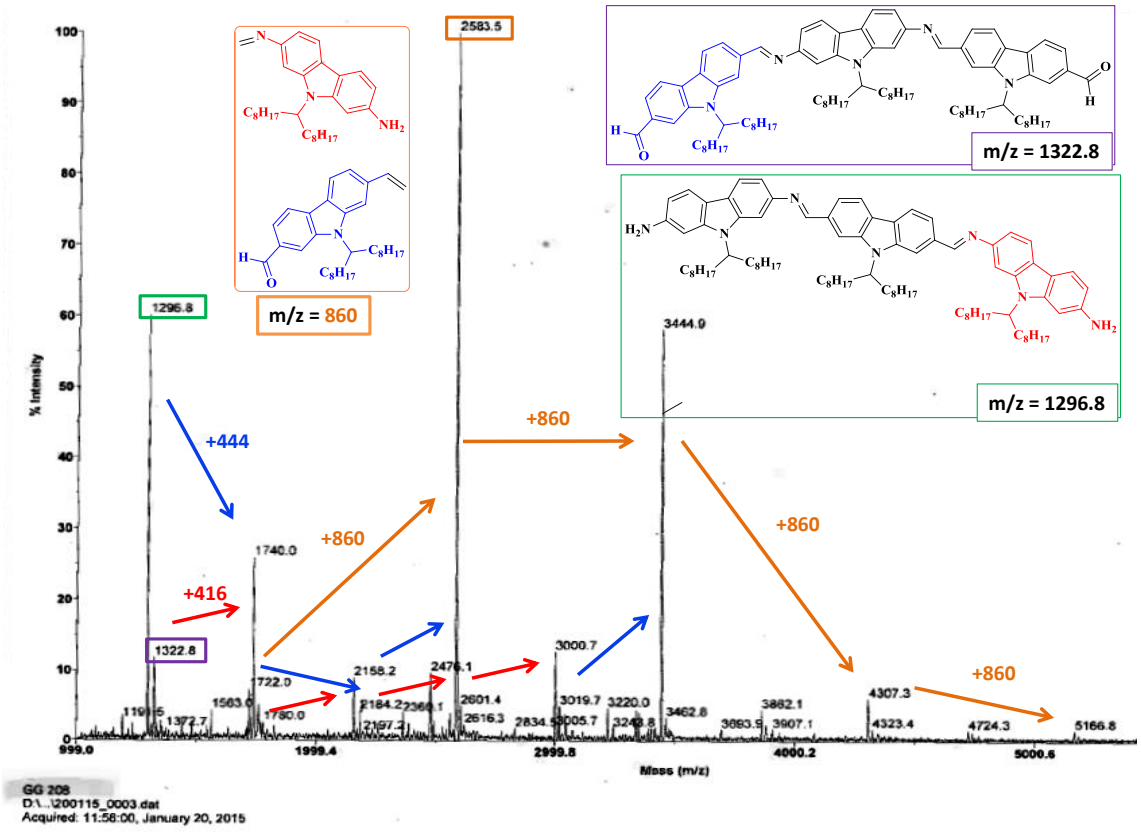

Figure 2-32: Mass spectra of the 2,7-2,7Cbz (EI).

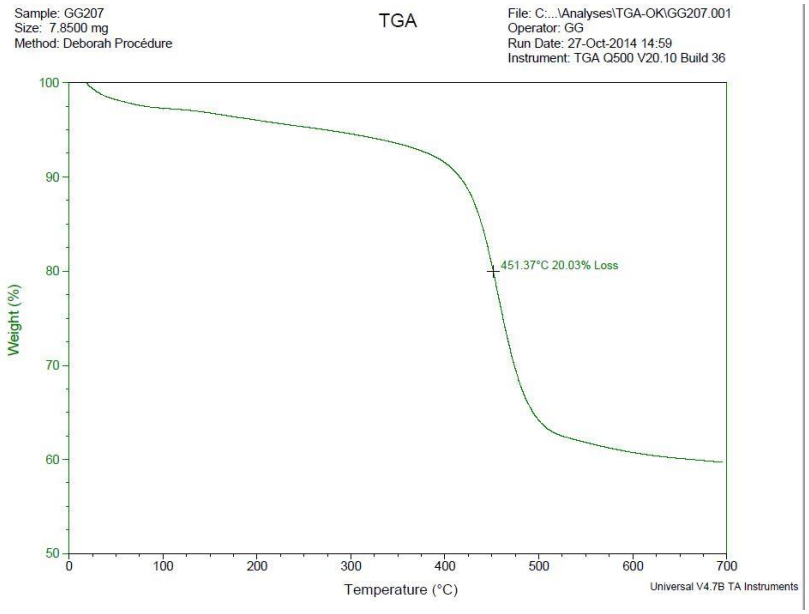

Figure 2-33: TGA trace of the 2,7-2,7Cbz (at a scan rate of 10°C per minute).

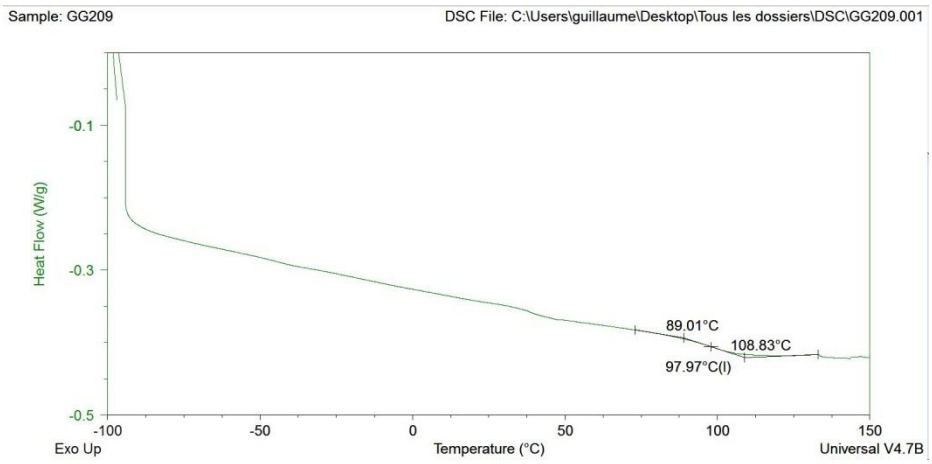

Figure 2-34: DSC trace of the 2,7-2,7Cbz (at a scan rate of 10°C per minute).

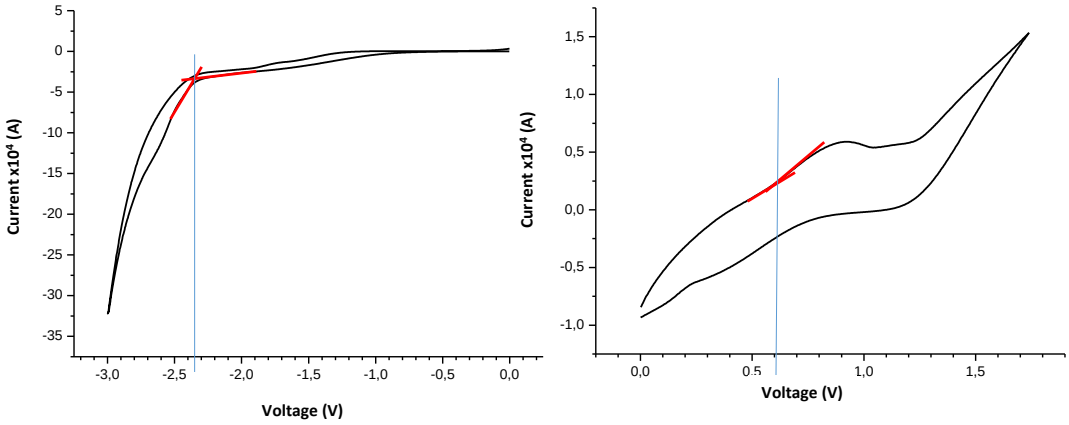

Figure 2-35: Cyclic voltammograms (left-reduction, right-oxidation) of 2,7-2,7Cbz in CH_2Cl_2 solution (0.1 $g.l^{-1}$) with $TBAPF_6$ as electrolyte.

Poly(2,7-diimino-N-dodecylcarbazole-*alt*-3,6-N-dodecylcarbazole) (2,7-3,6Cbz)

^{1}H NMR (400 MHz, $CDCl_3$): δ (ppm) 8.69-6.51 (m, 14H), 4.65 (s, 1H), 4.37 (s, 1H), 2.36 (s, 4H), 1.99 (s, 4H), 1.37-0.92 (m, 48H), 0.92 (m, 12H).
FT-IR (ATR): ν= 3370 (N-H stretch), 2925 (CH_2 asymmetric stretch), 2850 (CH_2 symmetric stretch), 1690 (CH=O stretch), 1590 (CH=N stretch), 1470 (C=C stretch) cm^{-1}

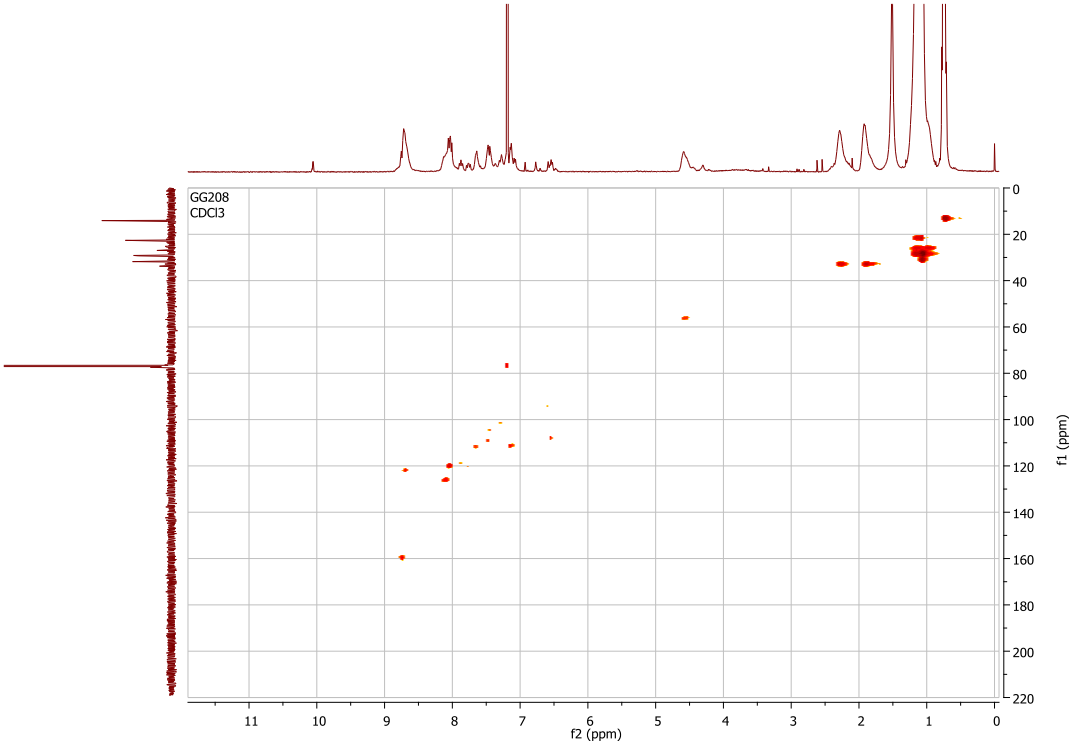

Figure 2-36: ^{1}H-^{13}C HSQC NMR spectrum of the 2,7-3,6Cbz (in $CDCl_3$).

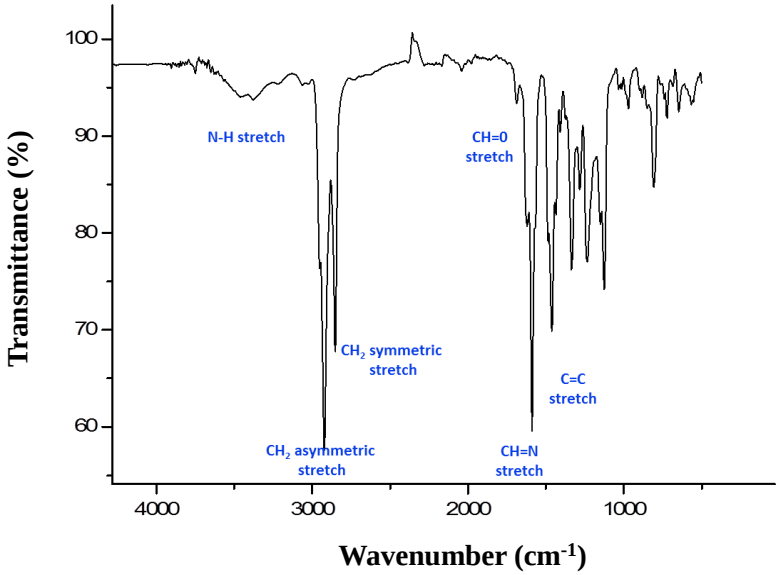

Figure 2-37: ATR-FTIR spectrum of the 2,7-3,6Cbz.

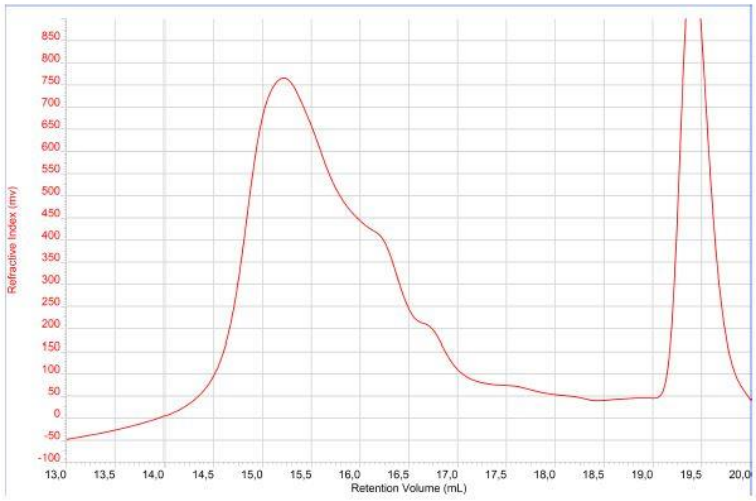

Peak	Mn	Mw	Mz	Mp	Mw/Mn	Ret Vol
1	3 660	13 708	23 401	18 037	3.745	15.210

Figure 2-38: SEC trace of the 2,7-3,6Cbz (in $CHCl_3$, polystyrene standard).

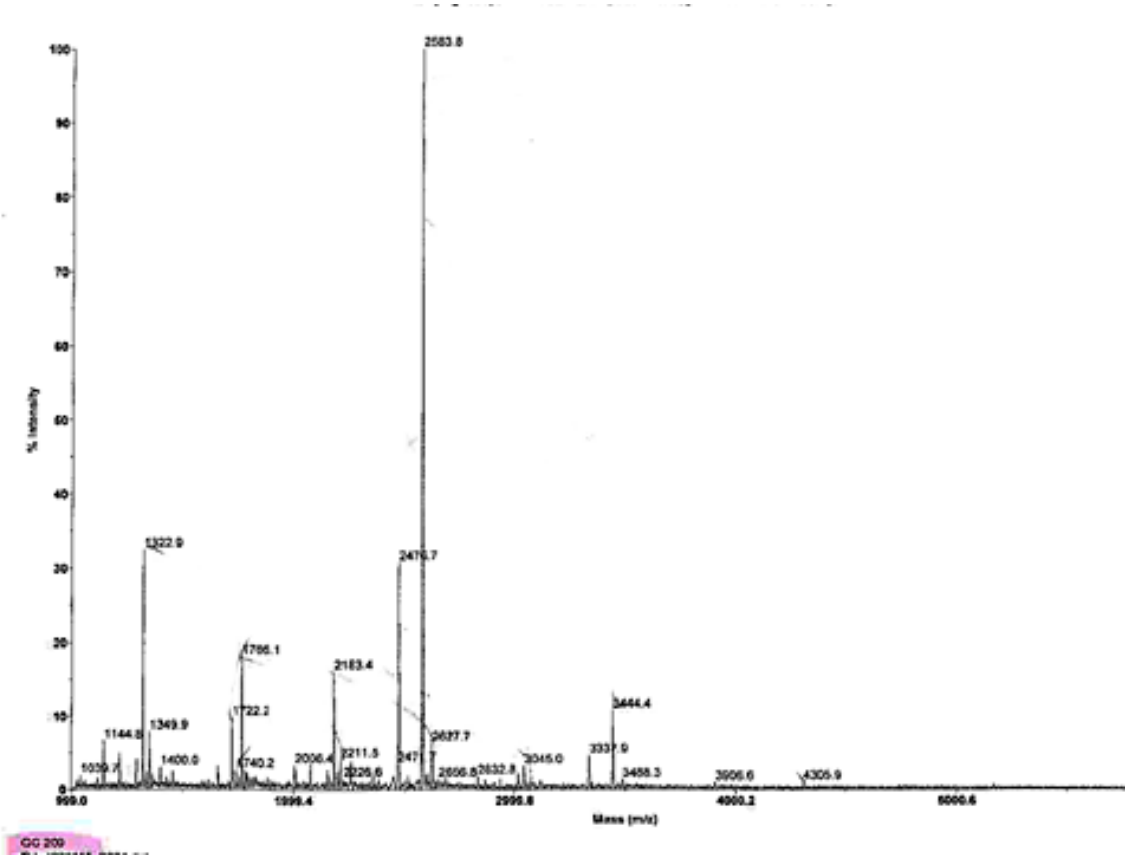

Figure 2-39: Mass spectra of the 2,7-3,6Cbz (EI).

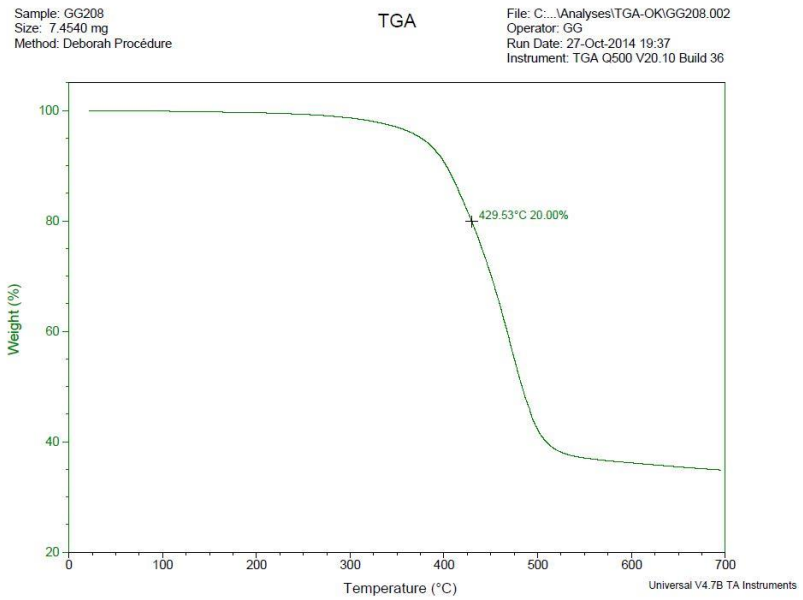

Figure 2-40: TGA trace of the 2,7-3,6Cbz (at a scan rate of 10°C per minute).

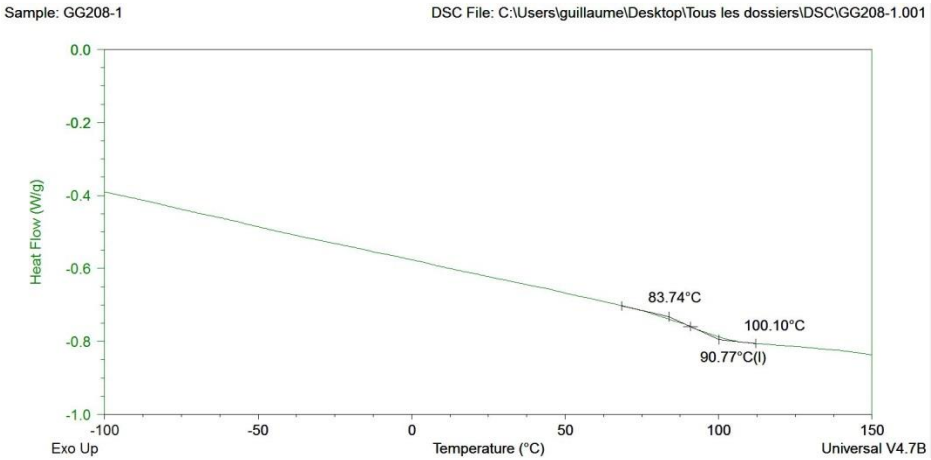

Figure 2-41: DSC trace of the 2,7-3,6Cbz (at a scan rate of 10°C per minute).

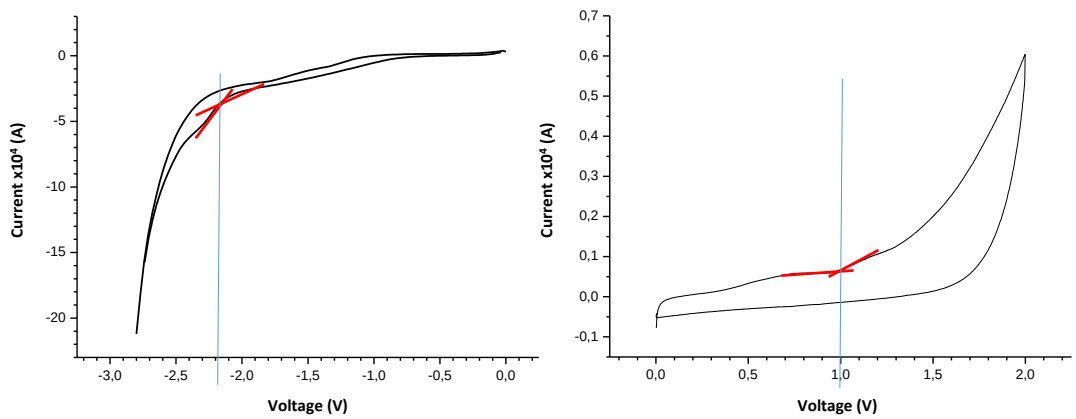

Figure 2-40: Cyclic voltammograms (left-reduction, right-oxidation) of 2,7-3,6Cbz in CH_2Cl_2 solution (0.1 g.l^{-1}) with $TBAPF_6$ as electrolyte.

Poly(3,6-diimino-N-dodecylcarbazole-*alt*-3,6-N-dodecylcarbazole) (3,6-3,6Cbz)

^{1}H NMR (400 MHz, $CDCl_3$): δ (ppm) 9.00–7.20 (m, 14H), 4.72-4.53 (m, 2H), 2.34 (s, 4H), 1.98 (s, 4H), 1.35-0.92 (m, 48H), 0.83 (m, 12H).

FT-IR (ATR): ν= 3393 (N-H stretch), 2931 (CH_2 asymmetric stretch), 2848 (CH_2 symmetric stretch), 1694 (CH=O stretch), 1582 (CH=N stretch), 1458 (C=C stretch) cm^{-1}

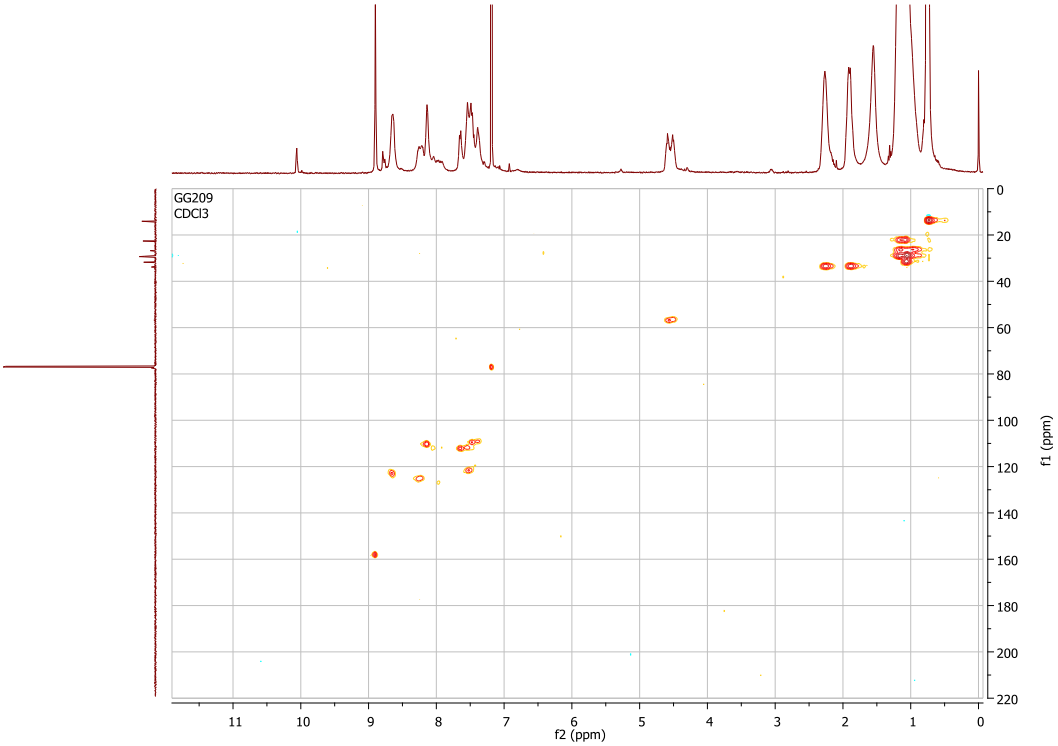

Figure 2-43: ^{1}H-^{13}C HSQC NMR spectrum of the 3,6-3,6Cbz (in $CDCl_3$).

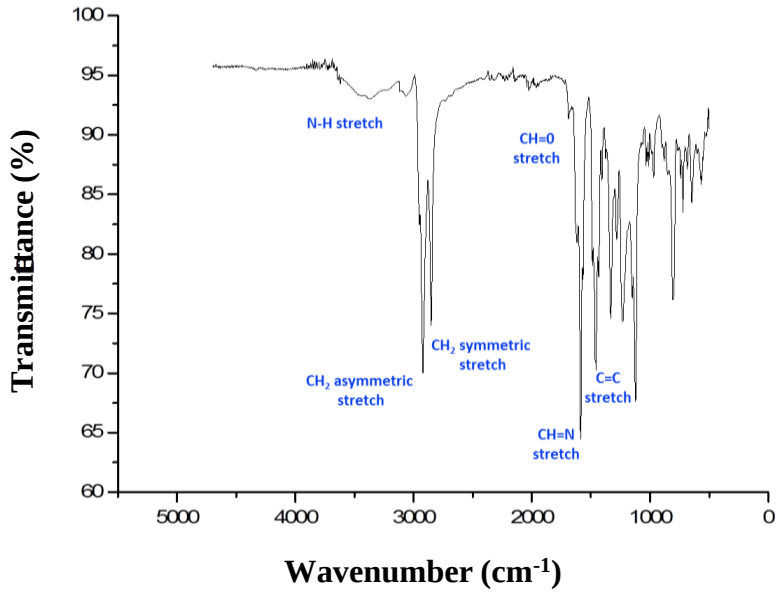

Figure 2-44: ATR-FTIR spectrum of the 3,6-3,6Cbz.

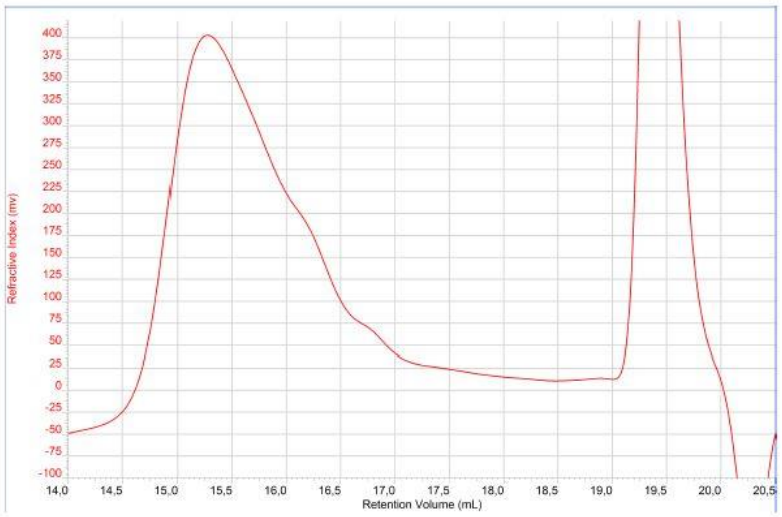

Peak	Mn	Mw	Mz	Mp	Mw/Mn	Ret Vol
1	3 686	11 688	17 124	16 989	3.171	15.263

Figure 2-45: SEC trace of the 3,6-3,6Cbz (in $CHCl_3$, polystyrene standard).

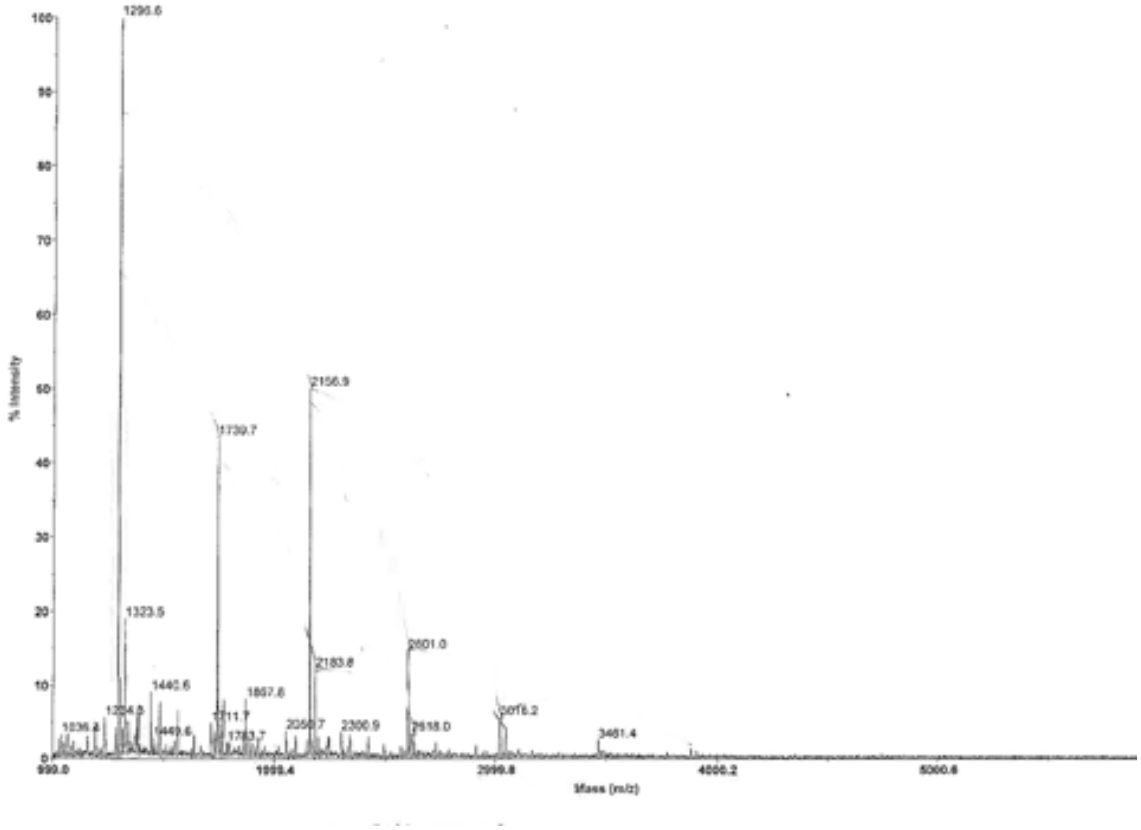

Figure 2-46: Mass spectra of the 3,6-3,6Cbz (EI).

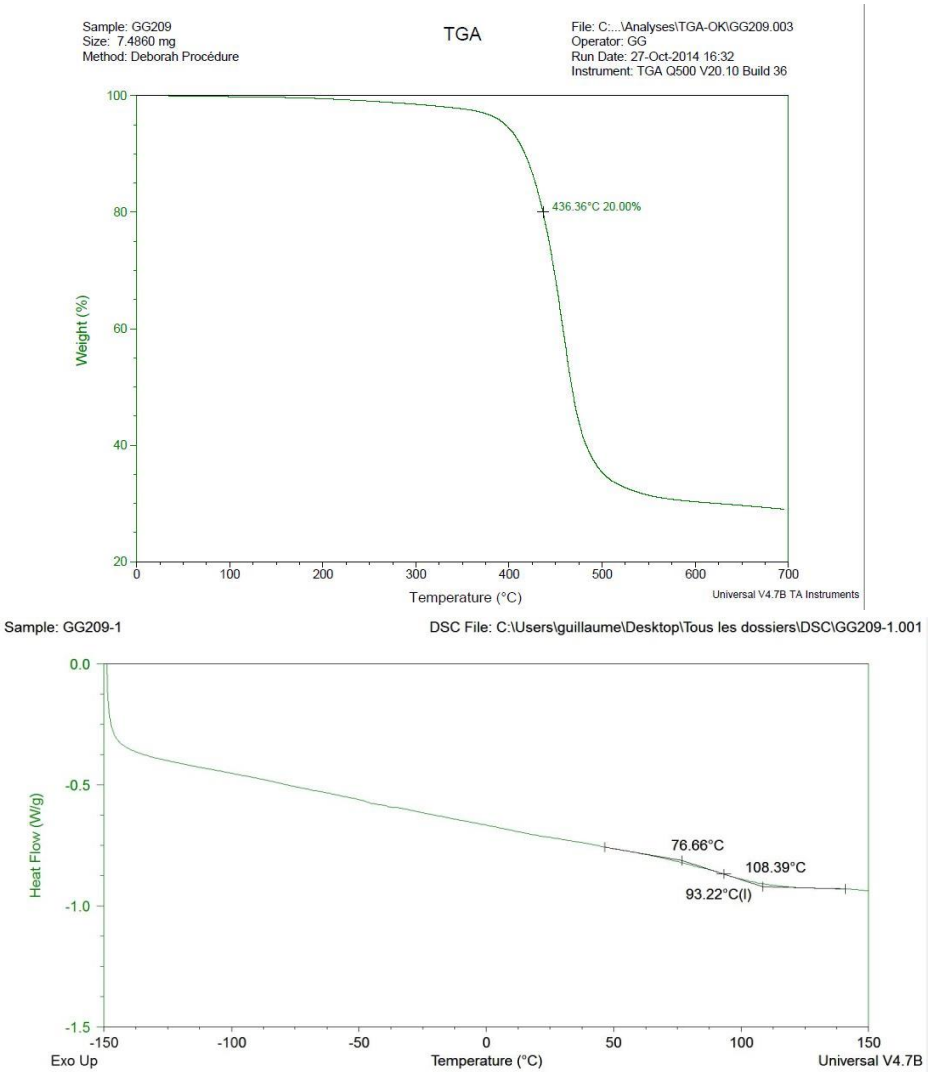

Figure 2-47: TGA (top) and DSC (bottom) traces of the 3,6-3,6Cbz (at a scan rate of 10°C per minute).

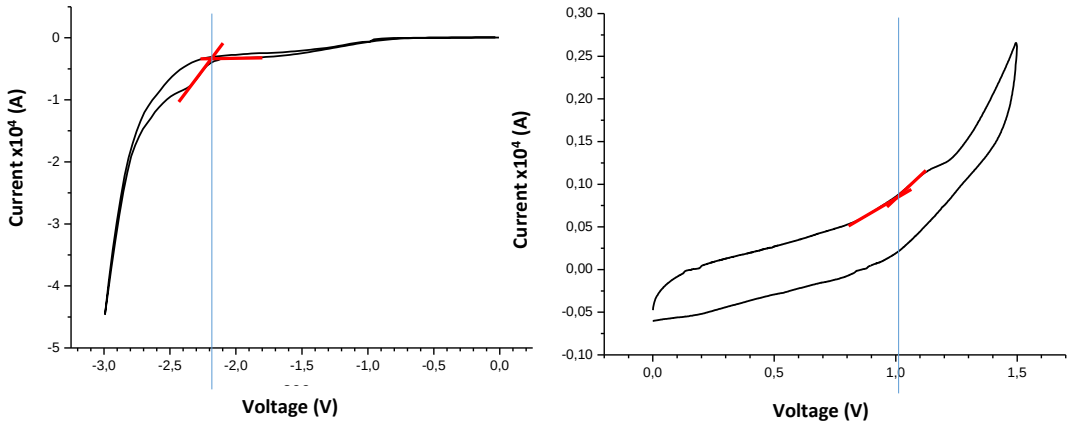

Figure 2-48: Cyclic voltammograms (left-reduction, right-oxidation) of 3,6-3,6Cbz in CH_2Cl_2 solution (0.1 g.l^{-1}) with $TBAPF_6$ as electrolyte.

Poly(3,6-diimino-N-dodecylcarbazole-*alt*-2,7-N-dodecylcarbazole) (3,6-2,7Cbz)

^{1}H NMR (400 MHz, $CDCl_3$): δ (ppm) 8.69-6.51 (m, 14H), 4.65 (s, 1H), 4.37 (s, 1H), 2.36 (s, 4H), 1.99 (s, 4H), 1.37-0.92 (m, 48H), 0.92 (m, 12H).

FT-IR (ATR): ν= 341 (N-H stretch), 2923 (CH_2 asymmetric stretch), 2849 (CH_2 symmetric stretch), 1688 (CH=O stretch), 1610 (CH=N stretch), 1463 (C=C stretch) cm^{-1}

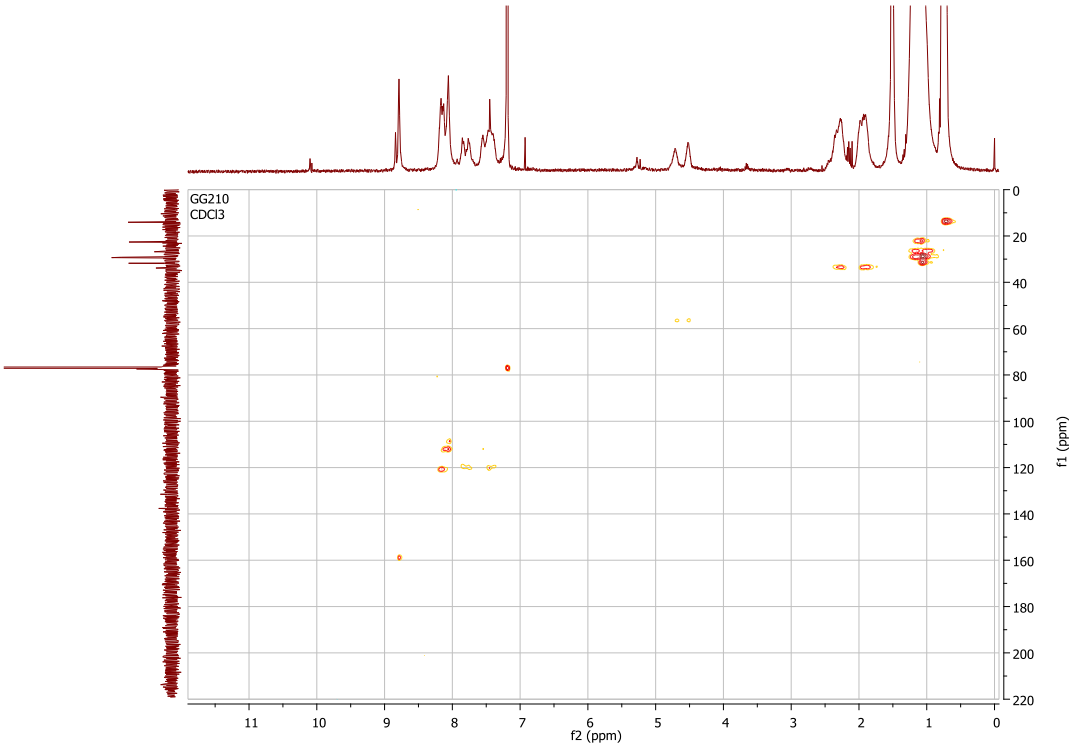

Figure 2-49: ^{1}H-^{13}C HSQC NMR spectrum of the 3,6-2,7Cbz (in $CDCl_3$).

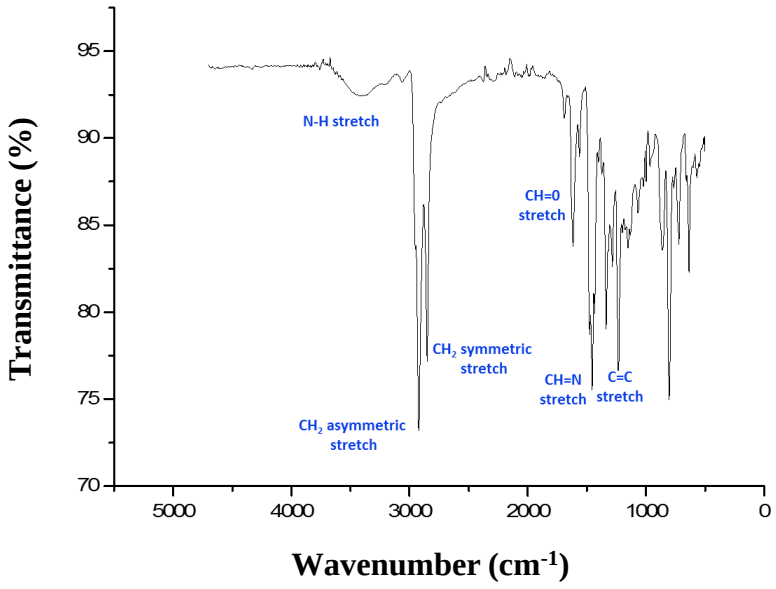

Figure 2-50: ATR-FTIR spectrum of the 3,6-2,7Cbz.

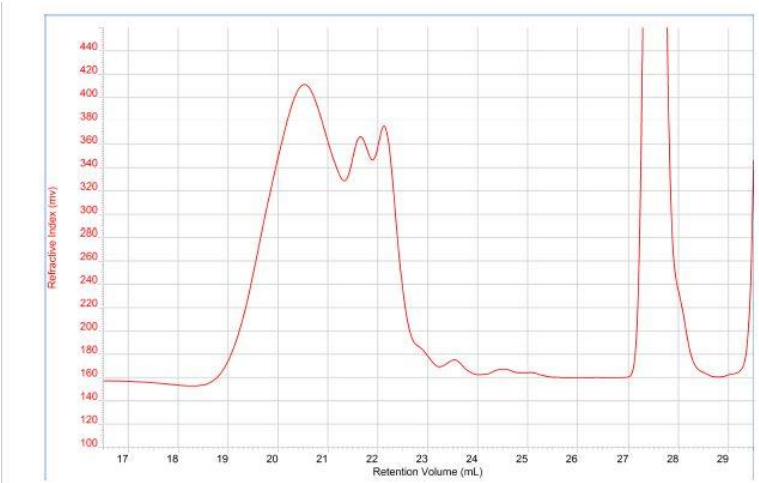

Peak	Mn	Mw	Mz	Mp	Mw/Mn	Ret Vol
1	3 499	10 044	18 372	11 116	2.871	20.520

Figure 2-51: SEC trace of the 3,6-2,7Cbz (in $CHCl_3$, polystyrene standard).

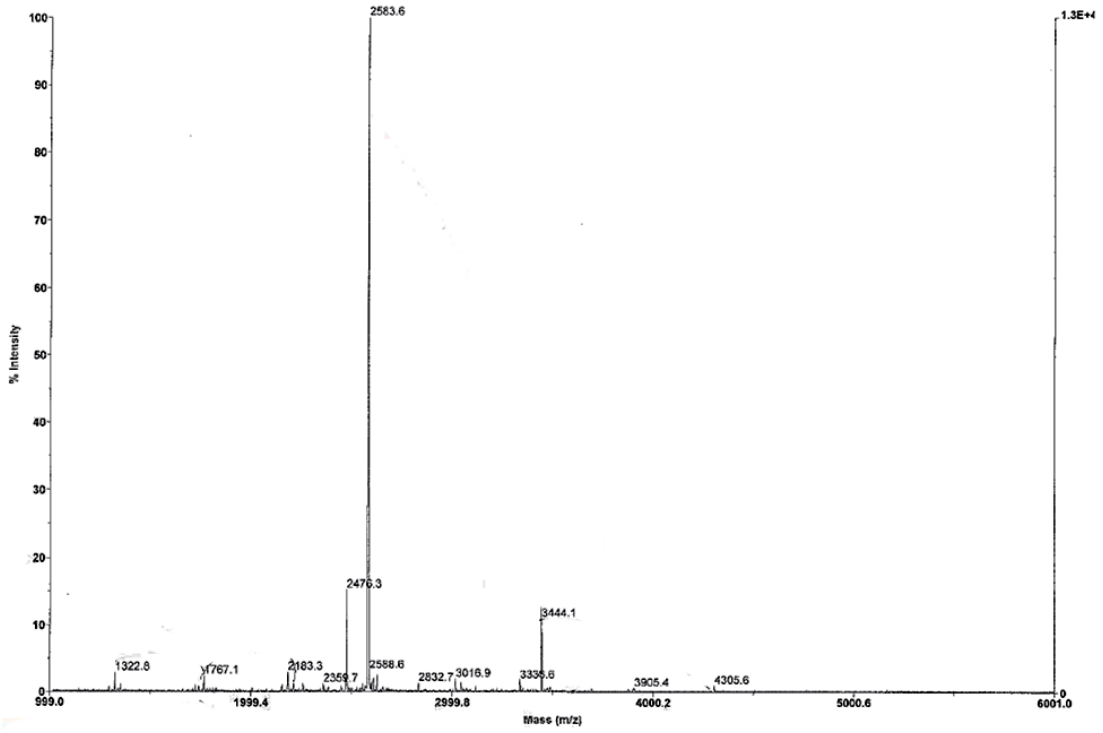

Figure 2-52: Mass spectra of the 3,6-2,7Cbz (EI).

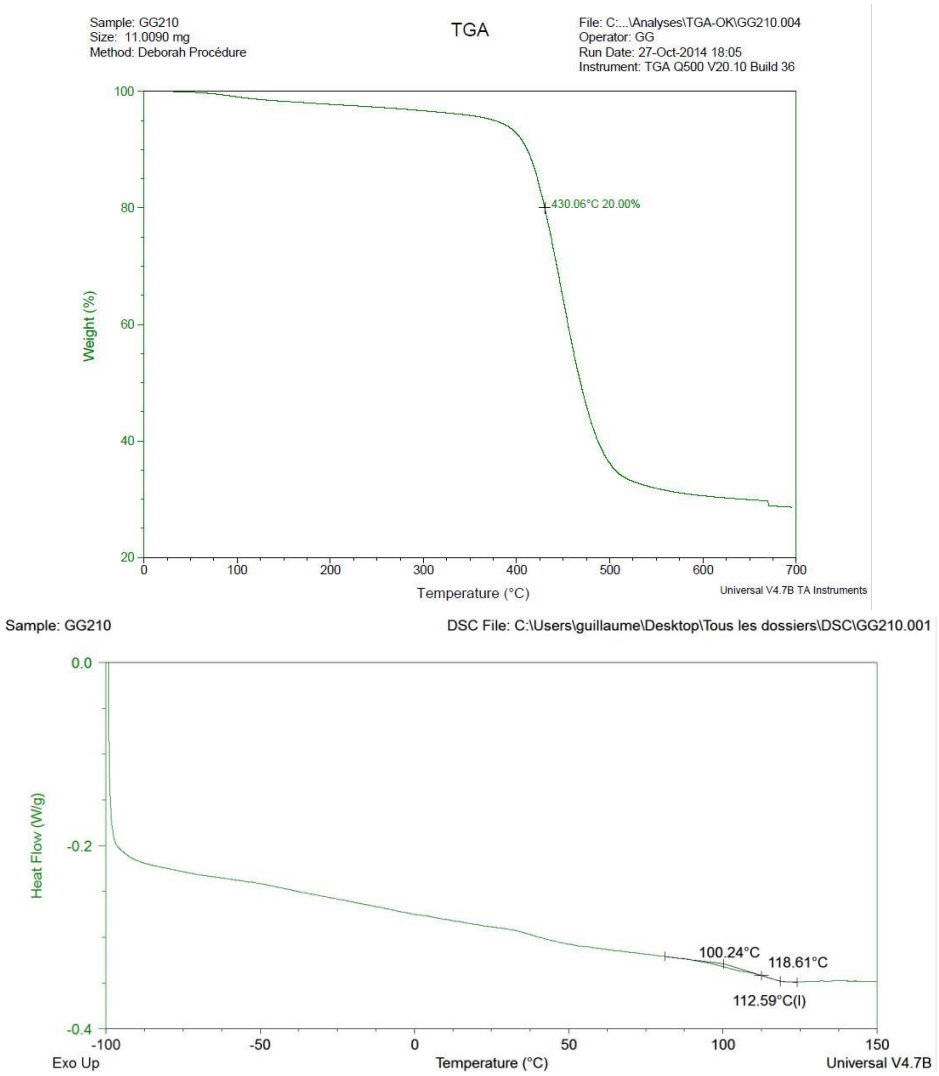

Figure 2-53: TGA (top) and DSC (bottom) traces of the 3,6-2,7Cbz (at a scan rate of 10°C per minute).

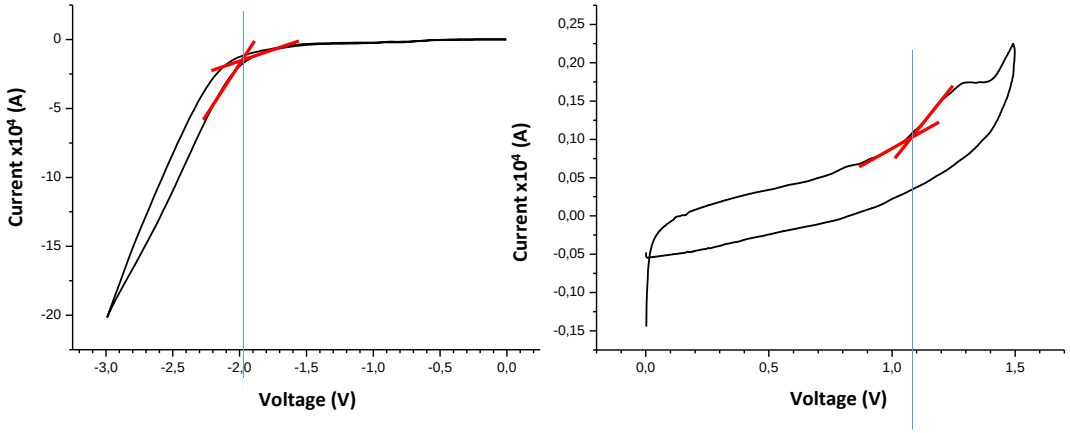

Figure 2-54: Cyclic voltammograms (left-reduction, right-oxidation) of 3,6-2,7Cbz in CH_2Cl_2 solution (0.1 $g.l^{-1}$) with $TBAPF_6$ as electrolyte.

Poly(2,7-diimino-N-dodecylcarbazole-*alt*-2,7-N-dodecylcarbazole-ran-2,7-diimino-N-dodecylcarbazole-*alt*-3,4-ethylenedioxythiophene) (2,7-EDOT-"EDOT percentage")

The ^{1}H NMR and FT-IR shift can be slightly moved depending of the amount of EDOT inserted. For ^{1}H NMR the only difference between them is the integration of the four EDOT protons around 4.45 ppm. For example, for the (**2,7-EDOT-50**):

^{1}H NMR (400 MHz, $CDCl_3$): δ (ppm) 8.79 (s, 2H) 9.05-7.30 (m, 6H), 7.23-6.52 (m, 2H), 4.57 (s, 1H), 4.44 (s, 2H), 2.32 (m, 2H), 2.96 (m, 2H), 1.36-1.00 (m, 24H), 0.83 (t, 6H).

FT-IR (ATR): ν= 2917 (CH_2 asymmetric stretch), 2852 (CH_2 symmetric stretch), 1697 (CH=O stretch), 1575 (CH=N stretch), 1459 (C=C stretch) cm^{-1}

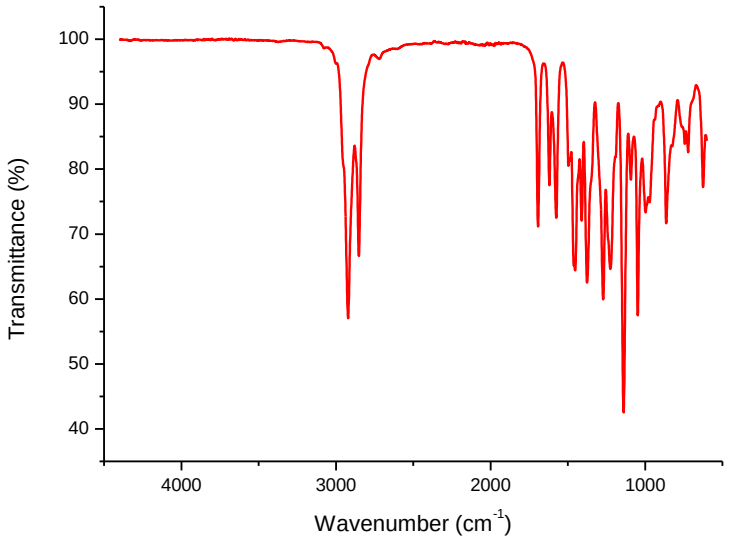

Figure 2-55: General ATR-FTIR spectrum of the 2,7-EDOT-X.

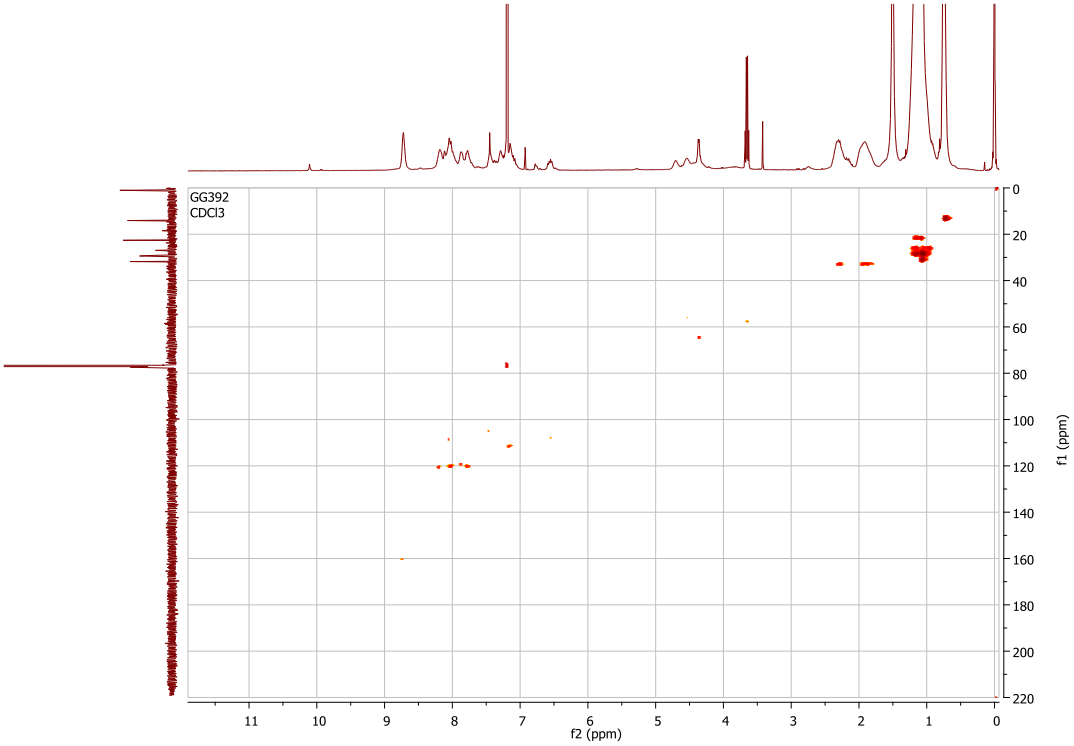

Figure 2-56: ^{1}H-^{13}C HSQC NMR spectrum of the 2,7-EDOT-25 (in $CDCl_3$).

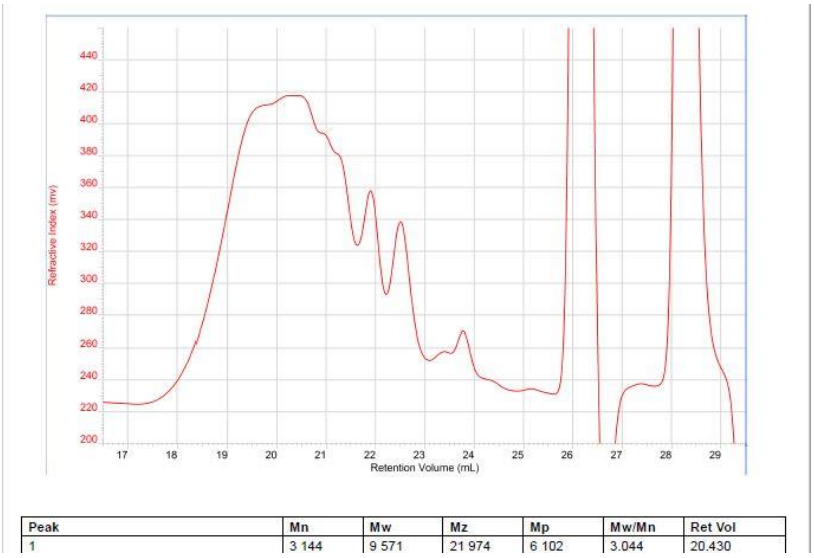

Peak	Mn	Mw	Mz	Mp	Mw/Mn	Ret Vol
1	3 144	9 571	21 974	6 102	3.044	20.430

Figure 2-57: SEC trace of the 2,7-EDOT-25 (in $CHCl_3$, polystyrene standard).

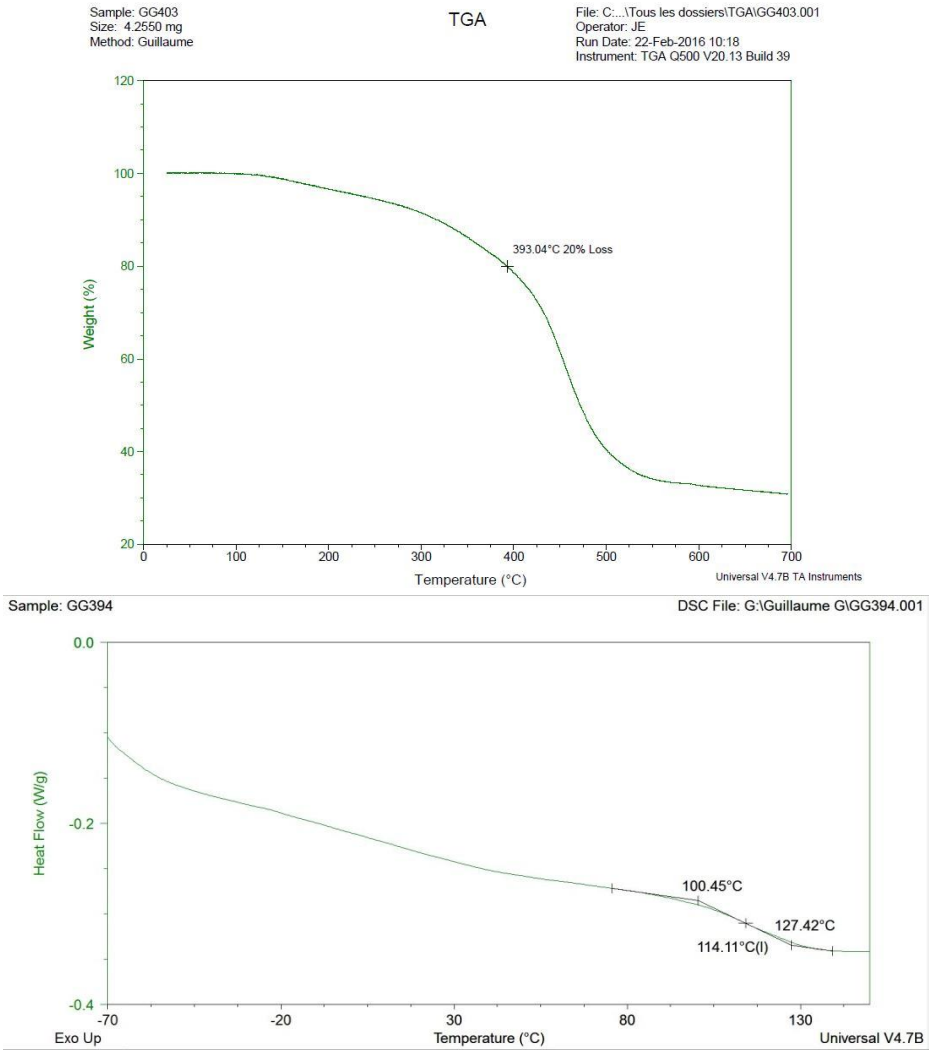

Figure 2-58: TGA (top) and DSC (bottom) traces of the 2,7-EDOT-25 (at a scan rate of 10°C per minute).

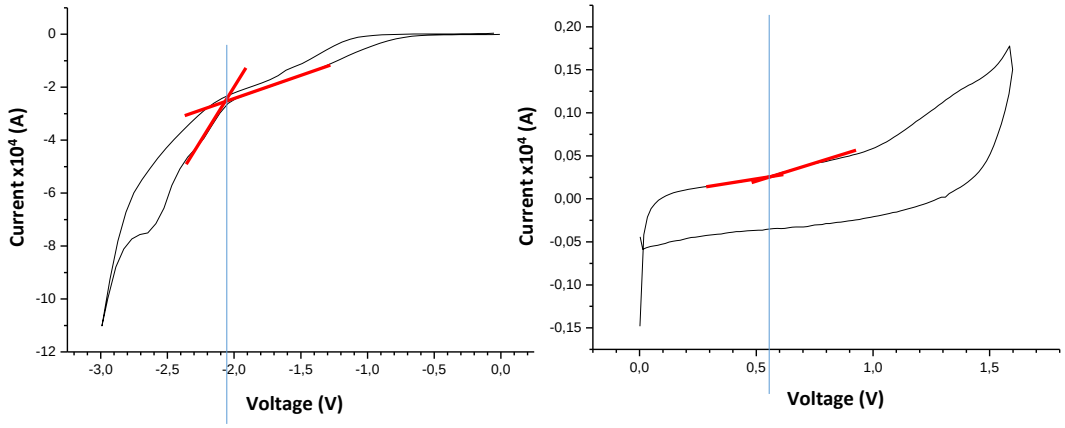

Figure 2-59: Cyclic voltammograms (left-reduction, right-oxidation) of 2,7-EDOT-25 in CH_2Cl_2 solution (0.1 $g.l^{-1}$) with $TBAPF_6$ as electrolyte.

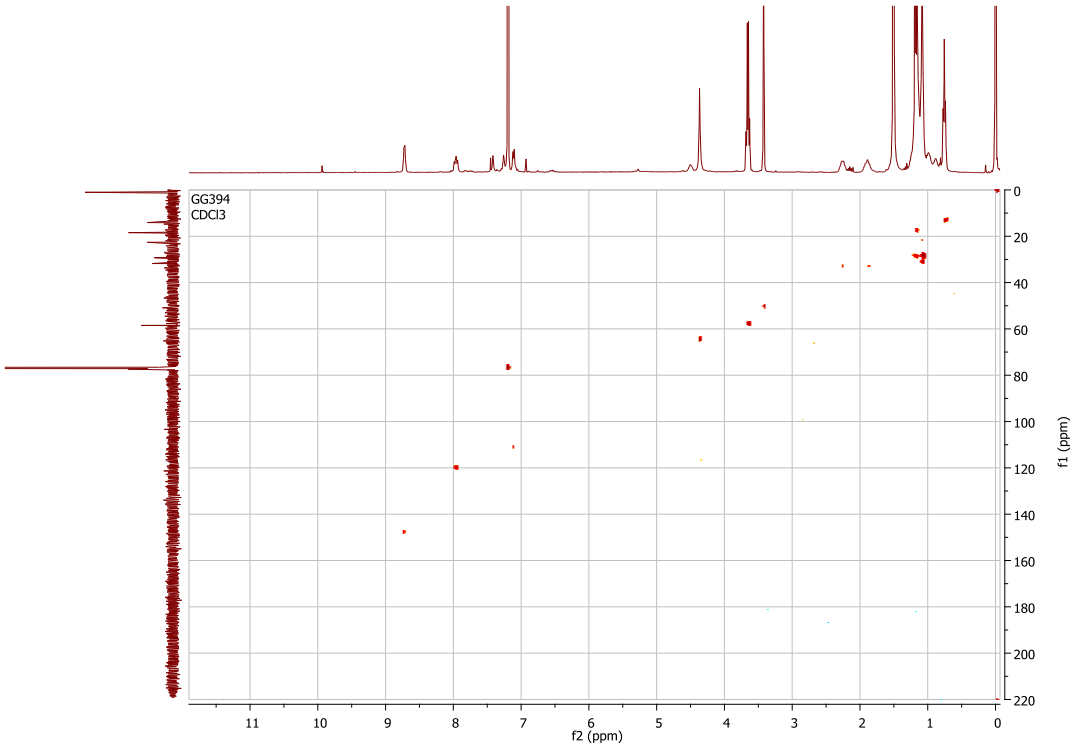

Figure 2-60: ^{1}H-^{13}C HSQC NMR spectrum of the 2,7-EDOT-50 (in $CDCl_3$).

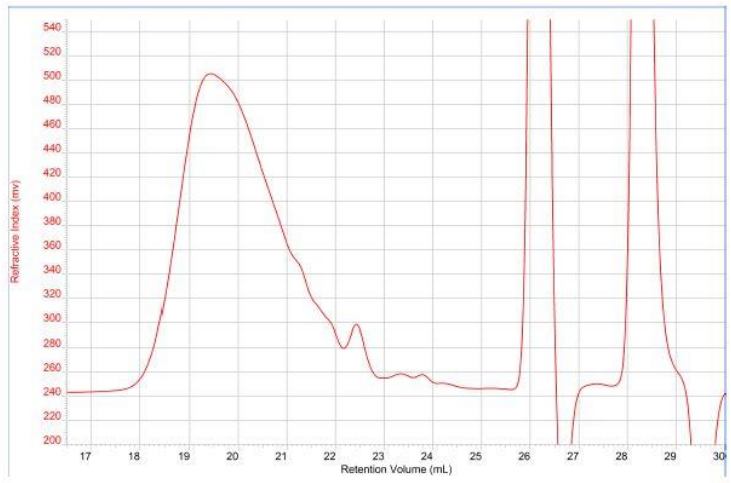

Peak	Mn	Mw	Mz	Mp	Mw/Mn	Ret Vol
1	4 214	10 085	17 349	12 281	2.393	19.417

Figure 2-61: SEC trace of the 2,7-EDOT-50 (in $CHCl_3$, polystyrene standard).

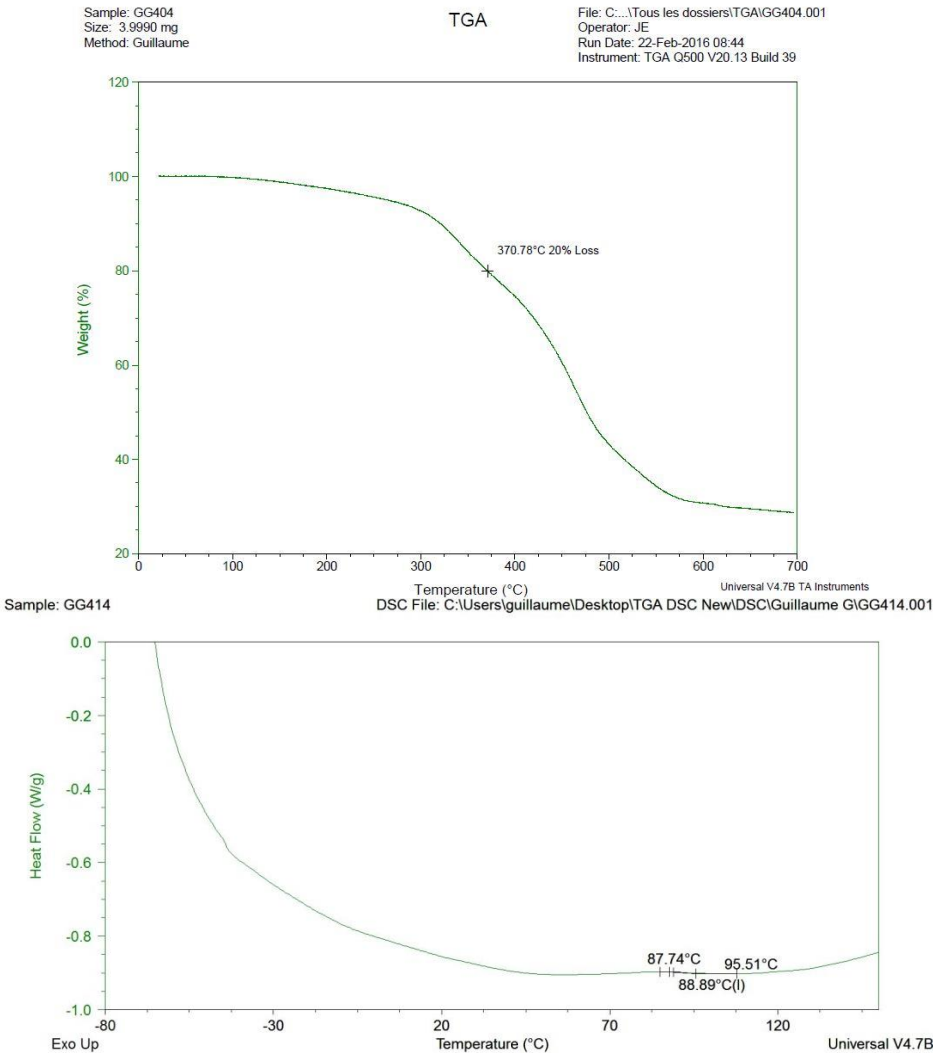

Figure 2-62: TGA (top) and DSC (bottom) traces of the 2,7-EDOT-50 (at a scan rate of 10°C per minute).

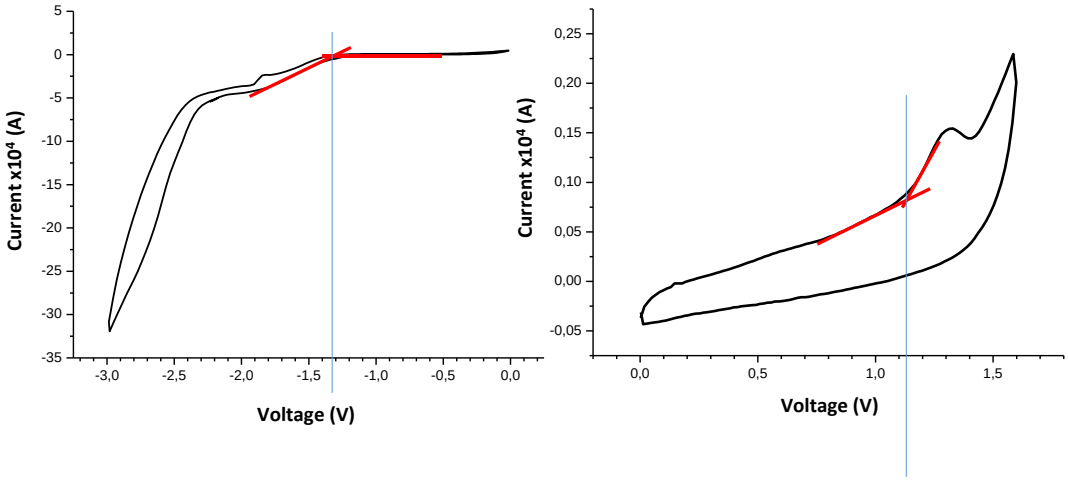

Figure 2-63: Cyclic voltammograms (left-reduction, right-oxidation) of 2,7-EDOT-50 in CH_2Cl_2 solution (0.1 $g.l^{-1}$) with $TBAPF_6$ as electrolyte.

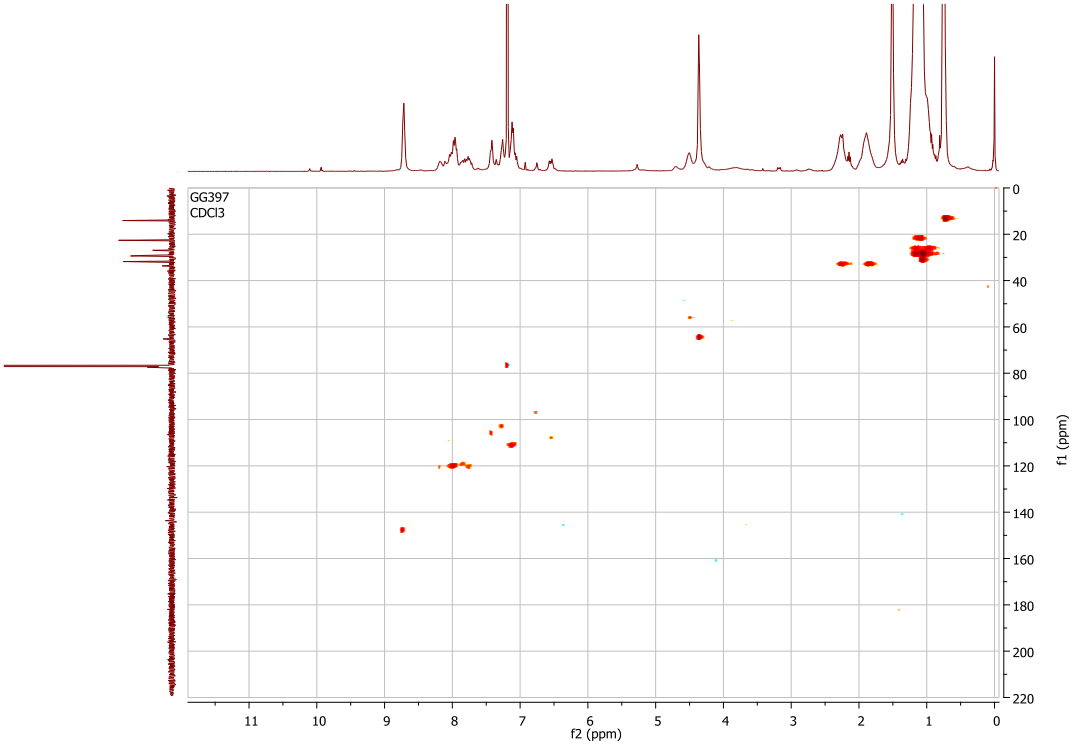

Figure 2-64: ^{1}H-^{13}C HSQC NMR spectrum of the 2,7-EDOT-75 (in $CDCl_3$).

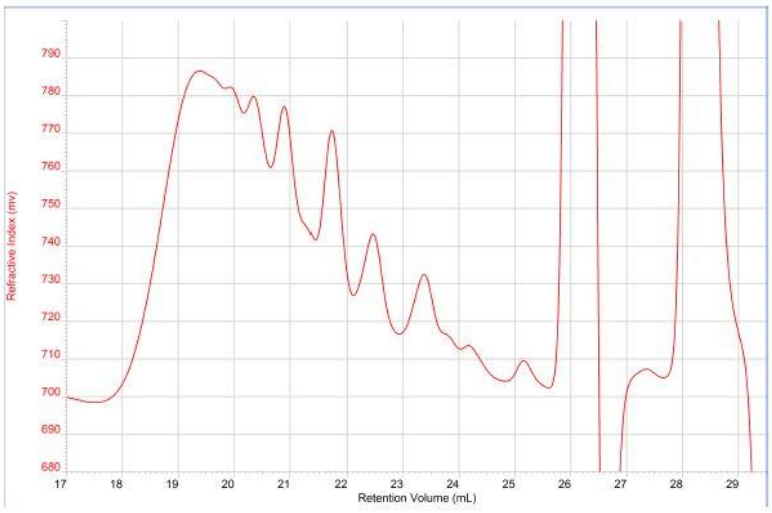

Peak	Mn	Mw	Mz	Mp	Mw/Mn	Ret Vol
1	2 487	7 936	15 904	12 412	3.190	19.383

Figure 2-65: SEC trace of the 2,7-EDOT-75 (in $CHCl_3$, polystyrene standard).

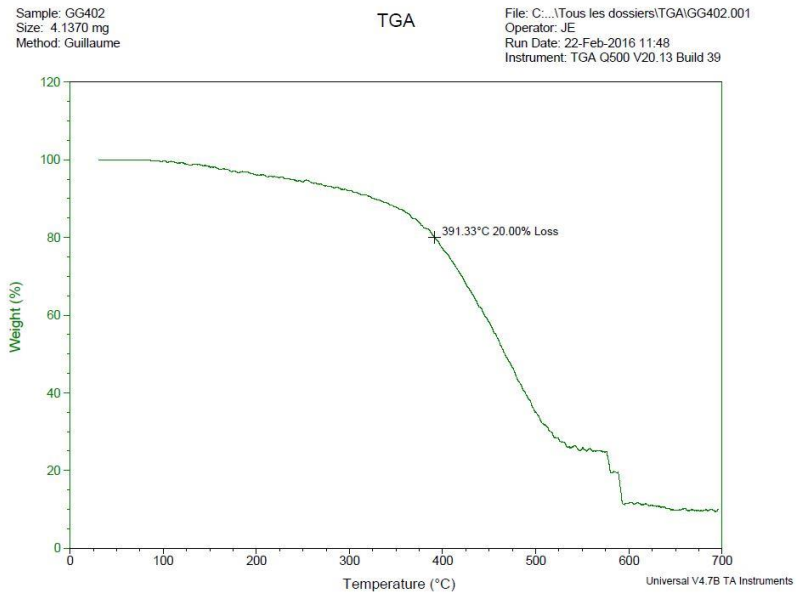

Figure 2-66: TGA trace of the 2,7-EDOT-75 (at a scan rate of 10°C per minute).

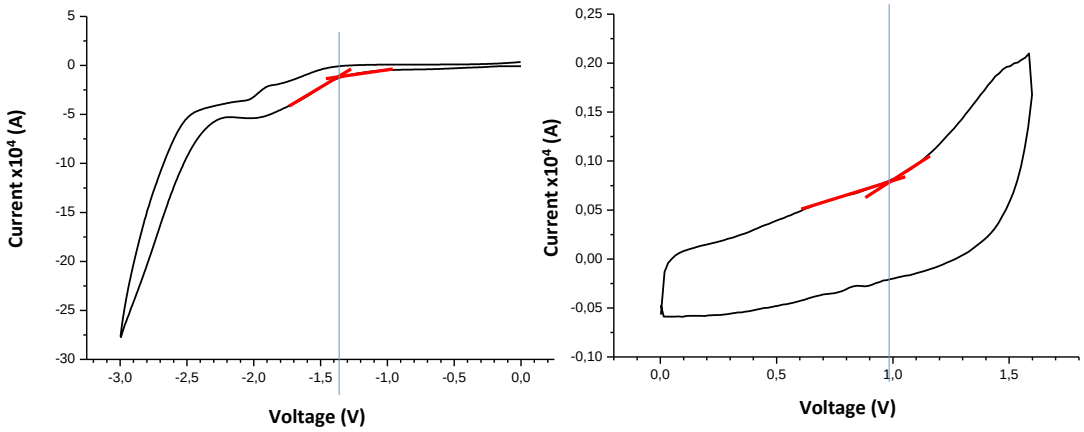

Figure 2-67: Cyclic voltammograms (left-reduction, right-oxidation) of 2,7-EDOT-75 in CH_2Cl_2 solution (0.1 $g.l^{-1}$) with $TBAPF_6$ as electrolyte.

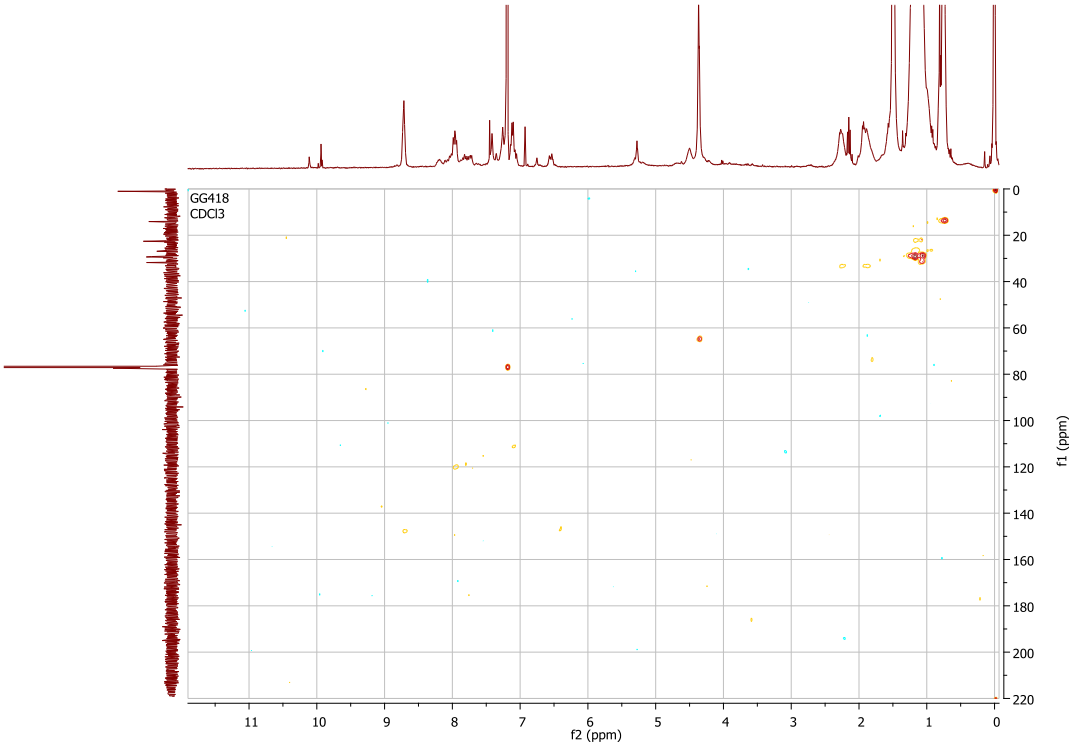

Figure 2-68: ^{1}H-^{13}C HSQC NMR spectrum of the 2,7-EDOT-100 (in $CDCl_3$).

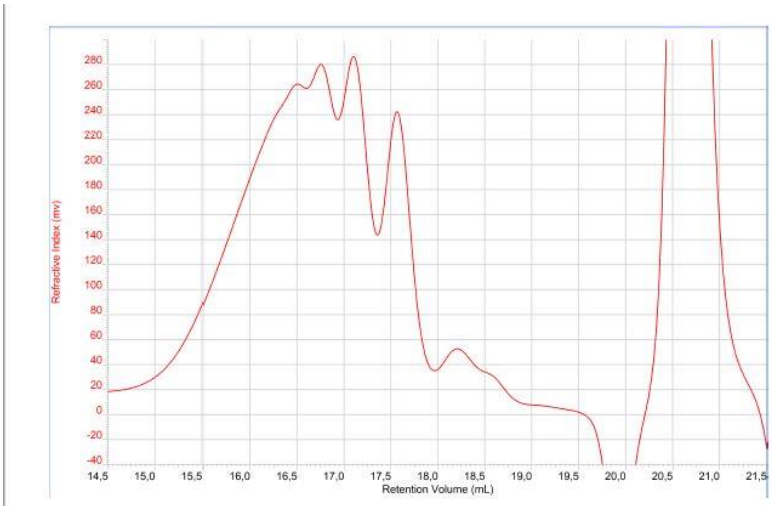

Peak	Mn	Mw	Mz	Mp	Mw/Mn	Ret Vol
1	2 421	4 877	9 133	2 247	2.014	17.097

Figure 2-69: SEC trace of the 2,7-EDOT-100 (in $CHCl_3$, polystyrene standard).

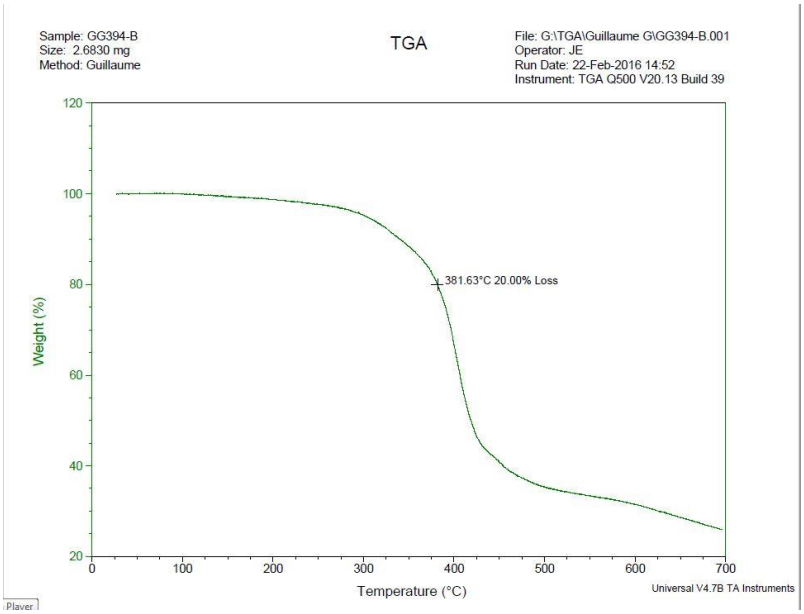

Figure 2-70: TGA trace of the 2,7-EDOT-100 (at a scan rate of 10°C per minute).

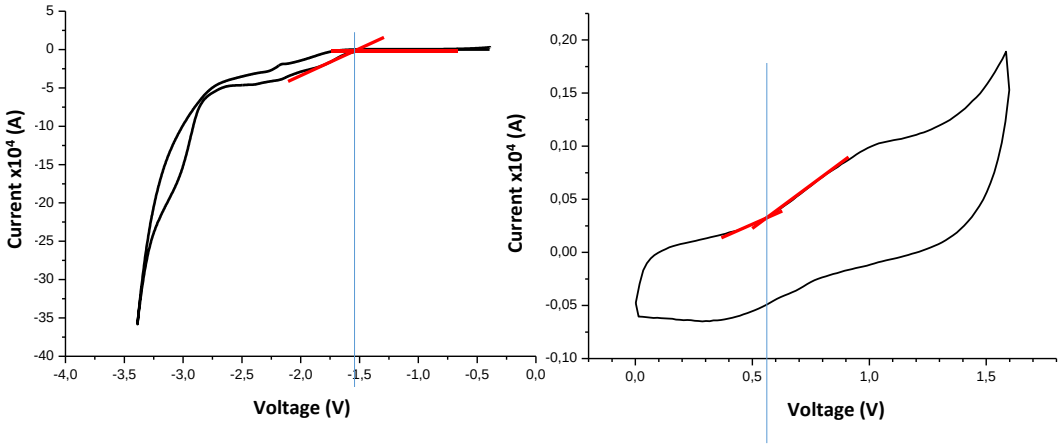

Figure 2-71: Cyclic voltammograms (left-reduction, right-oxidation) of 2,7-EDOT-100 in CH_2Cl_2 solution (0.1 g.l^{-1}) with $TBAPF_6$ as electrolyte.

Theoretical Analysis

All calculations were carried out with the PBE0 density functional using either Orca 3.03 or Gaussian09 C.01 packages.[57,58] Torsional potentials for the rotation about the C-N=R and R-C=N single bonds were evaluated with constrained minimizations of monomers, employing the TZVP basis set. The first torsion showed four local minima and the second two minima – see SI Figure S59. Azomethine dimers at all the possible 512 conformations, as identified by the minima in the torsional potentials, were first optimized with the PM6 semi-empirical method, fixing the C-N dihedrals d to -150,-40,+40,+150 degrees, and the R-C dihedrals fixed to either 0 or 180 degrees. Subsequently, PBE0/3-21G* geometry optimizations were performed,

removing the constraints in the dihedral values, in order to relax to the closest local minimum. Finally PBE0/Def2-SVP calculations were performed at the PBE0/3-21G* equilibrium geometry to obtain the energies E_i employed for calculating thermal-averaged properties (see discussion). The Boltzmann weighted averages were calculated at 300 K with the equation $\langle A \rangle = \sum_{i=1}^{512} A_i e^{-E_i/(k_B T)} / \sum_{i=1}^{512} e^{-E_i/(k_B T)}$.

The ground-state geometries of most stable dimers were further optimized with the def2-TZVP basis set. These geometries were employed as input for excited state energies calculations, carried out with the def2-SVP basis set and the Tamm Dancoff Approximation to time-dependent density functional theory. In all the calculations, the branched di-octyl side chain was replaced with a methyl group.

Theoretical Methodology. The ground-state geometry and electronic structure of the poly(azomethine)s were optimized by the hybrid density functional theory (DFT) method using
Basis set: def2-SVP
Functional: PBE0
Methods:
DFT (geometries, orbitals)
TDA (Tamm Dancoff Approximation, excited states)
Code: ORCA 3.03
Methodology for Absorption spectrum prediction:
Basis set: def2-TZVP
Functional: PBE0
Methods:
DFT (geometries, orbitals)
TDA (Tamm Dancoff Approximation, excited states)
Code: ORCA 3.03

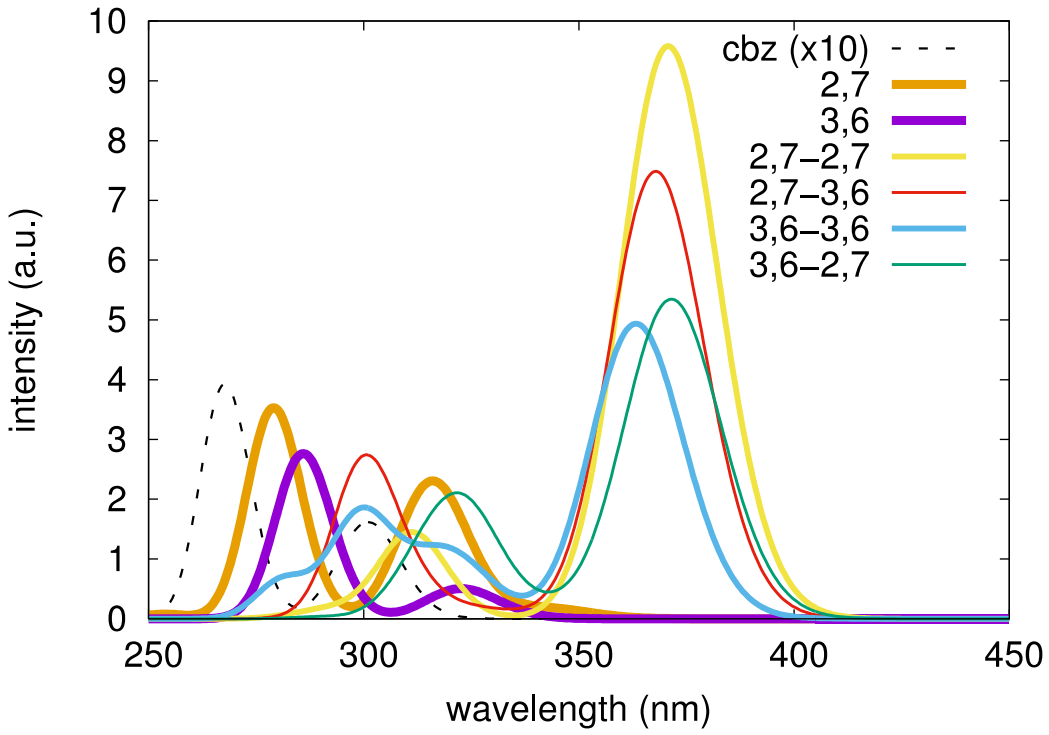

Figure 2-72: Absorption spectra prediction of the 4 carbazole-based azomethines (dimers).

Chapter 3: Synthesis of polysquaraines and polycroconaines

Résumé en français.

La synthèse de polysquaraines (*cf.* structure générale Figure 1) a été décrite pour la première fois en 1959 par S. Cohen, J. R. Lacher and J. C. Park.

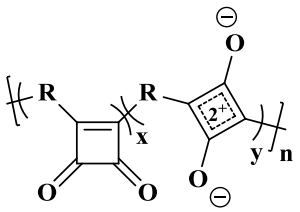

Figure 1 : Structure générale d'un polysquaraine.

Ces polymères présentaient déjà des caractéristiques optiques intéressantes. Plus récemment, les travaux de Havinga *et al.* ont remis au goût du jour cette famille de polymères avec notamment des structures originales combinant acide squarique et acide croconique avec du benzobisazole et du benzobisthiazole (Figure 2).

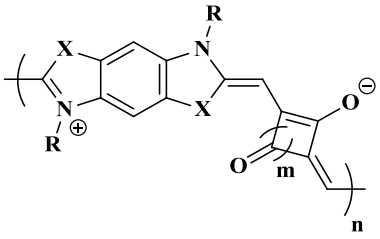

Figure 2 : Polysquaraine et polycroconaines conjugués et solubles dans les solvants organiques communs.

Il est important de souligner que ces structures sont obtenues en l'absence de catalyseurs métalliques. De la même manière, au cours de ce travail de thèse je me suis attaché à utiliser une diamine aromatique, la N,N'-didodecyldiphenyl-1,4-benzenediamine (**TPDA)**, comme comonomère des acides squariques et croconiques (Figure 3).

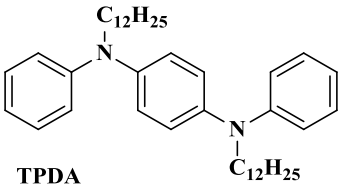

Figure 3 : Structure du TPDA

Différentes conditions ont été testées afin de modifier la position de la liaison entre l'acide squarique et le **TPDA**, comme un changement de solvant, l'ajout d'un co-solvant ou le contrôle de la stœchiométrie. Différents polysquaraines ont été synthétisés, et leurs propriétés optoélectroniques ont été étudiées. L'ajout de solvants di-fonctionnalisés dans le milieu réactionnel a permis l'obtention de polymères présentant une émission couvrant une grande partie du spectre visible (Figure 4).

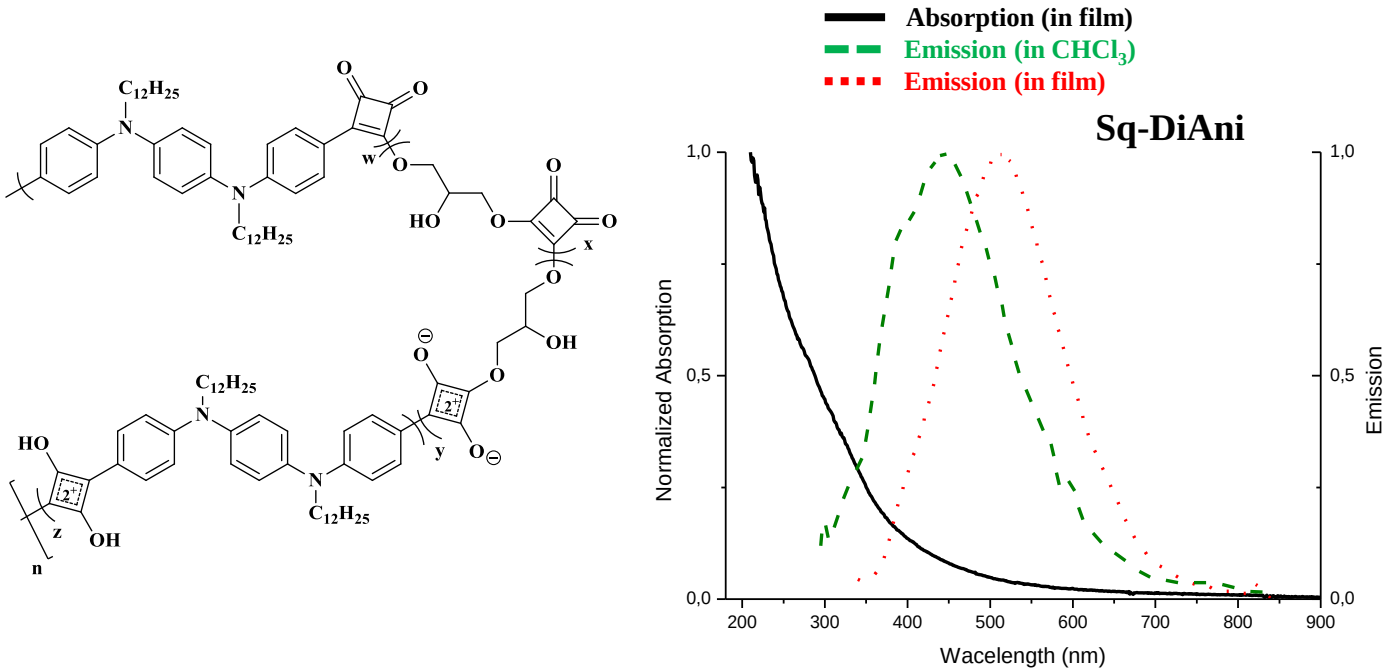

Figure 4: Structure proposée des polysquaraines intégrant du 1,3-propanediol (gauche) et spectres d'absorption et d'émission caractéristiques de ces polymères (droite)

Ils ont ensuite été intégrés dans des OLED, émettant une lumière blanche.

Structure and names of compounds synthesized in chapter 3.

Structure	Name and explanation	Solvent	Short Name
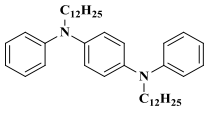	N,N'-didodecyldiphenyl-1,4-benzenediamine	/	**TPDA**
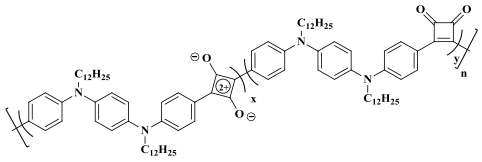	**TPDA-SqX, X** depending of the amount of **toluene (in %)** mixted with 1-butanol during the polymerization	**10% toluene**	**TPDA-Sq10**
		50% toluene	**TPDA-Sq50**
		90% toluene	**TPDA-Sq90**
	Polymer synthesized with **squaric acid** and **TPDA**	Mixture of **toluene and 1-propanol (50:50)**	**TPDA-Sq50-Prop**
	Polymer synthesized with **squaric acid** and **TPDA** and using **different DiOl**	**1-butanol**	**TPDA-Sq50-But**
		1-pentanol	**TPDA-Sq-PentDiol**
		1-dodecanol	**TPDA-Sq-DodDiol**
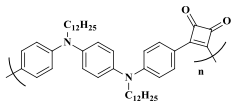	Polymer synthesized with the modified **squaric acid and TPDA** 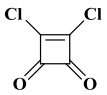	Mixture of **toluene and 1-butanol (50:50)**	**TPDA-SqCl**
		Mixture of **toluene and 1-propanol (50:50)**	**TPDA-SqCl-Prop**
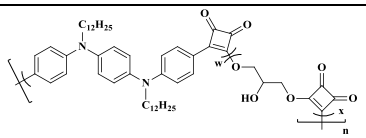		**Glycerol**	**TPDA-SqCl-Gly**
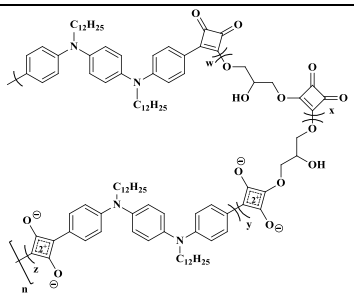	Polymer synthesized with **squaric acid** and **TPDA**	**Glycerol**	**TPDA-Sq-Gly**
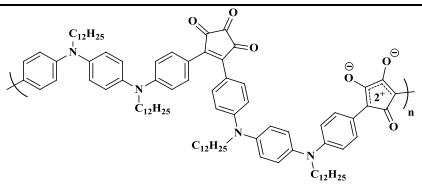	Polymer synthesized with **croconic acid** and **TPDA**	Mixture of **toluene and 1-butanol (50:50)**	**TPDA-Cro50**

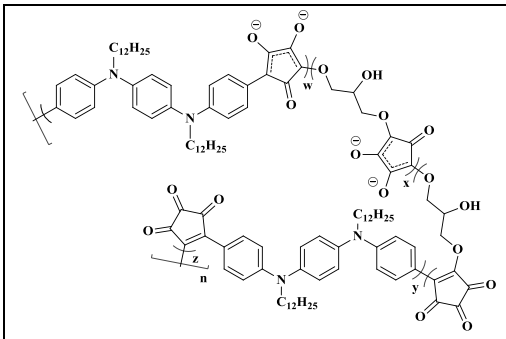	Polymer synthesized with **croconic acid** and **TPDA**	**Glycerol**	**TPDA-Cro-Gly**
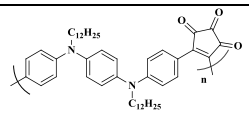	Polymer synthesized with modified **croconic acid** and **TPDA**		**TPDA-CroCl-Gly**
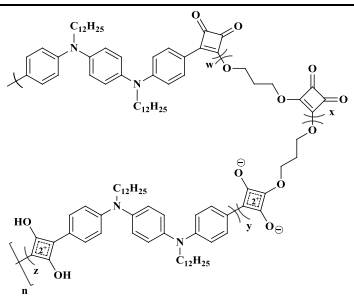	Polymer synthesized with **squaric acid** and **TPDA** and using **different ratio** of 1,3-propanediol	**1,3-propanediol**	**TPDA-Sq-PropDiol-1eq**
			TPDA-Sq-PropDiol-2eq
			TPDA-Sq-PropDiol-3eq
			TPDA-Sq-PropDiol-10eq

Chapter 3: Synthesis of polysquaraines and polycroconaines

3.1. Literature overview 119

3.2. Polycroconaine based on bis(indolium)thiophene 122

3.3. Poly(squaraine-*co*-triphenyldiamine) 124

3.3.1. Monomer synthesis 124

3.3.2. Polymer synthesis 126

3.3.3. Characterizations 127

3.3.4. Control of the linkage 128

3.3.4.1. Modification of the Squaric acid 128

3.3.4.2. Impact of the solvent 131

3.3.4.3. Investigation of various alcohol as comonomers and modification of alcohol ratio 138

3.3.4.3.1. Effect of the solvent 139

3.3.4.3.2. Effect of the solvent ratio 141

3.4. Toward integration in OLED 143

3.4.1. Optical and electrochemical characterization 143

3.4.2. Integration into OLED 147

3.5. Conclusions 151

3.6. References 152

3.7. Experimental part 155

3.7.1. Syntheses 155

3.7.2. Characterizations 160

3.1 Literature Overview

The squaric acid (diketocyclobutenediol in the original paper; 3,4-dihydroxycyclobut-3-ene-1,2-dione according the IUPAC nomenclature) is a compound first synthesized in 1959 by S. Cohen, J. R. Lacher and J. C. Park.[1] The squaric acid has then been developed in parallel for medicine and chemistry applications. Indeed, on the medical side, it has been described as a strong sensitizer [2] and its ester derivative is still developed as a treatment for alopecia areata (localized baldness) and warts.[3,4] Squaraines dyes have also been used as biological labelling[5], for photodynamic therapy[6,7], chemosensors and biosensors.[8]
From the chemistry point of view, the squaric acid has been studied for its chelating properties,[9–12] its ability to react with amine to form polyamides[13–15] and to react with aromatic moieties bearing a nitrogen in which the lone pair participates to the conjugation to form enamine (Figure 3-1).[16,17] The latter capacity will be particularly the object of investigations in this chapter.

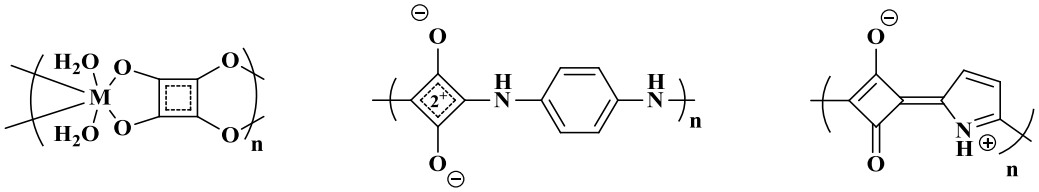

Figure 3-1: Squaric acid entering in the formation of: i) complexing metals ii) polyamide iii) enamine.

The first squaric acid based dyes have been synthesized in 1965 by A. Treibs and A. Jacob by performing the condensation of squaric acid with pyrrole and phenol derivatives (Figure 3-2).[16]

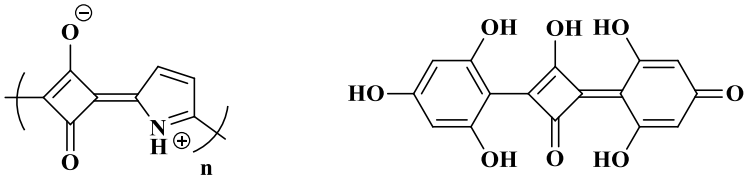

Figure 3-2: Structure of the first squaric acid based dyes (adapted from reference [16]).

While the first polysquaraines were also described in this paper, their low solubility impeded their full characterization. Bailey *et al.* studied the structure of the squaric acid once conjugated with aniline.[18] Different resonance structures have therefore been identified (Figure 3-3).

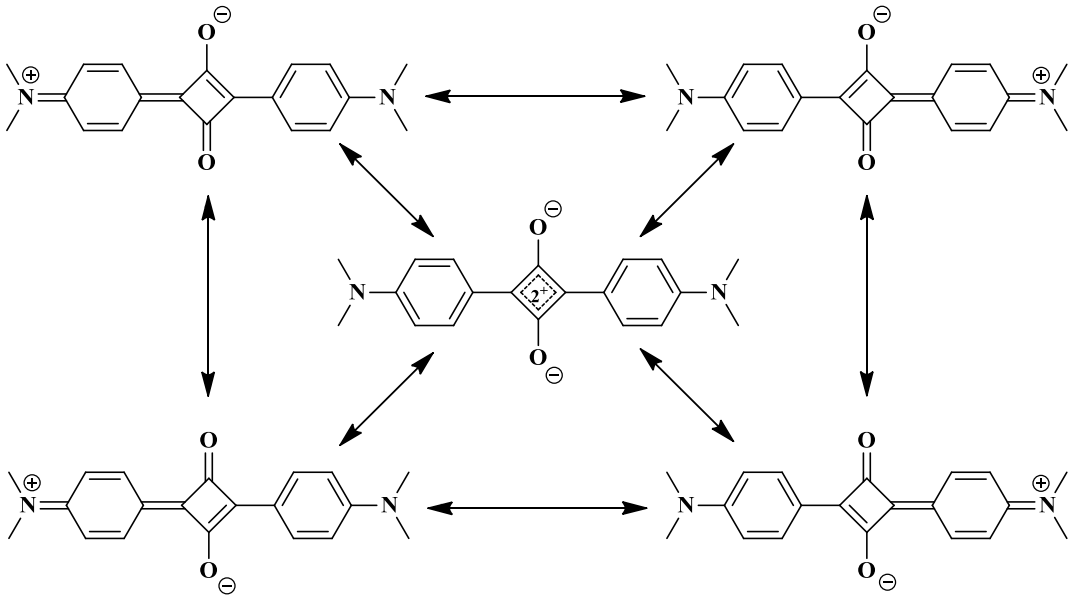

Figure 3-3: Resonance structures of squaraine dyes.[18]

Based on previously obtained results[19] and with the idea of synthesizing a low-band gap polymer, Havinga *et al.* synthesized a polysquaraine by alternating a strong donor moiety with a strong acceptor. They used the squaric or the croconic acid (considered as a stronger acceptor moiety)[8,20] as a withdrawing moiety (acceptor) and benzobisthiazole or benzobisazole as donating moieties.[21–23] The polymerization has been performed *via* a condensation reaction, to afford different squaric and croconic based polymers (Figure 3-4).

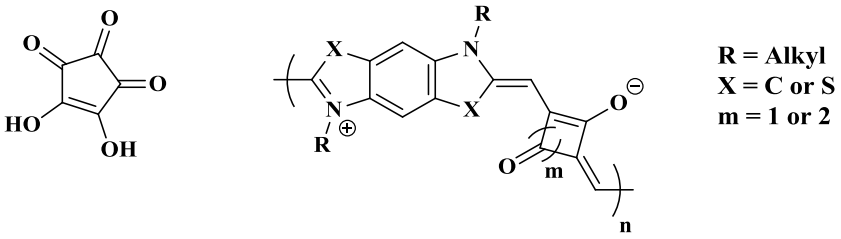

Figure 3-4: Structure of the croconic acid (left) and main structure of polysquaraine condensated with Benzobisazole and Benzobisthiazole (right).

It is noteworthy that the polymerization route leads to 1-2 or 1-3 linkages. Nevertheless, only 1-3 linkages are suited for near IR absorption and emission of dyes. For a better understanding, a mechanistic approach of the squaric dyes formation has been reported by Ronchi *et al.* in 2011 (Schema 3-1).[24]

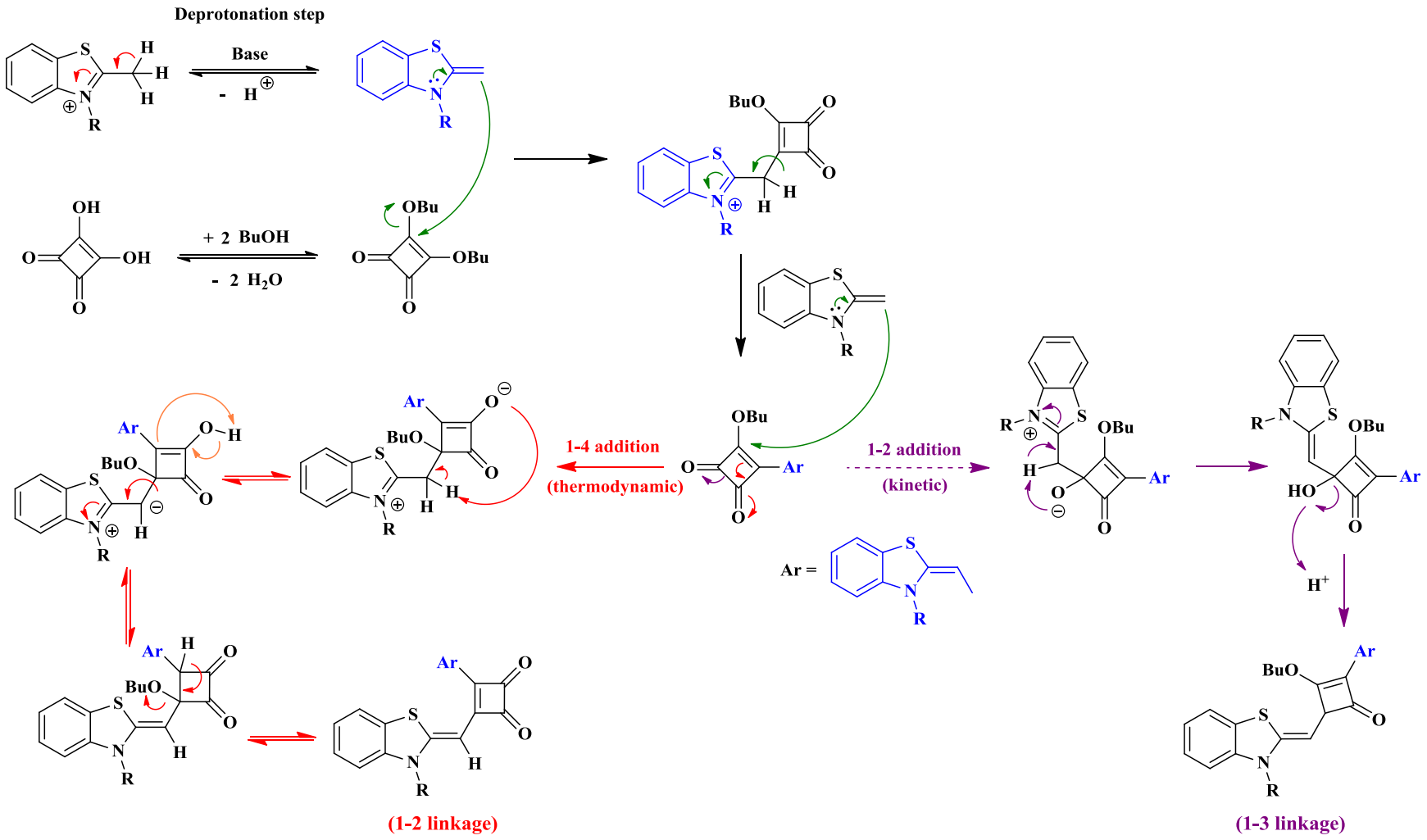

Schema 3-1: Mechanism of the squaric acid condensation on a benzothiazole (adapted from reference 24).

In both cases, the reaction is a condensation between the squaric acid and the aromatic moiety. Different mixtures of solvent have been used to obtain mostly the 1-3 linkage, the most used being a mixture of 50% of toluene and 50% of 1-butanol.[25]

Another important breakthrough was achieved thanks to the modification of the dyes. [26] By adding boronated and halides functions to the squaraine dyes, it was possible to polymerize them using the previously described transition-metal based coupling. This dramatically increased the range of co-monomer that can be polymerized with them. All these techniques allow the preparation of plethora of various polymers and dyes.[27–29] Their use in OLED devices has been particularly reported.

In present work, different objectives have been pursued. The first one has been to synthesize new polycroconaine and to compare them with previously synthesized indol based polysquaraine. Indeed these polymers presents near-IR absorption and can be synthesized without the need of transition-metal based catalyst.[30] Moreover, the croconic acid being considered as a stronger acceptor than the squaric acid, a red-shift in the absorption is expected.[8,20] Another objective was to perform the polymerization of the squaric acid with an alkylated N,N-Diphenyl-*p*-phenylenediamine by varying different parameters, such as the heating method, the temperature or the solvent used. An advantage of this kind of polymerization is that no base is needed.[31,32]

3.2. Polycroconaine based on bis(indolium)thiophene

A study has previously been performed in the lab, comparing polysquaraines obtained *via* metal-free and transition-metal based polymerization (Figure 3-5).[30]

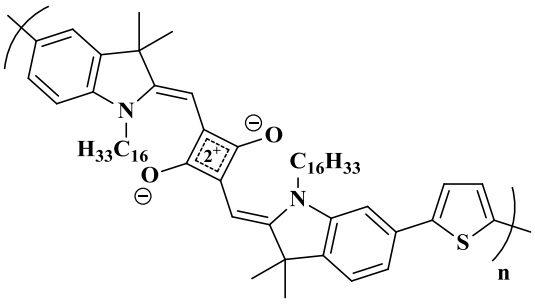

Figure 3-5: Structure of the poly(squaraine-*alt*-bis(indolium)thiophene))

To compare the properties of the polycroconaine based on bis(indolium)thiophene with the polysquaraine, the indol based monomer has been synthesized in 2 steps (Scheme 3-2).

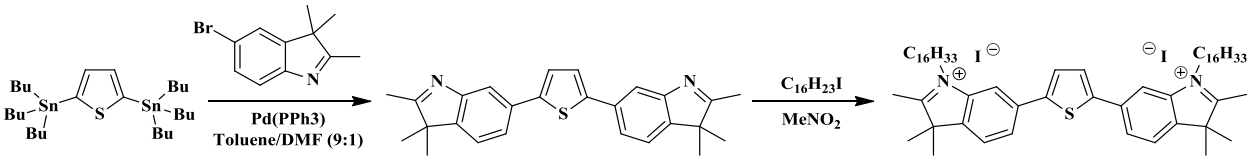

Scheme 3-2: Synthesis of the bis(indolium)thiophene.

As shown in Scheme 3-3, the first step of the reaction is the Stille coupling between the bis(dibutylstannyl)thiophene and two equivalents of the 5-bromoindol. The monomer has then been quaternized with 1-iodohexadecane in nitromethane. Characterizations of the compound are in agreement with the literature (see experimental section).[33] The polymerization with the commercial croconic acid has been performed following the same protocol than for the polymerization using the squaric acid (Scheme 3-3).

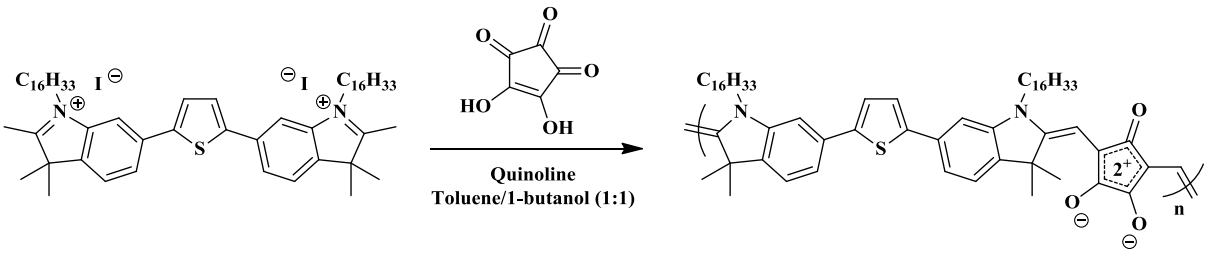

Scheme 3-3: Polycondensation of the croconic acid on the bis(indolium)thiophene.

Both the croconic acid and the bis(indolium)thiophene have been solubilized in stoichiometric amount in a mixture of 50% toluene and 50% 1-butanol (in volume). A Dean-Stark apparatus has been used to remove the water formed during the polycondensation. For the sake of comparison, the polymerization with the squaric acid has been performed in parallel using the same conditions. After 3 days of polymerization, the two polymers have been washed first with methanol, then with chloroform *via* a Soxhlet extraction. At the end of the extraction, around 10 weight % was still insoluble in hot chloroform in both cases. The optical properties of chloroform soluble fraction have then been measured in solution (Figure 3-5).

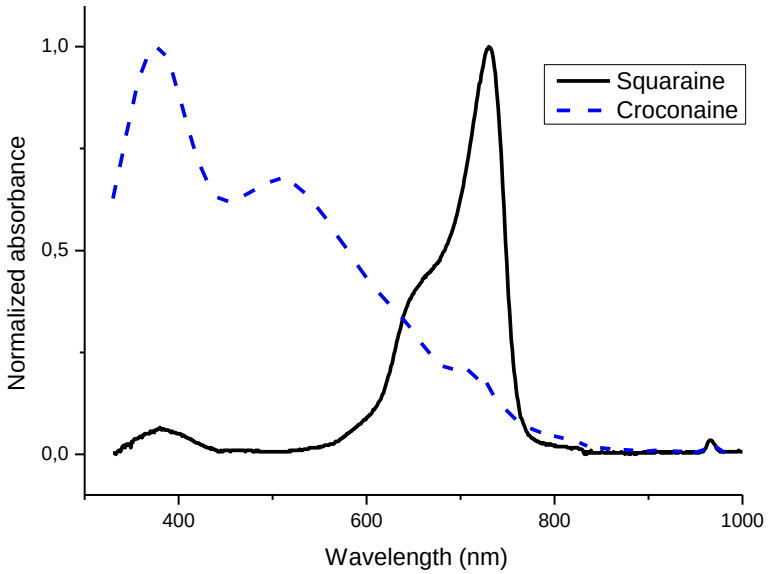

Figure 3-5: Absorption spectra of both polysquaraine and polycroconaine in chloroform.

Surprisingly, compared to the polysquaraine, the polycroconaine presents an absorption at a lower wavelength. The polysquaraine presents a maximum of absorption at 730 nm with a small absorption at 380 nm. On the contrary, the polycroconaine shows a maximum of absorption at 380 nm, a second peak at 510 nm and a small absorption at 730 nm. This reaction has been performed three times, constantly giving same results.

Based on these results, we decided to use a more accessible comonomer, instead of bis-indolium, combining squaric acid and croconic acid monomers with a di(arylamine), the N,N'-didodecyldiphenyl-1,4-benzenediamine (**TPDA**).

3.3. Poly(squaraine-*co*-triphenyldiamine)

3.3.1. Monomer synthesis

The first objective has been to synthesize a new polymer based on squaric acid and N,N-Diphenyl-*p*-phenylenediamine in a mixture of toluene and 1-butanol which are the common conditions used for the condensation of squaric acid with indolium for example.

The N,N'-didodecyldiphenyl-1,4-benzenediamine ou tripenylene diamine **(TPDA)** was synthesized in one step from the commercially available N,N'-diphenylbenzene-1,4-diamine, which was reacted with 1-bromododecane in the

presence of potassium hydroxide giving rise to the alkylated monomer N,N'-didodecyldiphenyl-1,4-benzenediamine (**TPDA**) (Scheme 3-4).

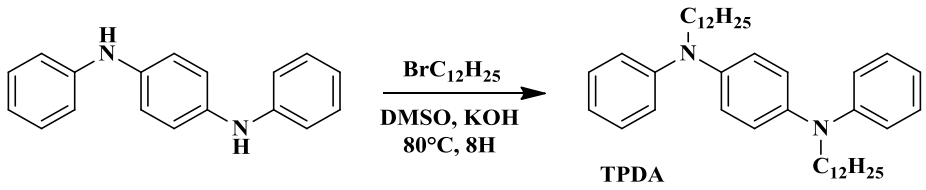

Scheme 3-4: Synthesis of the N,N'-didodecyldiphenyl-1,4-benzenediamine (TPDA).

IR, NMR (^{1}H, ^{13}C and ^{1}H-^{13}C HSQC) and HRMS analyses were performed to confirm its structure and were in good agreement with a previously reported similar structure.[34] NMR analysis has been performed using deuterated THF (THF-*d*8). No peak corresponding to amine protons were observed, confirming the double alkylation of the product. Additionally, integral values were consistent with the presence of two dodecyl chains (Figure 3-6).

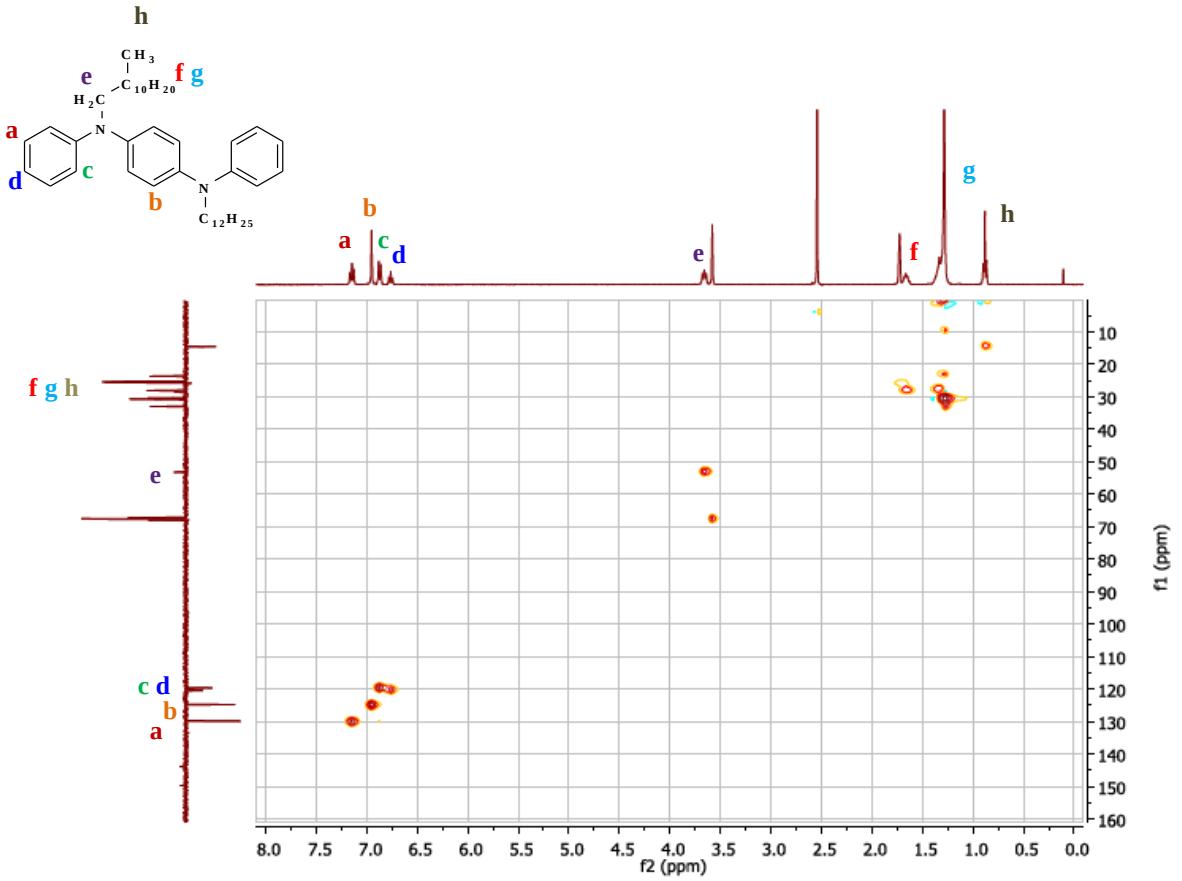

Figure 3-6: ^{1}H-^{13}C HSQC NMR spectra of the TPDA monomer (in THF-d8).

The double alkylation of the compound was also confirmed by FTIR, where there were no signals between 3300 and 3400 cm^{-1}, corresponding to the N-H stretch.

3.3.2. Polymer synthesis

The aniline-like monomer has then been polymerized with squaric acid using three different ratio of toluene and 1-butanol for studying the impact of the solvent on the optical properties. The squaric acid has been reacted with a stoichiometric amount of the **TPDA** compound in a mixture of toluene and 1-butanol with a different volume ratio between the solvents, to control the linkage between the **TPDA** and the squaric acid. The reaction has then been heated at reflux temperature during 24 hours (using a Dean-Stark apparatus to remove the water formed during the polymerization) (Scheme 3-5).

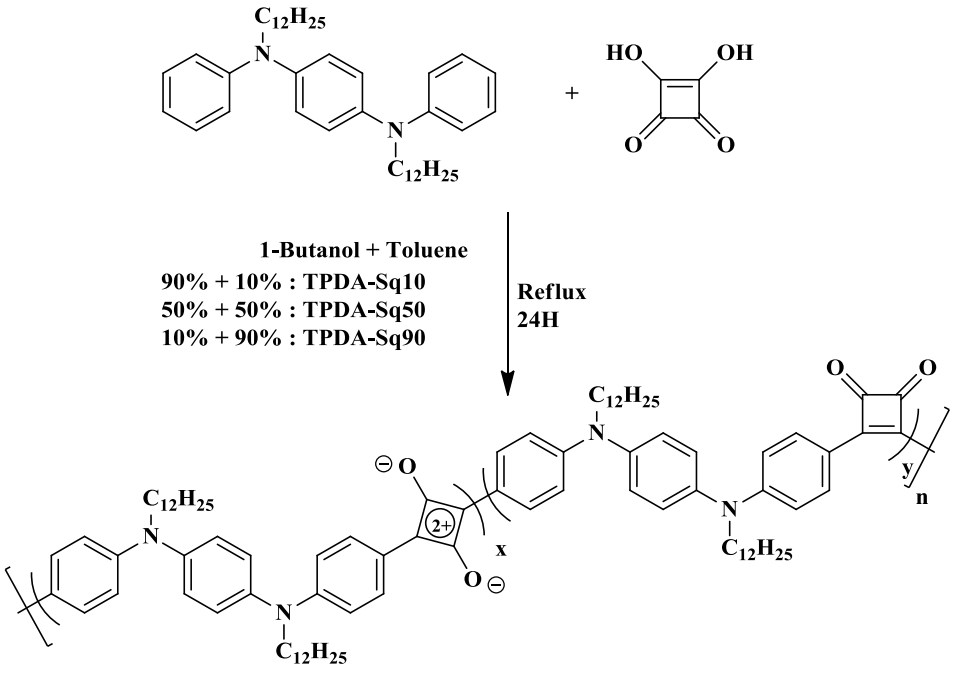

Scheme 3-5: General scheme for the synthesis of the different TPDA-Squaric acid based polymer (TPDA-Sq) synthesized with different toluene and 1-butanol ratio.

Three polymers have thus been synthesized, named poly(squaraine-*alt*-N,N'-didodecyldiphenyl-1,4-benzenediamine) or, as a short name, **TPDA-SqX**, **X** being the percentage of volume of the **toluene** in the mixture. It was not possible to perform the polymerization with only toluene or butanol, the **TPDA** compound being insoluble in 1-butanol and the squaric acid insoluble in toluene. The resulting polymer has been purified by repeated precipitation in MeOH from THF solution.

Control experiments, in acidic conditions or not, have been performed to make sure that the **TPDA** monomer was not subjected to homocoupling or other side reaction (by comparison to aniline derivatives). To reproduce an equivalent pH, 2 equivalents of

dichloroacetic acid have been added in the medium. After 24 hours of heating, no formation of polymer was observed (confirmed with SEC).

3.3.3. Characterizations

The absorption and emission spectra of the three polymers have then been performed in solution in THF (Figure 3-7).

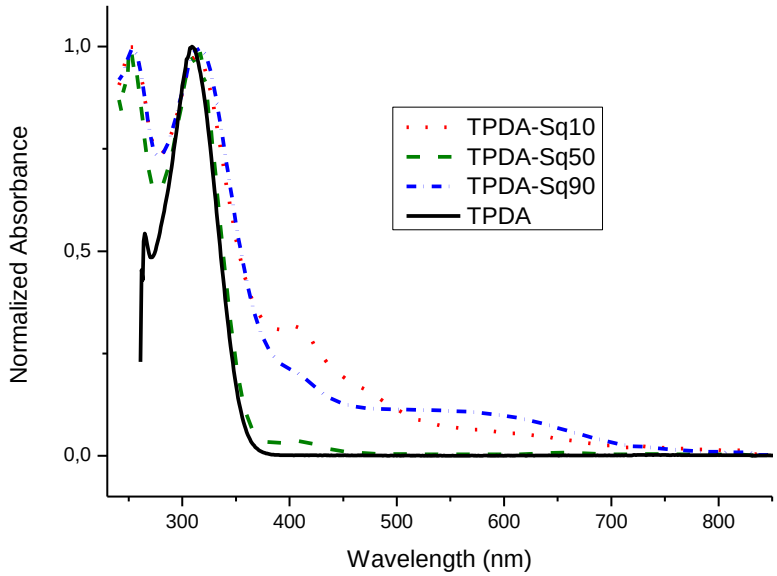

Figure 3-7: Absorption spectra of the TPDA-SqX polymers and monomer in solution in THF.

As shown in figure 3-7, two absorptions peaks are present at respectively 255 and 315 nm for all of the polymers. The absorption at 315 nm is also present for the absorption of the **TPDA.** However, for the three polymers, an absorption peak can also be observed around 400 nm, absorption which is not present in the monomer. Besides, an absorption peak could be observed at 600 nm which could be assigned to an extended conjugation length. This absorption can also be related to polyaniline (PANI) due to the protonation of aniline segments in acidic conditions.[35] In order to better investigate the type of linkage occurring with the squaraine subunit, we've carried out ATR-FTIR analysis (Figure 3-8).

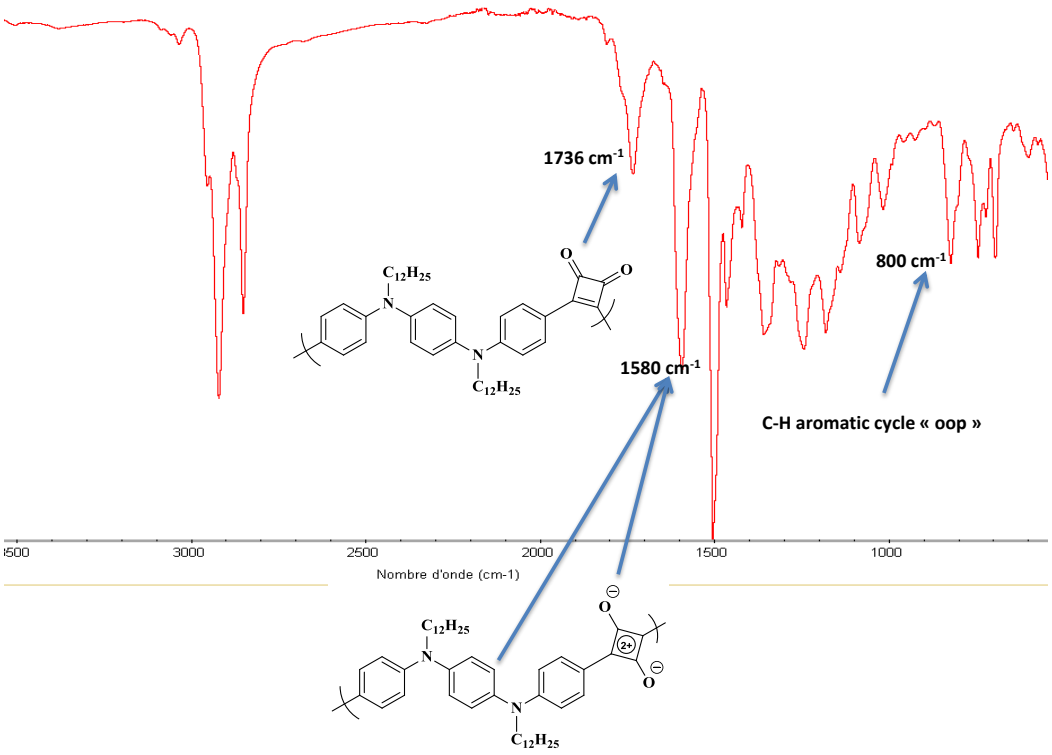

Figure 3-8: ATR-FTIR spectrum of the TPDA-Sq10 polymer.

Two signals are particularly noticeable for the understanding of the squaraine linkage formation. A signal at 1736 cm^{-1}, which corresponds to the ketone (C=O stretch) of the squaric acid (1-2 linkage) and a signal at 1580 cm^{-1} assigned to the zwitterionic form (C-O^- stretch) of the acid (1-3 linkage). Nevertheless, as the signal at 1622 cm^{-1} overlay with the C-H stretch from the **TPDA** monomer. A reference is needed in order to quantify the ratio between 1-2 and 1-3 linkages.[15,36,37]

3.3.4. Control of the linkage

In order to better access the catenation of the squaraine subunit within the polymer backbone we've investigated two pathways: a chemical modification of the squaric acid monomer and a variation of the solvent whether it is polar or protic which can drastically affect the coupling reaction.

3.3.4.1. Modification of the Squaric acid

To chemically control the reactivity of the squaric acid, and to favor the 1-2 linkage, different strategies can be employed. A first one is the use of Lewis acid (such

as $AlCl_3$) to complex with the ketones of the squaraïne. However, the polycondensation mechanism is too complex to predict the impact of such addition. The method we have used consisted in the substitution of the two hydroxyl groups of the squaric acid by chlorine atoms as good leaving groups. The methodology was reported in 1970 by R. C. De Selms *et al.* and is illustrated in Scheme 3-6.[38]

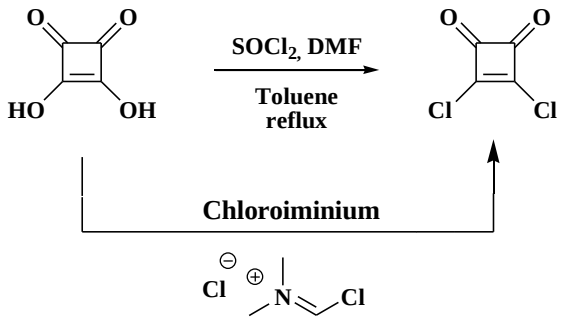

Scheme 3-6: Synthesis of dichlorinated squaric acid, (1,2-dichlorocyclobutene-3,4-dione, SqCl) thanks to a chloroiminium derivative.

This reaction, occurring in toluene at reflux, first consists in the reaction of the catalytic amount of DMF on the thionyl chloride to form a Vilsmeier-Haack reagent. Then the alcohol reacts on this chloroiminium intermediate to form the squaryl dichloride **SqCl**. The yellow compound has then been purified by sublimation, and the substitution of the alcohol functions by the chlorine has been confirmed by exact mass measurement. The same reaction has been performed on the croconic acid to obtain the chlorinated derivative **(CroCl)** which will be used further in this work. However, the croconic acid bearing three ketone functions, it can't be used as reference.

The purified monomer has then been polymerized with the **TPDA** monomer in a mixture of toluene and butanol, following the previously used procedure (Scheme 3-7).

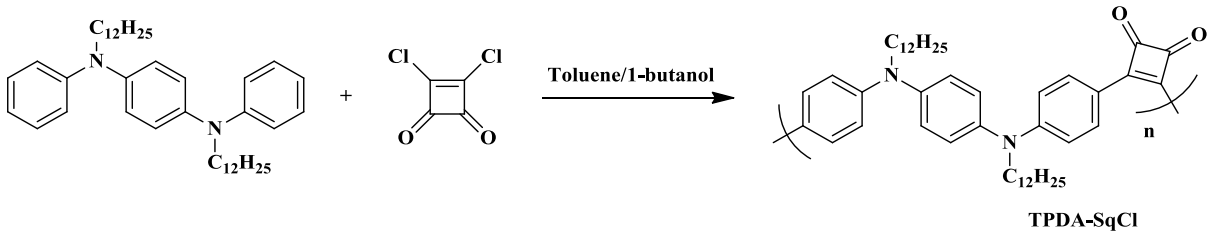

Scheme 3-7: Synthesis of the reference polymer (TPDA-SqCl).

The ATR-FTIR spectrum has then been performed. As shown in figure 3-9, characteristic signature of 1-2 linkage is confirmed and could be quantified by comparing intensity of the C=O signal (at 1700 cm^{-1}) and the C=C signal (at 1550 cm^{-1}) (Figure 3-9).

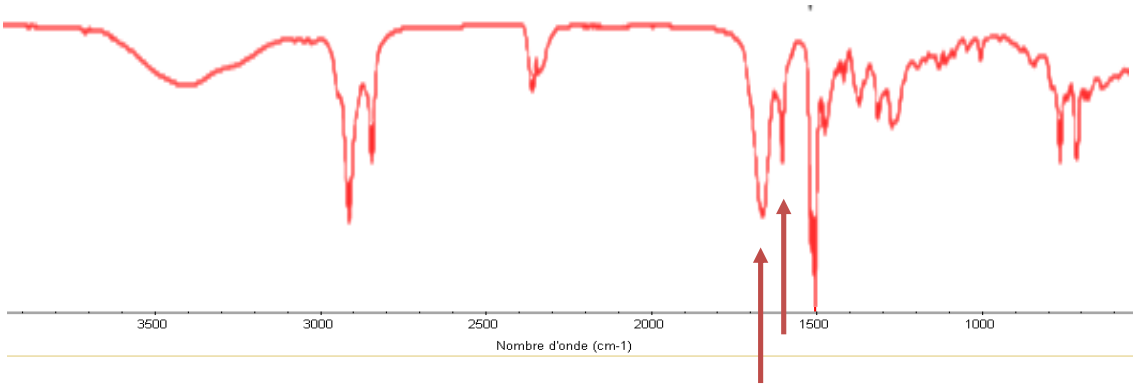

Figure 3-9: FTIR-ATR spectrum of the reference polymer (TPDA-SqCl).

The area ratio between two signals at 1700 and 1550 cm^{-1}, gave a value of 1.41 in the case of the full 1-2 linkages-based polymer. It was thus possible to estimate this value for all polymers (Table 3-1).

Polymer	Ratio of absorbance	Estimation of percentage of 1-2 linkage
Reference TPDA-SqCl	1.41	100%
TPDA-Sq10	0.43	30%
TPDA-Sq50	0.47	33%
TPDA-Sq90	0.38	27%

Table 3-1: Percentage of the 1,2 and 1,3 linkage present in the polymer chain, determined with their IR spectra.

It should be noted that the values reported in Table 3-1 cannot be taken as strictly quantitative due to possible experimental or interpretation errors. Anyway, these results allowed us to confirm that the absorbance at 600 nm was due to 1-3 linkages. Indeed, as illustrated in figure 3-10, the reference **TPDA-SqCl** doesn't show any absorption peak above 500 nm (Figure 3-10).

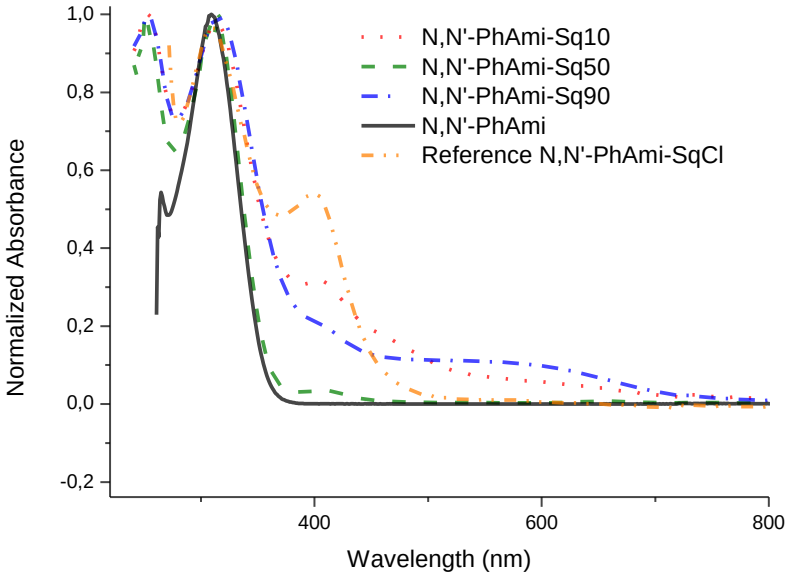

Figure 3-10: Absorption spectra of the different TPDA-Sq polymers (measured in $CHCl_3$).

From these, one can attest that main absorption peak (common to all polymers) at 400 nm is due to 1-2 linkages while the signal at 600 nm can be attributed to the 1-3 linkages. It can thus be interesting to envision to tune optical properties of such materials by playing with the 1-2/1-3 ratio. As discussed below, another way to control this ratio could be the variation of the solvent for the reaction.

3.3.4.2. Impact of the solvent

Reactions with a variation of the solvent have been performed to study the impact of the solvent on the addition of the monomer on the squaric or croconic acid. Different solvent have been tried, following the work of Eberhard W. Neuse and Brian R. Green *et al.* on poly(squaryl amide).[15] These reactions have been performed with the squaric acid, the squaryl dichloride **SqCl** and the croconic acid in order to compare optical properties of the different polymers. The general reaction is showed below (Scheme 3-8).

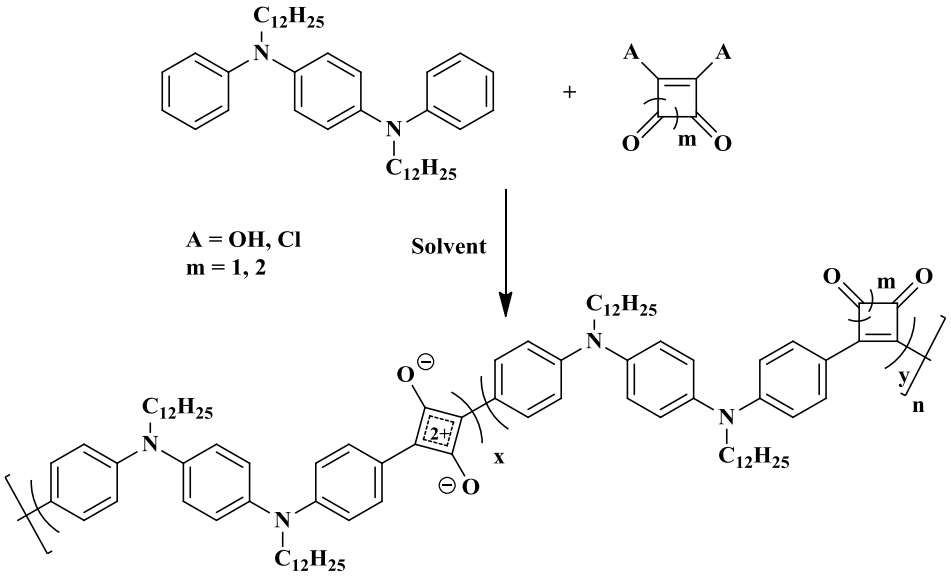

Scheme 3-8: General polycondensation reaction of TPDA and squaric acid like derivatives in different solvents.

Reactions have been performed in a conventional heating oil bath at 135°C or under µ-wave irradiation for 4 hours. All reactions performed in µ-wave reactors have first been performed one time under conventional heating to support that polymers obtained *via* the 2 polymerization methods present similar properties. The different conditions performed are reported in the table 3-2.

Monomer	First solvent (volume %)	Second solvent (volume %)	Heating method	Tempe-rature	Time
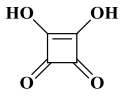 **Sq**	Toluene (90%)	1-Butanol (10%)	Oil bath	135°C	3days
	Toluene (50%)	1-Butanol (50%)	Oil bath	135°C	3days
	Toluene (10%)	1-Butanol (90%)	Oil bath	135°C	3days
	Toluene (50%)	Glycerol (50%)	Oil bath	135°C	3days
	Toluene (50%)	1-Propanol (50%)	Oil bath	135°C	3days
	NMP (100%)	/	µ-wave	200°C	4 hours
	DMF (100%)	/	µ- wave	120°C	4 hours
	Glycerol (100%)	/	µ- wave	200°C	4 hours
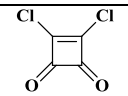 **SqCl**	Toluene (50%)	1-Butanol (50%)	Oil bath	135°C	3days
	Toluene (50%)	1-Propanol (50%)	Oil bath	135°C	3days
	Glycerol (100%)	/	µ- wave	200°C	4 hours
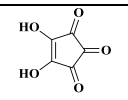 **Croco**	Toluene (50%)	1-Butanol (50%)	Oil bath	135°C	3days
	Glycerol (100%)	/	µ- wave	200°C	4hours

Table 3-2: Variation of solvent in polycondensation reactions between the squaric acid, SqCl or the croconic acid and the TPDA.

In these reactions, the different monomers have been polymerized in 1-butanol, propanol, or pure solvents like NMP, DMF or glycerol (not mixed with toluene). Polymers were characterized by NMR, SEC, DSC and TGA, results are gathered in Table 3-3. An example of ^{1}H-^{13}C HSQC NMR is shown below. All polymers synthesized in the presence of monofunctionnal alcohol present a similar spectrum. (Figure 3-11).

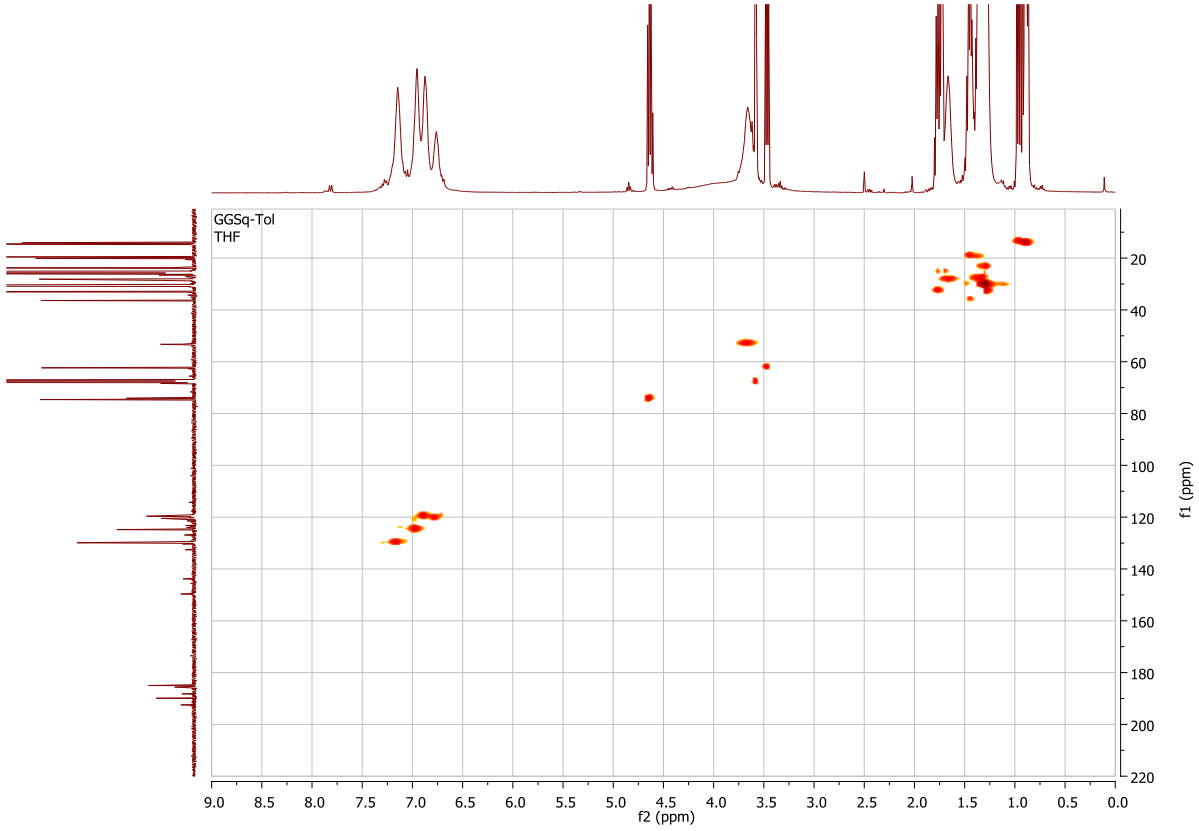

Figure 3-11: General ^{1}H-^{13}C HSQC NMR of different polysquaraines synthesized with a mixture of toluene and 1-butanol or 1-propanol (in THF-d_8)

The presence of the different linkages is confirmed thanks to the ^{13}C NMR spectrum, where signals between 150 and 200 ppm correspond to 1,2 and 1,3 linkages on the squaraine moiety.

Monomer	Second solvent (volume %)[a]	Polymer Name	$\overline{Mn}$ [b]	Đ[b]	T_d[c]
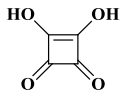 **Sq**	1-Butanol (10%)	**TPDA-Sq10**	2500	2.7	366°C
	1-Butanol (50%)	**TPDA-Sq50**	2100	2.2	372°C
	1-Butanol (90%)	**TPDA-Sq90**	2800	2.7	386°C
	1-Propanol (50%)	**TPDA-Sq50-Prop**	3700	3.4	350°C
	NMP (100%)	**TPDA-NMP**	642	1.1	/
	DMF (100%)	**TPDA-DMF**	839	1.5	/
	Glycerol (100%)	**TPDA-Sq-Gly**	2400	3.0	426°C
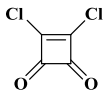 **SqCl**	1-Butanol (50%)	**TPDA-SqCl**	/	/	365°C
	1-Propanol (50%)	**TPDA-SqCl-Prop**	/	/	368°C
	Glycerol (100%)	**TPDA-SqCl-Gly**	1800	4.5	437°C
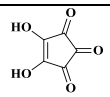 **Croco**	1-Butanol (50%)	**TPDA-Cro50**	/	/	372°C
	Glycerol (100%)	**TPDA-Cro-Gly**	/	/	428°C

Table 3-3: Polysquaraines and polycroconaines based on TPDA, effect of solvent synthesized in different solvents.
[a]With toluene as first solvent. [b]Measured by SEC in $CHCl_3/Et_3N$ (99:1) at 30 °C, relative to PS standards. [c]Obtained by TGA under N_2 at 10 °C min^{-1}.

Through DSC we were not able to observe any characteristic temperature, such as Tg or Tm. By TGA, all polymers showed degradation temperature above 300°C with a specific behavior when polymers are formed in presence of glycerol. The latter show a degradation temperature above 420°C. UV-Visible spectroscopy was then performed (Figure 3-12).

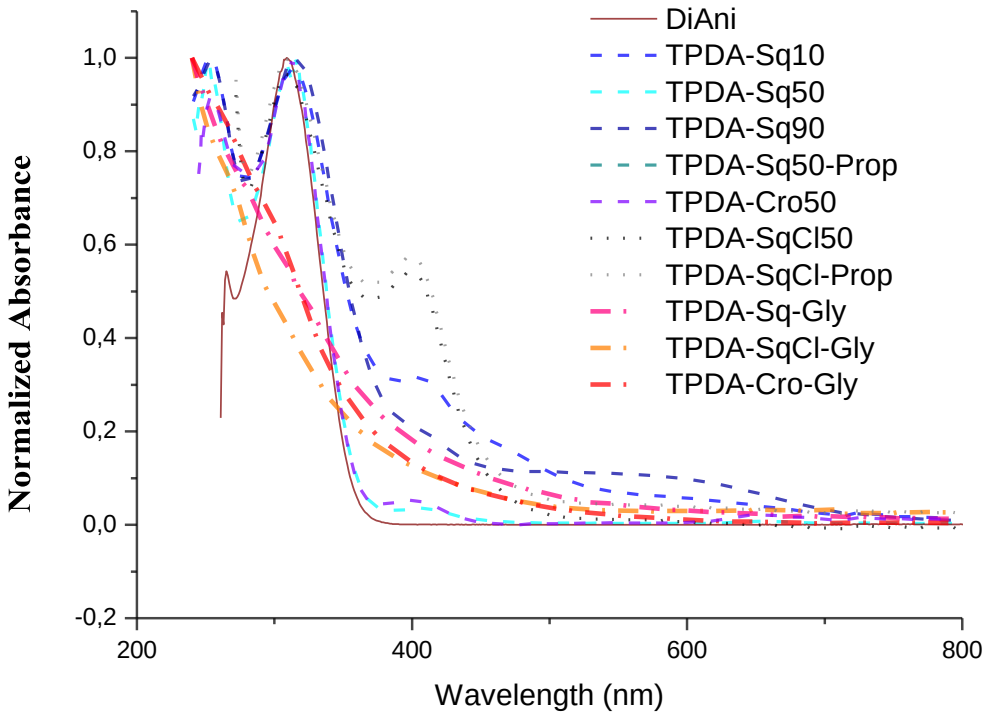

Figure 3-12: Absorption spectra of different polysquaraïne and polycroconaïne prepared using various solvents and mixtures (measured in solution in $CHCl_3$)

As previously shown, the different polymers exhibit different absorptions, depending on the solvent used. The use of propanol instead of butanol doesn't seem to impact the polymer absorption. It is noteworthy that polymers prepared from glycerol-based solutions gave different absorption behavior as compared to mono-alcohol solvent. The emission of such polymers is shown in Figure 3-13 below.

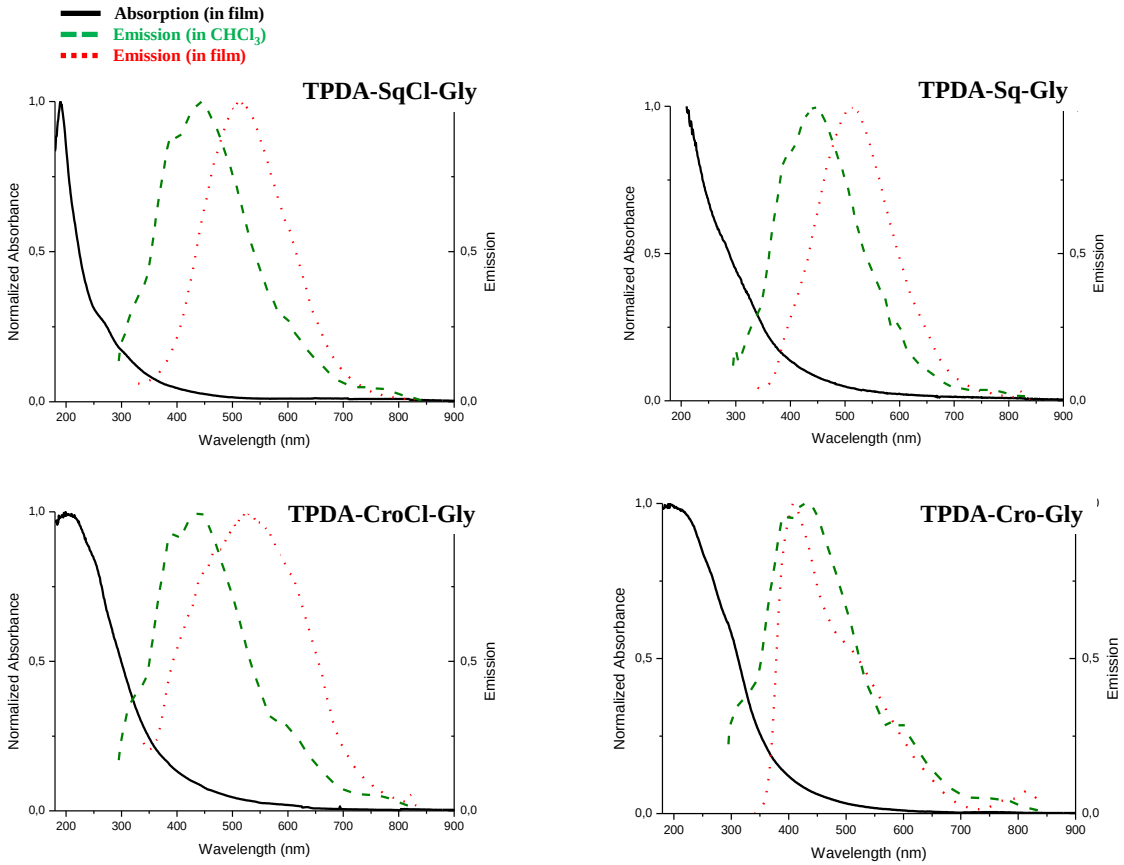

Figure 3-13: Absorption (black, plain, film) and emission spectra (red, dot, film and green, dash, in solution in $CHCl_3$) of the four glycerol based polymers.

A broad emission was also observed in all cases, all together with a noticeable Stoke shift which is a key feature for further use in OLED devices. This allow to avoid reabsorption phenomenon of the polymer emission by the polymer itself.

Therefore, we did focus on the study of the polymerization reaction in presence of glycerol. Indeed, as shown below, (see Scheme 3-9) the presence of alcohol functions on glycerol allows for its reaction with squaric acid monomer.

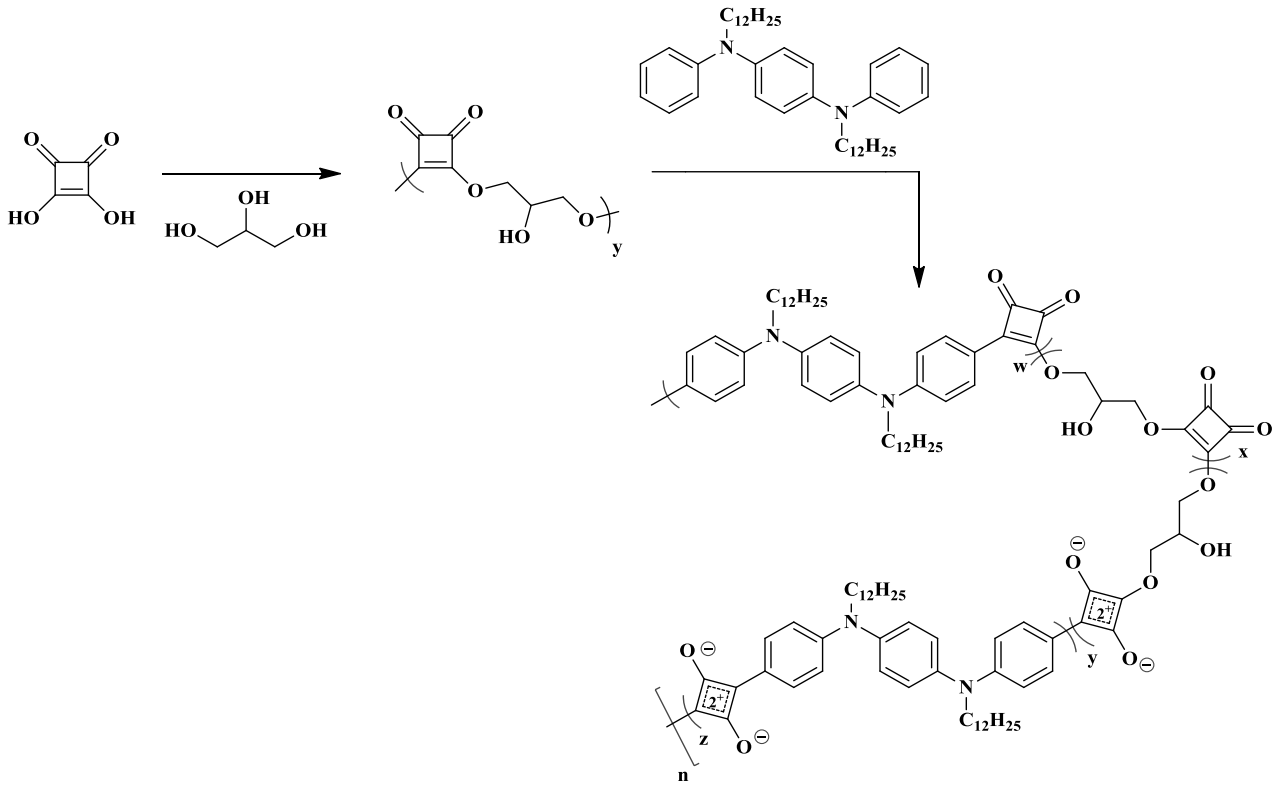

Scheme 3-9: Propose structure of the new random polymer based of squaric acid, glycerol and TPDA monomer.

It can thus be proposed the formation of a random copolymer between glycerol, squaric acid and **TPDA**. Glycerol insertion can be observed by fluorescence (broad emission due to a rupture in the conjugation) or TGA (different degradation temperature). Characterization by NMR was also performed in order to attest such structure (Figure 3-14).

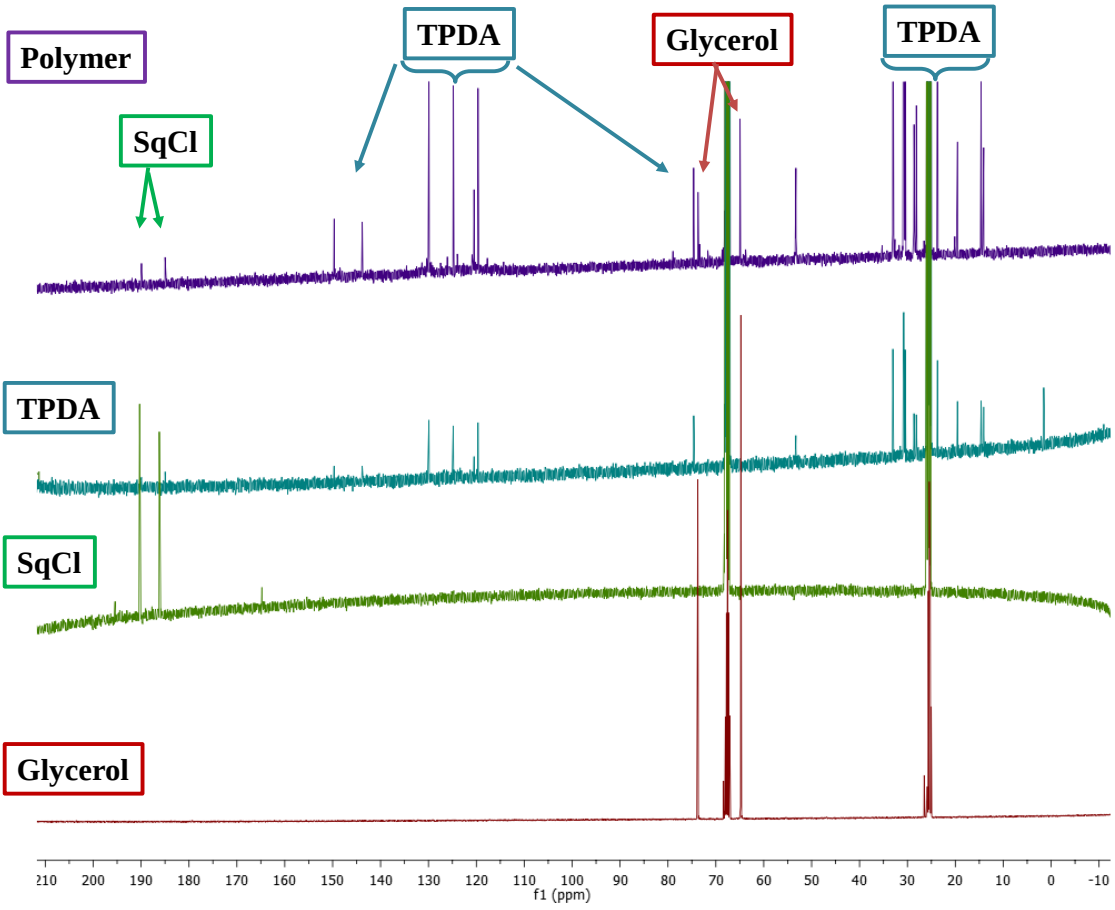

Figure 3-14: ^{13}C NMR (101 MHz) spectra of polysquaraines and monomers (example of TPDA-SqCl) in solution in THF-d_8

The polymer spectrum shows all signals corresponding to the different monomers without significant chemical shift. In addition, we have checked that the secondary alcohol function didn't react during polycondensation reaction as evidenced by the good solubility of final polymer in $CHCl_3$ or DMF and by ATR-FTIR (see experimental part). To confirm the link between the compounds, it could be interesting to perform a DOESY NMR.

In the continuation of this work, we wanted to take advantage of the reactivity of diols with squaric acid monomer to investigate the formation of various polymer structures thus by playing with different diol molecules.

3.3.4.3. Investigation of various alcohol as comonomers and modification of alcohol ratio.

A series of diols were tested as co-solvent or as comonomer in the polycondensation reaction between **TPDA** and squaric acid. (Table 3-4).

Monomer	Name	First solvent (volume %)	Second solvent (volume % or equivalent)	T_d[a]
Sq + TPDA	**TPDA-Sq50-PropDiol**	Toluene (50%)	1,3-Propanediol (50%)	426°C
	TPDA-Sq50 (Table 3-3)	Toluene (50%)	Butanol (50%)	372°C
	TPDA-Sq-Pent	Toluene (50%)	Pentanol (50%)	353°C
	TPDA-Sq-Dod	Toluene (50%)	Dodecanol (50%)	387°C
	TPDA-Sq-PEG	Toluene (50%)	PEG 10.000 $g.mol^{-1}$ (50%)	/
	TPDA-Sq-PropDiol-1eq	Toluene (100%)	Propanediol (1 eq)	/
	TPDA-Sq-PropDiol-2eq	Toluene (100%)	Propanediol (2 eq)	366°C 459°C
	TPDA-Sq-PropDiol-3eq	Toluene (100%)	Propanediol (3 eq)	367°C 425°C
	TPDA-Sq-PropDiol-10eq	Toluene (100%)	Propanediol (10 eq)	431°C

Table 3-4: Study of various alcohol solvents in the polycondensation between squaric acid and TPDA. [a]Obtained by TGA under N_2 at 10 °C min^{-1}.

As observed previously, all these polymers present a degradation temperature above 350°C. For the polymer synthesized with a few amount of propanediol, two degradation temperatures are observed, which is not the case when the amount of alcohol increases. This may be due to the presence of a mixture of chains without alcohol in their backbone and some random copolymer.

3.3.4.3.1. Effect of the solvent

In the case of PEG, for solubility reasons, no polymer are obtained. All other combinations allowed to obtain polymers that have been characterized by UV-Vis spectroscopy (Figure 3-15).

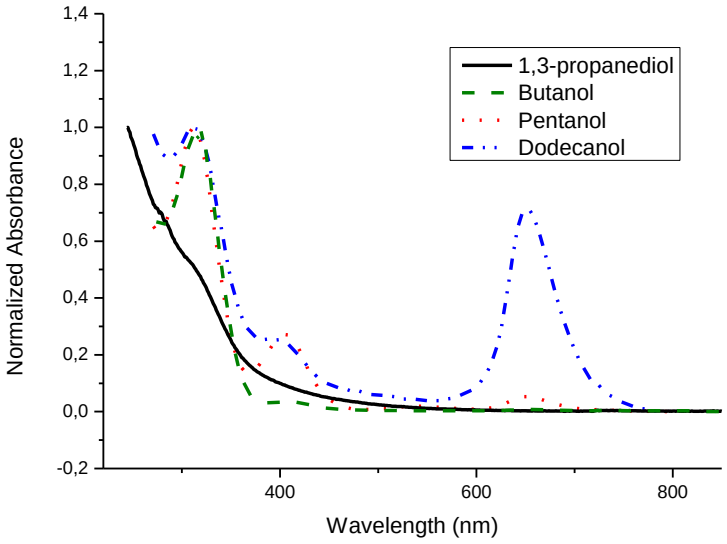

Figure 3-15: Absorption spectra of polymers synthesized with different alcohols as solvents (measured in $CHCl_3$).

The two absorptions peaks present at 255 nm and 310 nm are still observed except for the polymer synthesized with the 1-3 propanediol. However, the relative intensity of signals at 405 nm and 650 nm, which respectively correspond to 1-2 and 1-3 linkages are impacted by the solvent used. Longer is the alkyl chain, higher is the amount of 1-3 linkage in the chain. This may be due to the fact that during the condensation reaction, when a shorter alcohol is use, the kinetic pathway is favored, the propanolate being a better leaving group than the dodecanolate group. Moreover, the polymer synthesized with 1-3 propanediol as solvent doesn't exhibit clear absorption peak at wavelengths above 350 nm, meaning that the previously observed absorption at 400 nm and 650 nm are due to chromophore combining squaric acid and **TPDA** monomers (Figure 3-16).

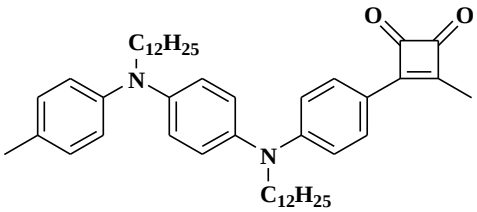

Figure 3-16: Probable structure of the chromophore sub-unit at the origin of the 400 nm absorption.

Moreover, the signal corresponding to the 1,2 linkage isn't observed on the FTIR spectra (see experimental part, Figure 3-66).

Another observation is that longer is the alcohol, higher is the absorption at high wavelength, which means that the absorption properties can be tuned toward near-IR only by changing the solvent used during the polymerization.

Then, 1,12-dodecanediol and 1,5-pentanediol have been used as co-solvent with toluene during the polymerization. Interestingly, similar results have been obtained in terms of optical properties. This may be due to a lower reactivity of longer alcohol toward the squaric acid greatly limiting the longer alcohol chain insertion. However, the reaction performed with 1,4-butanediol didn't allow to obtain polymers.

The impact of the solvent ratio added in the polymerization medium has then been studied.

3.3.4.3.2. Effect of the solvent ratio

The polymerization has then been performed in toluene, with different ratio of 1-3 propanediol, from one to ten equivalents, in order to "control" the amount of alcohol inserted in the chain (Scheme 3-10).

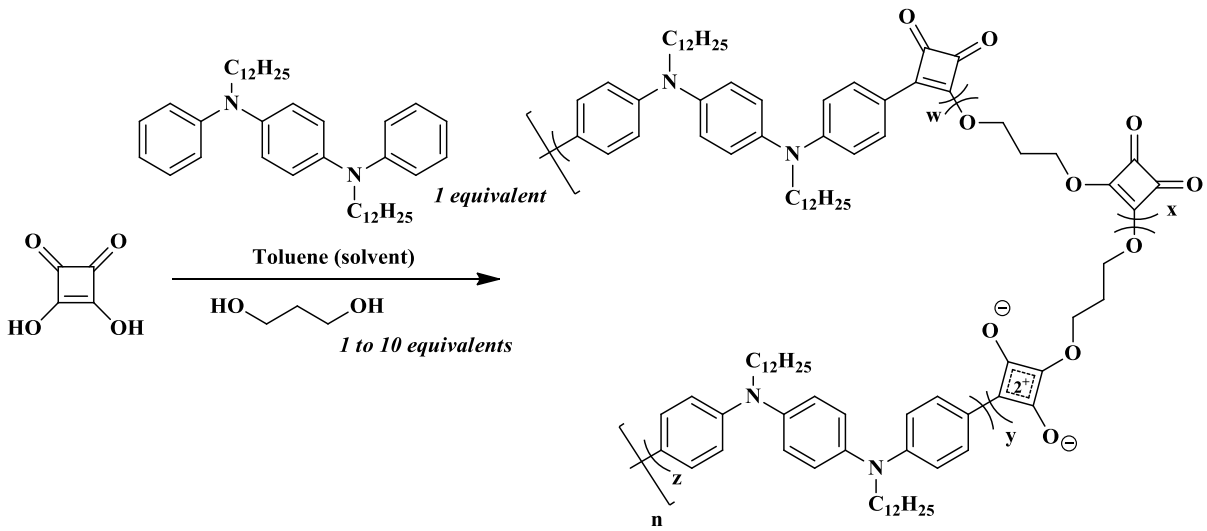

Scheme 3-10: Polymerization between squaric acid and TPDA in the presence of various amount of 1,3 propanediol from 1 to 10 equivalents.

With only 1 equivalent of propanediol the reaction isn't working due to the lack of solubility of the squaric acid. The addition of 1-butanol to solubilize the monomer leads to the same polymer obtained without the insertion of any diol. The polymerization was followed by UV-Vis spectroscopy (Figure 3-17).

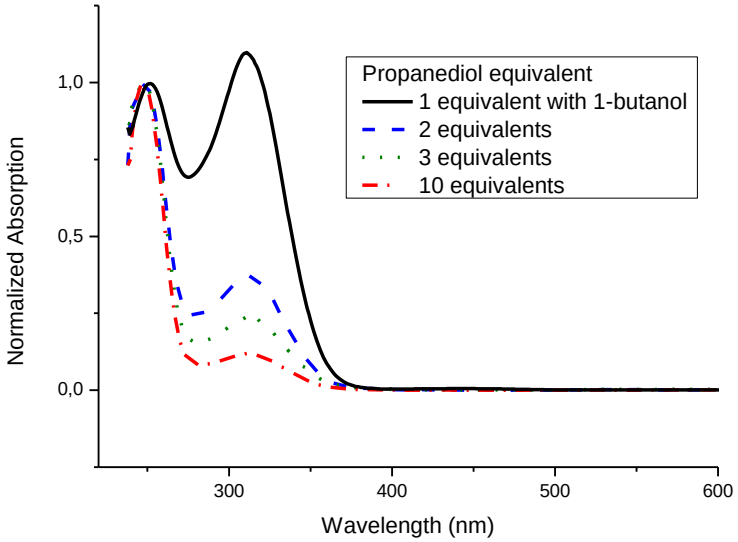

Figure 3-17: Absorption spectra of the four polymers (TPDA-Sq-PropDiol-Xeq) synthesized with a little amount of 1-3 propanediol in toluene (measured in CHCl3).

It's interesting to note that with the increase of propanediol added in the medium, the signal at 320 nm decreases, the absorption spectra of polysquaraines being more and more similar with the ones obtained with the glycerol. This can be due to the increase of the insertion of propanediol in the polymer chain at the expense of **TPDA** moiety. Moreover, the polymer doesn't show any absorption at higher wavelength than 350 nm, which confirms the first results obtained when the propanediol was used as a solvent. It can be noticed that the diol is inserted in the polymer backbone affecting the optical properties. Moreover, a large amount of diol is needed to achieve such insertion.

The emissions spectra of these polymers have been measured (Figure 3-18).

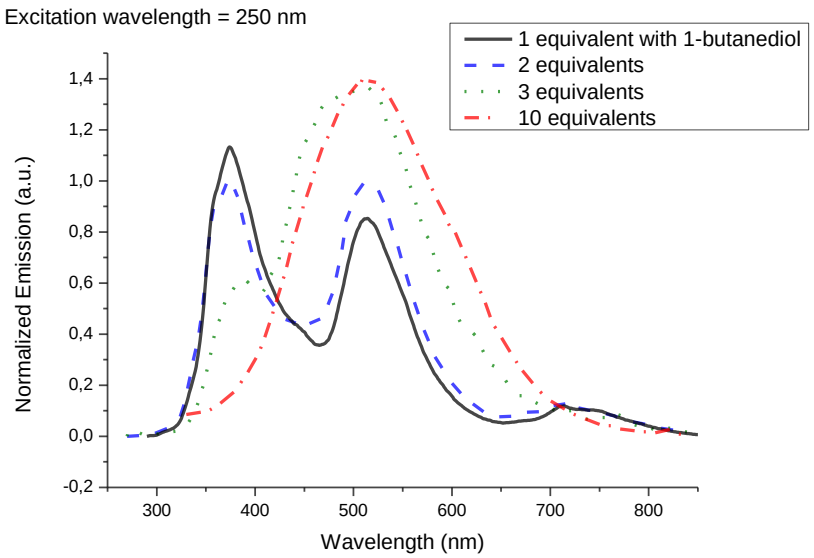

Figure 3-18: Emission spectra of the four polymers (TPDA-Sq-PropDiol-Xeq) synthesized with various amount of 1-3 propanediol in toluene (excited at 250 nm, measured in $CHCl_3$).

At low excitation wavelength, two emission peaks are present, one centered at 375 nm and the other at 510 nm. With the increase of propanediol added in the reaction mixture, the absorption at 510 nm increases and broadens, leading to the broad emission previously observed with 10 equivalents of propanediol added. Polymers synthesized with an excess of glycerol and propanediol present a broad emission, which could be of interest for further investigation in optoelectronic devices.

3.4. Toward integration in OLED

3.4.1. Optical and electrochemical characterization

Polysquaraines and polycroconaines incorporating glycerol subunits were first characterized by evaluating their emission spectra at various excitation wavelengths (Figure 3-19).

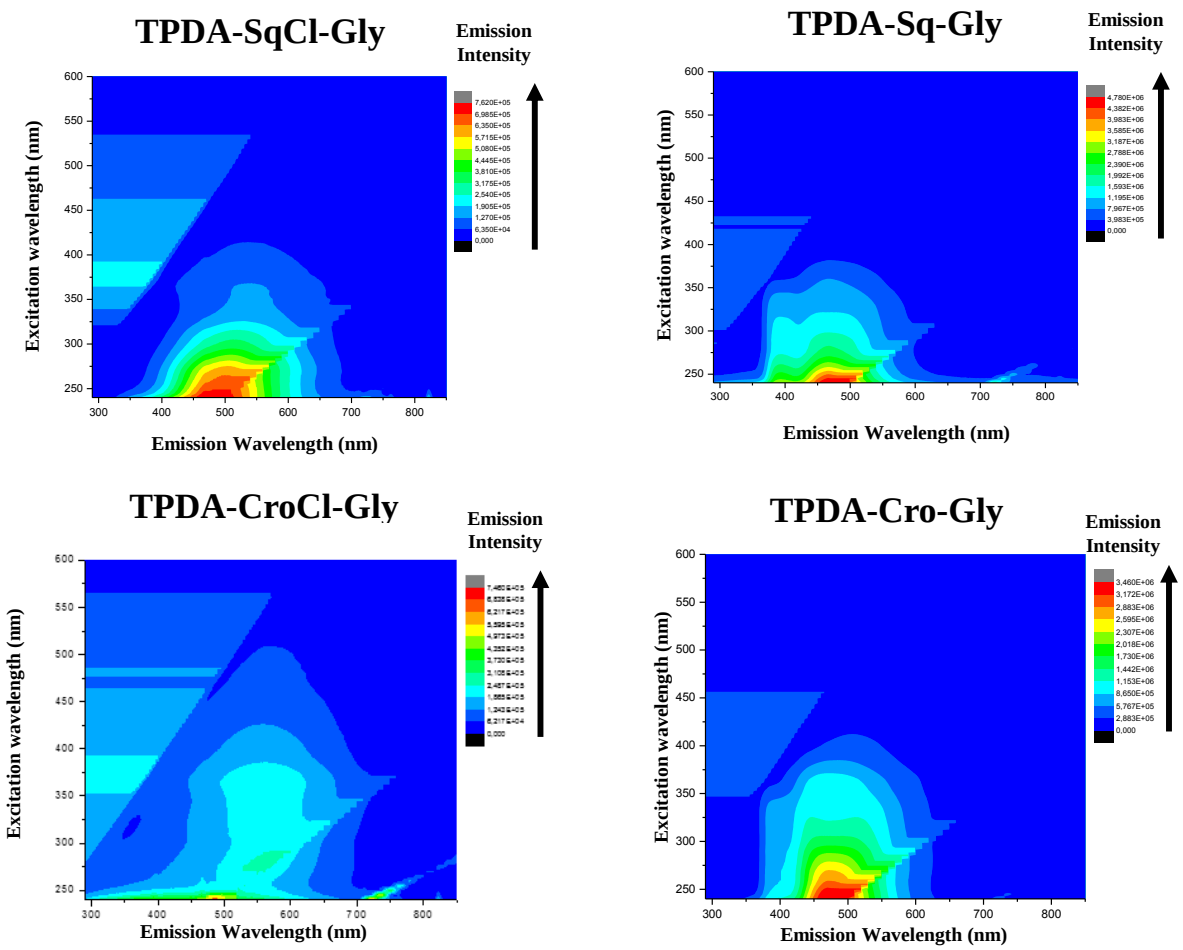

Figure 3-19: Emission spectra of the four glycerol based polymers at different excitation wavelengths (measured in $CHCl_3$)

The Y axes correspond to the excitation wavelength, the X to the emission wavelength (for one excitation) and the color corresponds to the emission intensity from blue (low emission) to red (strong emission). These 3D spectra give us information on the optimum excitation wavelength in order to obtain the more intense and broader emission. For all these polymers, the optimum excitation wavelength is between 220 and 250 nm.

Further optical characterizations were carried out using an integration sphere giving rise to the determination of the quantum yield and the chromaticity coordinates (according the CIE 1931 color space) (Table 3-5).

Compound	External Quantum Yield	Chromatic situation in X	Chromatic situation in y
TPDA-Sq-Gly	16.5 %	0.25	0.28
TPDA-SqCl-Gly	17.5 %	0.27	0.32
TPDA-Cro-Gly	16 %	0.23	0.26
TPDA-CroCl-Gly	17 %	0.26	0.28
Ideal white	/	0.33	0.33

Table 3-5: Chromaticity coordinates and quantum yields of the four polymers synthesized in glycerol, measured at $5x10^{-3}$ $g.L^{-1}$ (in $CHCl_3$) at an excitation wavelength of 275 nm.

The excitation wavelength chosen is higher than the optimum previously determined to avoid solvent interferences. The external quantum yield was found high enough for further development of these materials in devices. Moreover, for all the polymers obtained, their emission is close to a white emission in the CIE 1931 color space chromaticity diagram, the white having for coordinates (0.333;0.333). In fact, the one synthesized with the **SqCl** monomer, the **TPDA** and integrating glycerol in the chain is the closest to a white emission with its coordinate at (0.27;0.32) (Figure 3-20).

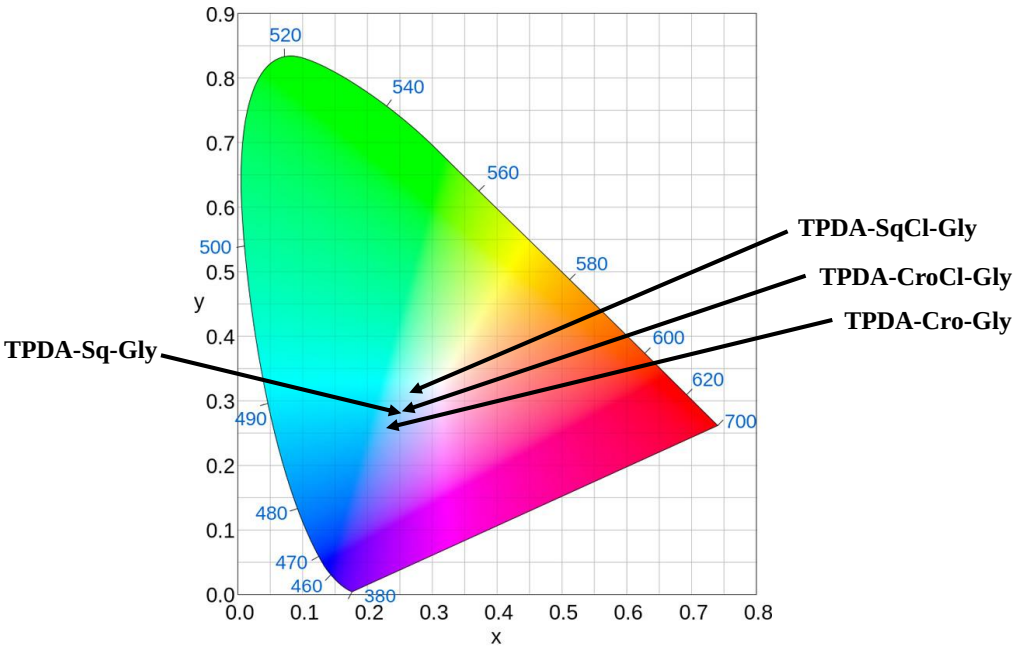

Figure 3-20: CIE 1931 color space chromaticity diagram showing coordinates of polymers synthesized using glycerol as solvent.

All polymers present a bluish emission in solution; however by performing the measurement in film, a red-shift of the emission can be expected, moving the emission toward the white light.

The more promising polymer in term of emission, the **TPDA-SqCl-Gly**, was investigated further in OLED devices. Priorly we have carried out cyclic voltammetry analysis in order to determine its HOMO and LUMO energy levels. The oxidation and reduction voltammograms (before calibration with ferrocene) are shown below (Figure 3-21).

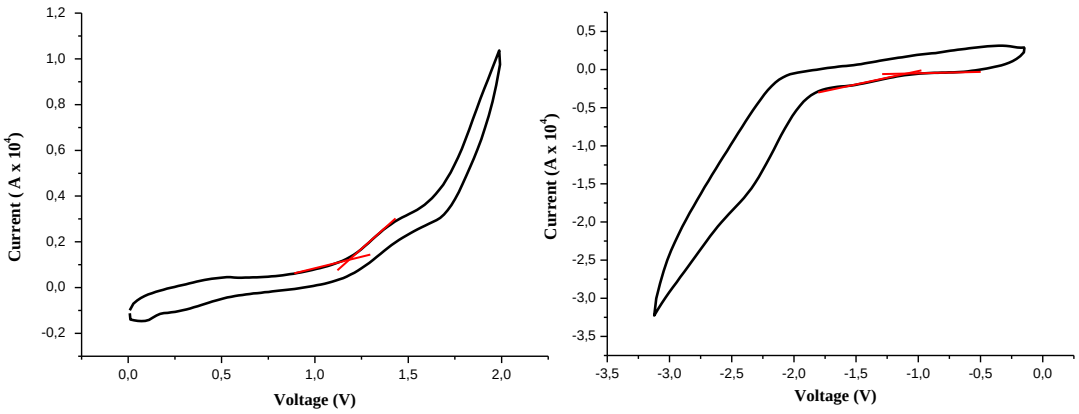

Figure 3-21: Cyclic voltammograms of TPDA-SqCl-Gly in CH_2Cl_2 solution (0.1 g.l^{-1} with $TBAPF_6$ as electrolyte); left-oxidation; right-reduction.

From the oxidation trace, E_{Ox} was determined at 1.2 V. Regarding the reduction curve, two reductions are noticeable, respectively at -1.15 V and -1.9 V corresponding to respectively the first reduction and the formation of di-anionic species.
HOMO and LUMO energy levels were thus deduced from the equations bellow taking into account the ferrocene calibration.

$$E_{HOMO}(eV) = -(E_{Ox}\ (V) + 4.4)$$
$$E_{LUMO}(eV) = -(E_{Red}\ (V) + 4.4)$$

Where 4.4 corresponds to the energetic position of the potential $E_{1/2}$ for the ferrocene/ferrocene+ (Fc/Fc+) redox couple, estimated from a ferrocene solution in chloroform using saturated calomel electrode as reference.[39,40]
The HOMO and LUMO levels for this polymer are respectively at -5.16 eV and -2.81 eV giving an electronic gap of 2.35 eV.
Investigation of the polymer showing a white emission in an OLED device was further performed..

3.4.2. Integration into OLED

In order to achieve a working OLED, energy levels of various materials have to be positioned in an appropriate way, to allow efficient electrons and holes hopping (Figure 3-22).

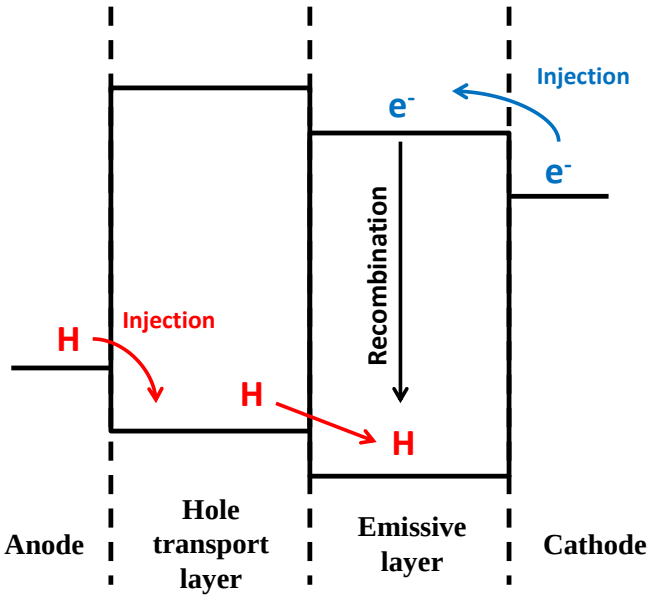

Figure 3-22: Energy level diagram for an OLED architecture.

ITO is conventionally used as the transparent anode (to inject holes)[41]. On the top of it, a layer of PEDOT-PSS (40-50 nm) has been added as electron blocking layer to improve the OLED efficiency. Then, the **TPDA**-SqCl-Gly (50 nm) has been spin-coated, followed by Calcium (20 nm) and Aluminum (100 nm) as cathode. Structure of the OLED designed in this work is shown in Figure 3-23.

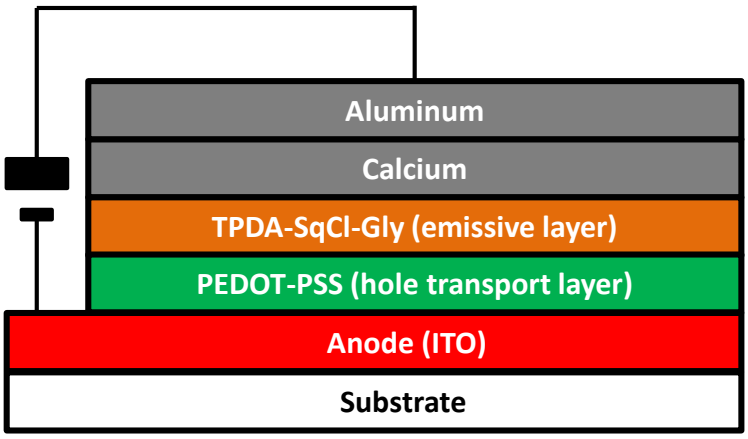

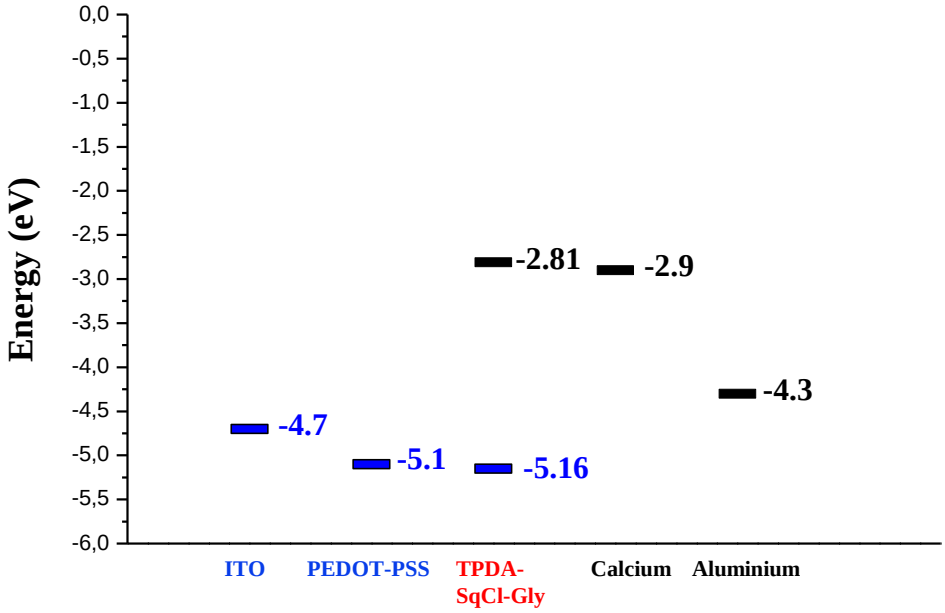

Figure 3-23: General structure of an OLED designed in this work (top) and energetic levels (bottom).

The first test performed on the OLED was a visual test. A picture was taken during operational OLED (Figure 3-24). The emission is stable during measurements (~1 hour).

Figure 3-24: Picture of the white OLED made from TPDA-SqCl-Gly copolymer, taken at 15V.

Once inserted into the integration sphere, much information can be obtained (Table 3-6).

OLED	Turn on voltage	Power efficiency ($lm.W^{-1}$)	Luminous flux (lm)	Chromaticity coordinate CIE 1931 (x;y)	Chromaticity coordinate CIE 1960 (u;v)	CCT (K)	CRI	Maximum emission wavelength (nm)
Best OLED	6V	$7.7x10^{-6}$	$6.1x10^{-6}$	0.359 ; 0.340	0.226 ; 0.321	4350	93	566
Average on 5 OLED	13V	$2.8x10^{-6}$	$2.3x10^{-6}$	0.368 ; 0.355	0.226 ; 0.326	4050	91	570

Table 3-6: Main characteristics of the OLED with TPDA-SqCl-Gly polymer as active layer (measured in an integration sphere).

The turn on voltage is at an average of 13V which is relatively high for organic materials, which can be due to the different layers roughness, especially the polymer one, which needs to be optimized.[42] The active layer roughness and thickness has been checked by AFM (see experimental part, Figure 3-25). The film thickness is around 90 nm and present defect with a thickness of 40 nm.

The power efficiency and luminous flux are two dependent values that are quite low (Figure 3-25). This can be due to some thickness irregularity spotted on the OLED surface or to losses, mainly due to surface plasmon (the thickness of the different layers being low).[43]

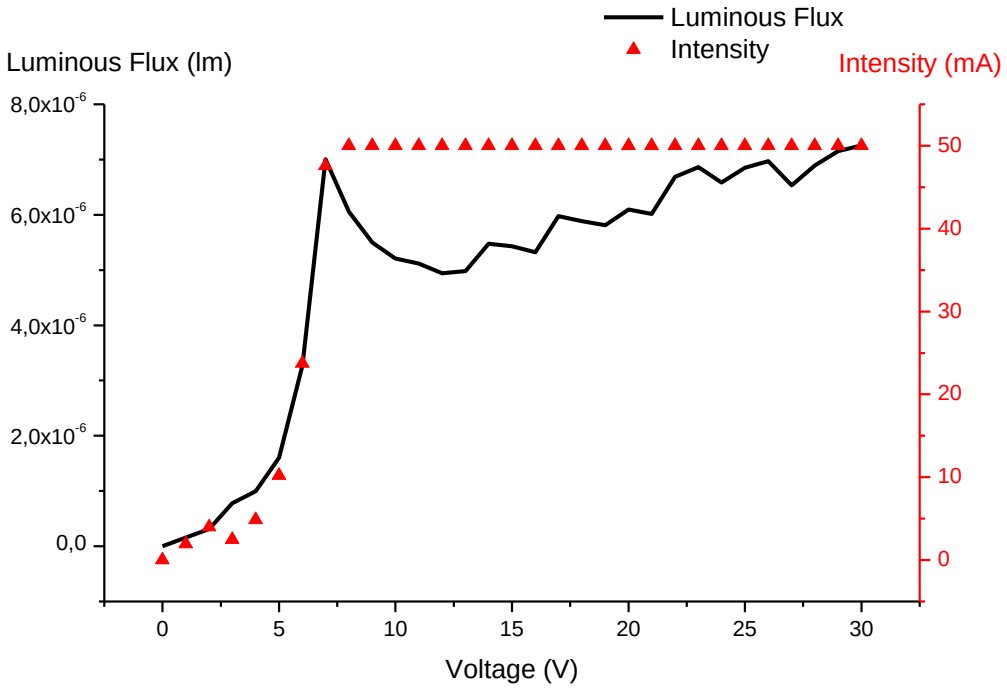

Figure 3-25: OLED luminous flux and intensity in function of the voltage applied.

However, the OLED shows a conventional IV curve until saturation. Furthermore, all color indicators proved than the light emitted is white.

Both the CIE 1931 and CIE 1960 color space show a white color. Moreover, their Correlated Color Temperature (CCT) of 4455K is coherent with the white emission. The x;y coordinate obtained during the measurement belongs to the CIE 1931 color space. In order to integrate them in the CIE 1960 color space, which integrates the CCT, a conversion can be performed according the two following equations:[44]

$$\mathbf{u} = \frac{4x}{-2x+12y+3} \quad \mathbf{v} = \frac{6y}{-2x+12y+3}$$

It's now possible to situate the OLED on both diagrams (Figure 3-27).

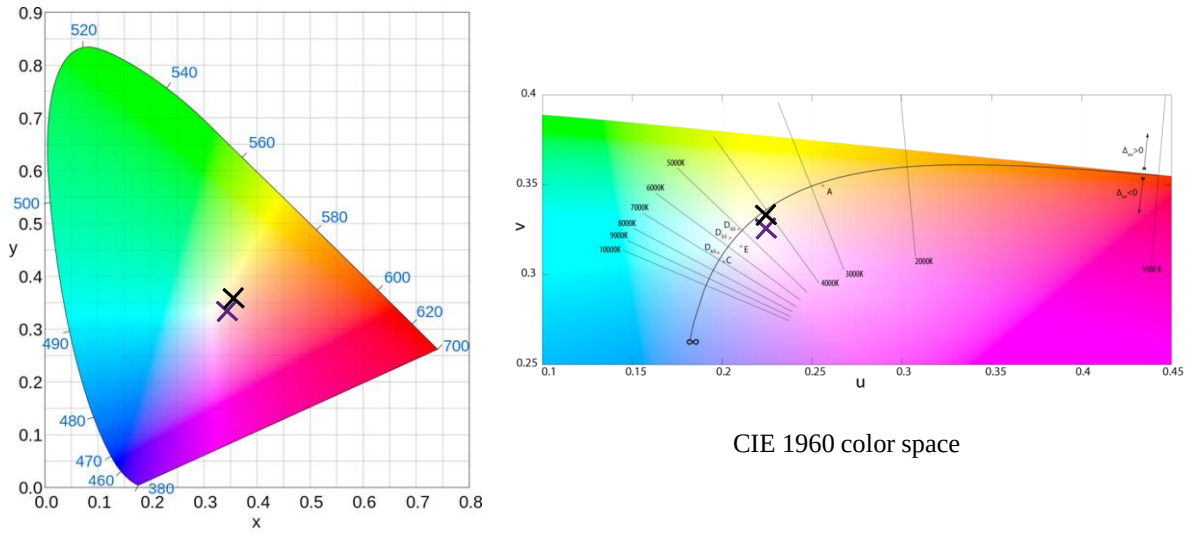

CIE 1931 color space

CIE 1960 color space

Figure 3-26: CIE 1931 color space chromaticity diagram (left) and CIE 1960 color space chromaticity diagram (right) showing coordinates of the OLED emission with TPDA-SqCl-Gly as active layer (black) and "ideal white" (purple).

The average emission of the OLED tested is white, slightly reddish. The best OLED obtained in term of color presents an almost pure white emission.
Finally, the Color Rendering Index (CRI) reached a value of 92 (versus a maximum of 100) which means that objects lighten by this OLED will almost appear under the same color as if they were lighten by an "ideal" natural light. This value is really high (if not the highest) for one single polymer based white OLED. Moreover, compared to commercial white OLED, it shows an emission covering the whole spectrum.[45]

3.5. Conclusion

New squaraine and croconaine based conjugated polymers and random co-polymers have been synthesized *via* metal-free polycondensation.

By modifying the squaric acid, a reference has been synthesized in order to relatively quantify the amount of one linkage compared to the other allowing a better understanding of the structure-properties relationship. Optical properties have also been modified by changing the solvent used during the polymerization, leading to polymers presenting for example near-IR absorption. A specific role was attributed to the co-solvent, for instance the glycerol. Thus, by using difunctional alcohol as co-solvent, statistic copolymers have been synthesized. They showed an absorption at low wavelength and a white emission centered around 450 nm in solution and 550 nm in film which means that they present a large Stoke-shift which is promising for their integration into emitting devices.

Finally, one of the co-polymers has successfully been integrated into OLED. Preliminary studies showed an OLED with a white emission, and high CRI. However, the luminescence and power efficiency are very low. In order to improve the efficiency, different option exist. One of them is the improvement of the film uniformity to improve contact between the different layers. Another possibility is to modify the OLED architecture, adding for example an electron transport layer (such as TiO_2), improving the electron transfer from the cathode to the emitting layer. Another option is to use a diffuser film which could help with the light extraction efficiency. From chemical point of view, a fine tuning of the polymer structure can be considered, as much as doping the polymer. All these options should be investigated in the lab, as well as the integration in devices.

3.6. References

[**1**] J. D. Park, J. R. Lacher, J. D. Park, *Journal of the American Chemical Society*, **1959**, *81*, 3480.

[**2**] U. Noster, B. M. Hausen, B. Krische, K. H. Schulz, *Contact Dermatitis*, **1976**, *2*, 99.

[**3**] T. Yoshimasu, F. Furukawa, *Autoimmunity Reviews*, **2016**, *15*, 8.

[**4**] S. Pandey, E. N. Wilmer, D. S. Morrell, *Pediatric Dermatology*, **2015**, *32*, 85.

[**5**] M. Sameiro, T. Gonçalves, *Chemical Reviews*, **2009**, *109*, 190.

[**6**] D. Ramaiaht, A. Joy, N. Chandrasekhar, N. V Eldho, S. Das, M. V George, *Synthesis*, **1997**, *65*, 783.

[**7**] D. Ramaiah, I. Eckert, K. T. Arun, L. Weidenfeller, B. Epe, *Photochemistry and photobiology*, **2004**, *79*, 99.

[**8**] W. Sun, S. Guo, C. Hu, J. Fan, X. Peng, *Chemical Reviews*, **2016**, *116*, 7768.

[**9**] R. West, Y. H. Niu, *Journal of the American Chemical Society*, **1963**, *85*, 2589.

[**10**] W. Beck, K. Sunkel, *Chemical Reviews*, **1988**, *88*, 1405.

[**11**] R. I. Geib, L. M. Schwartz, *Analytical Chemistry*, **1972**, *44*, 554.

[**12**] L. G. Cilindro, E. Stadlbauer, C. Keller, *Journal of Inorganic and Nuclear Chemistry*, **1972**, *34*, 2577.

[**13**] R. C. De Selms, C. J. Fox, R. C. Riordan, E. K. Company, D. Quadratswure, *Tetrahedron Letters*, **1970**, *10*, 781.

[**14**] R. R. Green, E. W. Neuse, *Hydrological Sciences Journal*, **1973**, *14*, 230.

[**15**] E. W. Neuse, B. R. Green, *Polymer*, **1974**, *15*, 339.

[**16**] A. Treibs, K. Jacob, *Angewandte Chemie International Edition in English*, **1965**, *4*, 694.

[**17**] N. Zugabe, O. Mol, G. Kristalle, U. Bonn, **1970**, 1.

[**18**] K.-Y. Law, F. C. Bailey, *Canadian Journal of Chemistry*, **1986**, *64*, 2267.

[**19**] S. Yasui, M. Matsuoka, T. Kitao, *Dyes and Pigments*, **1989**, *10*, 13.

[**20**] X. Song, J. W. Foley, *Dyes and Pigments*, **2008**, *78*, 60.

[**21**] E. E. Havinga, A. Pomp, W. ten Hoeve, H. Wynberg, *Synthetic Metals*, **1995**, *69*, 581.

[**22**] E. E. Havinga, W. ten Hoeve, H. Wynberg, *Synthetic Metals*, **1993**, *55*, 299.

[**23**] E. E. Havinga, W. ten Hoeve, H. Wynberg, *Polymer Bulletin*, **1992**, *29*, 119.

[**24**] E. Ronchi, R. Ruffo, S. Rizzato, A. Albinati, L. Beverina, G. A. Pagani, *Organic letters*, **2011**, *13*, 3166.

[**25**] J. K. Jeong, S. J. Choi, T. H. Rhee, N. C. Yang, D. H. Suh, *Polymer Bulletin*, **1999**, *42*, 183.

[**26**] S. F. Völker, S. Uemura, M. Limpinsel, M. Mingebach, C. Deibel, V. Dyakonov, C. Lambert, *Macromolecular Chemistry and Physics*, **2010**, *211*, 1098.

[**27**] S. Kuster, T. Geiger, *Dyes and Pigments*, **2012**, *95*, 657.

[**28**] W. Zhang, Z. Wang, Y. S. Tang, Z. G. Xu, Y. Li, Q. Jiang, *Chinese Chemical Letters*, **2010**, *21*, 245.

[**29**] J. Eldo, A. Ajayaghosh, *Chemistry of Materials*, **2002**, *14*, 410.

[**30**] J. Oriou, F. Ng, G. Hadziioannou, G. Garbay, M. Bousquet, L. Vignau, E. Cloutet, C. Brochon, *Polymer Chemistry*, **2014**, *5*, 7100.

[**31**] L. Beverina, P. Salice, *European Journal of Organic Chemistry*, **2010**, 1207.

[**32**] P. Marks, M. Levine, *Journal of Chemical Education*, **2012**, *89*, 1186.

[**33**] D. Scherer, R. Dörfler, A. Feldner, T. Vogtmann, M. Schwoerer, U. Lawrentz, W. Grahn, C. Lambert, *Chemical Physics*, **2002**, *279*, 179.

[**34**] W.-Y. Zheng, K. Levon, J. Laakso, J.-E. Oesterholm, *Macromolecules*, **1994**, *27*, 7754.

[**35**] W. S. Huang, **1993**, *34*, 1833.

[**36**] H.-C. Lu, W.-T. Whang, B.-M. Cheng, *Synthetic Metals*, **2010**, *160*, 1002.

[**37**] D. Yang, Z. Guan, L. Yang, Y. Huang, Q. Wei, Z. Lu, J. Yu, *Solar Energy Materials and Solar Cells*, **2012**, *105*, 220.

[**38**] R. C. De Selms, C. J. Fox, R. C. Riordan, *Tetrahedron Letters*, **1970**, *11*, 781.

[**39**] N. G. Tsierkezos, *Journal of Solution Chemistry*, **2007**, *36*, 289.

[**40**] C. M. Cardona, W. Li, A. E. Kaifer, D. Stockdale, G. C. Bazan, *Advanced Materials*, **2011**, *23*, 2367.

[**41**] C. W. Tang, S. A. Vanslyke, *Applied Physics Letters*, **1987**, *51*, 913.

[**42**] G. Liu, J. B. Kerr, S. Johnson, *Synthetic Metals*, **2004**, *144*, 1.

[**43**] S. Reineke, M. Thomschke, B. L??ssem, K. Leo, *Reviews of Modern Physics*, **2013**, *85*, 1245.

[**44**] D. L. MacAdam, *J. Opt. Soc. Am.*, **1937**, *27*, 294.

[**45**] Z. Wu, D. Ma, *Materials Science and Engineering: R: Reports*, **2016**, *107*, 1.

3.7. Experimental part

For general experimental informations, see the corresponding section page 235.

3.7.1. Synthesis

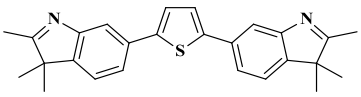

2,5-bis(2,3,3-trimethyl-3H-indol-6-yl)thiophene

5-bromo-2,3,3-trimethyl-3H-indole (1.61 g, 3.1 mmol), 2,5- bis(tributylstannyl)thiophene (2.02 g, 6.8 mmol) and tetrakis(triphenylphosphine)palladium(0) (67 mg, 0.06 mmol) were degassed via three vacuum/argon cycles, and 5 mL of a degassed toluene/DMF mixture (9:1 vol) was added under argon. The reaction mixture was refluxed under argon overnight. 10 ml of a 10%w KF aqueous solution was added, and the mixture was stirred for 1h at room temperature. The resulting white precipitate was filtered off, rinsed with toluene and the filtrate was washed three times with 20 ml of water. The organic phase was dried with MgSO4 and the solvent was removed under vacuum to give the crude product as an orange solid. A subsequent purification by flash chromatography (toluene:EtOH 96:4) followed by drying at 40°C under vacuum overnight afforded the pure compound as orange crystals (yield: 69 %).

^{1}H NMR (400 MHz, $CDCl_3$): δ (ppm) 7.59 (dd, J = 8.0, 1.8 Hz, 2H), 7.55 – 7.51 (m, 4H), 7.28 (s, J = 3.7 Hz, 2H), 2.30 (s, 6H), 1.35 (s, 12H).

^{13}C NMR (101 MHz, $CDCl_3$) δ (ppm) 188.56, 153.38, 146.62, 143.75, 131.69, 125.42, 123.97, 120.30, 118.88, 53.91, 23.28, 15.63.

FT-IR (ATR): ν= 2962, 1570, 1456, 1423, 1381, 1204, 1123, 891, 841, 828, 807, 728, 635, 589, 549 cm^{-1}.

HRMS (EI+, m/z) [M]+ calculated (%) for $C_{26}H_{26}N_2S$: 398.1817, found 398.1799.

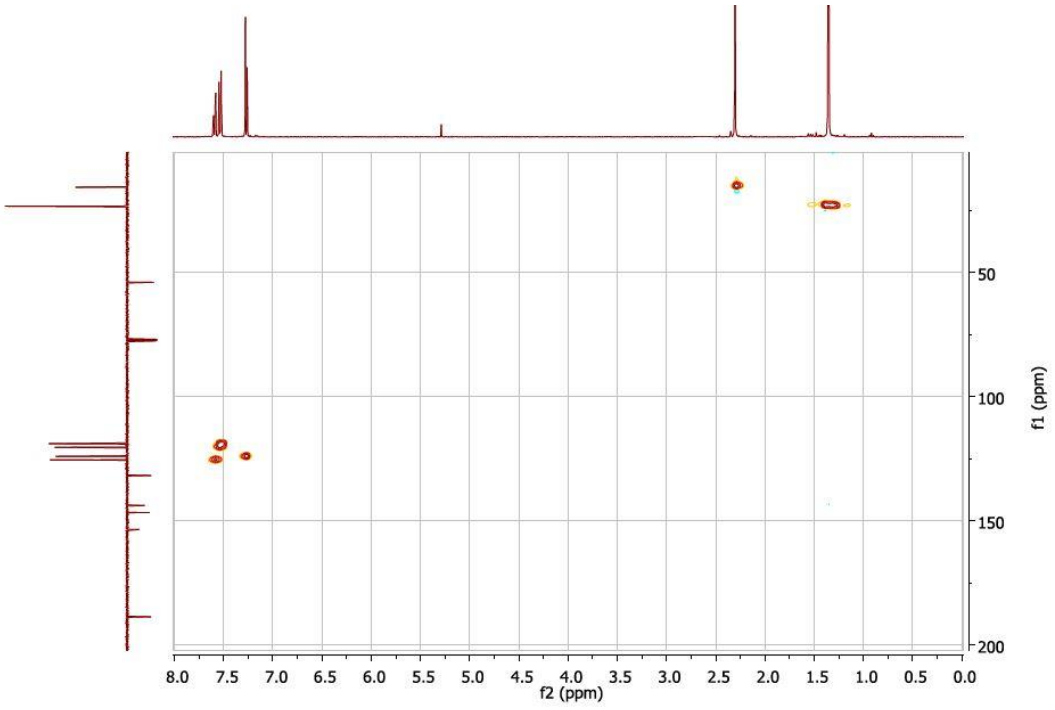

Figure 3-27: ^{1}H-^{13}C HSQC NMR of 2,5-bis(2,3,3-trimethyl-3H-indol-6-yl)thiophene (in $CDCl_3$).

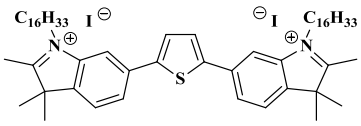

2,5-bis(1-hexadecyl-2,3,3-trimethyl-3H-indol-6-ium) thiophene diiodide

2,5-bis(2,3,3-trimethyl-3H-indol-6-yl)thiophene (0.80 g, 2.0 mmol), 1-iodohexadecane (7.03 g, 20.0 mmol) and 20 ml of nitromethane were bubbled under argon and then heated to reflux overnight. The solvent was removed under vacuum, and 50 ml of diethyl ether was added. The solution was cooled down at 5°C overnight, and a dark brown precipitate formed, which was recovered by filtration and rinsed with cold diethyl ether. The resulting solid was dried at 40°C under vacuum overnight to yield a brown powder (yield: 83 %).

^{1}H NMR (400 MHz, $CDCl_3$): δ (ppm) 7.90 (s, 2H), 7.74 (dd, *J* = 26.0, 8.4 Hz, 4H), 7.46 (s, 2H), 4.61 (t, *J* = 6.7 Hz, 4H), 3.01 (s, 6H), 1.92 (d, *J* = 6.8 Hz, 4H), 1.73 - 1.67 (m, 16H), 1.50 – 1.13 (m, 52H), 0.85 (t, *J* = 6.7 Hz, 6H).

^{13}C NMR (101 MHz, $CDCl_3$): δ (ppm) 194.80, 142.81, 142.70, 140.25, 135.99, 127.05, 126.80, 120.57, 116.51, 55.02, 50.42, 32.01, 29.79, 29.78, 29.75, 29.70, 29.62, 29.49, 29.45, 29.30, 28.19, 27.01, 23.50, 22.78, 16.77, 14.22.

FT-IR (ATR): ν=3443, 2920, 2850, 1608, 1586, 1539, 1465, 1367, 1337, 1297, 1219, 1164, 1065, 930, 805, 772, 720, 668, 538 cm^{-1}.

HRMS (EI+, m/z) [M-2H]+ calculated (%) for $C_{58}H_{90}N_2S$: 848.6981, found 846.7.

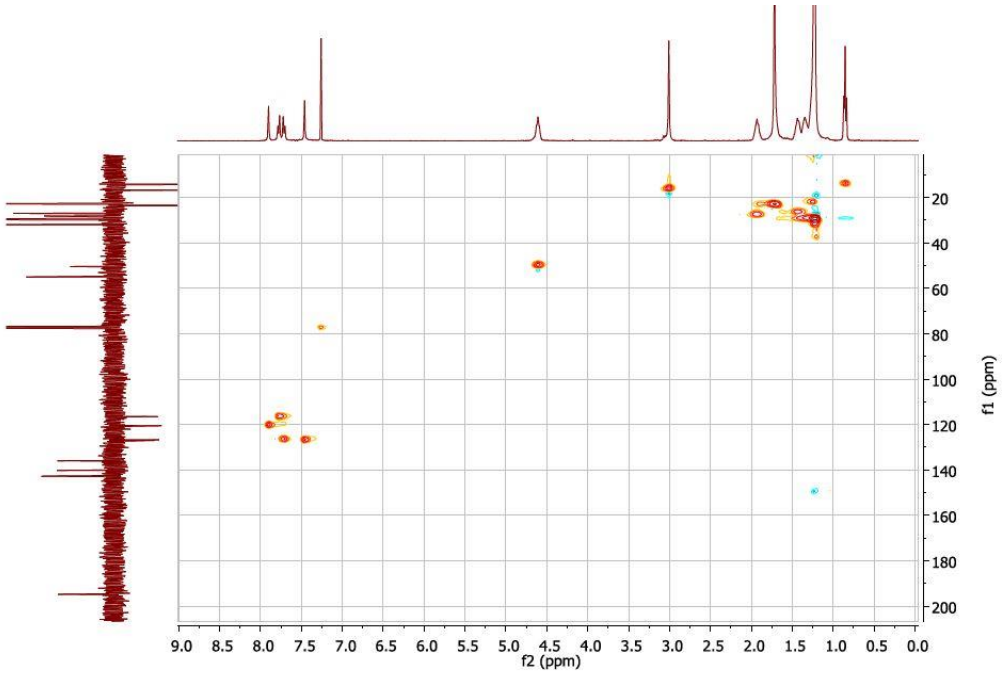

Figure 3-28: ^{1}H-^{13}C HSQC NMR of 2,5-bis(1-hexadecyl-2,3,3-trimethyl-3H-indol-6-ium)thiophene diiodide (in $CDCl_3$).

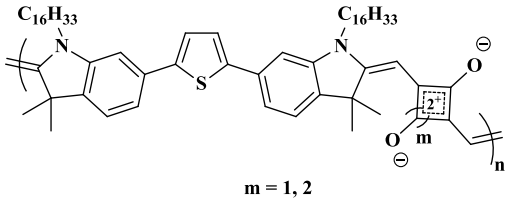

General procedure for Poly(bis(hexadecyl)squaraine-*alt*-thiophene) (m=1) and Poly(bis(hexadecyl)croconaine-*alt*-thiophene) (m=2)

2,5-bis(1-hexadecyl-2,3,3-trimethyl-3H-indol-6-ium) thiophene diiodide and squaric acid were added in a 25 ml round-bottom flask in stoichiometric amount, which was then connected to a Dean-Stark apparatus. The reaction media was degassed three times with vacuum/argon cycles, and 10 ml of a toluene/1- butanol mixture (1:1 vol, bubbled under argon) was added. Quinoline was then added and the mixture was then stirred and heated up to reflux for 3 days. Solubilization of the monomers was achieved only after stirring at reflux. A dark green color of the solution could be observed after few hours of reaction. The reaction mixture was then poured into cold MeOH/H_2O (9:1 vol) and the resulting precipitate was filtered and purified on Soxhlet apparatus with MeOH and $CHCl_3$. The $CHCl_3$ fractions was concentrated under vacuum, solubilized in a minimum amount of $CHCl_3$ and finally precipitated in MeOH/H_2O (9:1 vol). The solid was dried at 40°C under vacuum overnight.

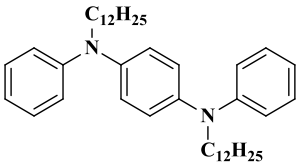

N^1,N^4-didodecyl-N^1,N^4-diphenylbenzene-1,4-diamine (TPDA)

N^1,N^4-diphenylbenzene-1,4-diamine (5.00 g, 19.2 mmol) and freshly powdered potassium hydroxide (5.39 g, 96.1 mmol) were introduced in a 500 ml round-bottom flask, and subsequently degassed *via* three vacuum/argon cycles. 200 ml of dry DMSO was then added under argon, and the mixture was stirred at 90°C for 2 H. 1-bromododecane (23.93 g, 23 ml, 96.0 mmol) was then added dropwise and the reaction was allowed to stir for 16 H. The mixture was poured in 500 mL of water, and extracted four times with 100 ml of diethyl ether. The combined organic phases were concentrated under vacuum, washed three times with 50 ml of water and dried over $MgSO_4$. The solvent was removed under vacuum. Flash chromatography (cyclohexane:ethyl acetate 95:5) followed by a recrystallization in pentane afforded the pure product as a white powder (yield: 75 %).

^{1}H NMR (400 MHz, THF): δ (ppm) 7.15 (t, *J* = 7.9 Hz, 4H), 6.95 (s, 4H), 6.87 (d, *J* = 7.9 Hz, 4H), 6.76 (t, *J* = 7.3 Hz, 4H), 3.70 – 3.62 (m, 4H), 1.71 – 1.61 (m, 4H), 1.31 (d, *J* = 19.3 Hz, 36H), 0.88 (t, *J* = 6.8 Hz, 6H).

^{13}C NMR (101 MHz, THF): δ (ppm) 149.69, 143.83, 129.89, 124.80, 120.48, 119.65, 53.28, 33.03, 30.80, 30.77, 30.74, 30.73, 30.62, 30.46, 28.62, 28.13, 23.72, 14.59. FT-IR (ATR): ν= 3038, 2916, 2848, 1594, 1494, 1467, 1358, 1256, 1143, 1094, 845, 742, 699, 612 cm^{-1}.
HRMS (EI+, m/z) [M]+ calculated for $C_{42}H_{64}N_2$: 596.5070, found 596.5080.

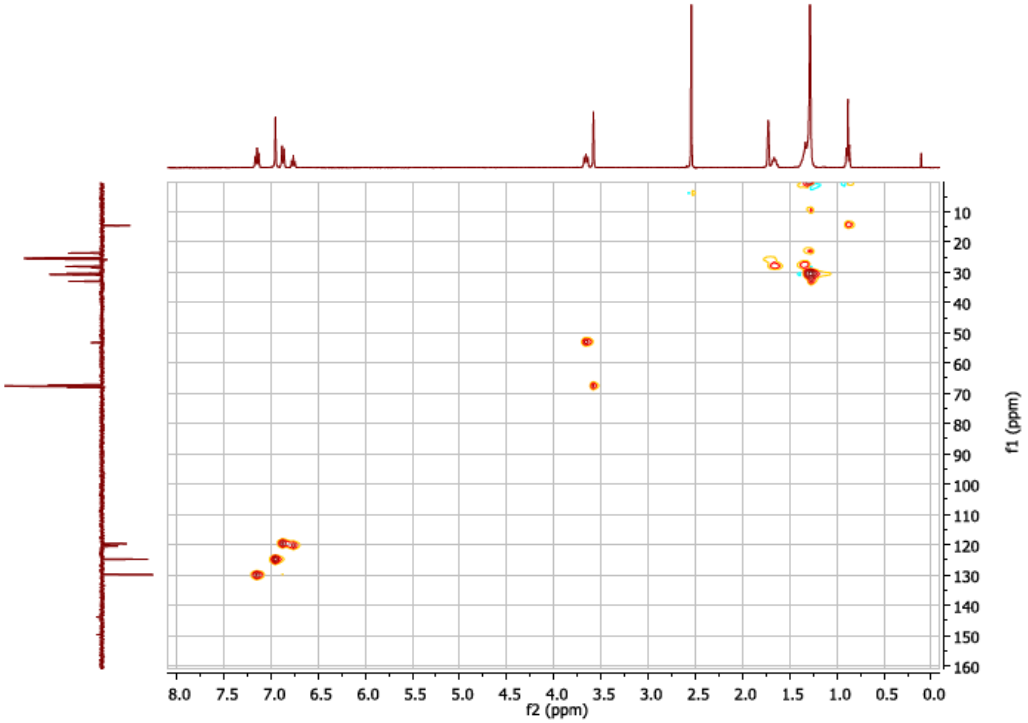

Figure 3-29: ^{1}H-^{13}C HSQC NMR spectrum of TPDA (in THF-d_8).

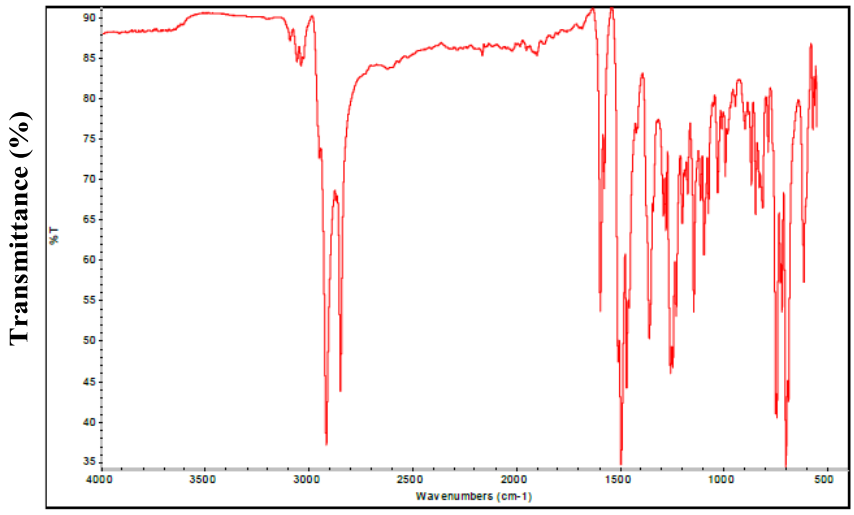

Figure 3-30: ATR-FTIR spectrum of TPDA.

1,2-dichlorocyclobutene-3,4-dione (SqCl)

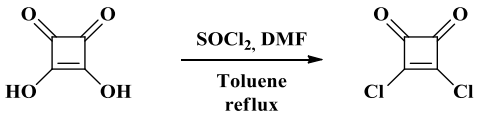

In a dried and nitrogen flushed 50 mL flask, 5 g (43.8 mmol) of squaric acid (3,4-Dihydroxycyclobut-3-ene-1,2-dione) has been solubilized in 10 mL of toluene. Then, 2 equivalents of thionyl chloride (6.36 mL, 87.7 mmol) were added as well as a droplet of DMF as catalyst (approximately 200 µL). The reaction was heated at reflux temperature for one hour before being allowed to cool down at room temperature. After evaporation of the toluene at room temperature with a small nitrogen flow, the pure yellow compound has been recovered after sublimation at 65°C under vacuum (yield: 95%)

The product doesn't present any protons, a ^{1}H NMR has been performed to confirm the absence of impurities.
^{13}C NMR (101 MHz, THF): δ (ppm) 190.12, 185.99
FT-IR (ATR): ν= 1810, 1760, 1530, 1171, 1048, 879, 736, cm^{-1}.
HRMS (EI+, m/z) [M]+ calculated for $C_4Cl_2O_2$: 150.93536, found 150.93586

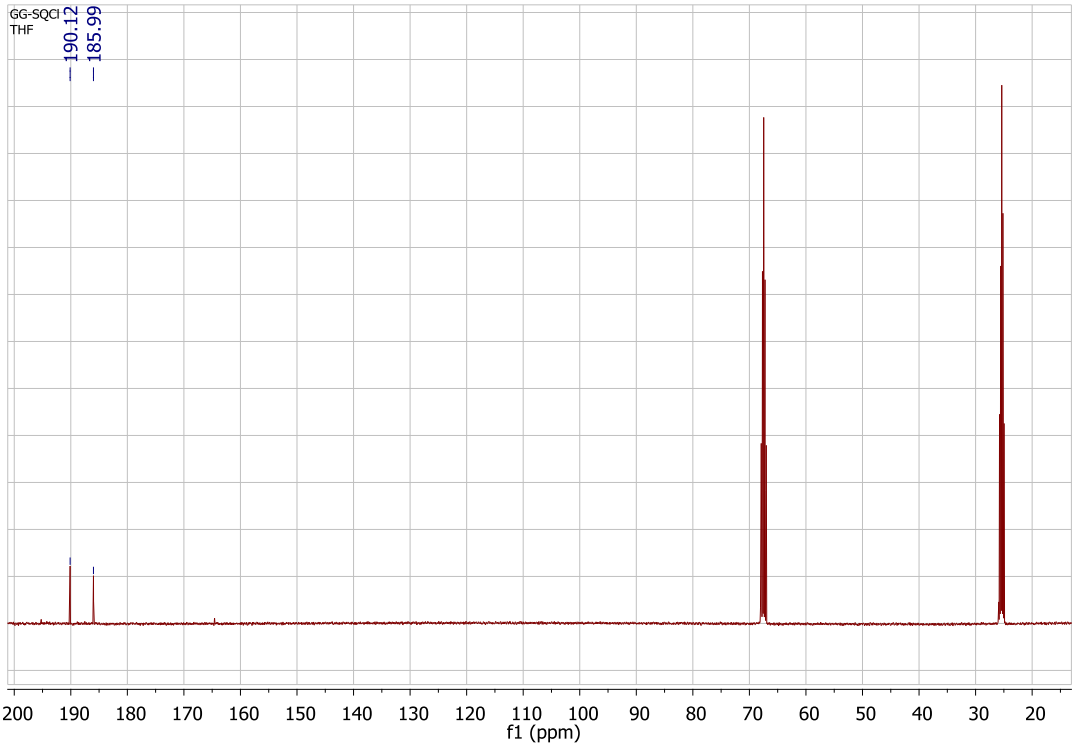

Figure 3-31: ^{13}C NMR spectrum (101 MHz) of SqCl in THF-d_8.

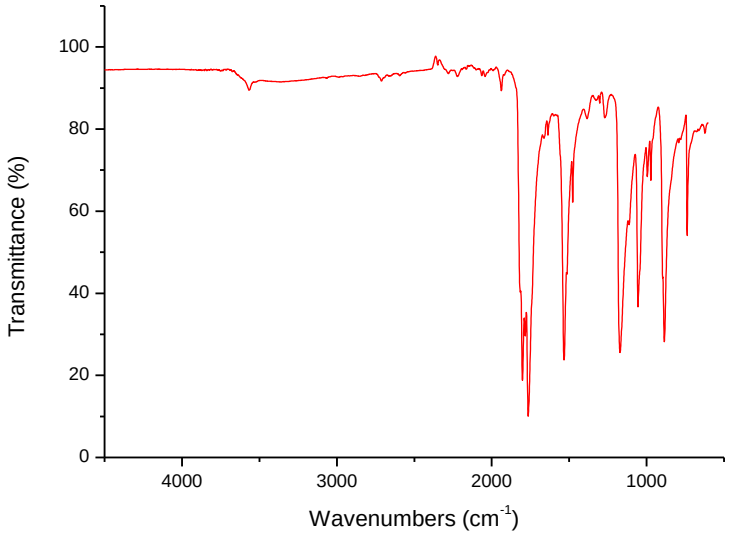

Figure 3-32: ATR-FTIR spectrum of TPDA-Sq10

General procedure polymerization.

Conventional heating

Squaric acid derivatives and **TPDA** have been added in a 25 mL flask, previously dried and nitrogen flushed. The solvent or solvent mixture (5 mL at total for a concentration of approximately 25 $mg.mL^{-1}$) has then been added and heated at reflux temperature for three days. The water formed during the polymerization has been removed thanks to a Dean-Stark apparatus.

µ-wave heating

Squaric acid derivatives and **TPDA** have been added in a 10 mL specific µ-wave glassware, previously dried and nitrogen flushed. The solvent or solvent mixture (4 mL at total for a concentration of approximately 25 $mg.mL^{-1}$) has then been added and heated at reflux temperature for four hours.

At the end of the reaction, regardless the heating method, the solvent has been evaporated under vacuum and polymers were purified using a Soxhlet apparatus using methanol and chloroform as solvent.

3.7.2. Characterization

Thickness and film roughness has been measured by AFM Dimension Fastscan, Bruker in tapping mode.

The OLED switched on at a voltage of 8V and stayed on above 30V. The intensity rapidly reaches the limitation of the source meter at 50 mA. The OLED has then been tested inside a External Quantum Efficiency Measurement System C9920-12 (HAMAMATSU) with an integration sphere and powered by a source meter and source measure unit.

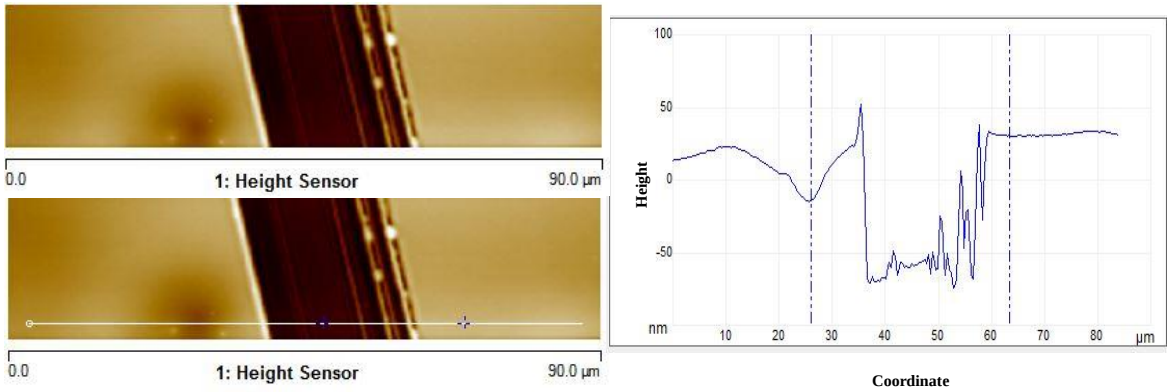

Figure 3-33: AFM picture (left) and surface profile (right) of the TDA-SqCl-Gly active layer.

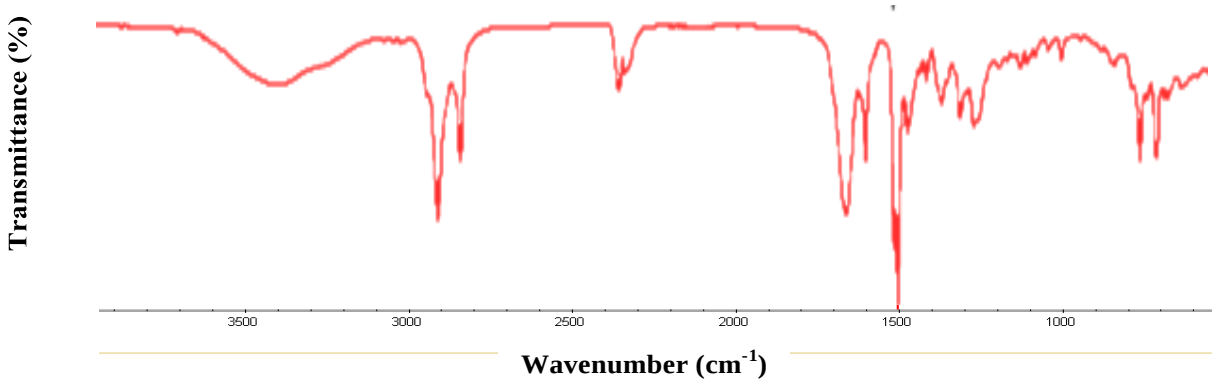

Figure 3-34: ATR-FTIR spectrum of Reference (TPDA-SqCl).

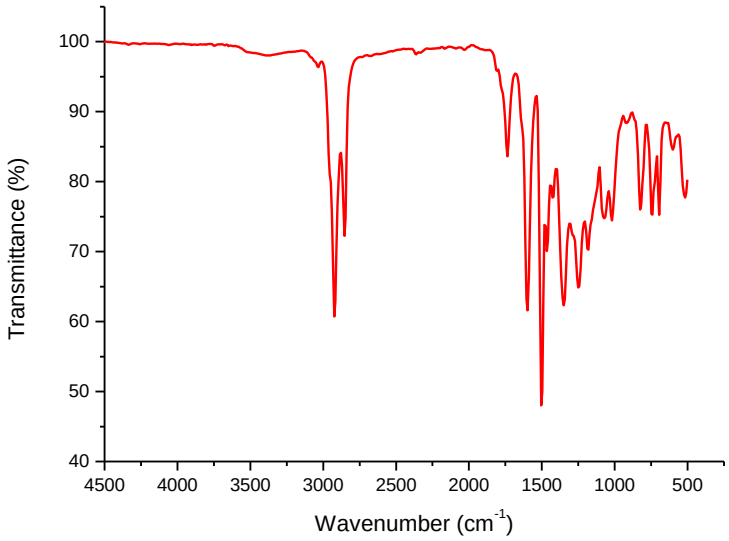

Figure 3-35: ATR-FTIR spectrum of TPDA-Sq10.

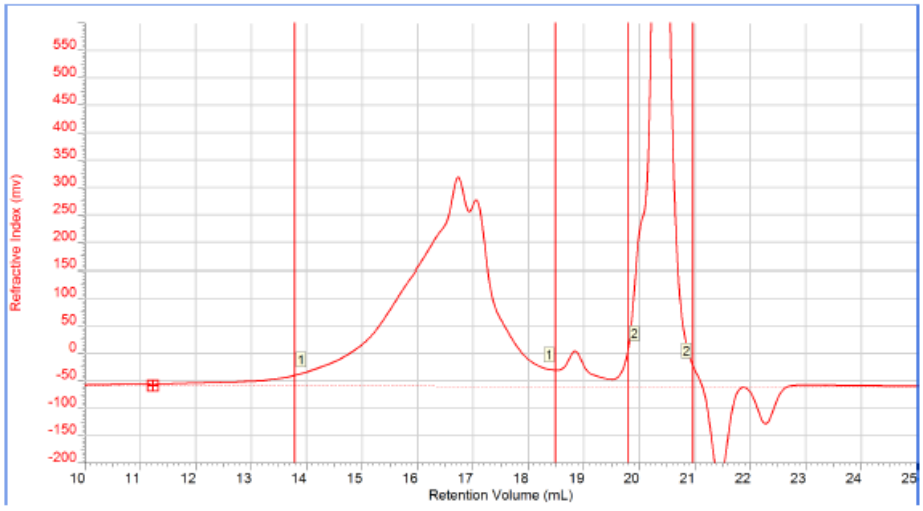

Peak	Mn	Mw	Mz	Mp	Mw/Mn	Ret Vol
1	2 476	6 752	20 470	2 706	2.727	16.720

Figure 3-36: SEC profile of TPDA-Sq10 (in $CHCl_3$, polystyrene standard).

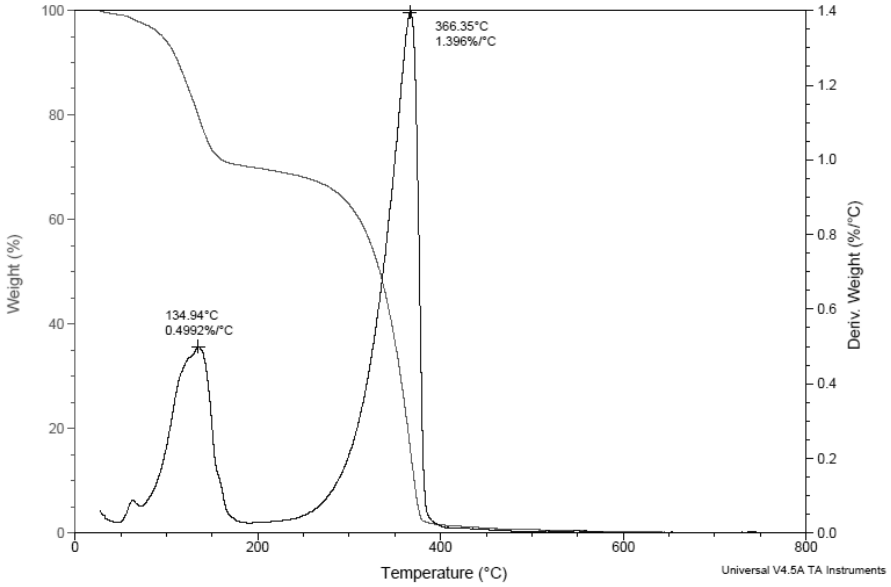

Figure 3-37: TGA of TPDA-Sq10 (scan rate of 10°C.min^{-1}).

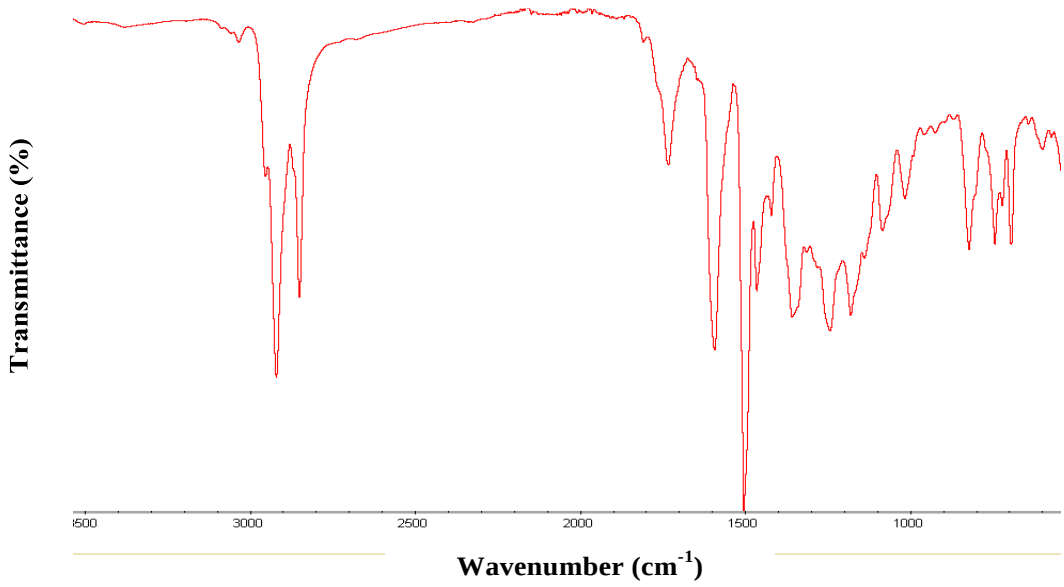

Figure 3-38: ATR-FTIR spectrum of TPDA-Sq50.

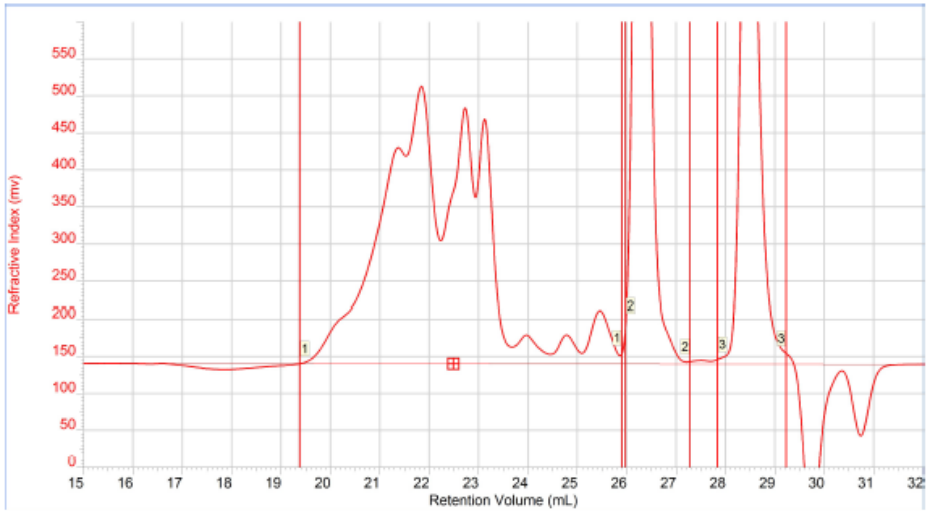

Peak	Mn	Mw	Mz	Mp	Mw/Mn	Ret Vol
1	2 110	4 511	8 158	4 025	2.137	21.833

Figure 3-39: SEC profile of TPDA-Sq50 (in $CHCl_3$, polystyrene standard).

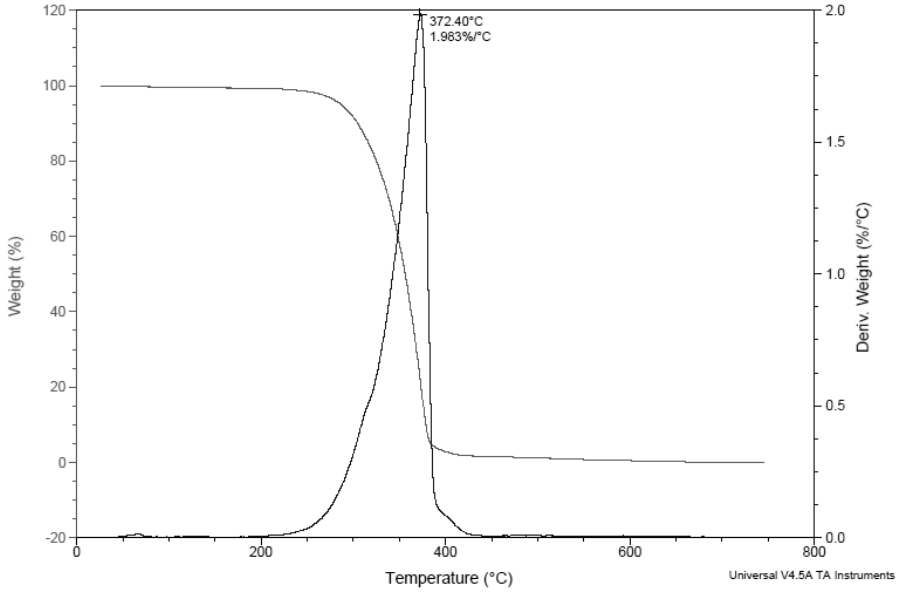

Figure 3-40: TGA of TPDA-Sq50 (scan rate of 10°C.min^{-1}).

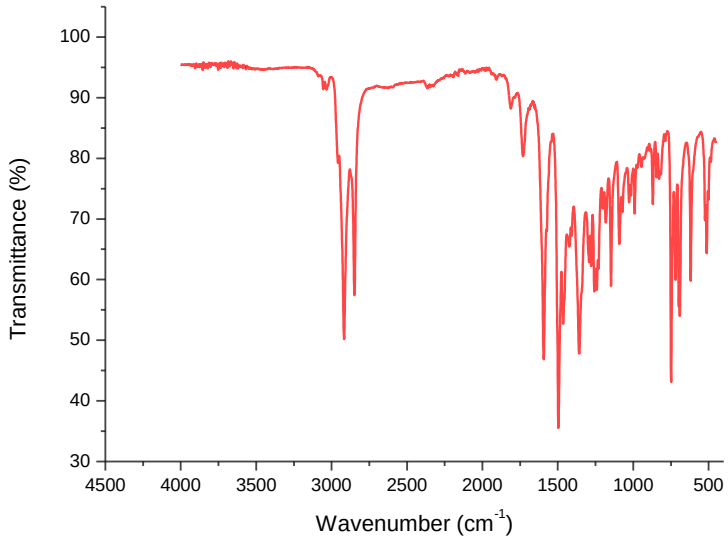

Figure 3-41: ATR-FTIR spectrum of TPDA-Sq90.

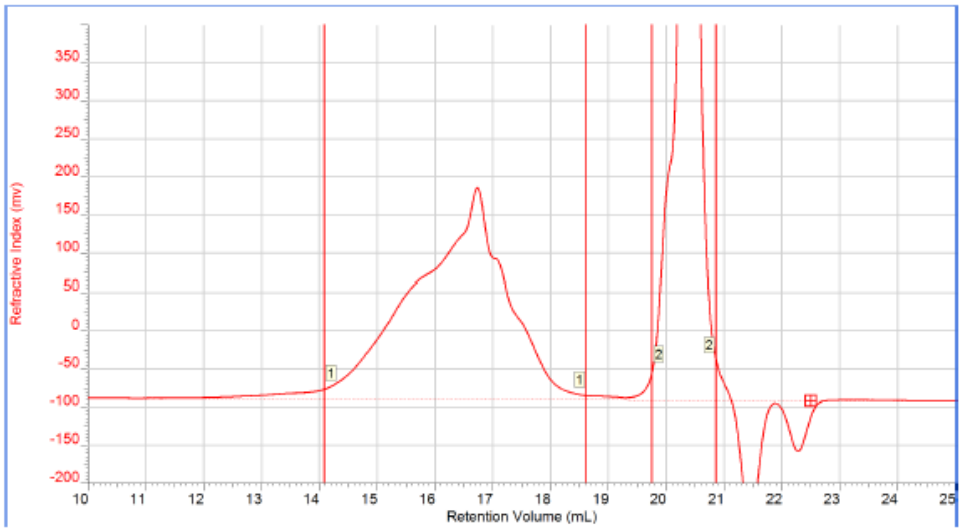

Peak	Mn	Mw	Mz	Mp	Mw/Mn	Ret Vol
1	2 759	6 699	15 067	2 710	2.428	16.720

Figure 3-42: SEC profile of TPDA-Sq90 (in $CHCl_3$, polystyrene standard).

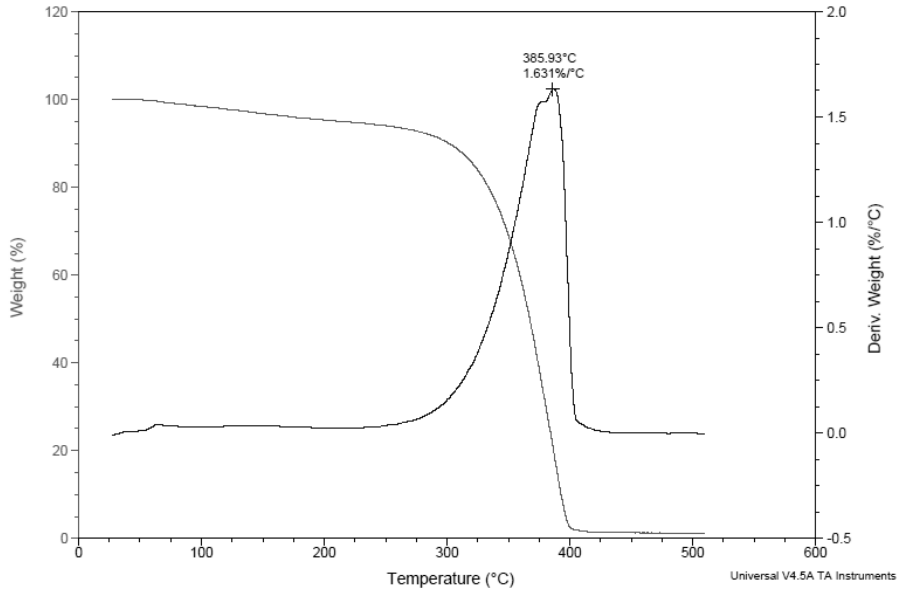

Figure 3-43: TGA of TPDA-Sq90 (scan rate of 10°C.min^{-1}).

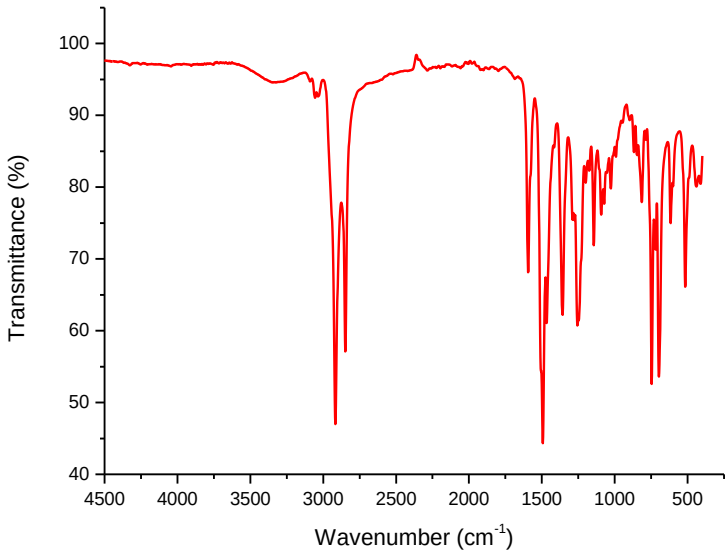

Figure 3-44: ATR-FTIR spectrum of TPDA-Sq50-Prop.

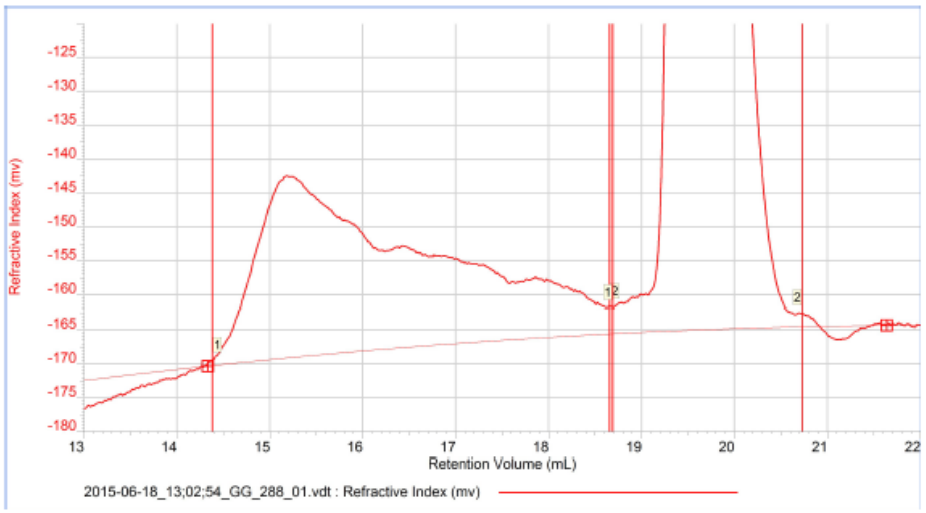

Peak	Mn	Mw	Mz	Mp	Mw/Mn	Ret Vol
1	3 720	12 686	22 289	22 728	3.410	15.187

Figure 3-45: SEC profile of TPDA-Sq50-Prop (in $CHCl_3$, polystyrene standard).

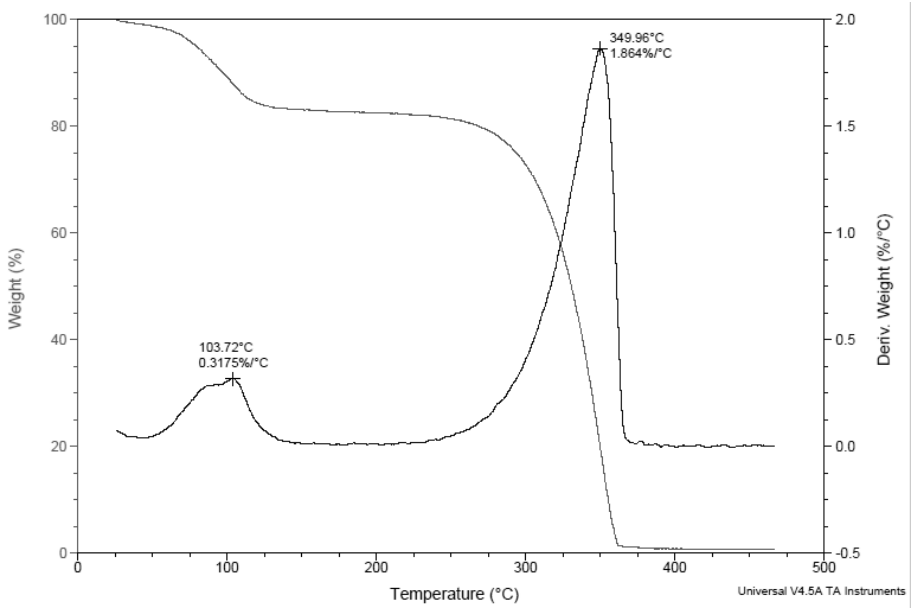

Figure 3-46: TGA of TPDA-Sq50-Prop (scan rate of 10°C.min^{-1}).

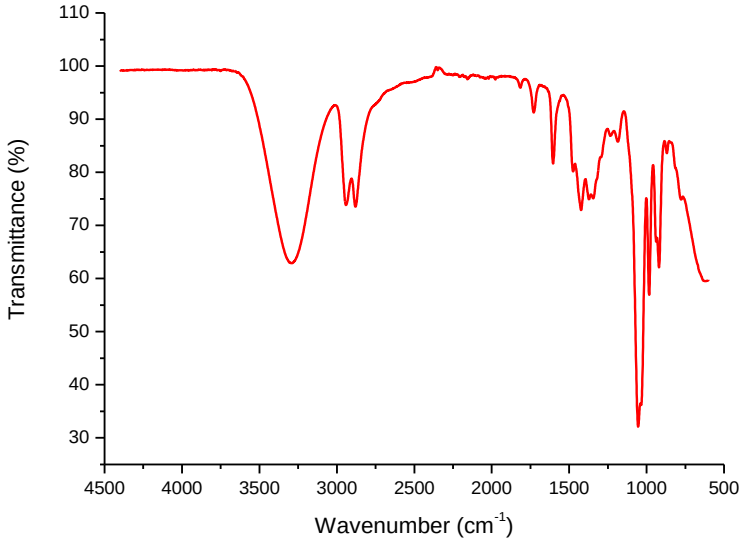

Figure 3-47: ATR-FTIR spectrum of TPDA-Sq-Gly.

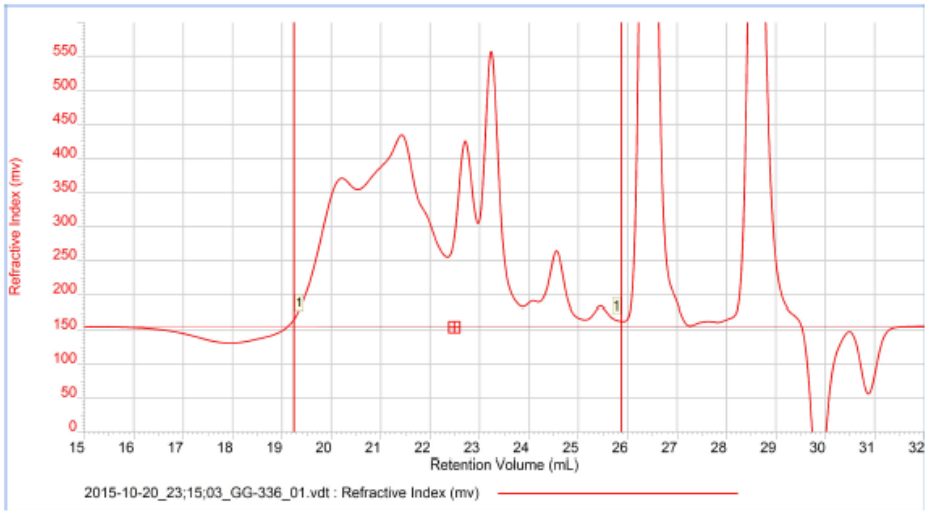

Peak	Mn	Mw	Mz	Mp	Mw/Mn	Ret Vol
1	2 407	7 200	14 703	1 434	2.991	23.223

Figure 3-47: SEC profile of TPDA-Sq-Gly (in $CHCl_3$, polystyrene standard).

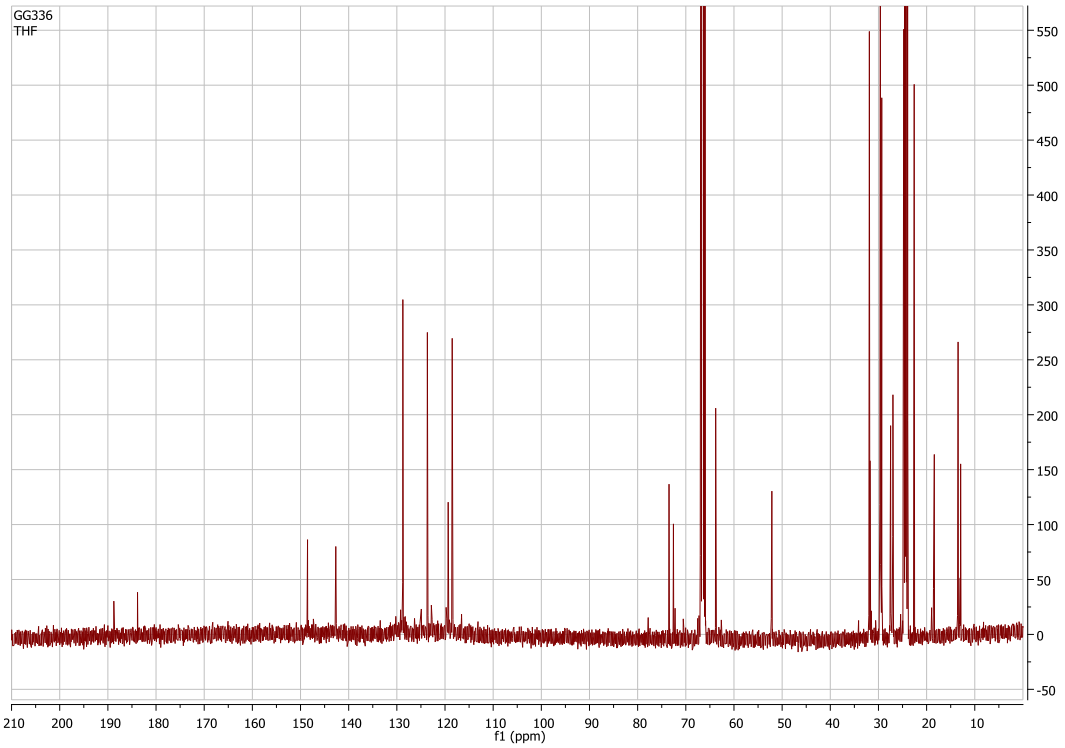

Figure 3-48: ^{13}C NMR spectrum (101 MHz) of TPDA-Sq-Gly in THF-d_8.

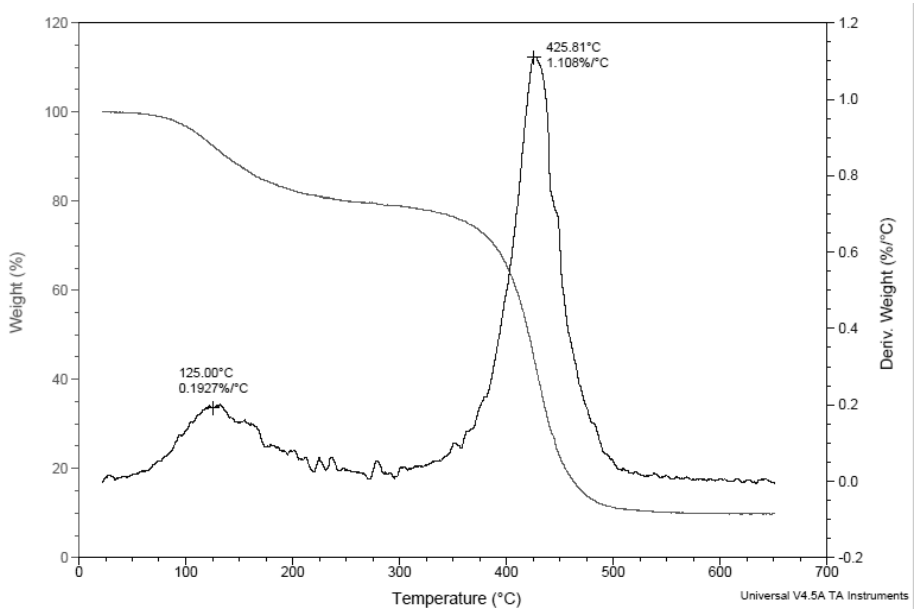

Figure 3-49: TGA of TPDA-Sq-Gly (scan rate of 10°C.min^{-1}).

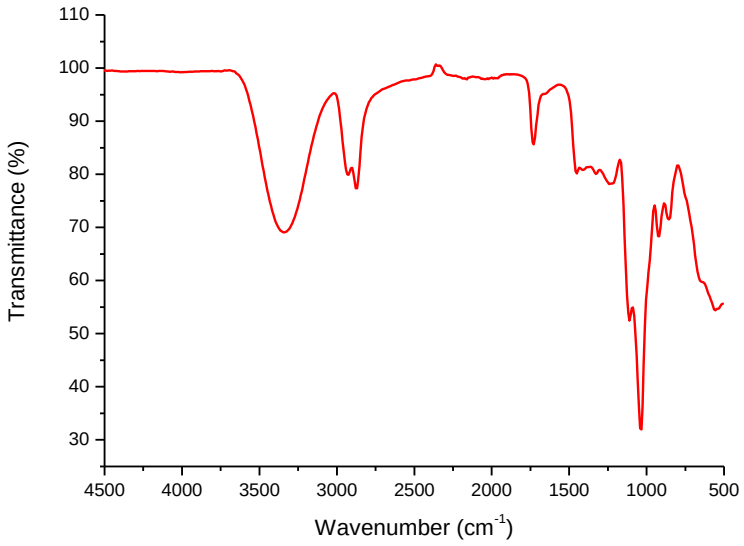

Figure 3-50: ATR-FTIR spectrum of TPDA-SqCl-Gly.

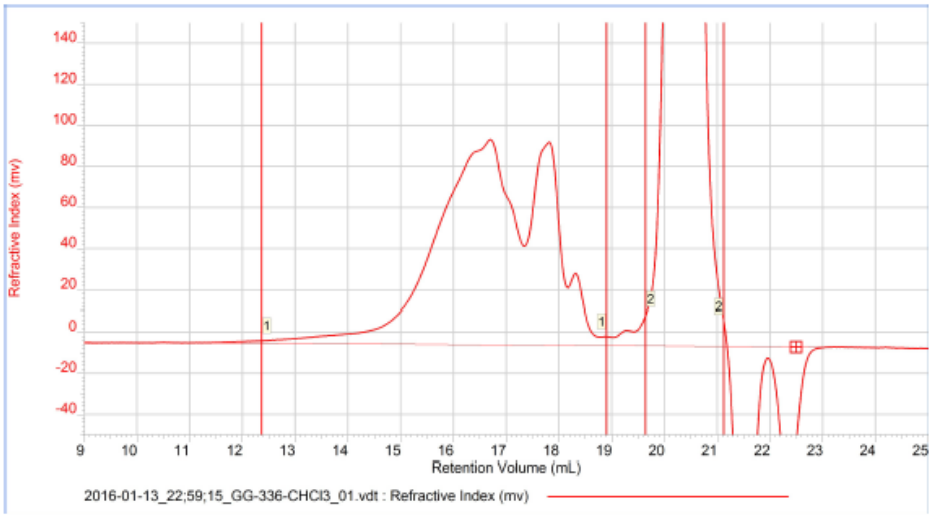

Peak	Mn	Mw	Mz	Mp	Mw/Mn	Ret Vol
1	1 782	8 064	88 450	3 036	4.525	16.683

Figure 3-51: SEC profile of TPDA-SqCl-Gly (in $CHCl_3$, polystyrene standard).

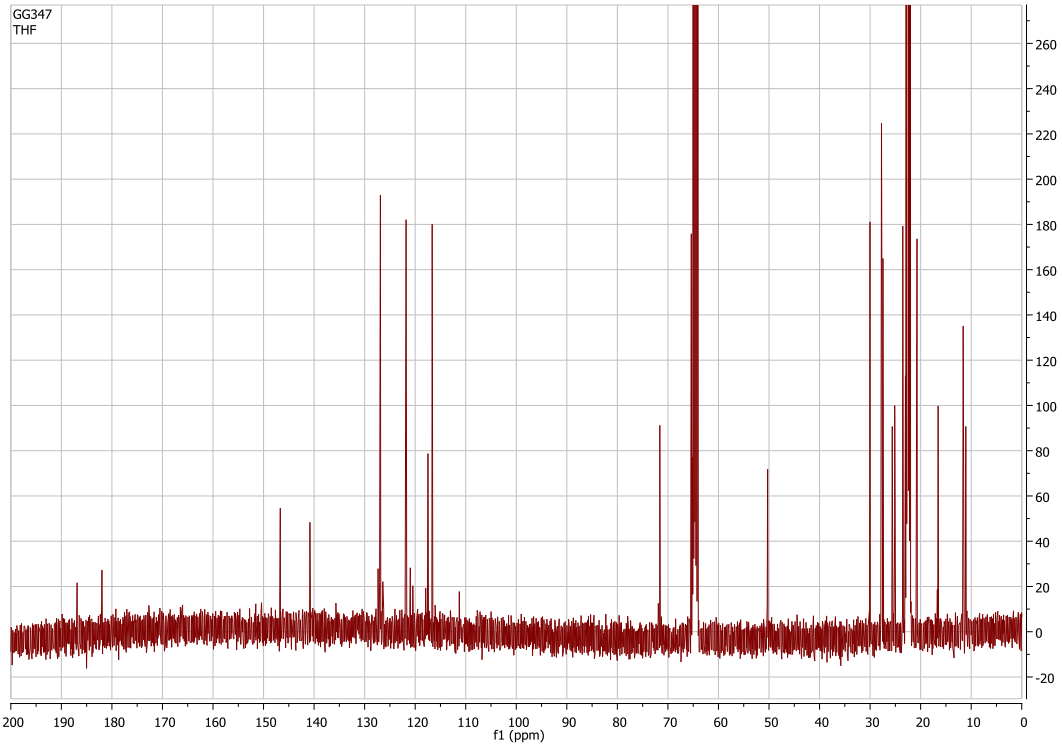

Figure 3-52: ^{13}C NMR spectrum (101 MHz) of TPDA-SqCl-Gly in THF-d_8.

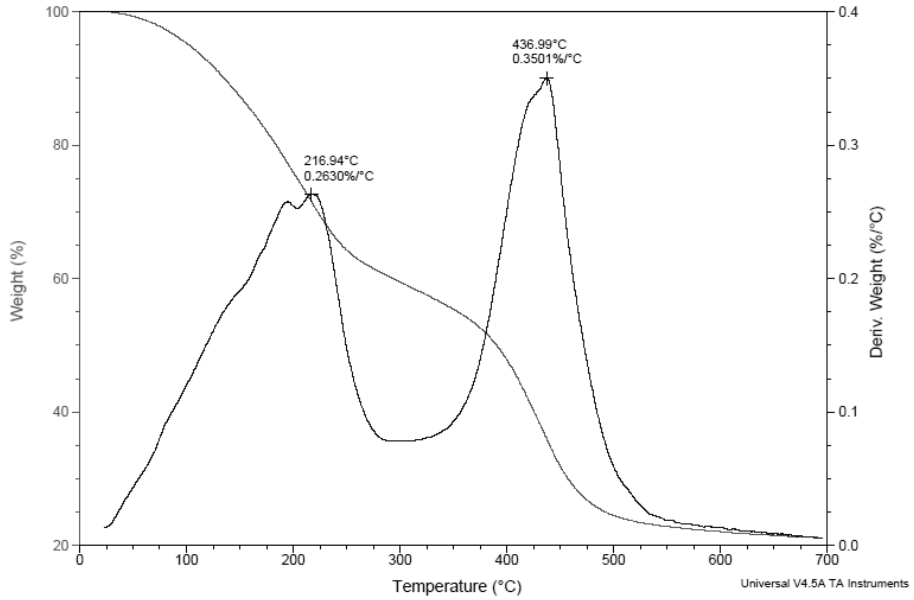

Figure 3-53: TGA of TPDA-SqCl-Gly (scan rate of 10°C.min^{-1}).

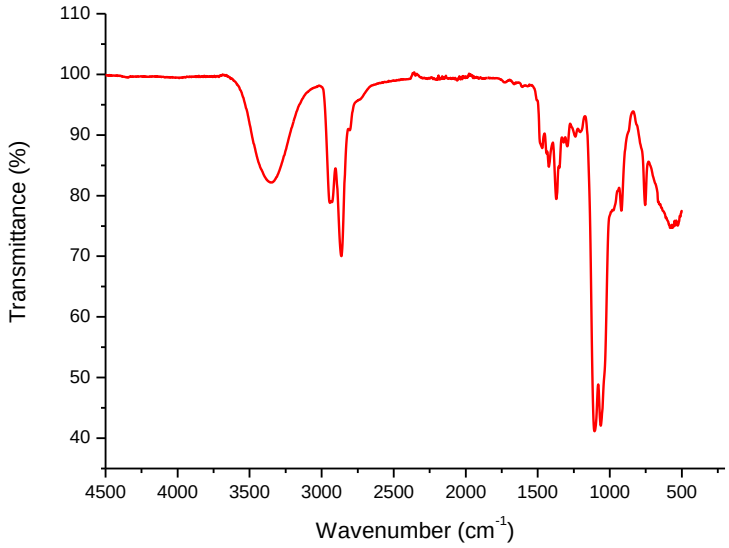

Figure 3-54: ATR-FTIR spectrum of TPDA-SqCl-Gly.

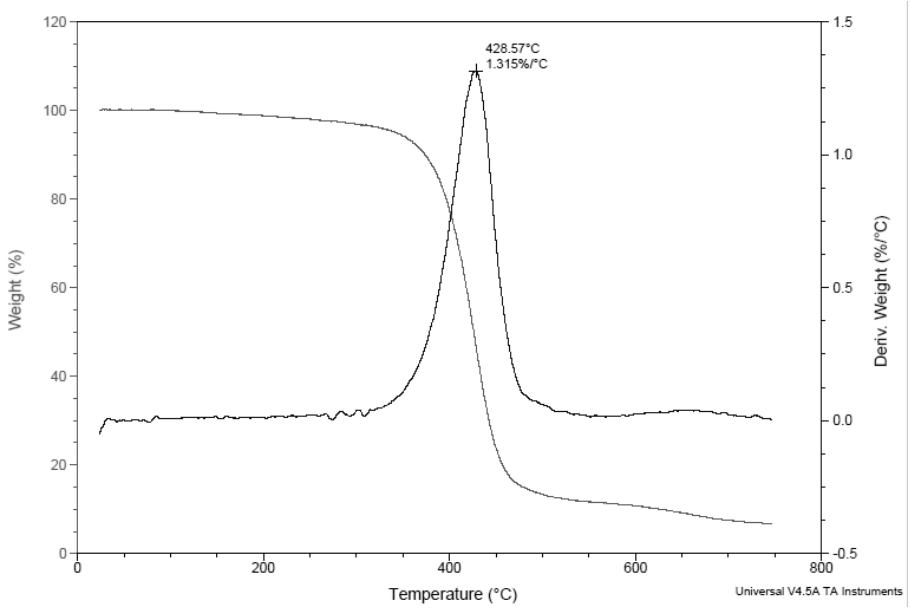

Figure 3-55: TGA of TPDA-Cro-Gly (scan rate of 10°C.min^{-1}).

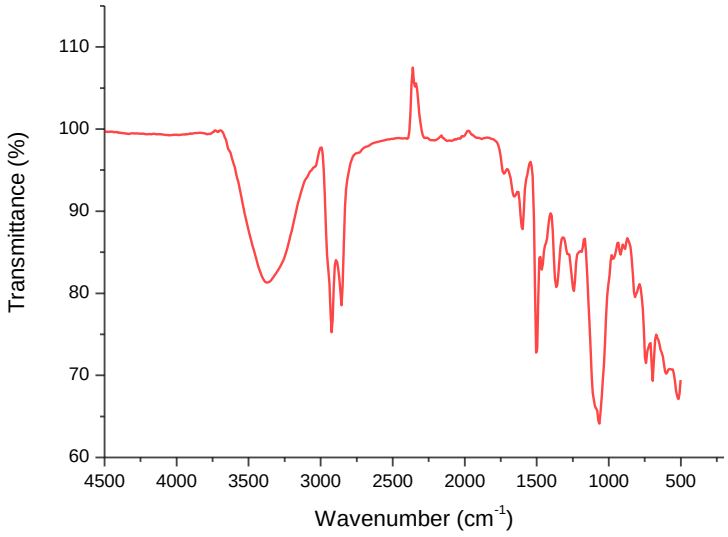

Figure 3-56: ATR-FTIR spectrum of TPDA-CroCl-Gly

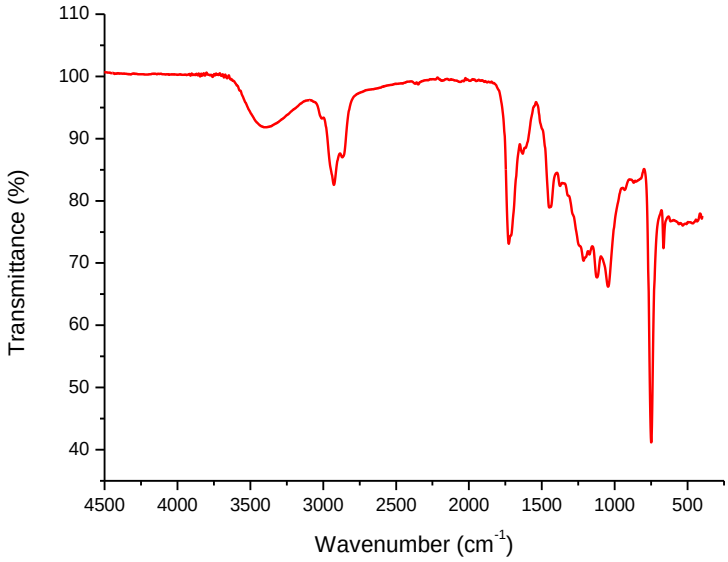

Figure 3-57: ATR-FTIR spectrum of TPDA-Sq50-PropDiol.

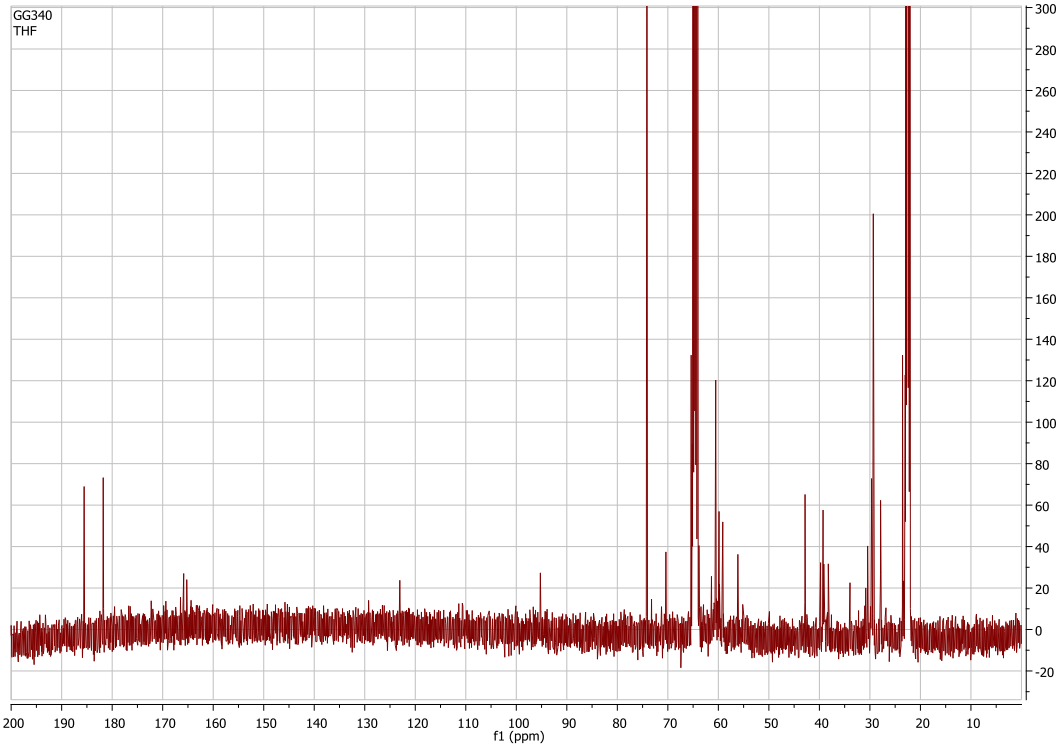

Figure 3-58: ^{13}C NMR spectrum (101 MHz) of TPDA-Sq50-PropDiol in THF-d_8.

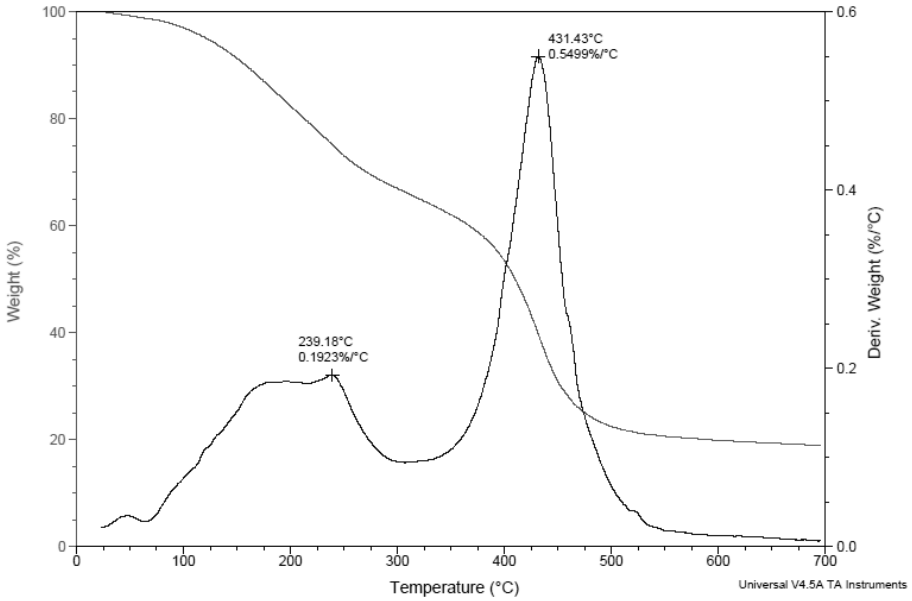

Figure 3-59: TGA of TPDA-Sq50-PropDiol (scan rate of 10°C.min^{-1})

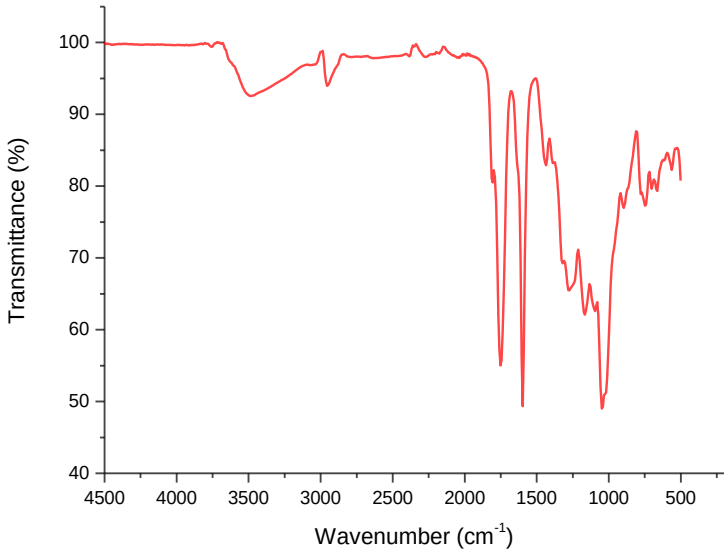

Figure 3-60: ATR-FTIR spectrum of TPDA-Sq50-ButDiol.

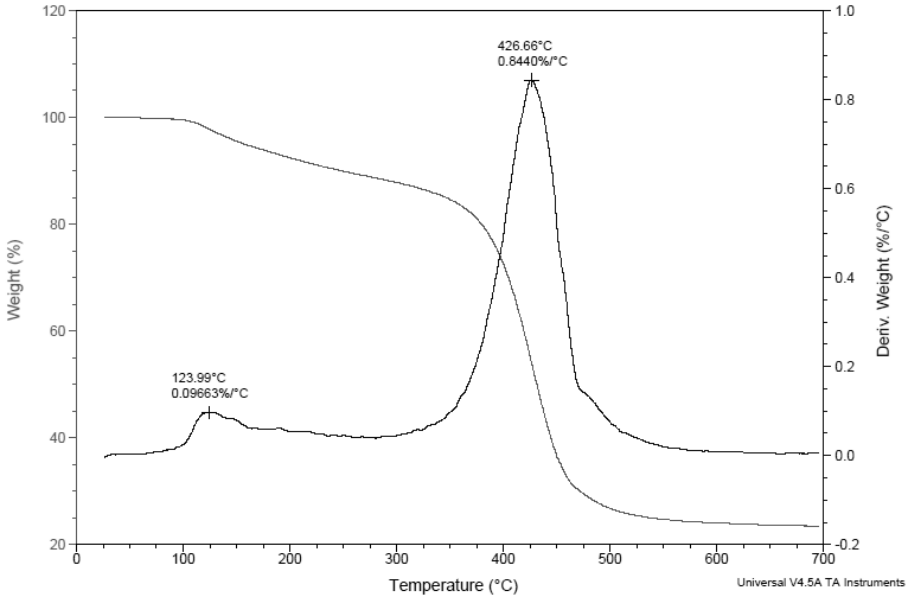

Figure 3-61: TGA of TPDA-Sq50-ButDiol (scan rate of 10°C.min^{-1}).

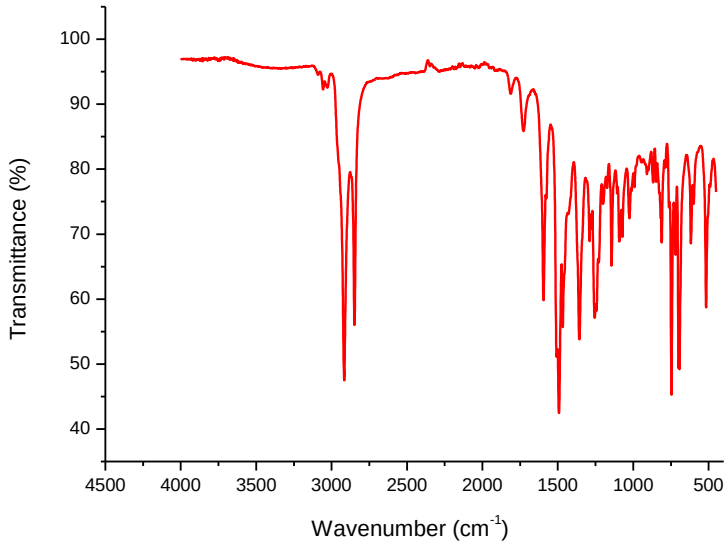

Figure 3-62: ATR-FTIR spectrum of TPDA-Sq50-Pent.

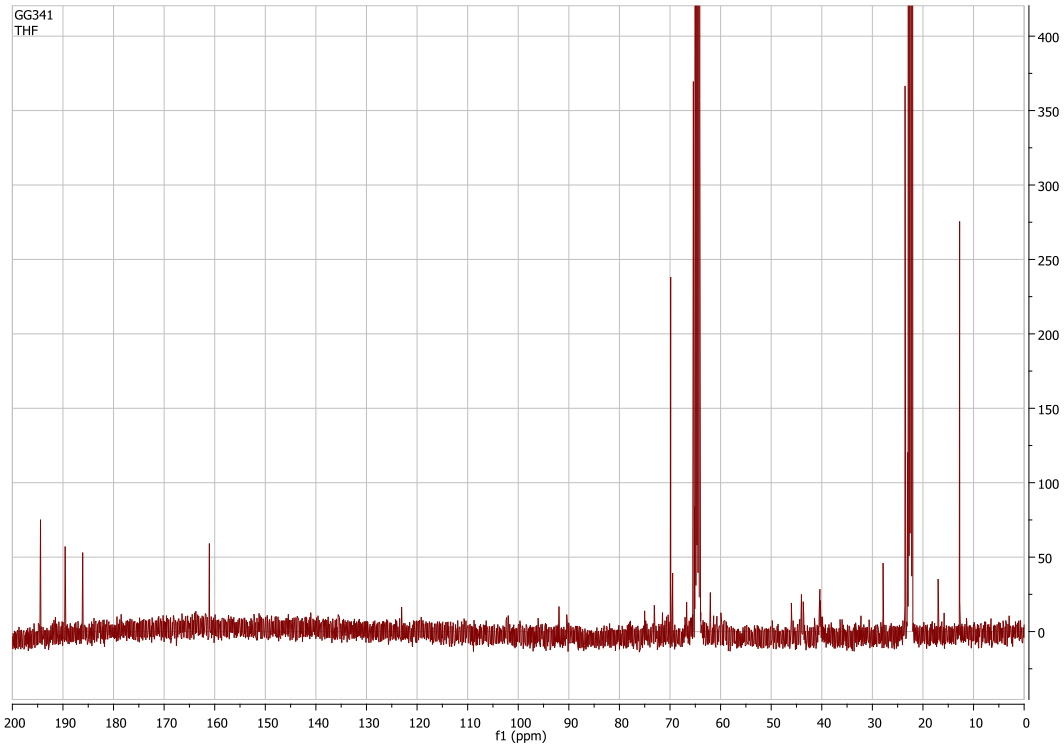

Figure 3-63: ^{13}C NMR spectrum (101 MHz) of TPDA-Sq50-Pent in THF-d_8.

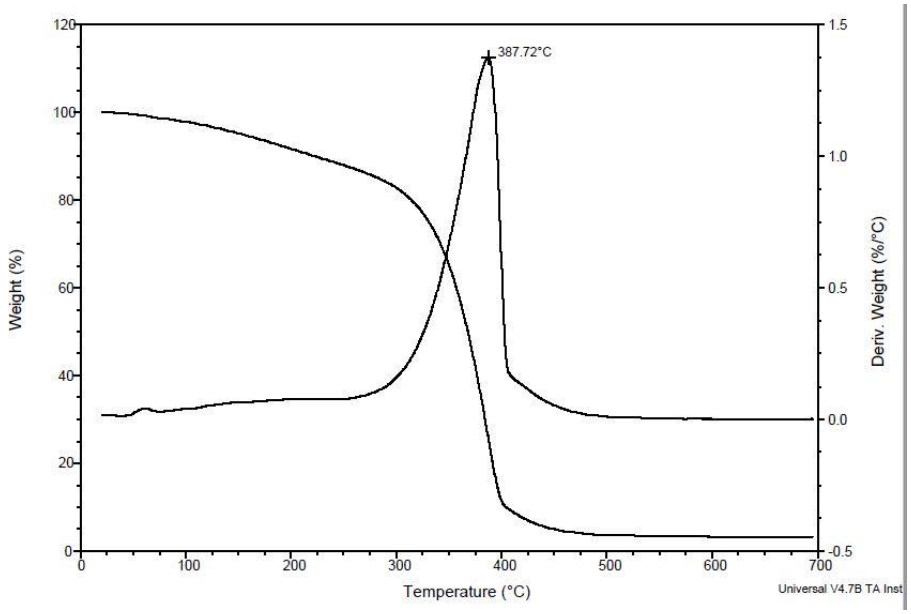

Figure 3-64: TGA of TPDA-Sq50-Pent (scan rate of 10°C.min^{-1})

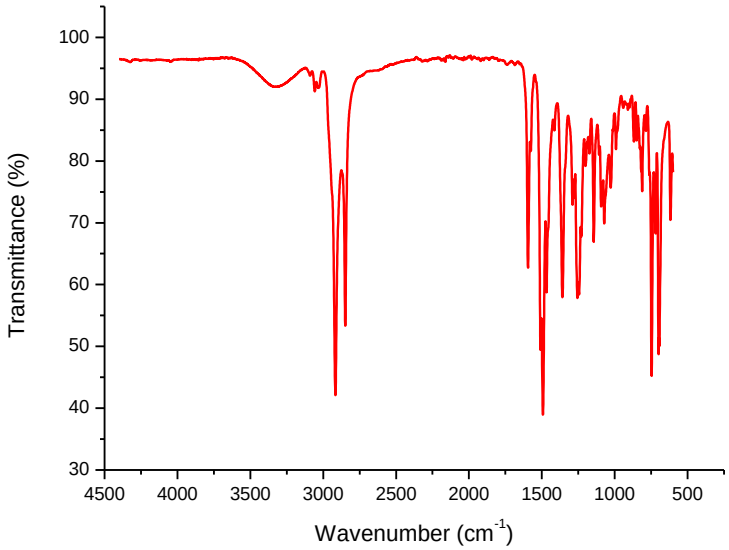

Figure 3-65: ATR-FTIR spectrum of TPDA-Sq50-PentDiol.

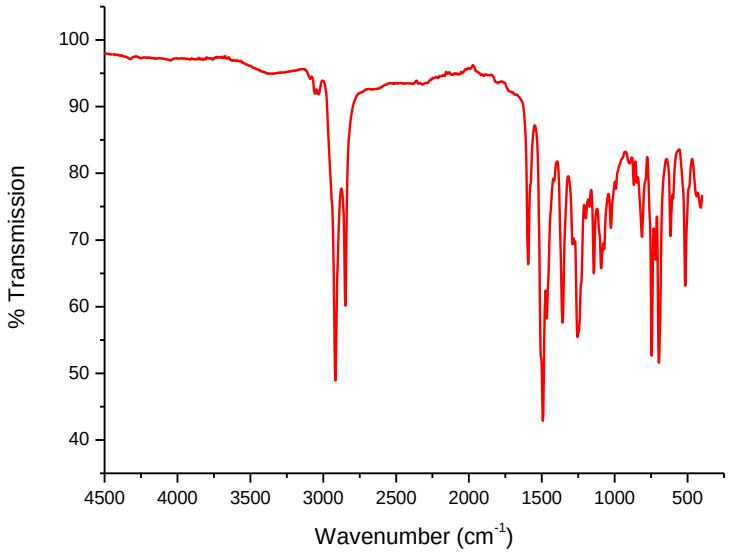

Figure 3-66: ATR-FTIR spectrum of TPDA-Sq50-Dod.

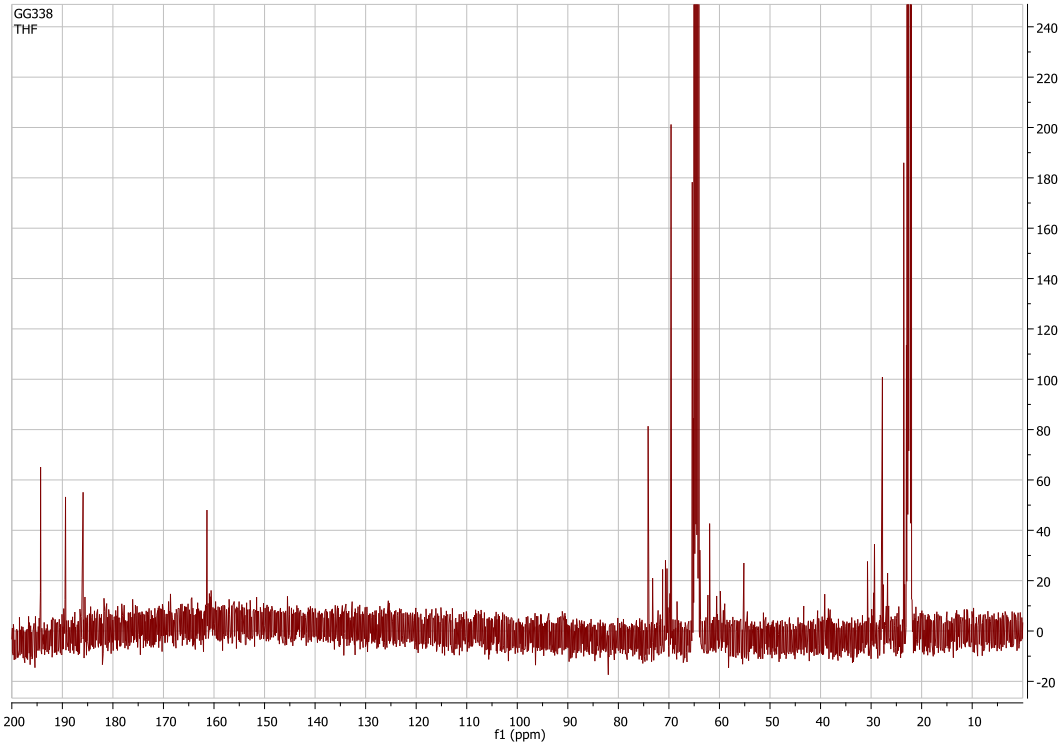

Figure 3-67: ^{13}C NMR spectrum (101 MHz) of TPDA-Sq50-Dod in THF-d_8.

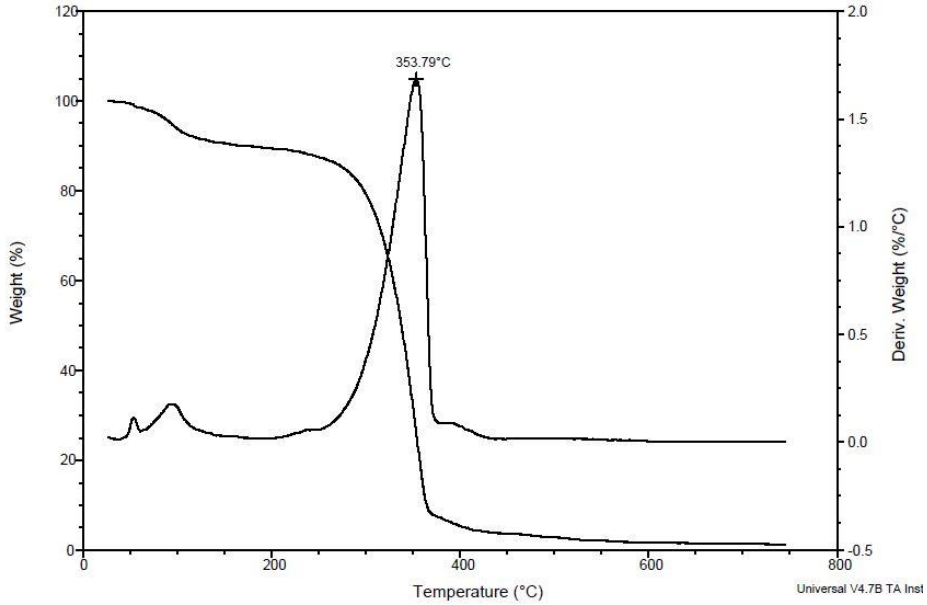

Figure 3-68: TGA of TPDA-Sq50-Dod (scan rate of 10°C.min^{-1}).

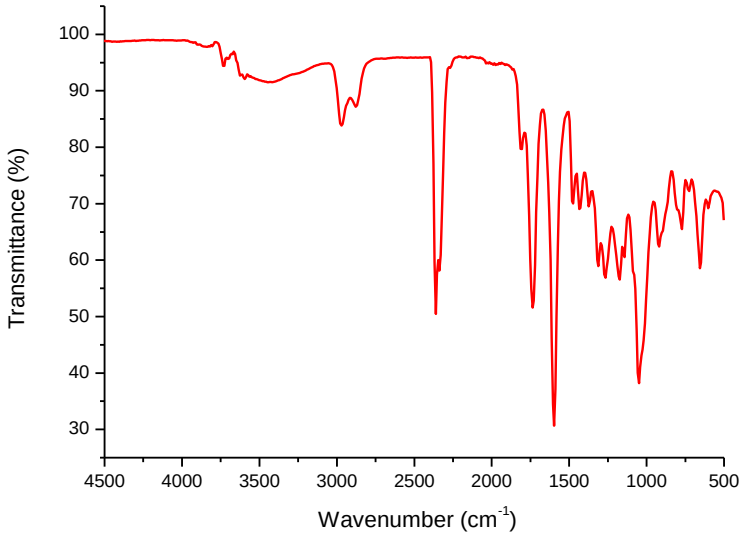

Figure 3-69: ATR-FTIR spectrum of TPDA-Sq50-PropDiol-2eq.

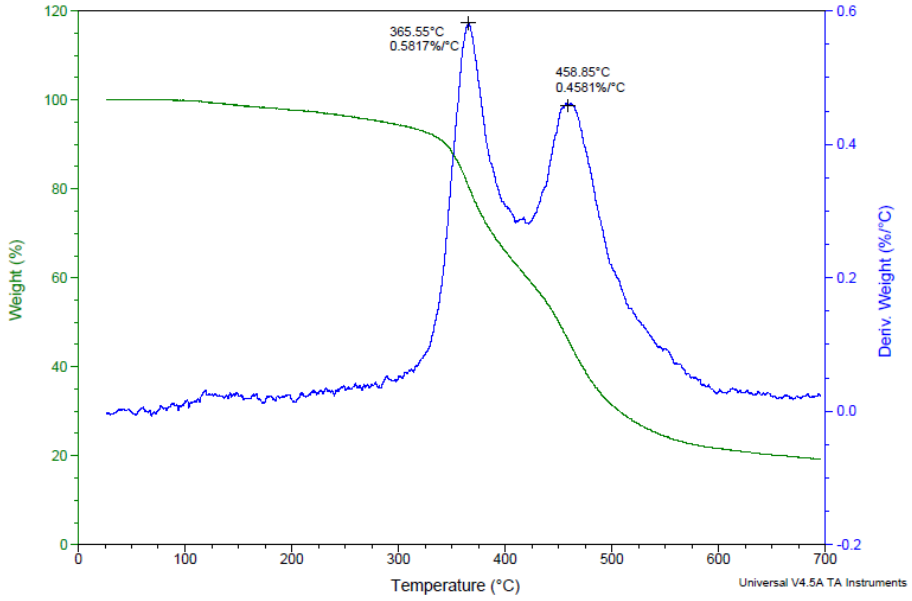

Figure 3-70: TGA of TPDA-Sq-PropDiol-2eq (scan rate of 10°C.min^{-1}).

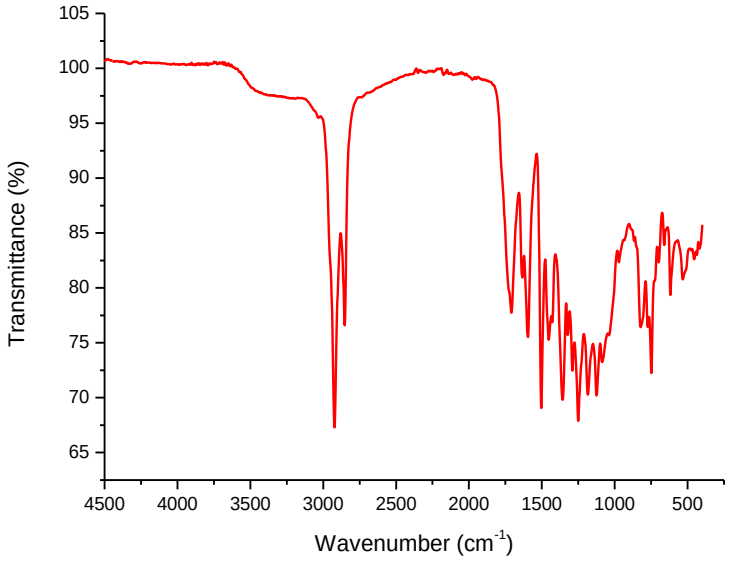

Figure 3-71: ATR-FTIR spectrum of TPDA-Sq-PropDiol-3eq.

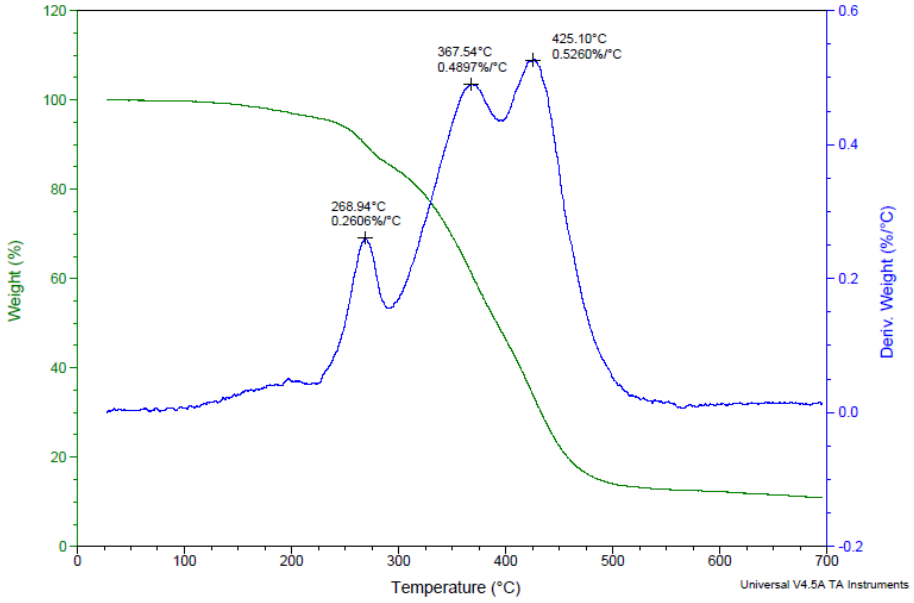

Figure 3-72: TGA of TPDA-Sq-PropDiol-3eq (scan rate of 10°C.min^{-1}).

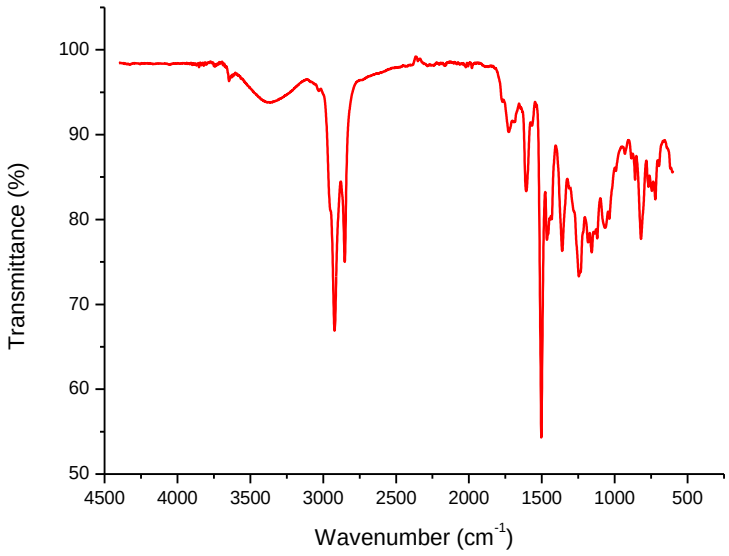

Figure 3-73: ATR-FTIR spectrum of TPDA-Sq-PropDiol-10eq.

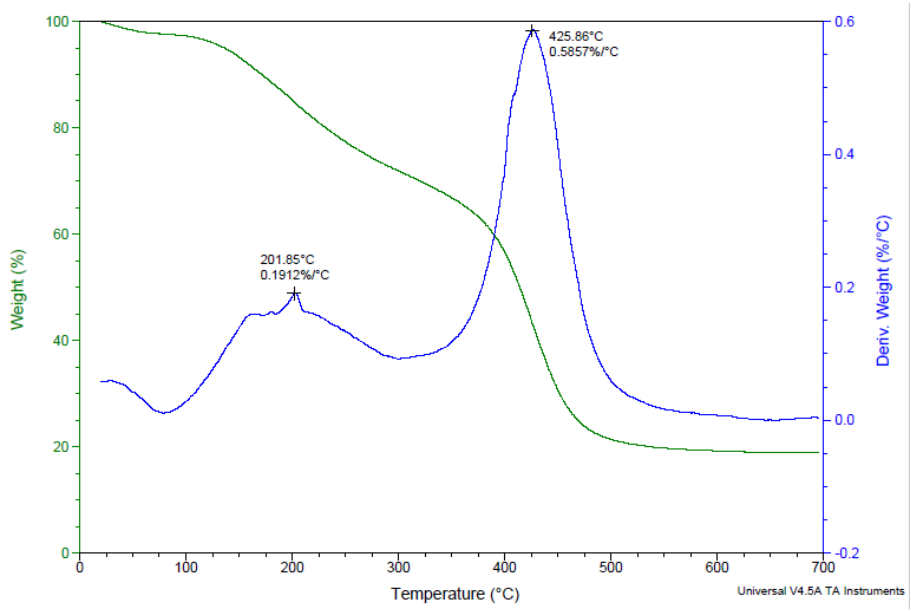

Figure 3-74: TGA of TPDA-Sq-PropDiol-10eq (scan rate of 10°C.min^{-1}).

Chapter 4: Exploratory study of new « bricks » for original π-conjugated polymers

Résumé en français.

Dans cette partie nous avons choisi d'étudier l'incorporation de nouvelles briques élémentaires dans la construction de chaines de polymères π-conjugués tels que le benzobisthiazole, la tetrazine et la divaniline (Figure 1).

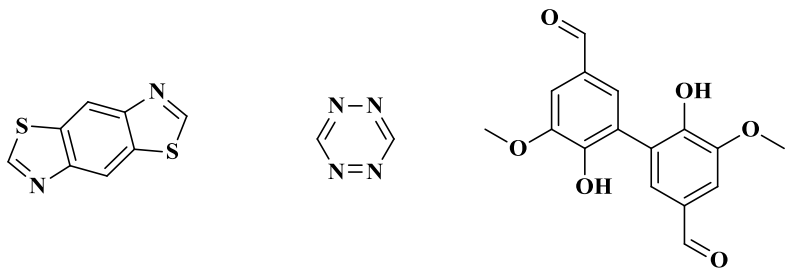

Figure 1 : Structures du Benzobisthiazole (gauche), de la 1,2,4,5-tétrazine (centre) et de la divanilline (droite).

Nous avons tout d'abord mis au point la formation du copolymère poly(2,7-carbazole-*alt*-benzobisthiazole) *via* la synthèse *in situ*, pour la première fois, de ce dernier à partir des fonctions aldéhyde (portées par le carbazole) et le 2,5-diamino-1,4-benzenedithiol dihydrochloride (Schéma 1).

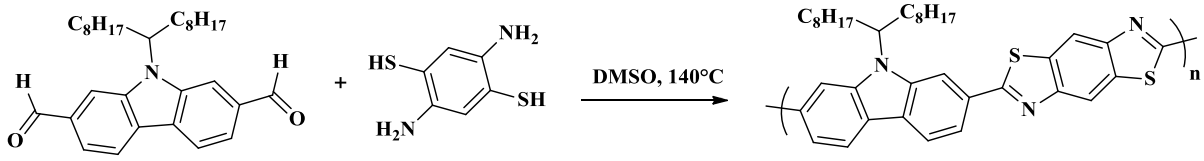

Schéma 1 : Synthèse du poly(2,7-carbazole-*alt*-benzobisthiazole) *via* la condensation du 2,5-diamino-1,4-benzenedithiol dihydrochloride sur le 2,7-diformylcarbazole.

Par ailleurs nous nous sommes intéréssés à des structures π-conjuguées riches en atomes d'azote telle que des poly(carbazole-*alt*-tétrazine) obtenus *via* une catalyse basique (Schéma 2).

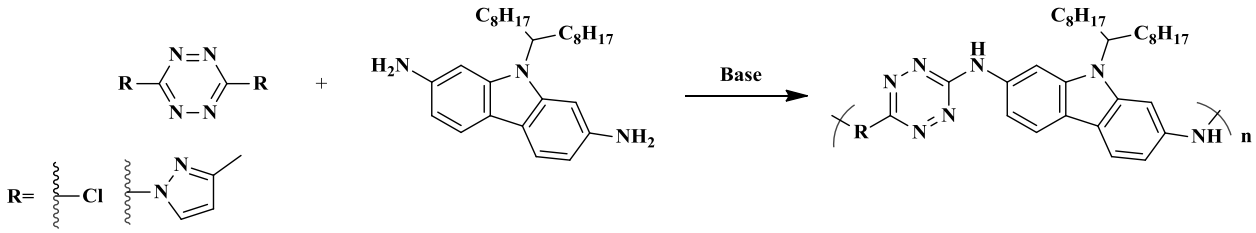

Schéma 2 : Polycondensation du 2,7-diaminocarbazole avec la tetrazine.

Finalement, la divanilline, monomère biosourcé dans notre cas, a été alkylée et polymérisée en présence de 1,4-diaminobenzène et de 2,7-diaminocarbazole *via* une réaction de polycondensation, formant ainsi des polyazométhines originales (Schéma 3).

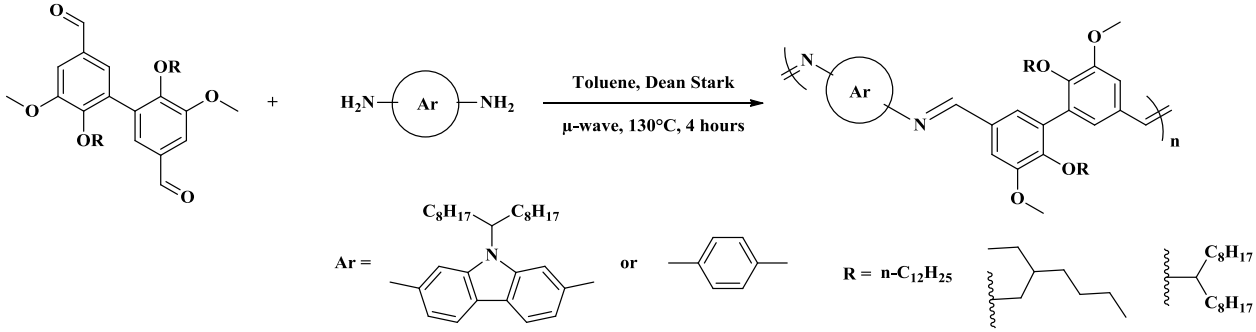

Schéma 3 : Polyazomethines obtenues via la condensation du 2,7-diamiocarbazole ou du benzène-1,4-diamine avec de la divanilline alkylée.

Les différentes conditions de synthèse ainsi que l'étude des propriétés optiques et électrochimiques sont discutées dans ce chapitre.

Chapter 4: Exploratory study of new « bricks » for original π-conjugated polymers.

4.1. π-conjugated polymers composed of Benzobisthiazole 189

4.1.1. State of the art 189

4.1.2. Synthesis and characterization 190

4.2. π-conjugated polymers composed of Tetrazine 192

4.2.1. State of the art 192

4.2.2. Preliminary results 195

4.3. π-conjugated polymers composed of Divanillin 198

4.3.1. State of the art 198

4.3.2. Synthesis 200

4.3.2.1. Monomer synthesis 200

4.3.2.2. Polymer synthesis 202

4.3.3. Optoelectronic properties 205

4.3.3.1. Optical characterizations 205

4.3.3.2. Electrochemical properties 207

4.4. Conclusion 209

4.5. References 210

4.6. Experimental Section 213

4.6.1. General procedure for the synthesis of Poly (Benzobisthiazole-*alt*-carbazole) 213

4.6.2. Tetrazine 213

4.6.3. Divanillin 215

In this chapter, the synthesis of some original compound and polymers is described. This is an exploratory study where different moieties have been studied. Some exhibit interesting properties, some are still under further investigations and some couldn't have been more developed for different reasons.

4.1. π-conjugated polymers composed of Benzobisthiazole

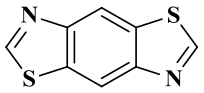

4.1.1. State of the art

Benzobisthiazole (benzo (1,2-4,5) di (3-alkyl 2 methylene thiazole)) based polymers and molecules have been shown to exhibit efficient π-stacking and strong intermolecular interactions in the solid state with a high degree of molecular order. Some of them present a high carrier mobility in thin film field-effect transistors and light-emitting diodes containing polybenzobisthiazole as electron transport layer were stable in air.[1–8] Benzobisthiazole has been used in different polymers, first to obtain polymers fiber with high modulus and high strength,[9,10] then to obtain polysquaraine and polycroconaine (as developed in chapter III).[11–13] It has then been coupled with thiophene unit and used as an electron donor molecule (p-type) in different polymers and single molecules.[6,14]

As described in the first chapter of this manuscript, the benzobisthiazole can be formed directly during the coupling of the 2,5-diamino-1,4-benzenedithiol dihydrochloride with a carboxylic acid (or an aldehyde) (Scheme 4-1). [6,9,10,14–16]

Scheme 4-1: Synthesis of poly(benzobisthiazole-*alt*-phenylene) (adapted from reference[16])

It is important to note that such polymerization reaction has only been described once, showing the formation of insoluble materials[15,16] and low yield[6,14] We decided to take advantage of the *in situ* formation of such benzobisthiazole subunit by testing the feasibility using a carbazole dialdehyde precursor. Indeed, the latter can be alkylated on the nitrogen giving rise to more soluble materials.

4.1.2. Synthesis and characterization

Condensation between 2,7-diformylcarbazole and 2,5-diamino-1,4-benzenedithiol dihydrochloride is shown below (Scheme 4-2).

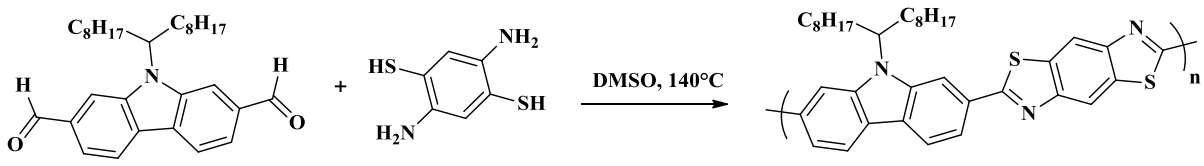

Scheme 4-2: Condensation of the 2,5-diamino-1,4-benzenedithiol dihydrochloride on previously synthesized 2,7-diformylcarbazole.

Such reaction was performed in absence of any metal catalyst in DMSO at 140°C. In order to optimize the reaction, different conditions have been tried, especially by varying the procedure (heating method and reaction time) (Table 4-1).

Polymer	Solvent (volume)	Heating method	Temperature	Time	Observation
Cbz-Bz1	DMSO (10 mL)	Oil bath	140°C	72 hours	Insoluble black powder
Cbz-Bz2	DMSO (5 mL)	µ-wave irradiation	140°C	4 hours	Insoluble black powder
Cbz-Bz3	DMSO (5 mL)	µ-wave irradiation	140°C	1 hour	Slightly soluble yellow powder

Table 4-1: Conditions used for the peparation of the different Carbazole-Benzobisthiazole (Cbz-Bz) polymers.

The first observation is that insoluble materials are rapidly formed, despite the presence of the 9-heptadecanyl chain on each carbazole moiety. This could suppose a high reaction yield and rate. The compound Carbazole-Benzobisthiazole obtained was characterized by UV-visible absorption and emission analysis.

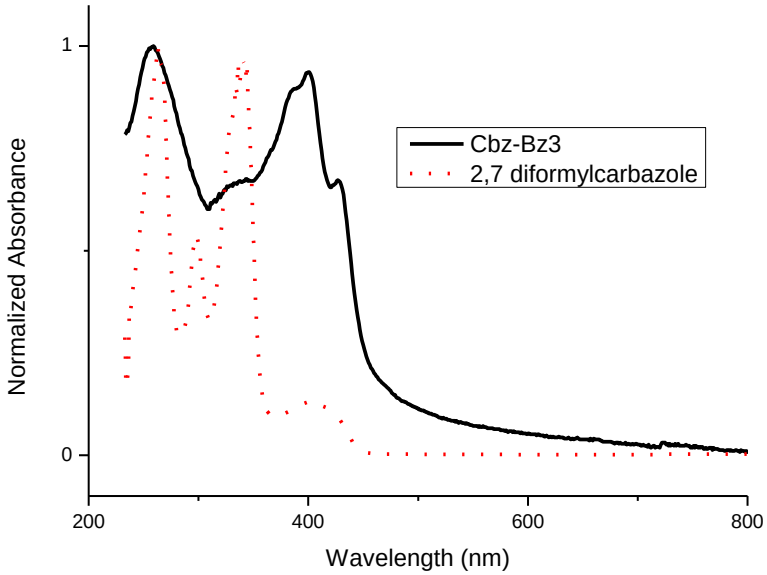

Figure 4-1: Absorption spectra (films on quartz) of the Cbz-Bz3 (black, solid) and the 2,7-diformylcarbazole (red, dot).

Formation of the copolymer is clearly evidenced by the absorption spectrum of **Cbz-Bz3** with a strong band centered at 400 nm and a kind of vibronic structure peaking at 430 nm. Thus emission spectra were recorded at 400 nm and 430 nm respectively, as illustrated in Figure 4-2.

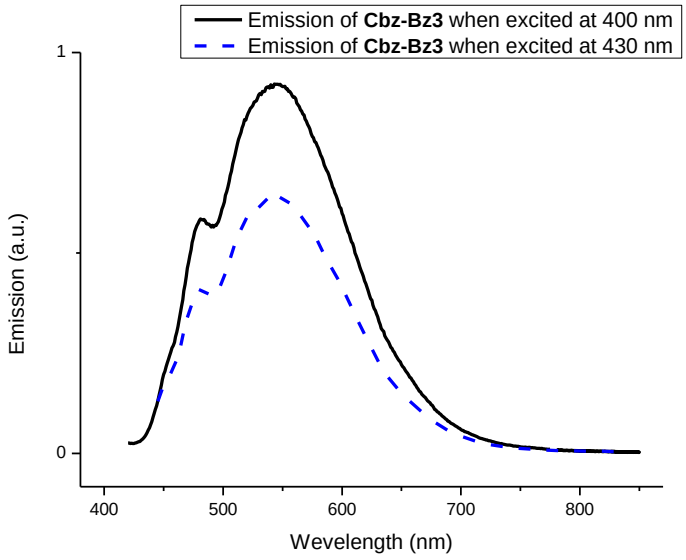

Figure 4-2: Emission spectra (film on quartz) of the Cbz-Bz3 polymer excited at 400 nm (black, solid) and 430 nm (blue, dash).

Both emission spectra are similar, showing that same chromophores are concerned.

On the basis of these results, such chemical reaction is quite promising and deserves to be investigated further. In particular, it would be helpful to derivatize soluble materials for a thorough characterization of the copolymers. In fact, the too low solubility of the copolymers impeded us to perform NMR, SEC or mass spectrometry along with cyclic voltammetry for instance.

4.2. π-conjugated polymers composed of Tetrazine

4.2.1. State of the art

Tetrazine is an old compound, already studied in 1933 for its metal complexing properties and more particularly known in explosives or energetic materials.[17–19] First polymers synthesized with this monomer were obtained by complexing tetrazine with multivalent metals (Figure 4-3).[20–22]

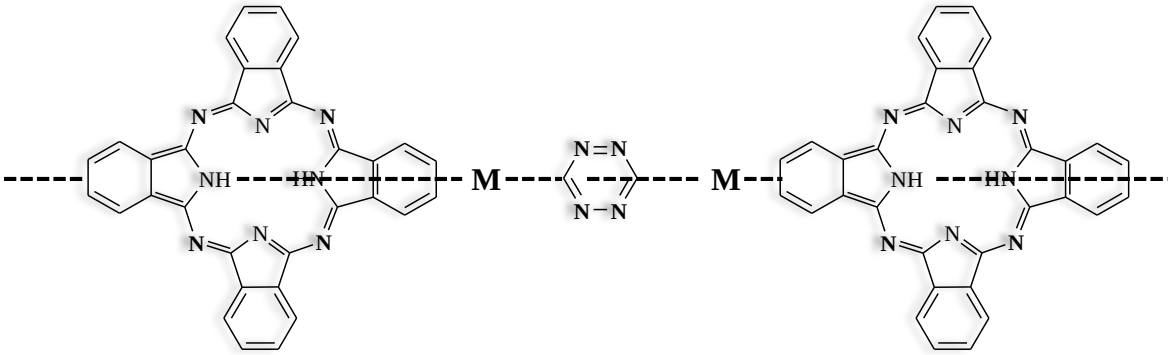

Figure 4-3: Polymer obtained with tetrazine being used as a ligand (M = Fe or Ru).

These polymers produce easily 1-D conducting polymers. This is due to the excellent electron affinity of the tetrazine, which allows charge transfer in a similar way that in a conducting polymer.

Though, it's not before 2003 that the first cross coupling reaction on tetrazine has been performed by Z. Novak and A. Kotshy, *via* Sonogashira and Negishi coupling allowing the insertion of new substituents to the tetrazine (Scheme 4-3).[23]

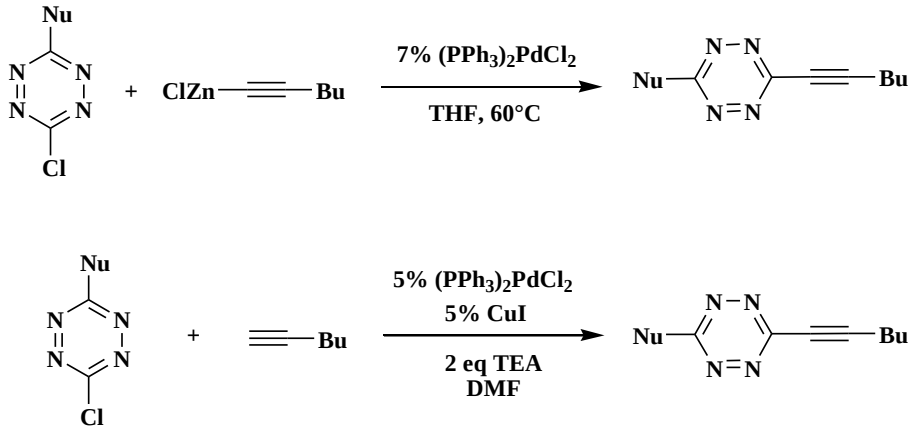

Scheme 4-3: Cross coupling reactions performed on tetrazine derivatives (top, Negishi cross coupling and bottom, Sonogashira cross coupling) (adapted from reference [23]).

Shortly after, the first electroactive copolymer alternating tetrazine and dithiophene subunit has been electrochemically synthesized by P. Audebert *et al.* (Figure 4-4).[24]

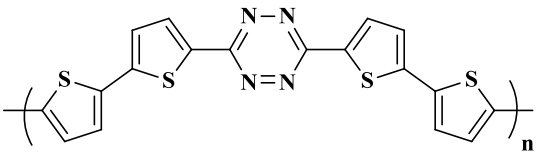

Figure 4-4: First electrochemically synthesized polymer integrating tetrazine.[24]

Many different substituents have been linked to tetrazine, giving rise to molecules exhibiting new opto-electronic properties.[25–29] Tetrazine based materials were for instance integrated in OPV by P. Ma *et al.*, showing a PCE of 5.3%.[30]

Nevertheless, only few polymers integrating tetrazine in their backbone have been synthesized, with the majority of them being obtained *via* electropolymerization or by complexation with metals.[31–33] Yet, a polymer containing carbazole and tetrazine has already been synthesized in 2012 with thiophene spacers *via* a Stille coupling (Scheme 4-4).[28]

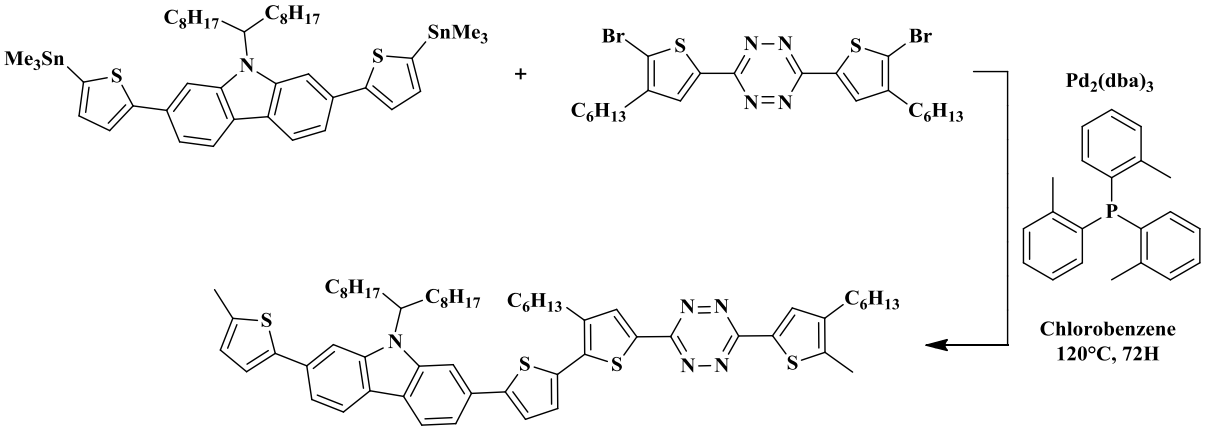

Scheme 4-4: Tetrazine and carbazole-based copolymer (adapted from reference [28]).

This copolymer presents a high absorption coefficient (higher than P3HT in solution) with a maximum of absorption, at around 480 nm.

Moreover, as developed by Novak *et al.* and by Audebert and coll., tetrazine can condensate on an amine, an alcohol or a thiol to obtain mono or di-substituted tetrazine.[34–38] In 2014, the team of P. Audebert even functionalized the tetrazine with phenols (Figure 4-5).[39]

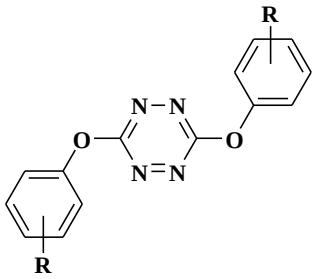

R= H, 4-CHO, 3-Cl, 4-Cl, 4-NO_2, 4-*t*Bu, 4-$OC_{10}H_{21}$, 4-Br

Figure 4-5: Small molecules combining tetrazine core and substituted phenoxy moieties (adapted from reference [39]).

By using a di-functional compound and by replacing the alcohol functions with amine, it could be possible to obtain conjugated polymers directly by condensing the diamino compound with the tetrazine. One can expect that the lone pair on the nitrogen linked to the tetrazine could participate to the molecule or polymer conjugation. We have started a collaboration with the group of Professor P. Audebert taking advantage of functionalities offered by tetrazine and functional carbazole molecules, such as the diamino derivative described earlier.

4.2.2. Preliminary results

Different molecules and polymers have been considered, all based on the nucleophilic behavior of the diaminocarbazole toward the tetrazine (Scheme 4-5).

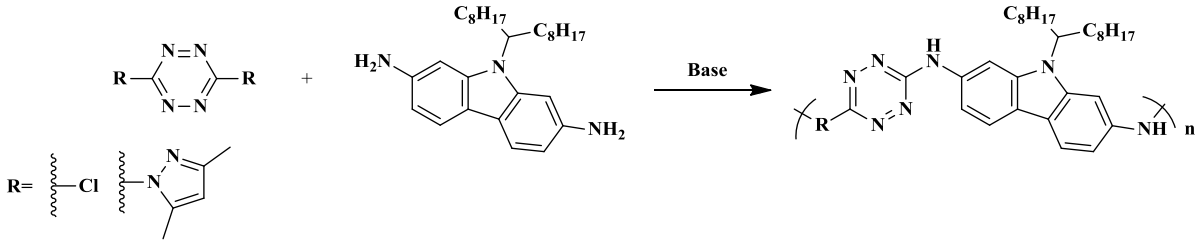

Scheme 4-5: General synthesis routes towards materials based on tetrazine and carbazole.

It is important to note that the base used for the above reaction should not be too nucleophilic in order to avoid a competition between the base and the diaminocarbazole. Thus, collidine (2,4,6-trimethylpyridine) or DMAP (4-Dimethylaminopyridine) have been used as non-nucleophilic base. Thanks to the group of P. Audebert, we could work with three different tetrazine: the dichlorotetrazine (**TzCl**),[40] the "Hiskey tetrazine" (3,6-bis(3,5-dimethylpyrazol-1-yl)-1,2,4,5-tetrazine, **TzHi**)[41] and the monofunctionnal chloroadamantane tetrazine **Ada-TzCl**,[42] synthesized in the lab (Scheme 4-6).

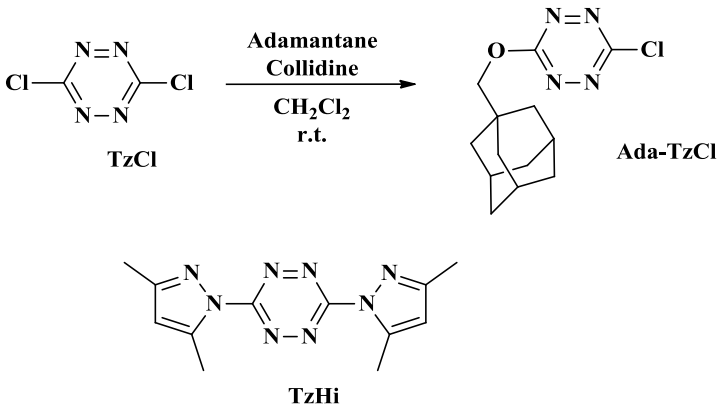

Scheme 4-6: Tetrazine derivatives as starting materials (TzCl, Ada-TzCl and TzHi).[40–42]

These three tetrazine derivatives present different reactivity towards nucleophilic substitutions, each group being more or less nucleofuge, and allowing a better tuning and control of the reactions.

Chemical pathways for the synthesis of tetrazine based copolymers are shown below (see Scheme 4-7).

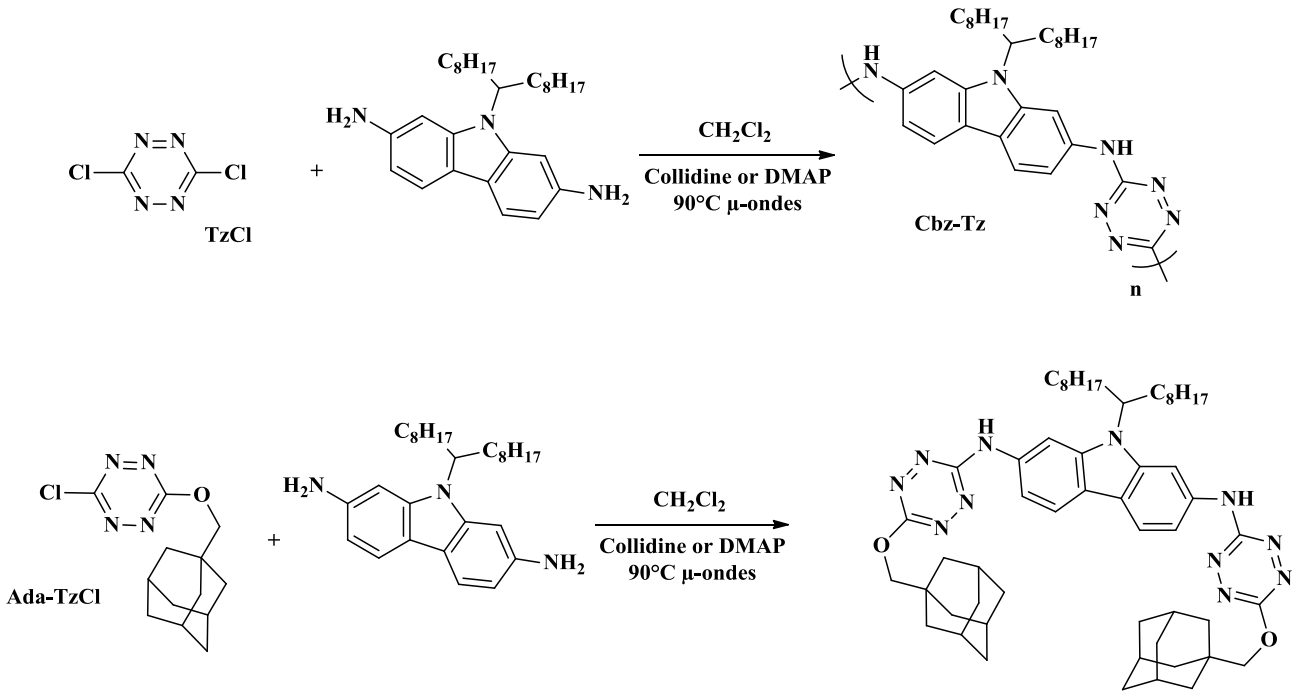

Scheme 4-7: Synthesis of the Cbz-Tz and Tz-Cbz-Tz componds.

Slightly soluble brown compounds with poor optical features were obtained impeding further characterization. To overcome this issue, a less reactive tetrazine **(TzHi)** was therefore tested to condensate with the diamino carbazole (Scheme 4-8).

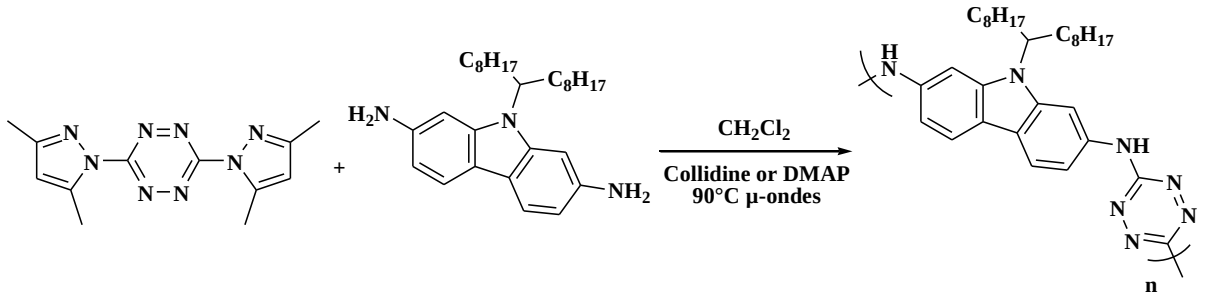

Scheme 4-8: Synthesis of the Cbz-Tz compound using a less reactive tetrazine derivative Tz-Hi.

Again, a poorly soluble compound was obtained. This can be due to the fact that primary amines are presents on the carbazole moieties, which implies the possibility to form network. Another possibility is that the remaining proton can interfere during the reactions.

Unfortunately, a similar result was obtained. This can be due to the presence of secondary amine in the polymer chain, which implies the possibility of a network formation. It was therefore decided to develop a methyl substituted diamino carbazole (see Scheme 4-9).

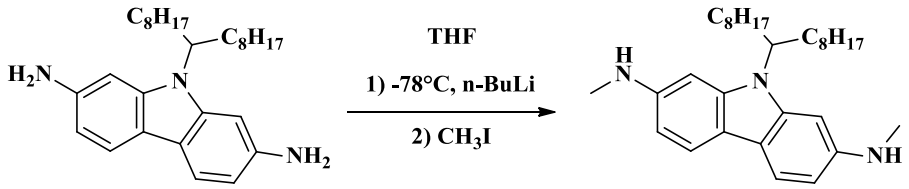

Scheme 4-9: Synthesis of the methylated 2,7-diaminocarbazole.

The crude product ^{1}H NMR has been performed (Figure 4-6).

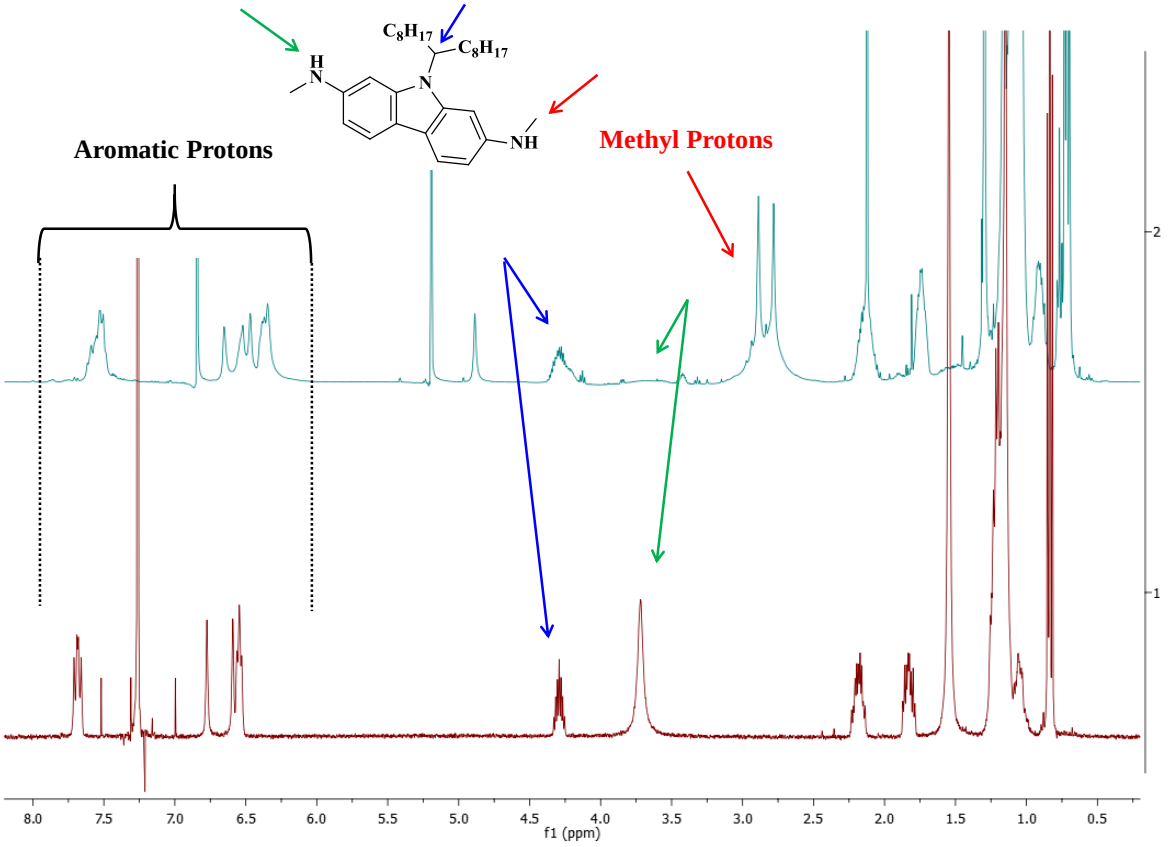

Figure 4-6: ^{1}H NMR (400 MHz) of the methylated 2,7-diaminocarbazole (top) and the 2,7-diaminocarbzole (bottom) (in $CDCl_3$)

The appearance of a doublet signal around 3 ppm confirms the methylation of the 2,7 diaminocarbazole

We are currently investigating this route as well as the condensation reaction with tetrazine derivatives.

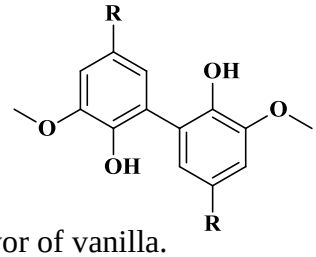

4.3. π-conjugated polymers composed of Divanillin

4.3.1. State of the art

Vanillin (4-hydroxy-3-methoxybenzaldehyde) is the main constituent flavor of vanilla. The alkaline oxidation of guaiacyl units (up to 25% of the lignin structure depending on the wood used) leads to vanillin.[43] Nowadays, the largest producer of vanillin from lignin is *Borregaard Industries*, in Norway. It represents 15% of the global vanillin production but this process attracts more and more interest due to continuous technical improvements.[44–46] In 2010, 15 000 tons of vanillin were produced from petrol and 2 000 tons from lignin. One of the main interest in Vanillin comes from its biomass availability.[46] Vanillin is widely used in food flavor formulations (chocolate, baking, beverage), perfumery and fragrances, odor masking (tires, plastics) and for the synthesis of several pharmaceuticals, chemicals and agrochemical intermediates. Vanillin has also been extensively used as a monomer to synthesize Schiff-base ligand for metals.[47,48]

Recent works on the oxidative coupling of phenolic molecules by enzymatic catalysis have made available a bio platform of aromatic molecules derived from lignin.[49,50] Llevot *et al.* developed an efficient enzymatic C–C coupling process using laccase from Trametes versicolor to obtain dimer of vanillin with a high yield and a high purity, giving access to a wide library of difunctional dimers (Scheme 4-10).

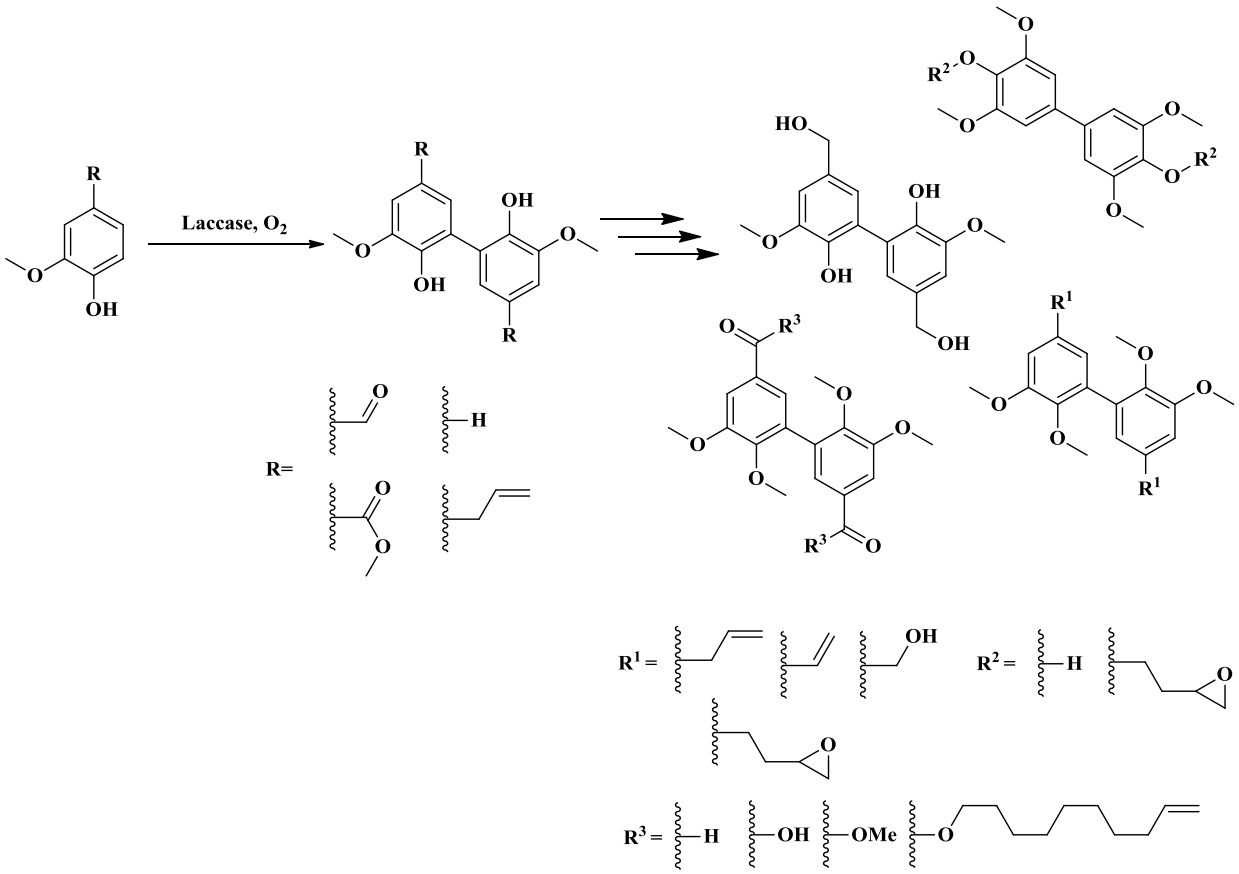

Scheme 4-10: Library of difunctional dimers based on vanillin.

Such library of difunctional dimers of vanillin prompted us to design π-conjugated polymers in combination with diamino compounds for instance. Indeed, we already discussed about interest in polyazomethine and metal-free process. Herein we come with another interesting feature due to an internal collaboration with the team of Professor H. Cramail, whose activity is dedicated to biosourced polymers. Targeted polymer structures are depicted below (Figure 4-7).

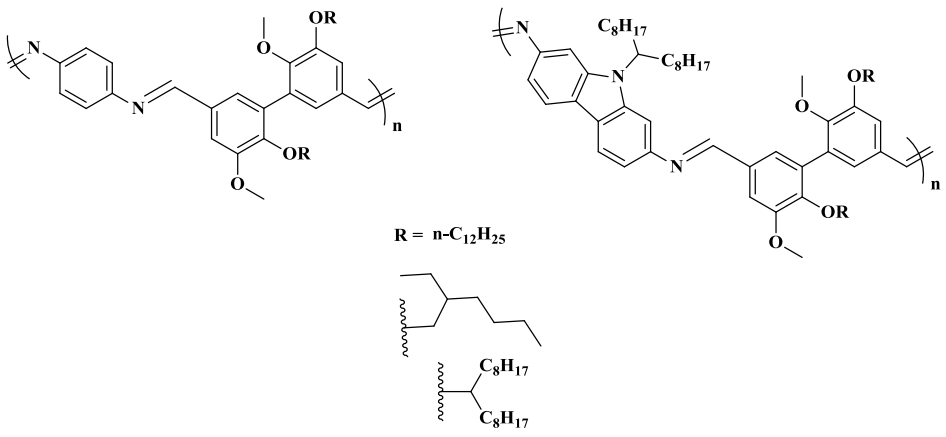

Figure 4-7: Polyazomethine based on 1,4-phenylenediamine (left) and 2,7-diaminocarbazole (right).

However, despite the presence of different functions linked to the divanillin, this monomer hasn't been used to synthesize conjugated polymers via metal-free polymerization.

In this work the synthesis of 3 divanillin monomers, alkylated with different alkyl chains has been performed. Thus, their polymerization with 1,4 benzene diamine or 2,7 carbazole diamine was carried out and their optical and electrochemical properties was studied.

4.3.2. Synthesis

4.3.2.1. Monomer synthesis

The 6,6-Dihydroxy-5,5-dimethoxy-[1,1-biphenyl]-3,3-dicarboxaldehyde **(DiVanillin)** has been synthesized from vanillin at room temperature using enzymatic coupling process (Scheme 4-11).[49]

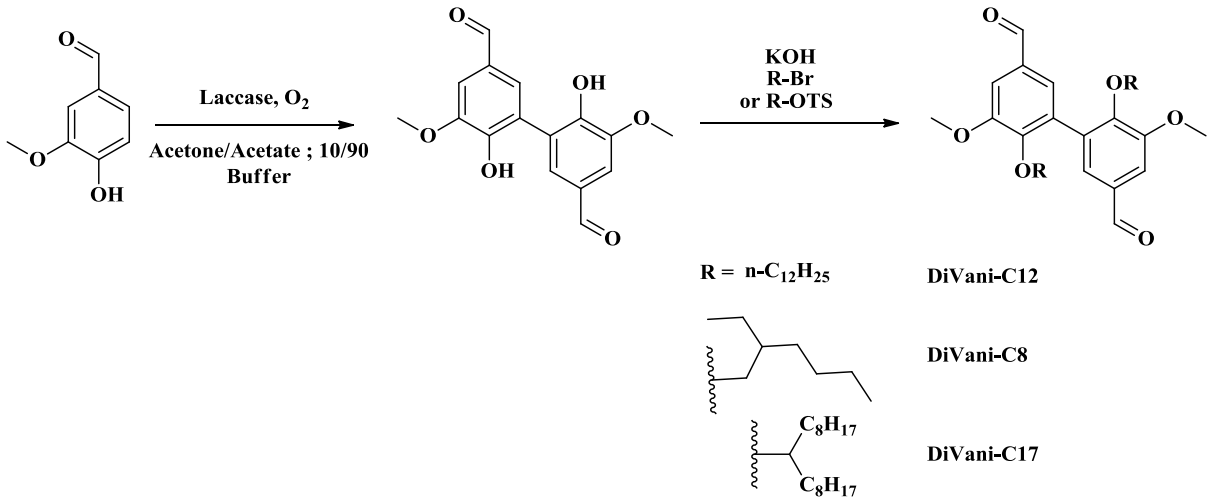

Scheme 4-11: Alkylation of the divanillin with dodecyl (DiVani-C12), ethylhexyl (DiVani-C8) and 9-heptadecanyl (DiVani-C17) chains.

A solution of vanillin in acetone was added to acetate buffer saturated in oxygen with laccase from Trametes Versicolor. In these conditions, the dimer precipitated and could be recovered by simple filtration. The filtrate has then simply been reloaded in vanillin and oxygen to start again the synthesis. Thus, it is possible to synthesize high purity divanillin (95%) in good yield and large amount. The divanillin structure has been attested by ^{1}H NMR, where the signal at 9.7 ppm corresponds to the 2 aldehyde protons and the signal at 7.5 and 7.2 ppm to the aromatic ones. The signal at 3.8 ppm corresponds to the methoxy groups (Figure 4-8).

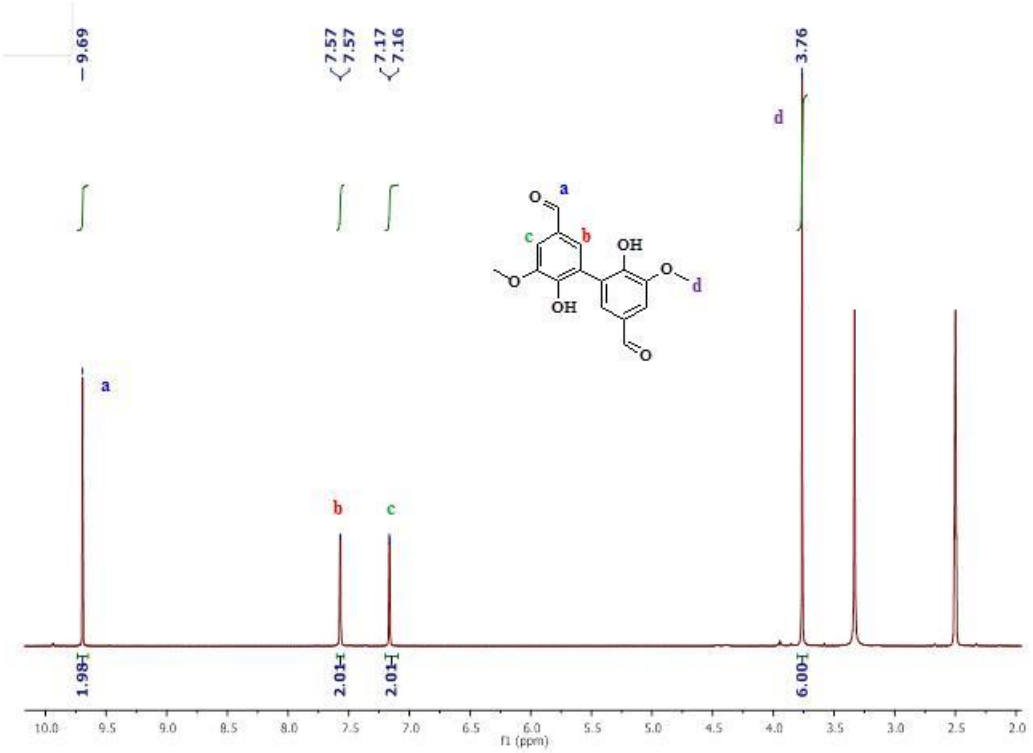

Figure 4-8: ^{1}H NMR (400 MHz) of the divanillin dialdehyde (in DMSO-d_6)

Divanillin was then alkylated by etherification reaction in DMSO in the presence of KOH with linear dodecyl, branched 2-ethylhexyl or previously synthesized 9-heptadecanyl chains (Scheme 2-3). They were varied in order to study their influence on solubility and properties of subsequent polyazomethines.[51–53] Alkylation was checked by NMR (see Figure 4-9).

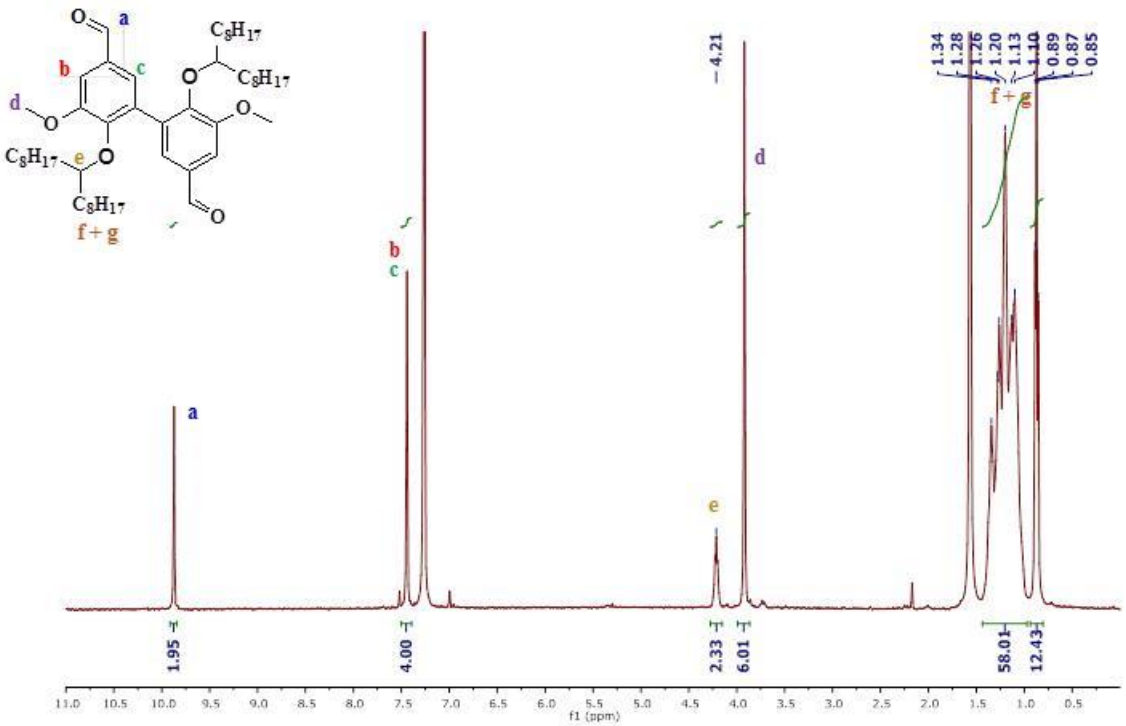

Figure 4-9: ^{1}H NMR (400 MHz) of the divanillin alkylated with the 9-heptadecanyl chain (DiVani-C17, in $CDCl_3$)

Signals at 3.8-4.4 ppm (O-C<u>H</u>$_2$) and at 0.6-1.6 ppm (C<u>H</u>$_2$) confirmed the attachment of alkyl groups on the vanillin monomer. Interestingly, aromatic protons protons arise as a singlet at 7.5 ppm Nevertheless, yields were found quite low as compared to literature data. This alkylation being usually performed with iodomethane, these yields could be explained by steric hindrance around alcohol functions of initial divanillin.[49]

4.3.2.2. Polymer synthesis

All three divanillin-based monomers were used in polycondensation reaction with commercially available benzene-1,4-diamine. Another material was targeted by reacting 2,7-diaminocarbazole and 2-ethylexyl divanillin (Scheme 4-12).

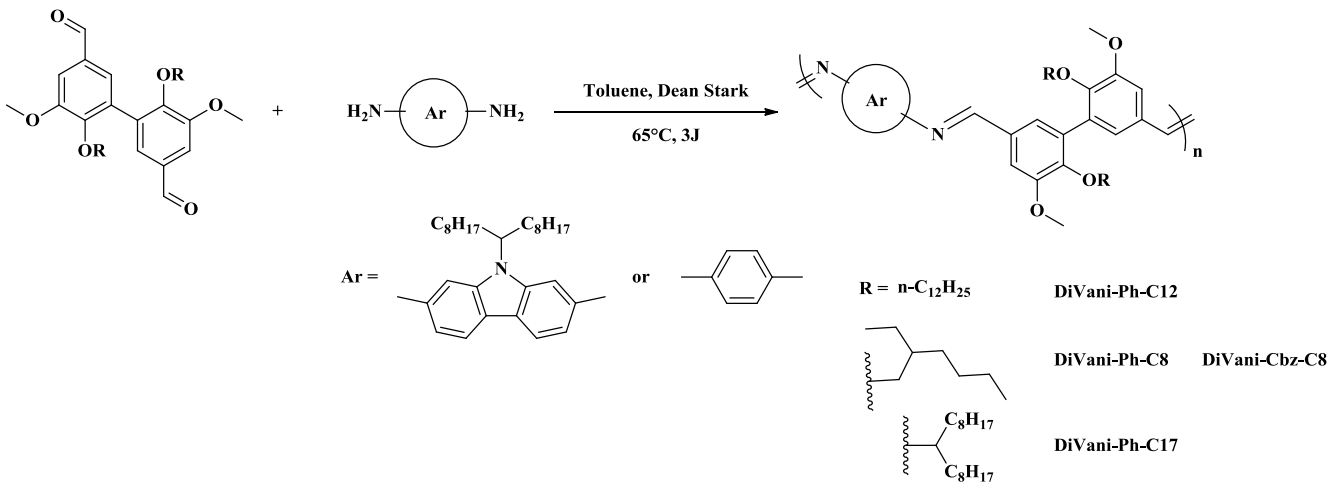

Scheme 4-12: Polymerization of the divanillin derivatives with diamino carbazole and *p*-phenylenediamine

As the polymerization using µ-wave was performed, stoichiometric amount of monomers were used along with silica as desiccant in order to push forward polymerization equilibrium. Classical filtration and washing could be performed for the easy recovery of copolymers. All materials were characterized by NMR and SEC. In ^{1}H NMR, the signal at 8.5 ppm clearly attested the formation of azomethine bound (-CH=N-) (Figure 4-10).

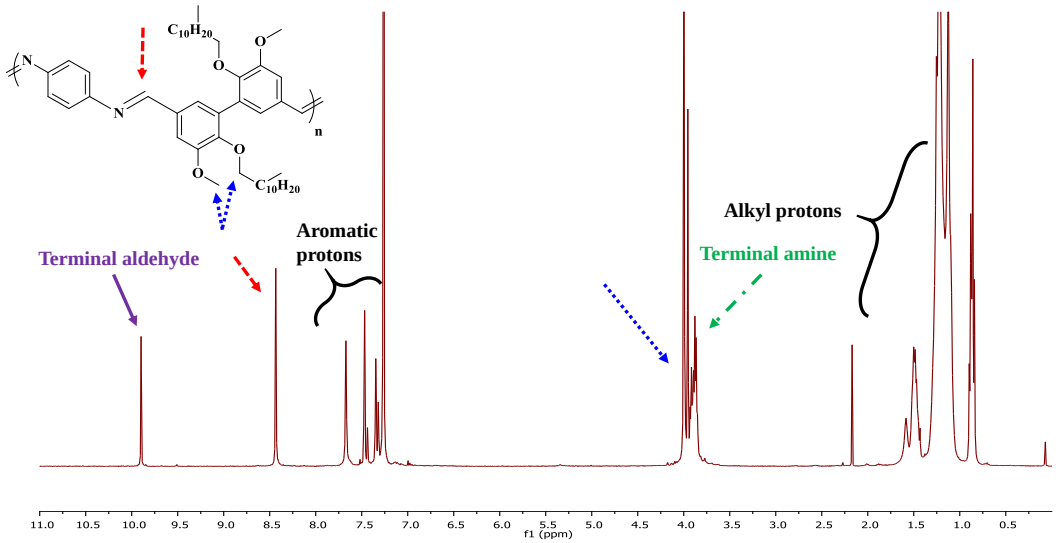

Figure 4-10: ^{1}H NMR (400 MHz) of the DiVani-Ph-C12 (in $CDCl_3$).

On this ^{1}H NMR, chain ends can be clearly seen (at 10.0 ppm) indicating a low degree of polymerization. Polymers were also analyzed by SEC in THF (Figure 4-11). A typical trace is shown, which is clearly representative of a polycondensation reaction showing series of oligomers. (see Figure 4-11).

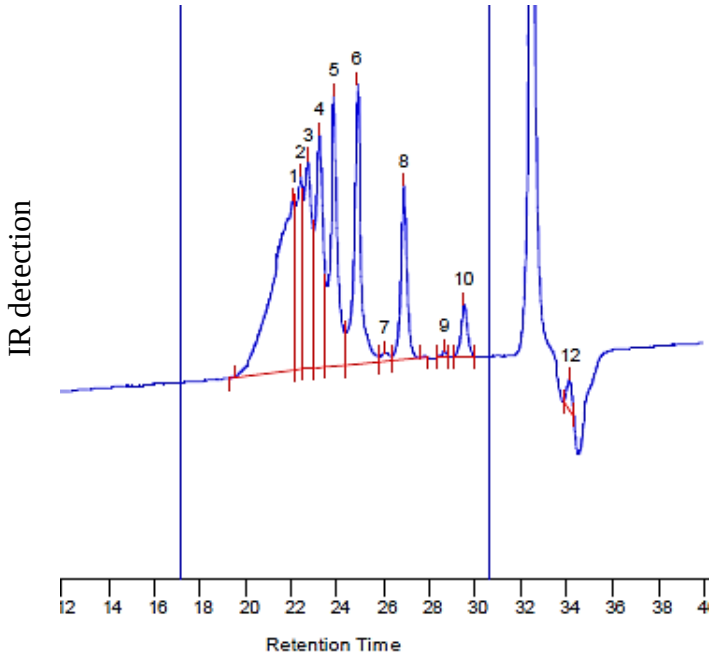

Peak N°	Mp	Mn	Mw
1	6839	9320	10427
2	5784	5820	5841
3	4752	4698	4719
4	3714	3674	3692
5	2741	2700	2718
6	1746	1718	1736
8	767	767	770
10	264	263	264

Figure 4-11: SEC data and trace of the DiVani-Ph-C8 polyazomethine (in THF, polystyrene calibration).

A discrepancy exists between the values obtained by SEC and the theoretical ones which can be due to the mode of detection and calibration made with polystyrene standard. For instance, Figure 4-12 illustrates 2 molecules that can be formed during reaction with their exact molar mass attesting a difference with values observed with SEC.

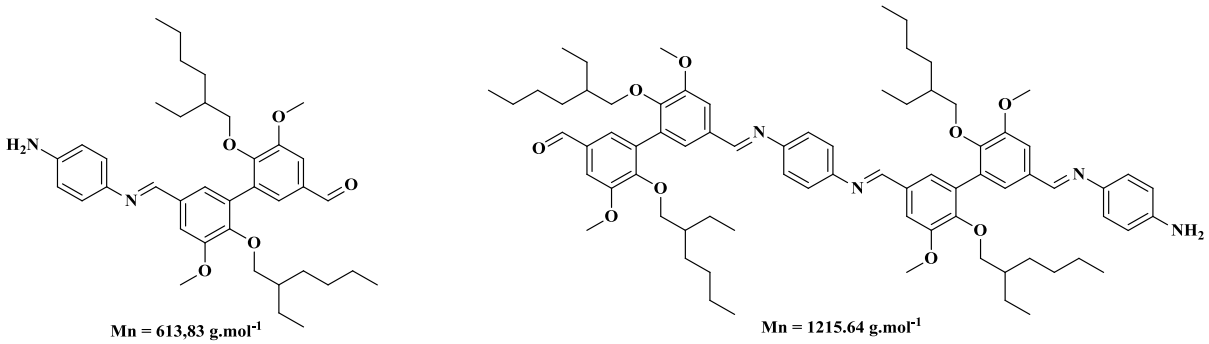

Figure 4-12: Molar mass of oligomers for n=1 and n=2.

All the molecular characteristics, thermal and optical properties of vanillin-based polyazomethines are reported in the Table 4-2 below.

Polymer	$\overline{M_n}$[a] [g.mol^{-1}]	$\overline{M_w}$[a] [g.mol^{-1}]	Đ[a]	$\overline{DP}_n$[a]	T_d[b] [°C]	Absorption[c] λ_{max} [nm]	Emission[c] λ_{max} [nm]	Φ_f[d]	
DiVani-Ph-C8	2200	3800	1.8	4	401	285-364	435	0.07	0.03
DiVani-Ph-C12	2500	4600	1.9	4	402	285-364	460	0.05	0.03
DiVani-Ph-C17	2800	5500	2.0	4	404	285-364	485	0.05	0.02
DiVani-Cbz-C8	6200	15400	2.5	7	401	270-390	580	0.09	0.05

Table 4-2: Molar masses, thermal and optical properties of carbazole based polyazomethines.
[a]Determined by gel permeation chromatography (GPC) relative to polystyrene standards from the soluble part of PCBT in THF at 40°C. [b]Decomposition temperature at 20% weight loss, evaluated under N_2 at a heating rate of 10 °C/min. [c]Determined in chloroform solution. [d]Determined respectively in film and solution with an integration sphere.

All of the divanillin based polymers present a number-average size of 2200 g.mol^{-1}, increasing with the size of the alkyl chain used, with a dispersity close to 2.0 which is coherent with a step-growth mechanism (at high conversion). However, the carbazole based polyazomethine presents a higher molar mass, mainly due to a higher molar mass of the repeating unit (912.4 g.mol^{-1} instead of 597.83 g.mol^{-1}) but also due to the synthesis of longer chains (probably due to a globally better solubility), with a $\overline{DP}_n$ of 7. In all phenylene based oligomers, the number of repeating unit is around 3.

Thermal properties of the polymers were determined by thermogravimetric analysis under N_2 atmosphere at a heating rate of 10°C per minutes. All polyazomethines present a good thermal stability with a degradation temperature around 405°C. It seems that the alkyl chain used doesn't have a significant impact on this temperature. For differential scanning calorimetry, analyses between -80°C and 200°C did not show any clear glass transition or crystallinity behavior, indicating the amorphous nature of these materials (see experimental part).

4.3.3. Optoelectronic properties

4.3.3.1. Optical characterizations

The absorption spectra of the obtained polymers have then been performed (Figure 4-13).

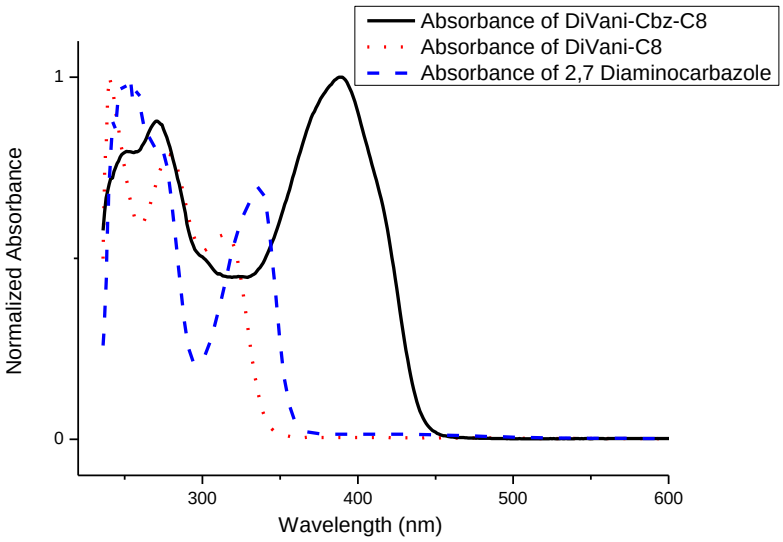

Figure 4-13: Absorption spectra of the polymer Cbz-Vani-C8 and of the two monomers; the 2,7-diaminocarbazole (blue, dash) and the DiVani-C8 (red, dot).

There is a clear red-shift and broadening of absorption spectrum when going from monomers to polymer confirming the occurrence of the polycondensation reaction. As shown below (see Figure 4-14) similar absorption band (at 400 nm) could be observed for the phenyl subunits based copolymers whatever the alkyl chain substituent.

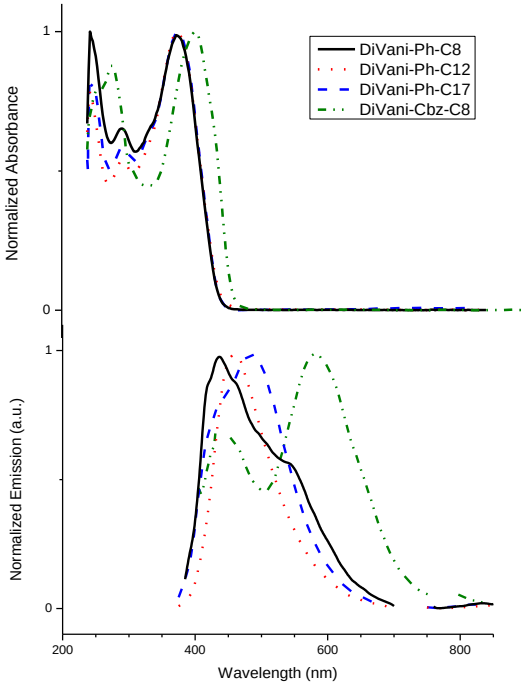

Figure 4-14: Absorption spectra (top) and emission spectra (excited at 360 nm, bottom) of the four DiVani-based polymers.

Again, the use of carbazole instead of a phenyl subunit shows a specific feature where the absorption band is red-shifted from 364 to 390 nm. This bathochromic effect is due to an electronic effect, the carbazole being more electron donating than the 1,4 benzene diamine. The same effect is observed on the emission spectrum, with a 100 to 150 nm red-shift between the carbazole and 1,4 benzene diamine. In the case of the emission, a shift in the maximum of absorption is observed. Depending of the alkyl chain used, there is a red-shift of up to 50 nm between the divanillin bearing the dodecyl chain compared to the one with the heptadecanyl chain. This may be due to some stacking effect.[54] Regardless this difference, the three *p*-phenylenediamine based polyazomethines emissions cover a broad wavelength from 380 to 650 nm, when the carbazole-based one covers a wavelength range from 400 to 700 nm which makes them interesting candidates for their insertion into emitting devices. To support this statement, their absolute fluorescence quantum efficiency has been measured with an integration sphere. In solution, the absolute fluorescence quantum efficiency goes from 4 to 9% and in solid state these values go lower, from 2 to 4%. This diminution from solution to film is coherent and is not as important as expected. This can be the combination of two processes, a low self-quenching and a diminution of the intramolecular rotation (non-radiative deactivation process) from solution to film. However, the solid state value of $\mathbf{\Phi_f}$ is still low, suggesting that there is still self-quenching or intramolecular rotation, both decreasing the fluorescence (in our case, both phenomenon are probably present). The effect of the alkyl chain can also be important. Indeed, aggregates present in solution can reduce the intramolecular rotation, the quantum efficiency value being dependent of the alkyl chain size. [55] In our case, the oligomer presenting the shorter (ethylhexyl) chain presents a slightly higher fluorescence quantum yield in solution only. In any case all these values are too low for their future integration into devices. However, as previously mentioned, these yields can be increased by lowering the temperature or doping the polymer for instance through the addition of 2,2,2-Trifluoroethanoic acid (trifluoroacetic acid). [56,57]

4.3.3.2. Electrochemical properties

Electrochemical properties were estimated by cyclic voltammetry using dichloromethane solutions of tetrabutylammonium hexafluorophosphate ($TBAPF_6$) as electrolyte, silver for the reference electrode and platinum for the working and counter-electrodes. Finally the material was solubilized in the electrolyte solution at a concentration of 0.1 $g.L^{-1}$ (Figure 4-15).

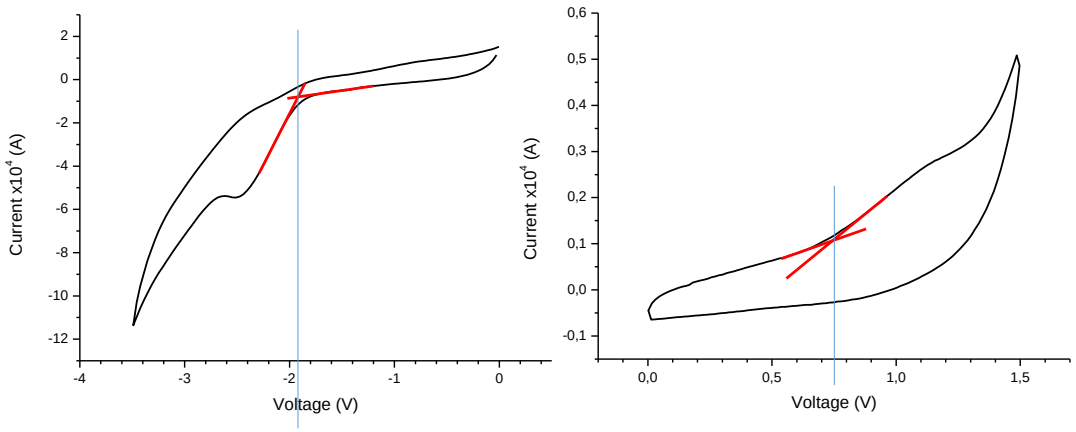

Figure 4-15:Cyclic voltammograms (left-reduction, right-oxidation) of DiVani-Ph-C17 in CH_2Cl_2 solution (0.1 g.l^{-1}) with $TBAPF_6$ as electrolyte.

The calculated values of the energy levels are summarized in Table 4-3.

Polymer	HOMO [eV][a]	LUMO [eV][a]	Eg^{elec} [eV][b]	Eg^{opt} [eV][c]
395 (C17)	- 5.15	- 2.3	2.85	3.02
424 (C12)	- 5.15	- 2.25	2.90	3.05
425 (C8)	- 5.21	- 2.35	2.86	3.06
Cbz	- 5.18	-2.52	2.66	2.85

Table 4-3: Electrochemical properties of Divanillin based polyazomethines.
[a]Estimated from the oxidation and reduction potentials measured by cyclic voltammetry in CH_2Cl_2 solution.
[b]Calculated by difference between oxidation and reduction potentials. [c]Calculated by Tauc method

The slight differences between the electrochemical and optical band-gaps can be explained by the fact that the redox peaks result from localized sites rather than from the conjugated backbone.[58] For all the three 1,4-diaminobenzene based polymers, both optical and electrochemical gap are comparable within experimental errors, with a value around 2.87 eV for the electrochemical gap and 3.05 eV for the optical one. For the carbazole based polyazomethine, these values reach respectively 2.66 eV and 2.85 eV. These gap reductions are coherent with the red-shift observed in both absorption and emission spectra.

4.4. Conclusion

In this chapter, syntheses of different polymers integrating original "bricks" such as vanillin, tetrazine or *in situ* formed benzobisthiazole have been presented. They all have been obtained *via* metal-free reactions and are original in the sense that these reactions or these compounds haven't been extensively studied. Oligomers have been synthesized, alternating carbazole and benzobisthiazole but with a too low solubility, impeding further characterization. Different tetrazine derivatives have then been coupled with 2,7-diaminocarbazole, leading to the formation of an insoluble brown compound, which we assumed being a network. Efforts have to be made to improve the solubility of these new compounds. Finally, alkylated divanillin has been synthesized and polymerized via a metal-free polycondensation reaction involving the 1,4 benzene diamine and an alkylated 2,7-diaminocarbazole. Interestingly, all polyazomethines present a broad emission. As expected, the carbazole-based polyazomethine show a red-shift absorption and emission due to the lower band-gap for the polymer, which is coherent with the replacement of the phenyl moiety with a carbazole one which is more electron-donating. However, the main advantage of the polycondensation between the divanillin and the 1,4 benzene diamino compound is that these conjugated polymers have been synthesized in environment friendly conditions, without transition-metal based catalyst, under micro-wave irradiation, in just three steps in a quantitative yield, and by coupling a bio-based monomer with a highly commercially available one. Moreover, first results concerning the optical and electrochemical properties are really promising for futures applications. The next step will be to improve their absolute fluorescence quantum efficiency by protonating the polymers and eventually integrating them into devices.[56,57] These very encouraging results open the way on a whole family of biosourced conjugated polymers.

4.5. References

[**1**] E. Ahmed, S. Subramaniyan, F. S. Kim, H. Xin, S. A. Jenekhe, *Macromolecules*, **2011**, *44*, 7207.

[**2**] D. Ades, A. Siove, G. Sauvet, *Journal de chimie physique*, **1998**, *95*, 1242.

[**3**] J. J. Intemann, J. F. Mike, M. Cai, C. A. Barnes, T. Xiao, R. A. Roggers, J. Shinar, R. Shinar, M. Jeffries-EL, *Journal of Polymer Science Part A: Polymer Chemistry*, **2013**, *51*, 916.

[**4**] S. Subramaniyan, F. S. Kim, G. Ren, H. Li, S. A. Jenekhe, *Macromolecules*, **2012**, *45*, 9029.

[**5**] S. Subramaniyan, T. Earmme, N. M. Murari, S. A. Jenekhe, *Polymer Chemistry*, **2014**, *5*, 5707.

[**6**] A. Dessì, G. Barozzino Consiglio, M. Calamante, G. Reginato, A. Mordini, M. Peruzzini, M. Taddei, A. Sinicropi, M. L. Parisi, F. Fabrizi de Biani, R. Basosi, R. Mori, M. Spatola, M. Bruzzi, L. Zani, *European Journal of Organic Chemistry*, **2013**, *2013*, 5961.

[**7**] A. P. Kulkarni, C. J. Tonzola, A. Babel, S. A. Jenekhe, *Chemistry of Materials*, **2004**, *16*, 4556.

[**8**] A. Ajayaghosh, *ChemInform*, **2003**, *34*, 181.

[**9**] J. F. Wolfe, B. H. Loo, *Macromolecules*, **1981**, *14*, 915.

[**10**] S. R. Allen, A. G. Filippov, R. J. Farris, E. L. Thomas, *Macromolecules*, **1981**, *14*, 1135.

[**11**] E. E. Havinga, A. Pomp, W. ten Hoeve, H. Wynberg, *Synthetic Metals*, **1995**, *69*, 581.

[**12**] E. E. Havinga, W. ten Hoeve, H. Wynberg, *Synthetic Metals*, **1993**, *55*, 299.

[**13**] E. E. Havinga, W. ten Hoeve, H. Wynberg, *Polymer Bulletin*, **1992**, *29*, 119.

[**14**] E. Ahmed, F. S. Kim, H. Xin, S. A. Jenekhe, *Macromolecules*, **2009**, *42*, 8615.

[**15**] T. Hattori, H. Akita, M. Kakimoto, Y. Imai, *Macromolecules*, **1992**, *25*, 3351.

[**16**] Y. I. Yoshio Imai, Isao Taoka, Keikichi Uno, *Die Makromolekulare Chemie*, **1964**, *83*, 167.

[**17**] W. J. Dennistoun, F. W. Bergstrom, *Journal of the American Chemical Society*, **1933**, *55*, 3648.

[**18**] D. M. Badgujar, M. B. Talawar, S. N. Asthana, P. P. Mahulikar, *Journal of Hazardous Materials*, **2008**, *151*, 289.

[**19**] D. E. Chavez, M. A. Hiskey, D. L. Naud, *Propellants, Explosives, Pyrotechnics*, **2004**, *29*, 209.

[**20**] M. Hanack, S. Deger, U. Keppeler, A. Lange, A. Leverenz, R. Manfred, *Synthetic Metals*, **1987**, *19*, 739.

[**21**] M. Hanack, K. Dürr, A. Lange, J. Osio Barcina, J. Pohmer, E. Witke, *Synthetic Metals*, **1995**, *71*, 2275.

[**22**] M. Hanack, A. Lange, R. Grosshans, *Synthetic Metals*, **1991**, *45*, 59.

[**23**] Z. Novak, A. Kotschy, *Organic Letters*, **2003**, *5*, 3495.

[**24**] P. Audebert, S. Sadki, F. Miomandre, G. Clavier, *Electrochemistry Communications*, **2004**, *6*, 144.

[**25**] P. Audebert, S. Sadki, F. Miomandre, G. Clavier, M. C. Vernieres, M. Saoud, P. Hapiot, *New Journal of Chemistry*, **2004**, *28*, 387.

[**26**] P. Audebert, F. Miomandre, G. Clavier, M. C. Verniéres, S. Badré, R. Méallet-Renault, *Chemistry - A European Journal*, **2005**, *11*, 5667.

[**27**] Y. Kim, E. Kim, P. Audebert, *Chemical Communications*, **2006**, *2*, 3612.

[**28**] M. J. Baek, W. Jang, S. H. Lee, Y. S. Lee, *Synthetic Metals*, **2012**, *161*, 2785.

[**29**] S. Pluczyk, P. Zassowski, L. Galmiche, P. Audebert, M. Lapkowski, *Electrochimica Acta*, **2016**, *212*, 856.

[**30**] P. Ma, C. Wang, S. Wen, L. Wang, L. Shen, W. Guo, S. Ruan, *Solar Energy Materials and Solar Cells*, **2016**, *155*, 30.

[**31**] G. Clavier, P. Audebert, *Chemical Reviews*, **2010**, *110*, 3299.

[**32**] N. Saracoglu, *Tetrahedron*, **2007**, *63*, 4199.

[**33**] W. Kaim, *Coordination Chemistry Reviews*, **2002**, *230*, 127.

[**34**] Y. H. Gong, F. Miomandre, R. Méallet-Renault, S. Badré, L. Galmiche, J. Tang, P. Audebert, G. Clavier, *European Journal of Organic Chemistry*, **2009**, 6121.

[**35**] A. Cutivet, E. Leroy, E. Pasquinet, D. Poullain, *Tetrahedron Letters*, **2008**, *49*, 2748.

[**36**] D. E. Chavez, M. A. Hiskey, R. D. Gilardi, *Angewandte Chemie - International Edition*, **2000**, *39*, 1791.

[**37**] D. E. Chavez, M. A. Hiskey, *Journal of Heterocyclic Chemistry*, **1998**, *35*, 1329.

[**38**] Z. Novak, B. Bostai, M. Csékei, K. Lörincz, A. Kotschy, *Heterocycles*, **2013**, *60*, 2653.

[**39**] E. Jullien-Macchi, V. Alain-Rizzo, C. Allain, C. Dumas-Verdes, P. Audebert, *RSC Advances*, **2014**, *4*, 34127.

[**40**] D. E. Chavez, M. A. Hiskey, *Journal of Energetic Materials*, **2004**, 37.

[**41**] M. D. Coburn, G. A. Buntain, B. W. Harris, M. A. Hiskey, K.-Y. Lee, D. G. Ott, *Journal of Heterocyclic Chemistry*, **1991**, *28*, 2049.

[**42**] Z. Qing, P. Audebert, G. Clavier, F. Miomandre, J. Tang, T. T. Vu, R. Méallet-Renault, *Journal of Electroanalytical Chemistry*, **2009**, *632*, 39.

[**43**] Z. Wong, K. Chen, J. Li, *BioResources*, **2010**, *5*, 1509.

[**44**] E. A. B. da Silva, M. Zabkova, J. D. Aranjo, C. A. Cateto, M. F. Barreiro, M. N. Belgacem, A. E. Rodrigues, *Chemical Engineering Research and Design*, **2009**, *87*, 1276.

[**45**] J. D. P. Araújo, C. A. Grande, A. E. Rodrigues, *Chemical Engineering Research and Design*, **2010**, *88*, 1024.

[**46**] M. Fache, B. Boutevin, S. Caillol, *Green Chemistry*, **2016**, *18*, 712.

[**47**] I. Kaya, M. Yildirim, M. Kamaci, *European Polymer Journal*, **2009**, *45*, 1586.

[**48**] M. Andruh, *Dalton Transactions*, **2015**, *44*, 16633.

[**49**] A. Llevot, E. Grau, S. Carlotti, S. Grelier, H. Cramail, *Polymer Chemistry*, **2015**, *6*, 6058.

[**50**] S. Kobayashi, A. Makino, *Chemical Reviews*, **2009**, *109*, 5288.

[**51**] C. Yang, S. A. Jenekhe, *Chemistry of Materials*, **1991**, *3*, 878.

[**52**] K. S. Lee, J. C. Won, J. C. Jung, *Makromolekulare Chemie-Macromolecular Chemistry and Physics*, **1989**, *190*, 1547.

[**53**] B. A. Reinhardt, M. R. Unroe, *Polymer Preprints*, **1990**, 620.

[**54**] S. M. Mcafee, P. Josse, A. Labrunie, S. Dabos-seignon, J. Roncali, G. C. Welch, P. Blanchard, **2016**, *37*, 479.

[**55**] Y. Liu, Y. Lei, M. Liu, F. Li, H. Xiao, J. Chen, X. Huang, W. Gao, H. Wu, Y. Cheng, *Journal of Materials Chemistry C*, **2016**, *4*, 5970.

[**56**] S. Barik, W. G. Skene, *Polymer Chemistry*, **2011**, *2*, 1091.

[**57**] S. Barik, T. Bletzacker, W. G. Skene, *Macromolecules*, **2012**, *45*, 1165.

[**58**] P. L. T. Boudreault, A. Najari, M. Leclerc, *Chemistry of Materials*, **2011**, *23*, 456.

4.6. Experimental Section

For general experimental informations, see the corresponding section page 235.

4.6.1. General procedure for the synthesis of Poly (Benzobisthiazole-*alt*-carbazole)

The synthesis and characterization of the 9-Heptadecanyl-2,7-diformylcarbazole has already been described in the second chapter of this manuscript. The 2,5-diamino-1,4-benzenedithiol di-hydrochloride has been directly used as received. 2,7-Diformylcarbazole (100 mg, 0.22 mmol) was dissolved in DMSO (5 mL). Then, in stoichiometric amount, 2,5-diamino-1,4-benzenedithiol di-hydrochloride (53.1 mg) were added to the reaction. The reaction mixture has then been heated, either at 140°C in an oil bath for 72 hours, or under µ-wave radiation during 4 hours or 1 hour. The crude product has been washed with methanol to remove the eventual residual monomer (too few to be quantified).

4.6.2. Tetrazine

Both the 3,6-Dichloro-1,2,4,5-tetrazine **Tz-Cl** and the 3,6-bis(3,5-dimethylpyrazol-1-yl)-1,2,4,5-tetrazine **Tz-Hi** have been gracefully furnished by P. Audebert.

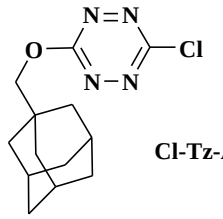

Cl-Tz-Ada

3-(adamantane-1-yloxy)-6-chloro-1,2,4,5-tetrazine (Cl-Tz-Ada)

3,6-Dichloro-1,2,4,5-tetrazine (750 mg, 5 mmol) and 1-(Hydroxymethyl)adamantane (1-adamantanmethanol) (830 mg, 5.1 mmol) were solubilized in dichloromethane. Then 650 mg of 2,3,5-Trimethylpyridine (2,3,5 collidine) were added (5.3 mmol). The reaction was then mixed at room temperature for two hours. The crude product was purified by flash chromatography in a mixture of cyclohexane and dichloromethane (10:90) to afford a pink powder (yield: 99%).

^{1}H NMR (400 MHz, DMSO-d_6, ppm): d 4.22 (s, 2H); 2.05 (s, 3H); 1.79-1.70 (m, 12H)

^{13}C NMR (101 MHz, DMSO-d_6, ppm): d 167.10; 164.08; 80.32; 39.01; 36.84; 33.78; 27.95

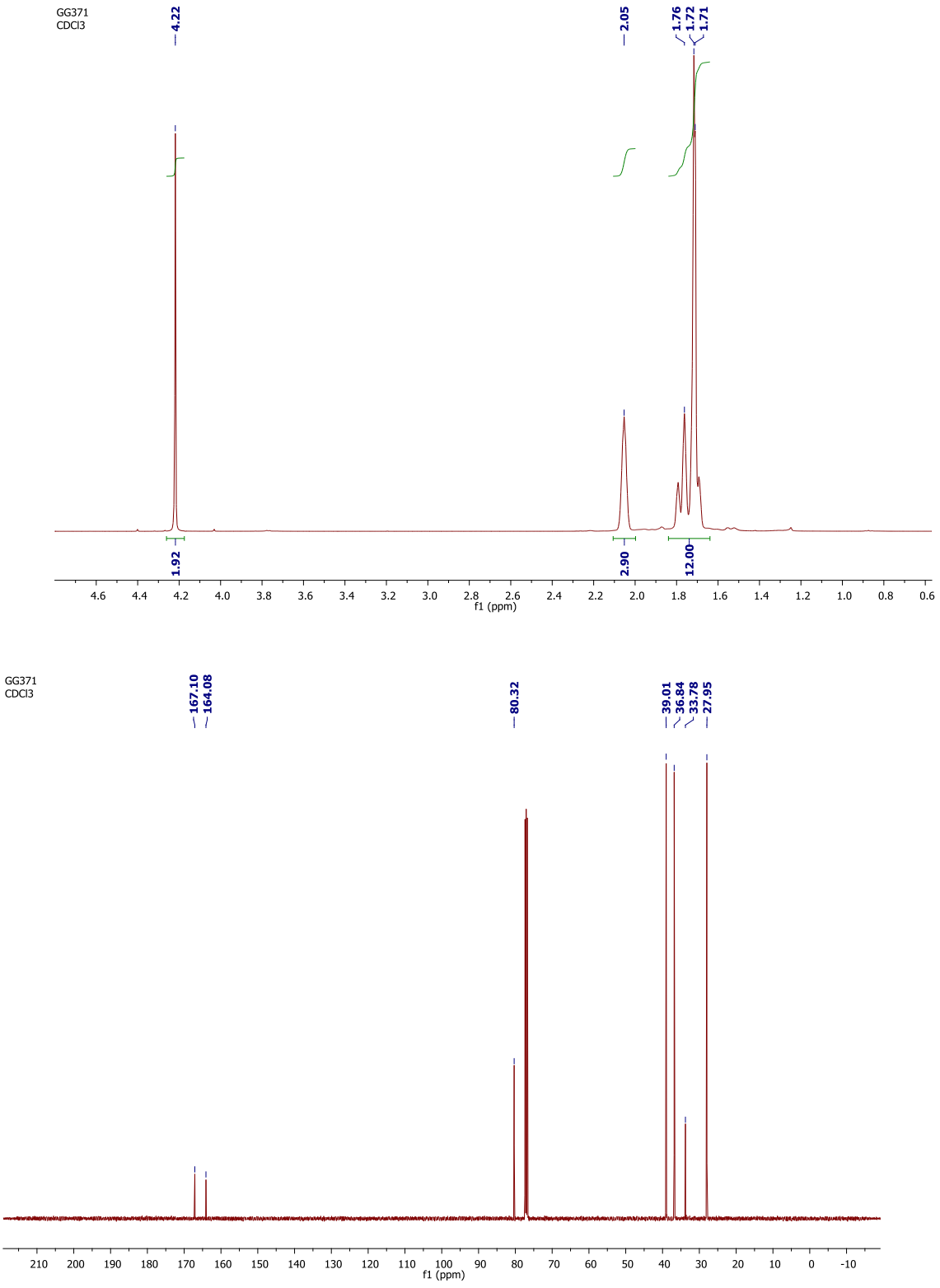

Figure 4-16: ^{1}H NMR (400 MHz, top) and ^{13}C NMR (101 MHz, bottom) of 3-(adamantane-1-yloxy)-6-chloro-1,2,4,5-tetrazine (Cl-Tz-Ada) in ($CDCl_3$).

Tz-Cbz-Tz: 2,7-diaminocarbazole (100 mg, 0.23 mmol) was solubilized with 141.4 mg of **Cl-Tz-Ada** (0.5 mmol, 2.2 equivalents) in dichloromethane. Then 55.5 mg of 2,3,5 collidine (2 equivalents) have been added to the reaction mixture. The reaction was then heated at 90°C under micro-wave irradiation for 2 hours. A brown product has then been recovered.

Cbz-Tz: 2,7-diaminocarbazole (100 mg, 0.23 mmol) was solubilized with 34.6 mg of **Tz-Cl** (0.23 mmol), in dichloromethane. Then 2.8 mg of 2,3,5 collidine (0.1 equivalent) have been added to the reaction mixture. The reaction was then heated either at 90°C under micro-wave irradiation for 4 hours or at 70°C in an oil bath for 24 hours. In both cases, a brown product has then been recovered.

4.6.3. Divanilline

Vanillin, 1-bromododecane and 2-Ethylhexyl bromide have been used as received and *p*-phenylenediamine has been recrystallized in water prior utilization. The syntheses and characterizations of the 2,7-diaminocarbazole and the 9-heptadecane *p*-toluenesulfonate have already been described in the second chapter of this work.

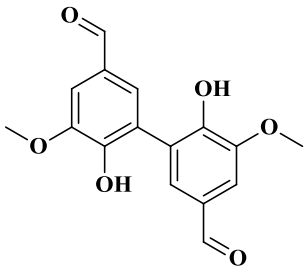

6,6′-Dihydroxy-5,5′-dimethoxy-[1,1′-biphenyl]-3,3′-dicarboxaldehyde (Divanillin) :

A solution of vanillin in acetone was added to acetate buffer saturated in oxygen with laccase from Trametes Versicolor. In these conditions, the dimer formed precipitates and can be recovered by simple filtration. The filtrate has then simply been reloaded in vanillin and oxygen to start again the synthesis.

^{1}H NMR (400 MHz, DMSO-d_6, ppm): d 9.69 (s, 2H); 7.57 (d, J=1.9 Hz, 2H); 7.16 (d, J = 1.9 Hz, 2H); 3.76 (s, 6H)

^{13}C NMR (101 MHz, DMSO-d_6, ppm): d 191.17; 150.42; 148.16; 128.19; 127.75; 124.57; 109.15; 56.03

FT-IR (ATR): ν= 3220, 1676, 1587, 1413, 1245, 1127, 750 cm^{-1}

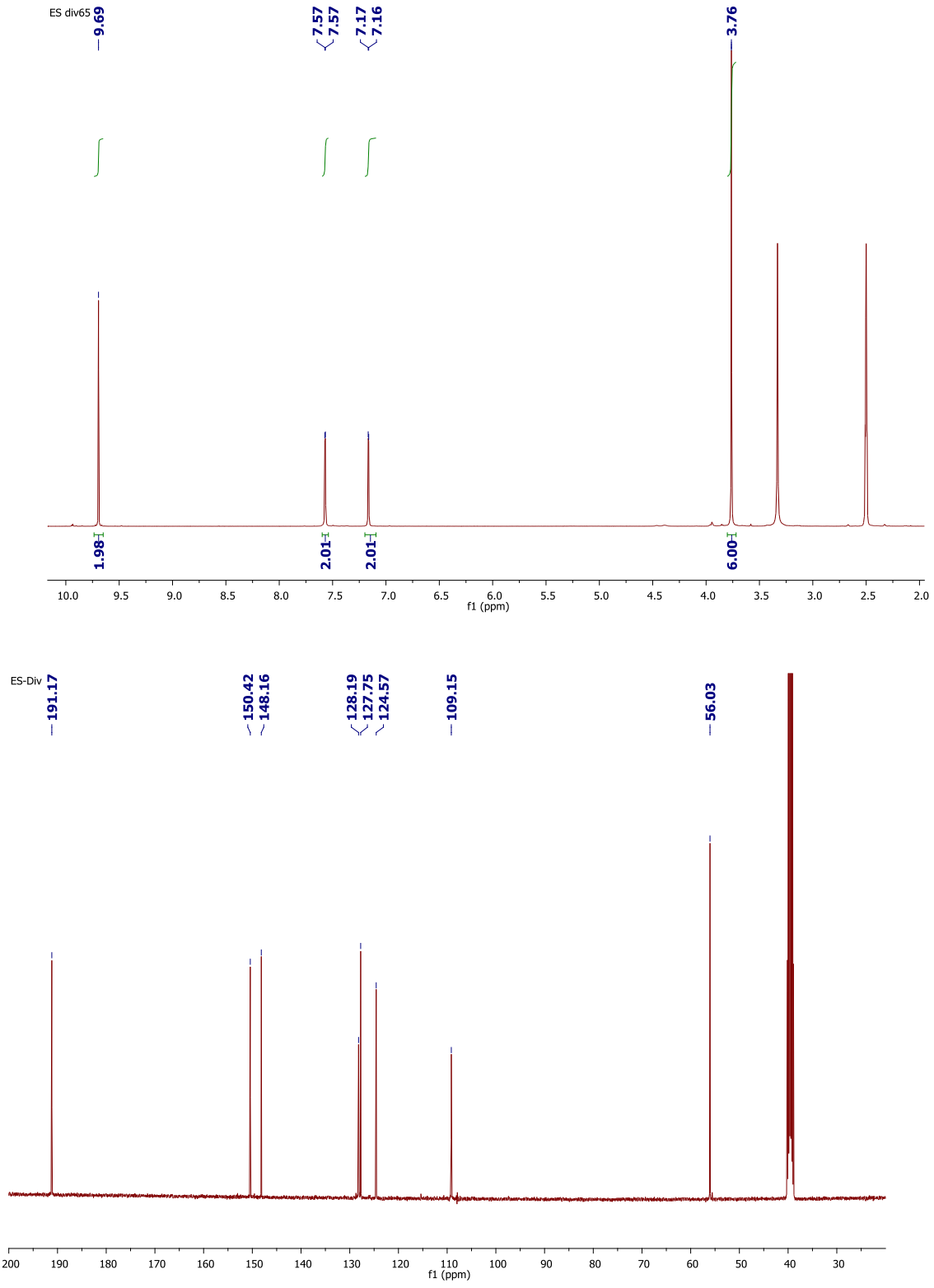

Figure 4-17: ^{1}H NMR (400 MHz, top) and ^{13}C NMR (101MHz, bottom) spectra of the divanillin (in DMSO-d_6).

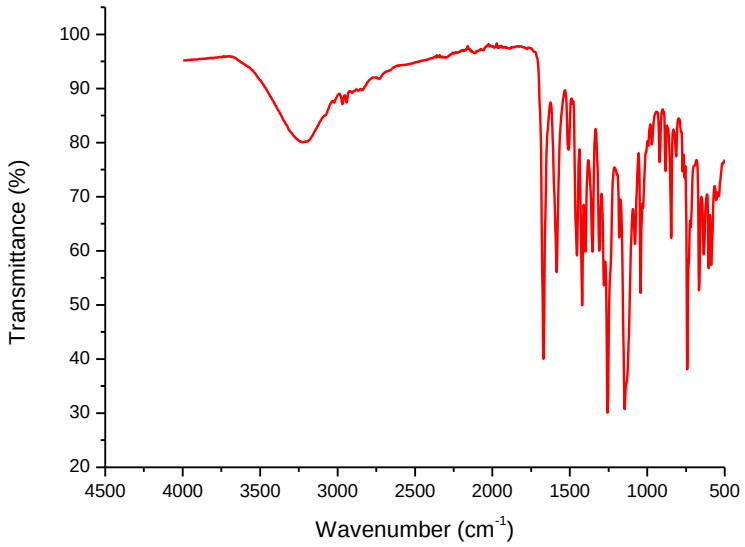

Figure 4-18: ATR-FTIR spectrum of the divanillin.

6,6′-Dialkylated-5,5′-dimethoxy-[1,1′-biphenyl]-3,3′-dicarboxaldehyde (Alkylated Divanillin, DiVani-C8; DiVani-C12; DiVani-C17)

General procedure.

In a dried and nitrogen flushed 100 mL glassware, divanillin (2 g, 6.62 mmol) was solubilized in 20 mL of previously dried DMSO. Then KOH (0.89 mg, 15.9 mmol) was added to the reaction mixture which was heated at 80°C for 2 hours. Then, 2.2 equivalent of the chosen alkyl chain (ethylhexyl, dodecyl or heptadecanyl) have been added to the reaction mixture and heated for 12 more hours. The reaction mixture has then been poured into 300 mL of water and extracted with 100 mL of diethyl ether, 3 times. The crude product recovered after the diethyl ether evaporation, has been purified with flash chromatography in a mixture of cylcohexane/ethyl acetate (95/5), yield > 55 %

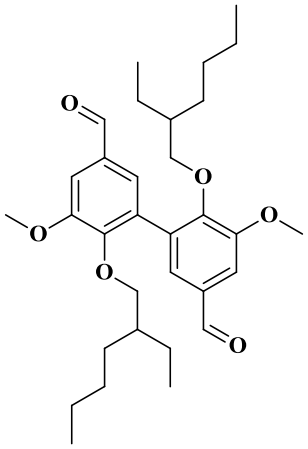

DiVani-C8

^{1}H NMR (400 MHz, $CDCl_3$, ppm): d 9.89 (s, 2H); 7.46 (dd, J=8.7, 1.9 Hz, 4H); 3.95 (s, 6H); 3.81 (m, 4H), 1.39-1.06 (m, 18H), 0.80 (t, J=7 Hz, 6H), 0.69 (t, J=7.4 Hz, 6H)
^{13}C NMR (101 MHz, $CDCl_3$, ppm): d 191.17; 153.72; 152.08; 132.24; 131.86; 128.40; 109.96; 73.74; 56.13; 32.07; 30.19; 29.80; 29.74; 29.71; 29.51; 29.41; 25.84; 22.84; 14.26
FT-IR (ATR): ν= 3220, 1676, 1587, 1413, 1245, 1127, 750 cm^{-1}
HRMS (EI+, m/z) [M]+ calculated (%) for $C_{32}H_{46}O_6Na$: 549.3186, found 549.3163

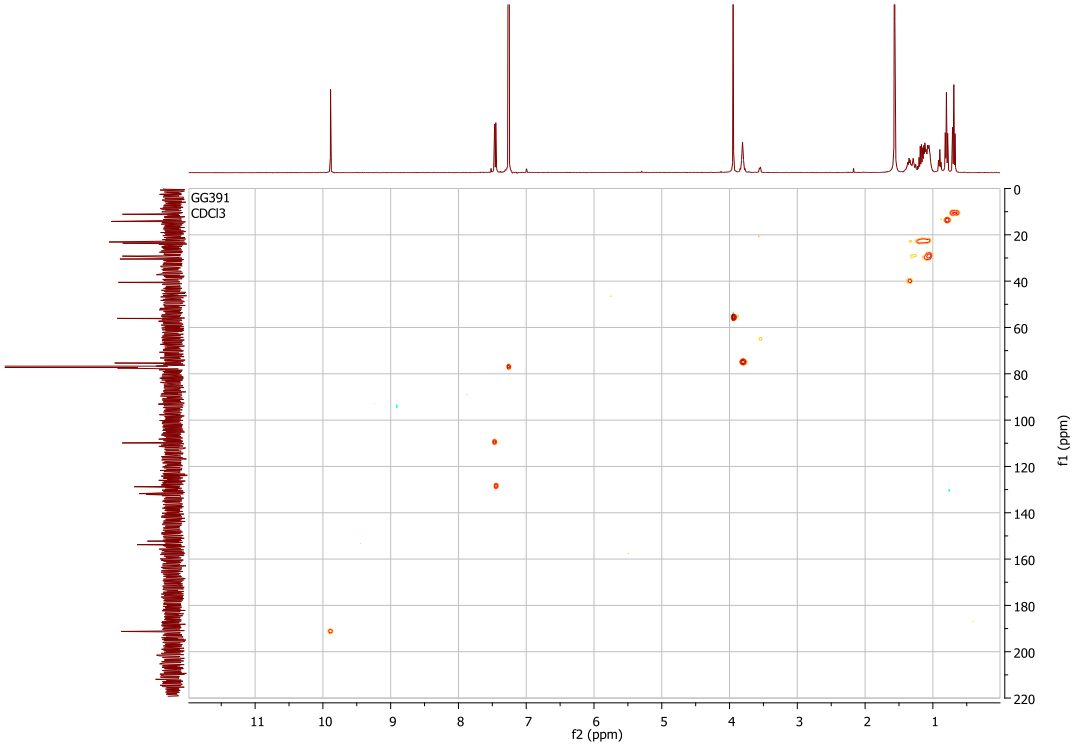

Figure 4-19: ^{1}H-13C HSQC NMR spectra of DiVani-C8 (in $CDCl_3$).

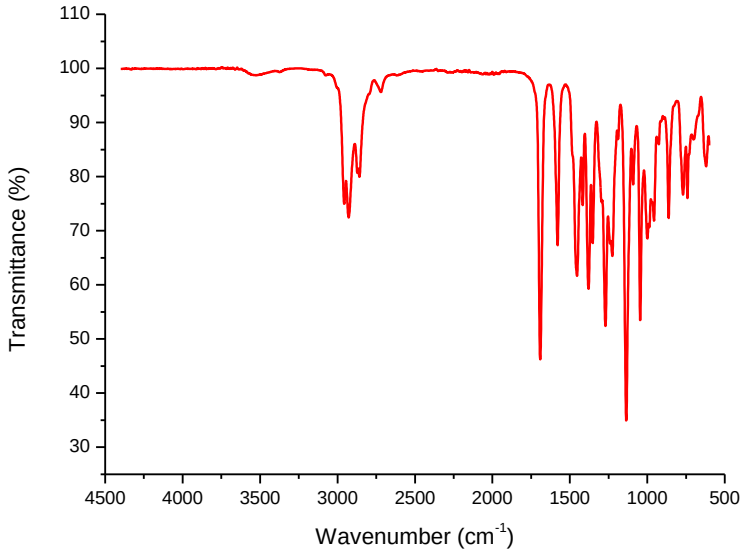

Figure 4-20: ATR-FTIR spectrum of DiVani-C8.

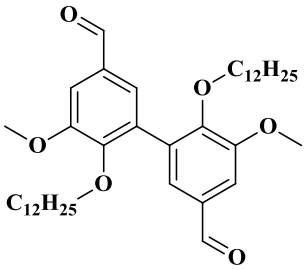

DiVani-C12

^{1}H NMR (400 MHz, $CDCl_3$, ppm): d 9.89 (s, 2H); 7.46 (dd, J=16.1 Hz, 1.9 Hz, 4H); 3.95 (s, 6H); 3.90 (t, J=6.4Hz 4H); 1.46 (m, 4H); 1.39-1.00 (m, 36H), 0.88 (t, J=6.9 Hz, 6H)

^{13}C NMR (101 MHz, $CDCl_3$, ppm): d 191.25; 153.76; 152.26; 132.12; 131.75; 128.74; 109.86; 75.36; 56.09; 40.53; 30.45; 29.20; 23.63; 23.11; 14.23; 11.13

FT-IR (ATR): ν= 2930, 2850, 1676, 1587, 1413, 1245, 1127, 750 cm^{-1}

HRMS (EI+, m/z) [M]+ calculated (%) for $C_{29}H_{41}Br_2N$: 561.16057, found 561.16261

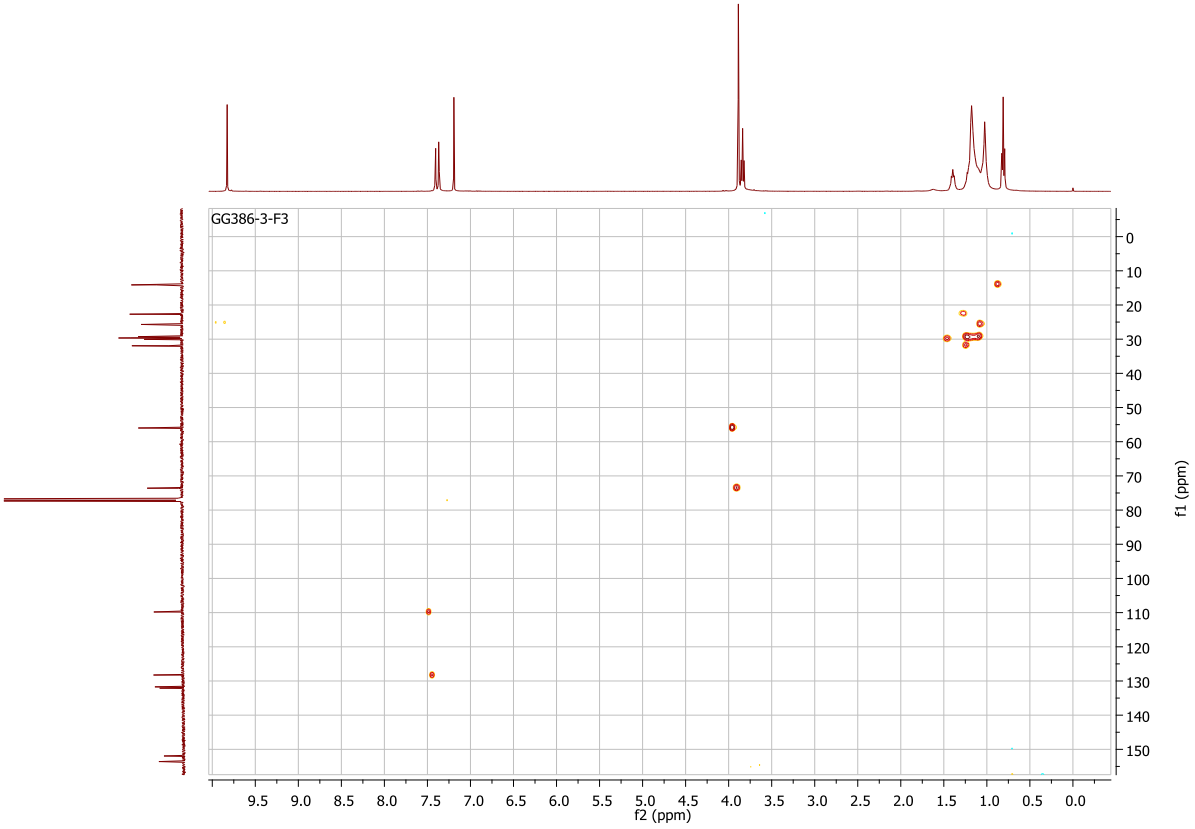

Figure 4-21: ^{1}H-13C HSQC NMR spectra of DiVani-C12 (in $CDCl_3$).

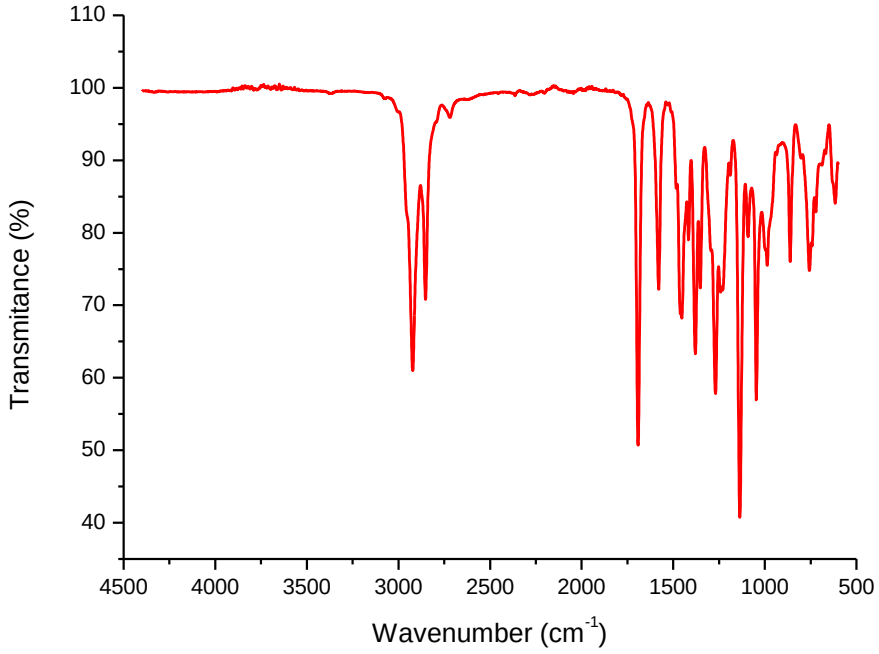

Figure 4-22: ATR-FTIR spectrum of DiVani-C12.

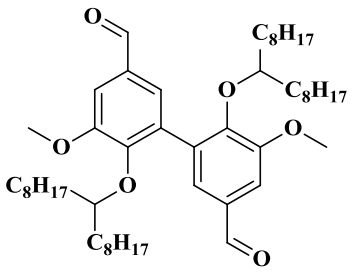

DiVani-C17

^{1}H NMR (400 MHz, $CDCl_3$, ppm): d 9.87 (s, 2H); 7.44 (m, 4H); 4.21 (m, 2H); 3.92 (s, 6H), 1.57 (s, 8H); 1.40-1.00 (m, 52H), 0.87 (t, J=7 Hz, 12H)

^{13}C NMR (101 MHz, $CDCl_3$, ppm): d 191.25; 153.76; 152.26; 132.12; 131.75; 128.74; 109.86; 75.36; 56.09; 40.53; 30.45; 29.20; 23.63; 23.11; 14.23; 11.13

FT-IR (ATR): ν= 3220, 1676, 1587, 1413, 1245, 1127, 750 cm^{-1}

HRMS (EI+, m/z) [M]+ calculated (%) for $C_{50}H_{82}O_6Na$: 801.6003, found 801.6012

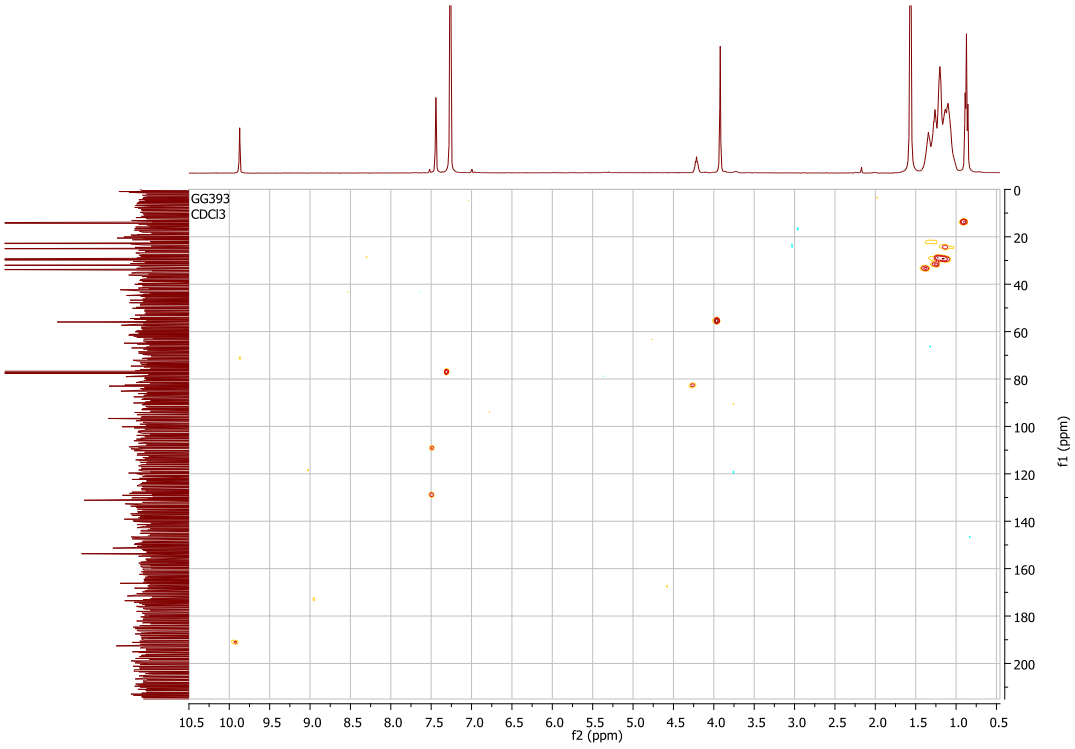

Figure 4-23: ^{1}H-13C HSQC NMR spectra of DiVani-C17 (in $CDCl_3$).

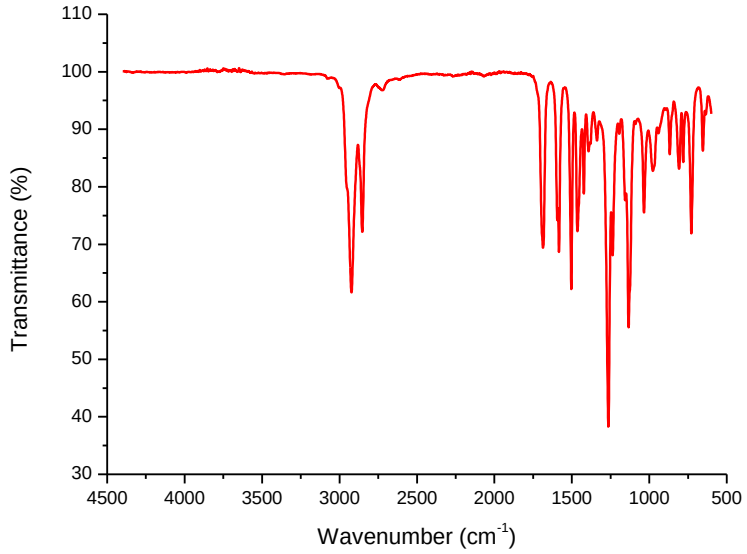

Figure 4-24: ATR-FTIR spectrum of DiVani-C17.

Polyazomethines, general procedure:

In a 10 mL micro-wave dedicated glassware, a stoeichiometric amount of *p*-phenylenediamine or 2,7-diaminocarbazole is solubilized with the previously alkylated DiVani monomers in 2 mL of toluene. Silica (3 mg) was then added and the reaction heated at 130°C for 4 hours. The crude polymer was then purified on Soxhlet apparatus with methanol and then chloroform to afford the final polymers.

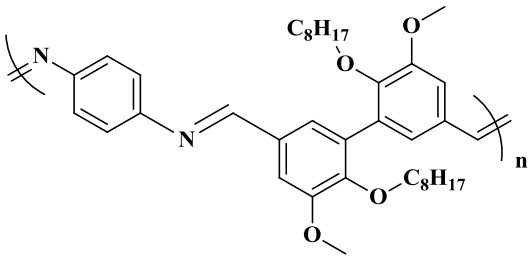

DiVani-Ph-C8

^{1}H NMR (400 MHz, $CDCl_3$, ppm): d 9.89 (s, 2H); 7.46 (dd, J=8.7, 1.9 Hz, 4H); 3.95 (s, J = 6H); 3.81 (m, 4H), 1.39-1.06 (m, 18H), 0.80 (t, J=7 Hz, 6H), 0.69 (t, J=7.4 Hz, 6H)

^{13}C NMR (101 MHz, $CDCl_3$, ppm): d 191.25; 153.76; 152.26; 132.12; 131.75; 128.74; 109.86; 75.36; 56.09; 40.53; 30.45; 29.20; 23.63; 23.11; 14.23; 11.13

FT-IR (ATR): ν= 3220, 1676, 1587, 1413, 1245, 1127, 750 cm^{-1}

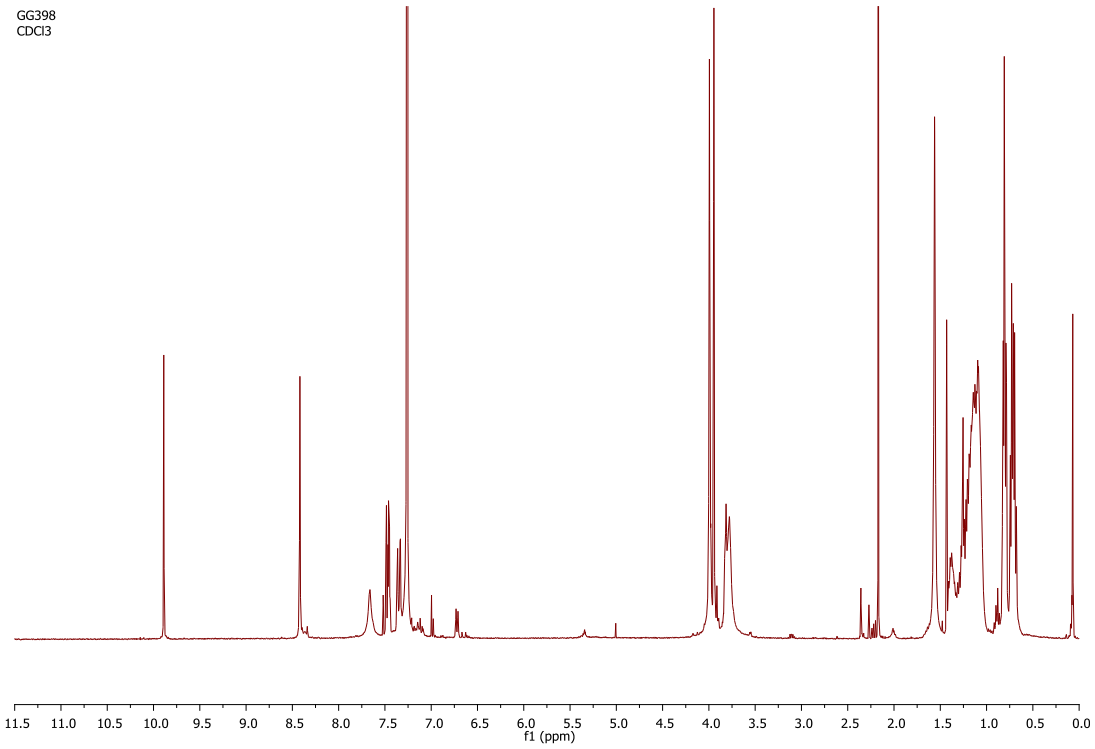

Figure 4-25: ^{1}H NMR (400 MHz) spectrum of DiVani-Ph-C8 (in $CDCl_3$).

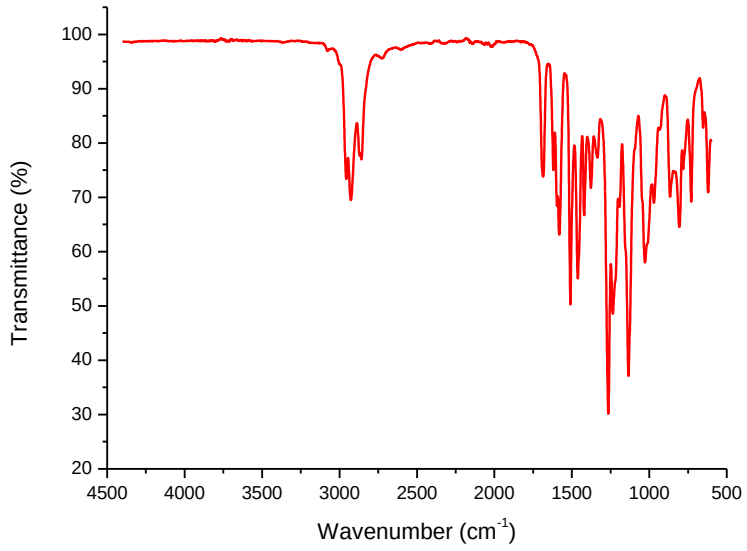

Figure 4-26: ATR-FTIR spectrum of DiVani-Ph-C8.

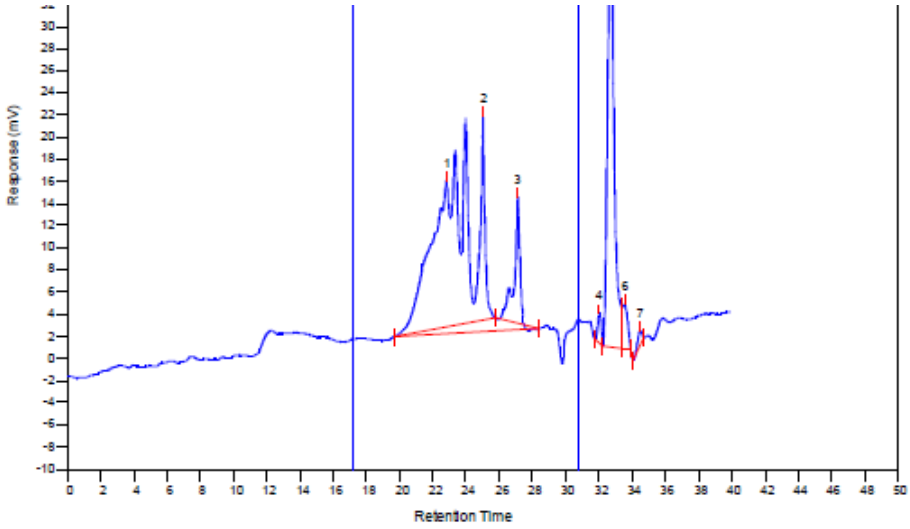

MW Averages

Peak No	Mp	Mn	Mw	Mz	Mz+1	Mv	PD
1	1684	2147	3808	6376	9587	3502	1.77364
2	2620	3118	4398	6538	9437	4149	1.41052
3	743	783	792	803	815	791	1.01149

Figure 4-27: SEC trace of the DiVani-Ph-C8 (in THF, polystyrene standard).

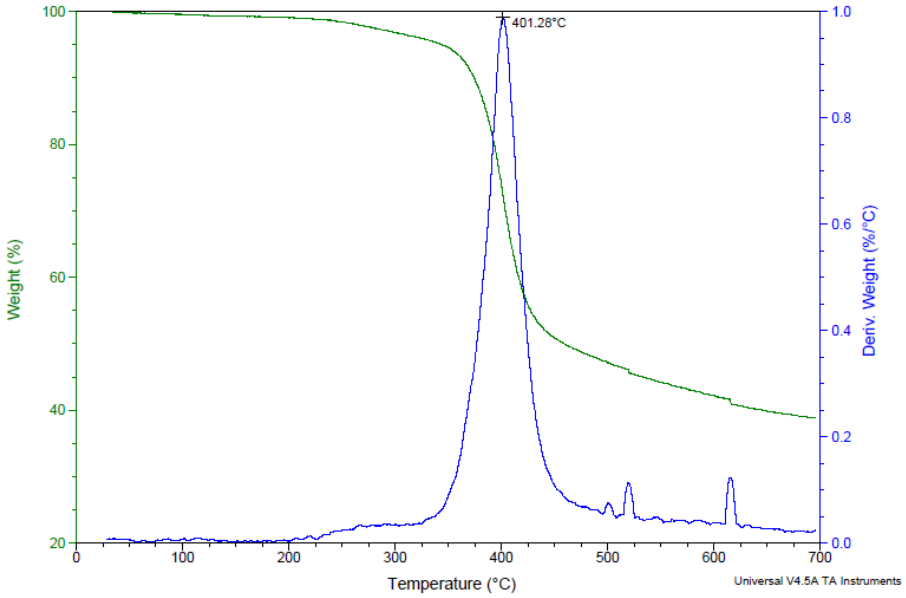

Figure 4-28: TGA trace of the DiVani-Ph-C8 (at a scan rate of 10°C per minute).

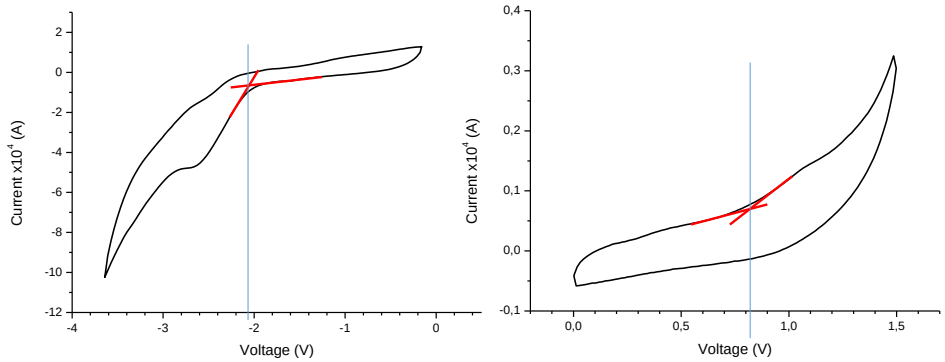

Figure 4-29: Cyclic voltammograms (left-reduction, right-oxidation) of DiVani-Ph-C8 in CH_2Cl_2 solution (0.1 $g.l^{-1}$).

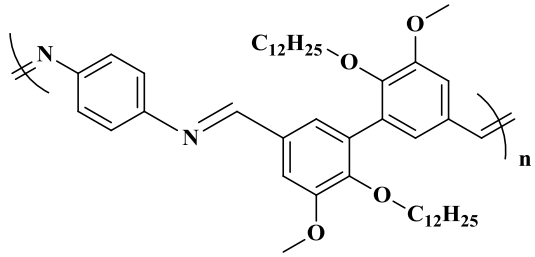

DiVani-Ph-C12

^{1}H NMR (400 MHz, $CDCl_3$, ppm): d 9.89 (s, 2H); 7.46 (dd, J=8.7, 1.9 Hz, 4H); 3.95 (s, J = 6H); 3.81 (m, 4H), 1.39-1.06 (m, 18H), 0.80 (t, J=7 Hz, 6H), 0.69 (t, J=7.4 Hz, 6H)
^{13}C NMR (101 MHz, $CDCl_3$, ppm): d 191.25; 153.76; 152.26; 132.12; 131.75; 128.74; 109.86; 75.36; 56.09; 40.53; 30.45; 29.20; 23.63; 23.11; 14.23; 11.13
FT-IR (ATR): ν= 3220, 1676, 1587, 1413, 1245, 1127, 750 cm^{-1}

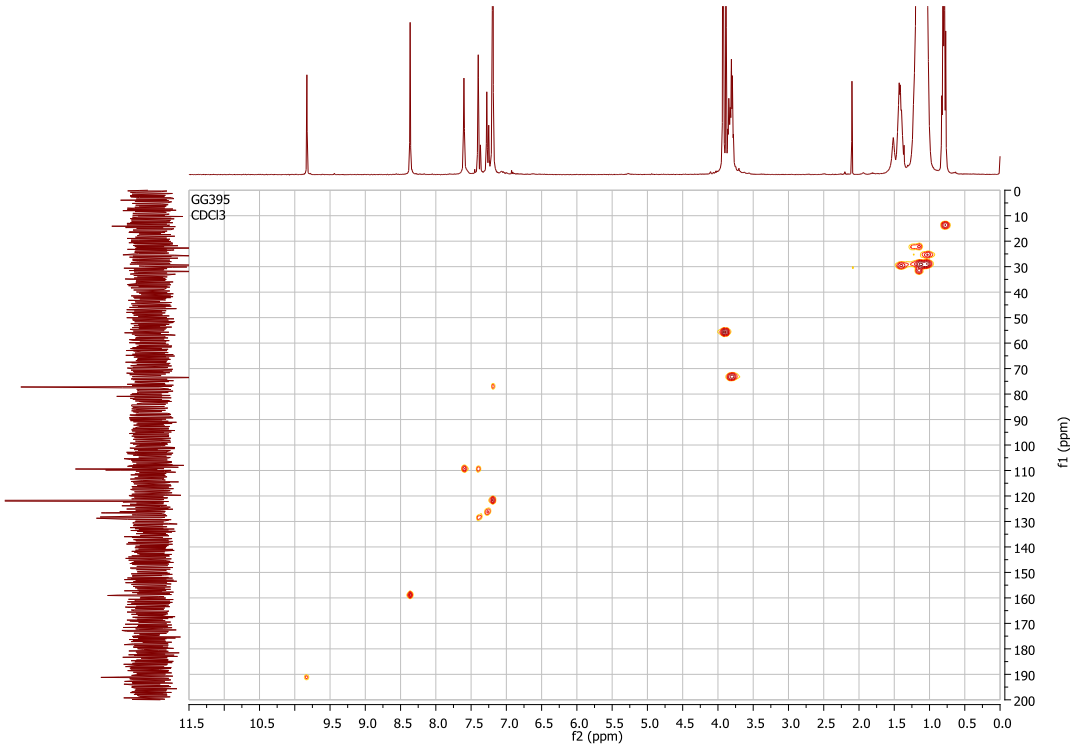

Figure 4-30: ^{1}H-13C HSQC NMR spectra of DiVani-C12 (in $CDCl_3$).

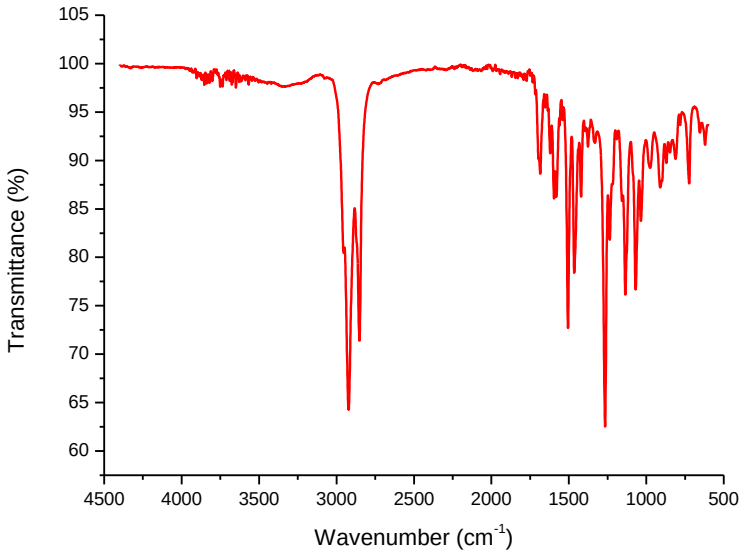

Figure 4-31: ATR-FTIR spectrum of DiVani-Ph-C12.

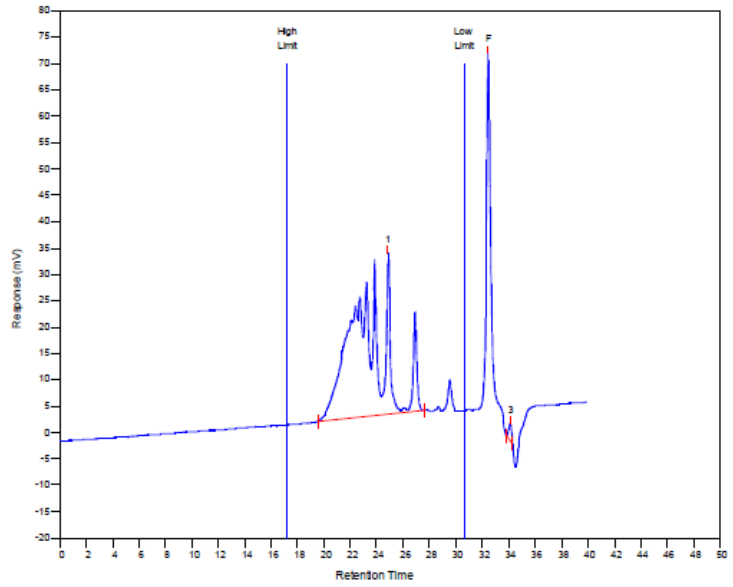

MW Averages

Peak No	Mp	Mn	Mw	Mz	Mz+1	Mv	PD
1	1746	2490	4617	7834	11782	4232	1.85422

Figure 4-32: SEC trace of the DiVani-Ph-C12 (in THF, polystyrene standard).

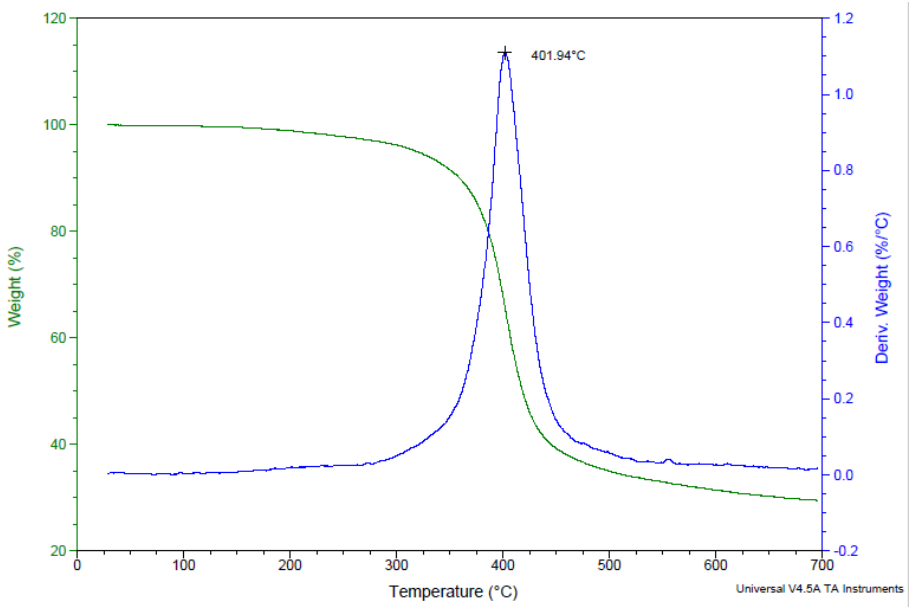

Figure 4-33: TGA trace of the DiVani-Ph-C12 (at a scan rate of 10°C per minute).

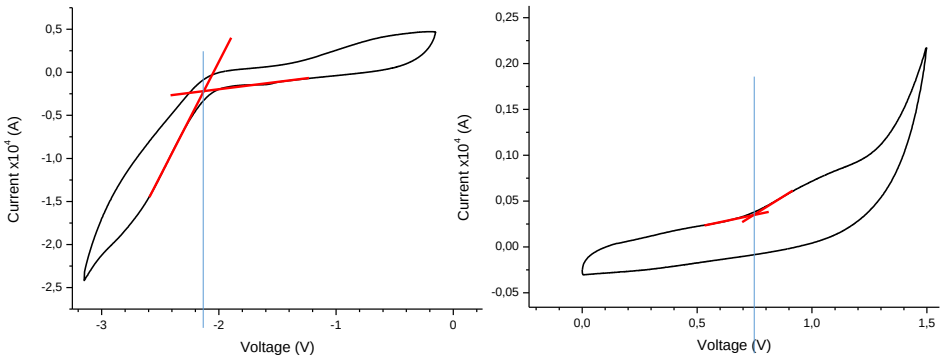

Figure 4-34: Cyclic voltammograms (left-reduction, right-oxidation) of DiVani-Ph-C12 in CH_2Cl_2 solution (0.1 $g.l^{-1}$).

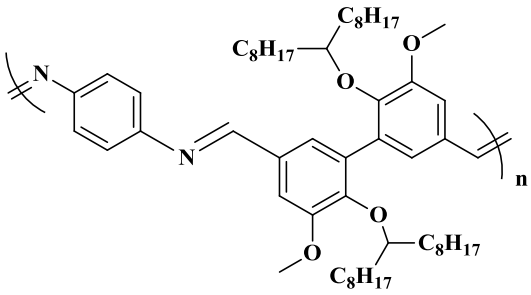

DiVani-Ph-C17

^{1}H NMR (400 MHz, $CDCl_3$, ppm): d 9.89 (s, 2H); 7.46 (dd, J=8.7, 1.9 Hz, 4H); 3.95 (s, J = 6H); 3.81 (m, 4H), 1.39-1.06 (m, 18H), 0.80 (t, J=7 Hz, 6H), 0.69 (t, J=7.4 Hz, 6H)
^{13}C NMR (101 MHz, $CDCl_3$, ppm): d 191.25; 153.76; 152.26; 132.12; 131.75; 128.74; 109.86; 75.36; 56.09; 40.53; 30.45; 29.20; 23.63; 23.11; 14.23; 11.13
FT-IR (ATR): ν= 3220, 1676, 1587, 1413, 1245, 1127, 750 cm^{-1}

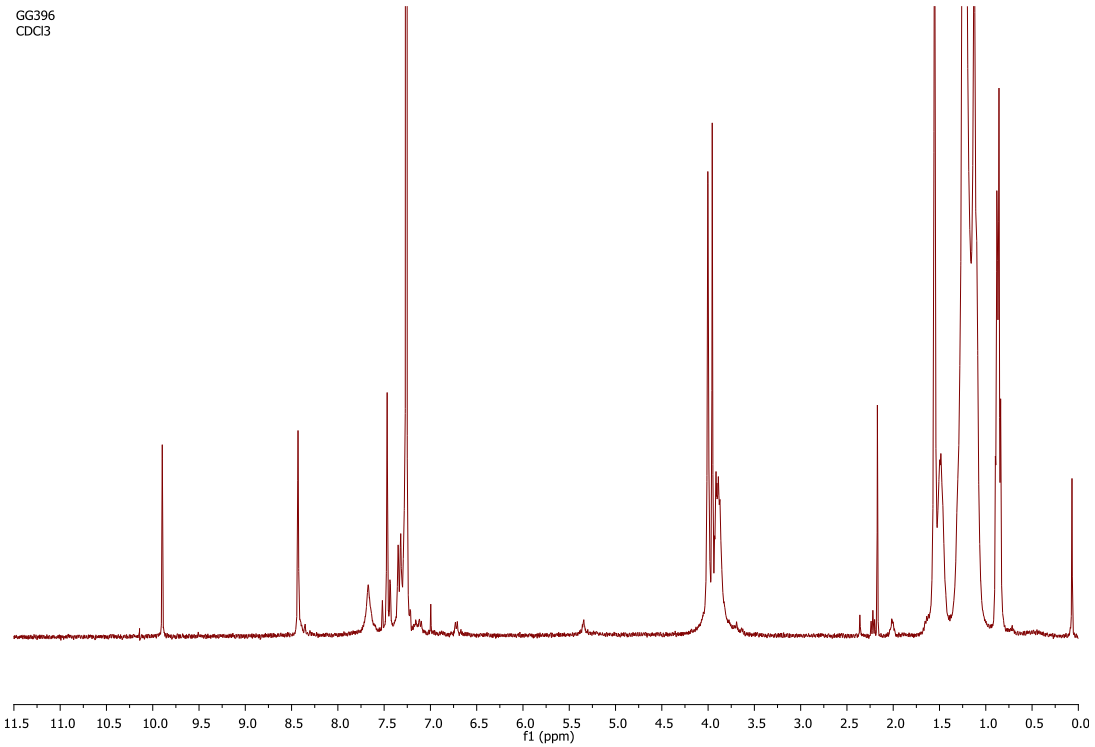

Figure 4-35: ^{1}H NMR (400 MHz) spectrum of DiVani-Ph-C17 (in $CDCl_3$).

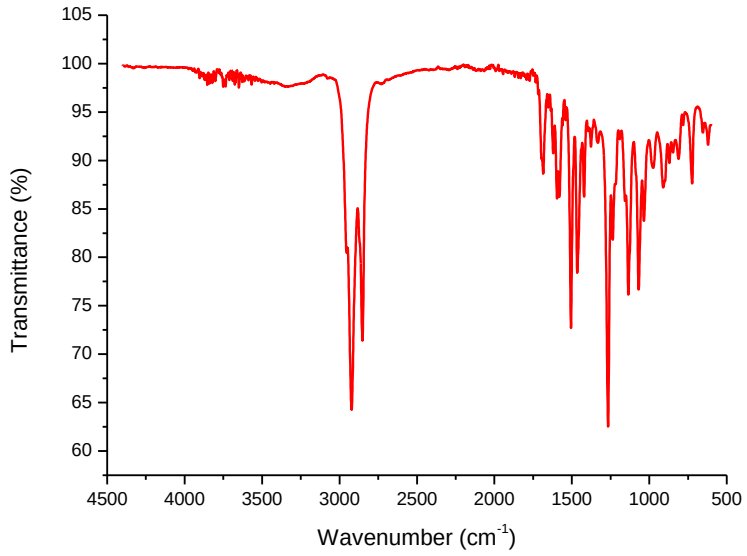

Figure 4-36: ATR-FTIR spectrum of DiVani-Ph-C17.

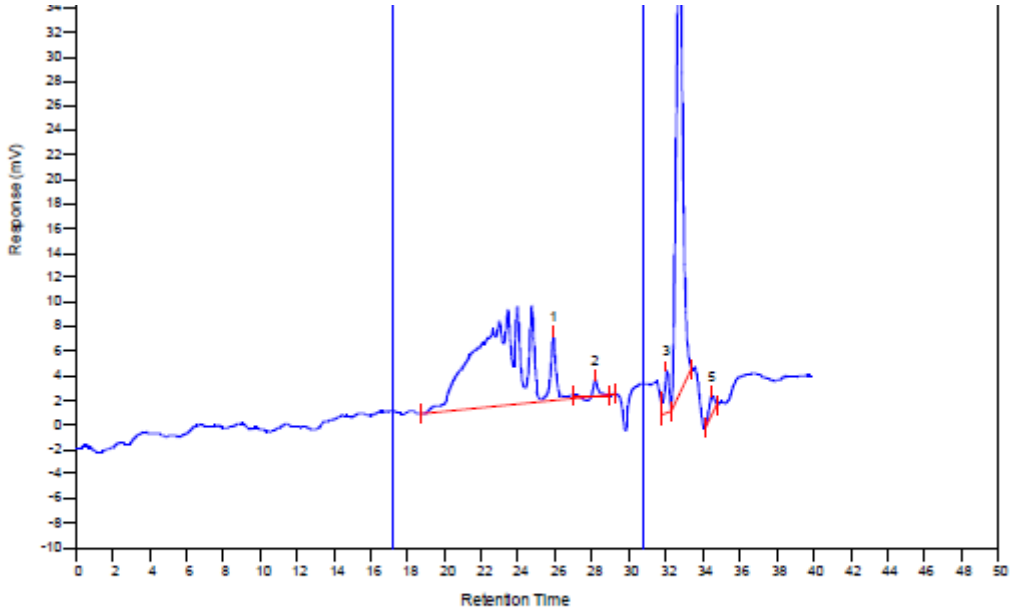

MW Averages

Peak No	Mp	Mn	Mw	Mz	Mz+1	Mv	PD
1	2660	2759	5464	10787	18989	4922	1.98043
2	493	479	481	484	487	481	1.00418

Figure 4-37: SEC trace of the DiVani-Ph-C17 (in THF, polystyrene standard).

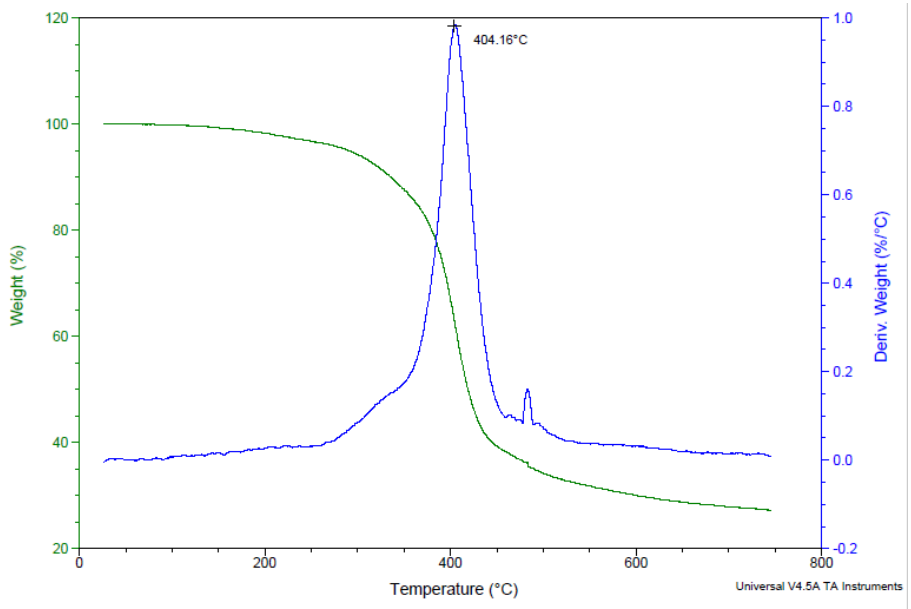

Figure 4-38: TGA traces of the DiVani-Ph-C17 (at a scan rate of 10°C per minute).

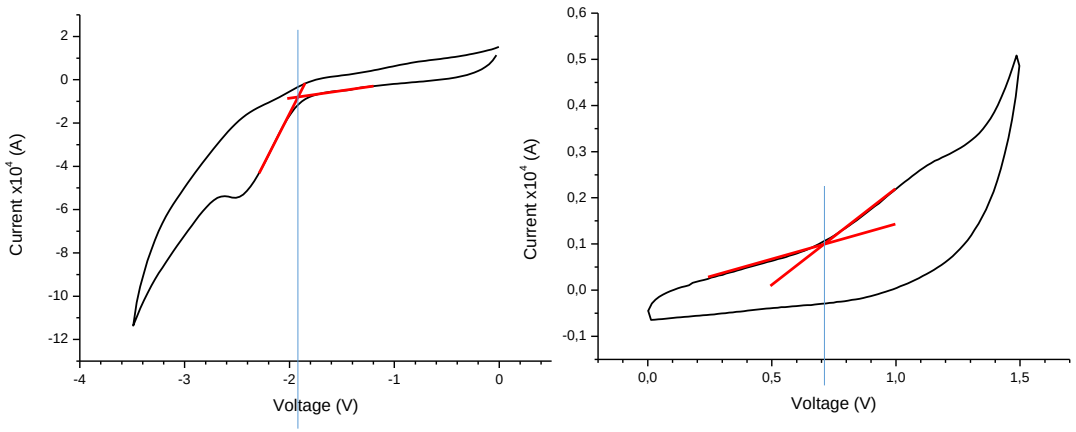

Figure 4-39: Cyclic voltammograms (left-reduction, right-oxidation) of DiVani-Ph-C17 in CH_2Cl_2 solution (0.1 g.l^{-1}).

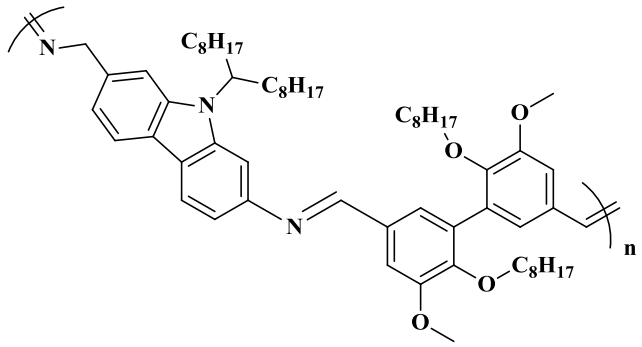

DiVani-Cbz-C8

^{1}H NMR (400 MHz, $CDCl_3$, ppm): d 9.89 (s, 2H); 7.46 (dd, J=8.7, 1.9 Hz, 4H); 3.95 (s, J = 6H); 3.81 (m, 4H), 1.39-1.06 (m, 18H), 0.80 (t, J=7 Hz, 6H), 0.69 (t, J=7.4 Hz, 6H)
^{13}C NMR (101 MHz, $CDCl_3$, ppm): d 191.25; 153.76; 152.26; 132.12; 131.75; 128.74; 109.86; 75.36; 56.09; 40.53; 30.45; 29.20; 23.63; 23.11; 14.23; 11.13
FT-IR (ATR): ν= 3220, 1676, 1587, 1413, 1245, 1127, 750 cm^{-1}

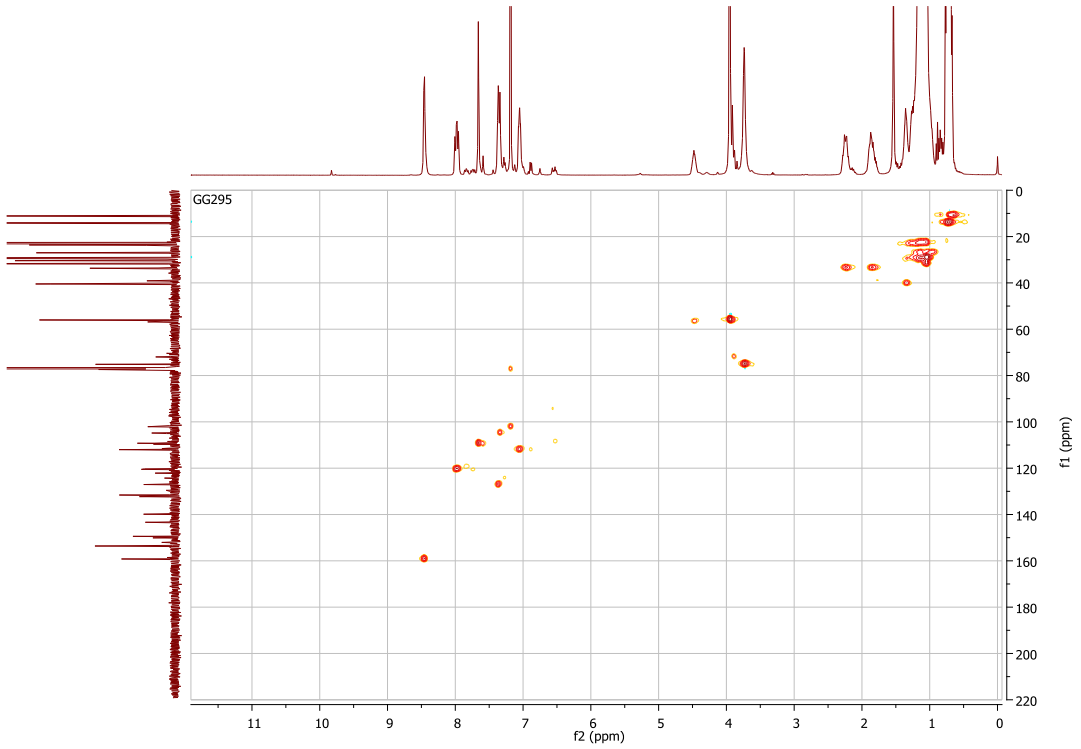

Figure 4-40: ^{1}H-^{13}C HSQC NMR spectra of DiVani-Cbz-C8 (in $CDCl_3$).

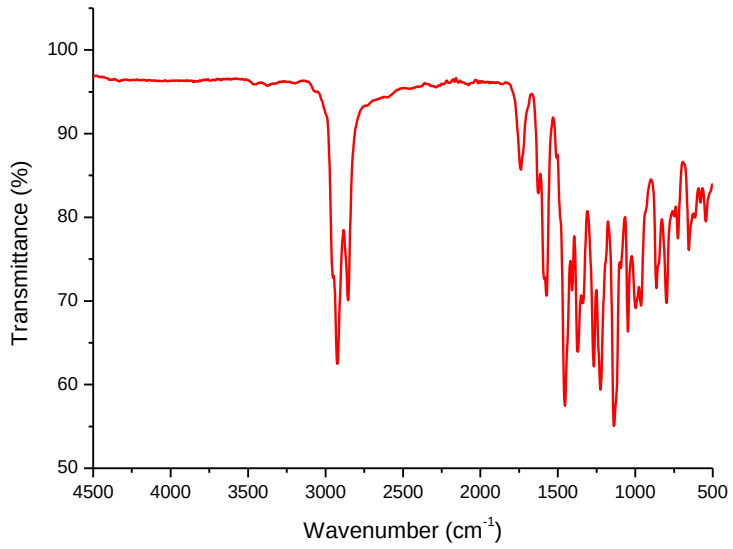

Figure 4-41: ATR-FTIR spectrum of DiVani-Cbz-C8.

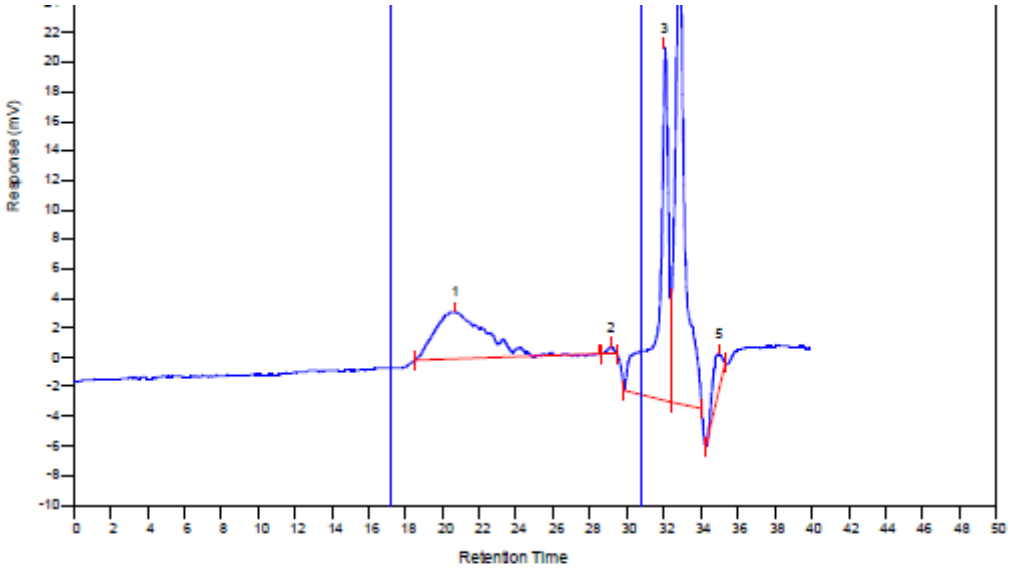

MW Averages

Peak No	Mp	Mn	Mw	Mz	Mz+1	Mv	PD
1	15698	7182	14550	25045	35776	13237	2.0259
2	329	335	337	339	341	337	1.00597

Figure 4-42: SEC trace of the DiVani-Cbz-C8 (in THF, polystyrene standard)

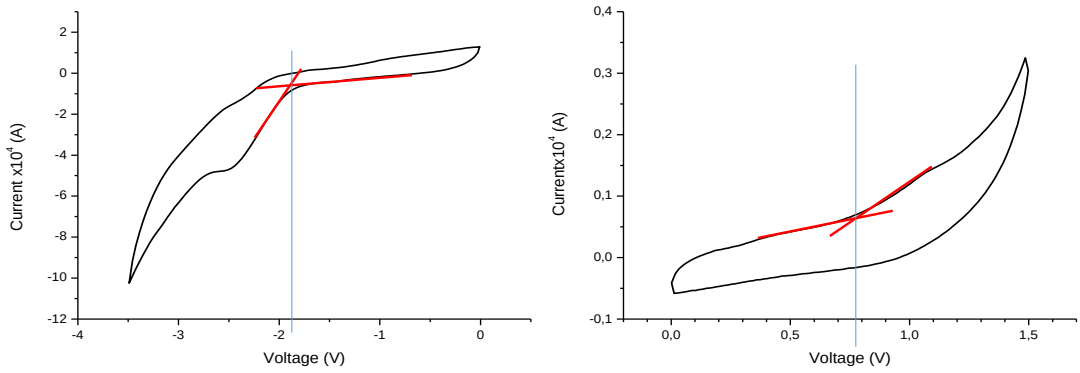

Figure 4-39: Cyclic voltammograms (left-reduction, right-oxidation) of DiVani-Cbz-C8 in CH_2Cl_2 solution (0.1 $g.l^{-1}$).

Conclusion générale et perspectives

Depuis leur découverte dans les années 70-80, les polymères semi-conducteurs ont été énormément étudiés pour les rendre notamment plus efficaces et rentables vis-à-vis des technologies utilisant du Silicium. En effet, ces composés sont une alternative intéressante à l'utilisation de ces dispositifs inorganiques et permettent surtout le développement de dispositifs pour des applications bas coût, flexibles et légers. Néanmoins, il a été mis en évidence que les impuretés métalliques résiduelles pouvaient être nocives pour toutes ces applications potentielles. Différentes stratégies ont donc vu le jour, consistant à ne pas utiliser de catalyseurs métalliques et à diminuer le nombre d'étapes de purification des matériaux polymères. C'est dans ce cadre que se sont déroulées ces recherches.

Dans un premier temps, des polyazométhines (équivalents des phenylènes vinylènes) ont été synthétisés à base de carbazole d'une part puis intégrant des unités EDOT d'autre part. Pour les polycarbazole azométhines, les enchainements aux positions 2,7 du carbazole se sont révélés intéressants pour leurs caractéristiques électroniques. Les meilleurs résultats, en termes de masse molaire et de faible gap, ont été obtenus pour les co-polyazomethines à base de carbazole et d'EDOT. Il faut noter que des calculs théoriques ont permis de valider nombre de résultats obtenus dans ce chapitre. Bien que les caractéristiques optoélectroniques de ces composés demeurent faibles, de nombreux paramètres restent à être étudiés et optimisés, tels que la modification des unités de répétition ou des substituants pour ne citer que ceux là.

Dans un deuxième temps, des « polycolorants » type polysquaraines et polycroconaines ont été synthétisés. La nature des enchainements s'est montrée cruciale pour les caractéristiques optoélectroniques de ces matériaux. De façon plus originale, la nature du solvant utilisé, en particulier des diols, a permis de mettre en évidence l'insertion de ces derniers dans les structures type polysquaraine modifiant les signatures optiques de ces polymères. Ils ont ensuite été intégrés dans des OLEDs pour servir de couche émissive. Des OLEDs, composées d'une couche d'ITO, de PEDOT-PSS, du polymère servant de couche active et de la cathode de Calcium recouverte d'une couche d'Aluminium, ont été réalisées et permis l'obtention d'une émission très proche du blanc avec un indice de rendu de couleur de 91 sur 100. Cependant, l'efficacité et les performances restent faibles ouvrant la voie à des optimisations possibles, soit *via* des changements sur la structure même des polysquaraines, soit en modifiant l'architecture et les couches des OLEDs ou encore en optimisant le dépôt des différentes couches des OLEDs.

Enfin, de façon plus exploratoire, des polymères plus originaux, composés de tétrazine, de divanilline ou de benzobisthiazole ont été explorés. En effet, le chapitre de ce manuscrit a permis d'explorer de nouvelles voies s'ajoutant à nos préoccupations de synthétiser des polymères sans métaux. L'insertion d'unités tetrazine dans un polymère conjugué permet d'étudier des structures plus riches en atomes d'azote. La copolymérisation de la vanilline ouvre la voie à toute une chimie des polymères π-conjugués bio-sourcés. Enfin, l'unité benzobisthiazole a été obtenue *in situ* dans la chaine polymère par condensation.

Tous les composés synthétisés dans ces travaux sont synthétisés *via* des réactions de polymérisations ne nécessitant pas l'ajout de métaux dans le milieu réactionnel. Nombreuses de ces réactions, menant à des composés conjugués, sont encore à explorer. L'utilisation de carbènes peut, par exemple, être envisagée. Il est aussi possible de réaliser la condensation du carbazole sur l'acide squarique.[1–3] En utilisant un carbazole mono-fonctionnalisé il a été possible de synthétiser un composé présentant une couleur bleu-vert et pouvant être impliqué dans des réactions de polycondensations par exemple (Schéma 1).

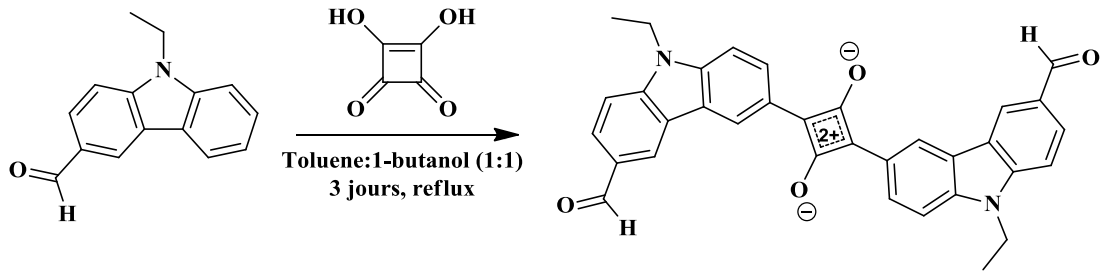

Schéma 1 : Condensation du N-Ethylcarbazole-3-carboxaldehyde sur l'acide squarique

Enfin, grâce à ces résultats encourageants, une thèse financée par Solvay et la région Aquitaine a débuté, afin notamment d'explorer plus en détails cette nouvelle famille de polymères conjugués biosourcés et d'étudier les propriétés de ces nouveaux polymères, continuant ainsi le développement des ces voies de synthèse plus propres et originales.

[**1**] S. Soman, M. A. Rahim, S. Lingamoorthy, C. H. Suresh, S. Das, *Physical Chemistry Chemical Physics*, **2015**, *17*, 23095.

[**2**] D. Yang, Q. Yang, L. Yang, Q. Luo, Y. Huang, Z. Lu, S. Zhao, *Chemical communications (Cambridge, England)*, **2013**, *49*, 10465.

[**3**] Y.-Y. Chen, H. K. Hall, *Polymer Bulletin*, **1986**, *16*, 419.

Experimental (general)

Materials

Tetrahydrofuran (THF), methylene chloride (CH_2Cl_2), chloroform ($CHCl_3$), diethylether (Et_2O), dimethylsulfoxide (DMSO) and toluene were purified from a solvent purification system (MBraun MB-SPS-800) prior to use. N,N-dimethylformamide (DMF) was dried over calcium hydride (CaH_2) and distilled prior to use. Squaric acid was recrystallized in boiling water and then rinsed with cold water and acetone, followed by drying under vacuum at 40°C overnight prior to use. Unless otherwise specified, all other solvents and chemicals were purchased from commercial suppliers (Alfa Aesar, Sigma-Aldrich, TCI, Acros Organics, Orgalight or Strem Chemicals) and used as received. Poly(3,4-ethylenedioxy-thiophene):poly(styrene sulfonate) (PEDOT:PSS) was purchased from Baytron P and passed successively through a 0.8 μm and a 0.45 μm PVDF syringe filter before spin-coating. All reactions were carried out under argon at 1 atmosphere unless mentioned otherwise.

Characterization apparatus

^{1}H, ^{13}C and ^{1}H-^{13}C HSQC NMR measurements were performed with a Bruker AC-400 NMR spectrometer at room temperature. ^{1}H-^{1}H NOESY measurement was performed with a Bruker AC-400 NMR spectrometer with a Bruker CryoProbe

IR spectra were recorded with Bruker Tensor 27 spectrometer using a 0.6 mm-diameter beam. Samples were analyzed with the attenuated total reflexion (ATR) method.

High resolution mass spectroscopy analyses were performed on a AutoSpec-Waters spectrometer (EI).

Optical absorption spectra were obtained with a UV-visible spectrophotometer (UV-3600, Shimadzu).

Photoluminescence spectra were obtained from a spectrofluorometer (Fluoromax-4, Horiba Scientific).

Molar masses of polymers samples measured in THF were determined by size exclusion chromatography (SEC) using a 3-columns set of TSK gel TOSOH (G2000, G3000, G4000 with pore sizes of 20, 75, and 200Å respectively, connected in series) calibrated with narrow polystyrene standards from polymer Laboratories using both refractometric and UV detectors (Varian). THF was used as eluent (1 mL/min) and trichlorobenzene as a flow marker at 40°C.

Molar masses of polymers samples measured in $CHCl_3$, were measured by SEC at 40°C with THF as eluent, using a Viscotek VE2001-GPC. Polymer laboratories-Varian (one guard column and three columns based on cross-linked polystyrene, pore size = 200 Å, 75 Å and 20 Å), and PS standards were used for calibration.

DSC analysis have been performed on a TA instrument, under Helium flow, with an LN2 cooling and modulated with +/- 0,64 °C every 60 seconds. Sample were heated at $10°C.min^{-1}$ and cooled down at $5°C.min^{-1}$.

TGA have been performed on a TA-Q50, from 25°C to 600 - 700 °C with a heating of 10°C.min^{-1} under nitrogen flow.

Electrochemical measurements and HOMO-LUMO calculation were performed in solution. A solution of 0.1 g.l^{-1} of the investigated polymer in CH_2Cl_2 with 0.1 M tetrabutylammonium hexafluorophosphate ($TBAPF_6$) as electrolyte was prepared in a glove box under N_2. CV measurements were then performed on the solution under N_2, using silver wire as reference electrode and platinum for the working and counter electrodes. A solution of ferrocene (1 mM in the same solvent) was prepared in the same conditions and the redox potential of Fc/Fc+ vs Ag ($E_{Fc/Fc+}$ Ag) was measured.

Quantum yields have been measured in an integration sphere, with a spectrometer Quantaurus-QY from Hamamatsu photonics (in film and in solution in $CHCl_3$ or DMF).

Titre : Nouvelles voies de synthèse sans métaux d'oligomères et de polymères pour l'électronique organique

Résumé : Dans cette thèse sont développées les synthèses et caractérisations de nouveaux polymères conjugués pour des applications dans l'électronique organique. Ces polymères ont été synthétisés *via* des réactions de polymérisation sans utilisation de métaux de transition. Des polyazomethines à base de carbazole ont ainsi été synthétisés par polycondensation entre des carbazole portant des fonctions amine et aldéhyde en positions 2,7 et 3,6. Leurs propriétés optiques et électroniques ont été étudiées en fonction de la position des fonctions imines ainsi formées. Un comonomère de type EDOT a ensuite été intégré dans le polymère et l'impact de ce comonomère sur les propriétés du copolymère ainsi formé a été étudié.
Des polymères à base d'acide squarique et croconique ont ensuite été synthétisés. En faisant varier les conditions de synthèse, les propriétés optoélectroniques ont pu être contrôlées, permettant d'obtenir des composés présentant une émission blanche, qui ont ensuite été intégrés en tant que couche active dans des dispositifs de type OLED.
Enfin, des polymères plus originaux ont été étudiés, utilisant des réactions de polymérisation originale, permettant par exemple la formation de benzobisthiazole *in situ*. D'autres polymères ont été synthétisés en intégrant dans leur chaine des monomères originaux, comme la tetrazine ou la divanilline. Les propriétés optoélectroniques de ces composés ont ensuite été étudiées en vue de leur éventuelle intégration dans des dispositifs.

Mots clés : Acide squarique, Acide croconique, Carbazole, Imine, Azomethine, Tetrazine, Divanilline, OLED, Electronique organique, Polymères

---

Title : Original metal-free synthesis routes of semi-conducting oligomers and (co)polymers for organic electronics.

Abstract : In this work, synthesis and characterizations of new conjugated polymers are described. These polymers, developed for their integration into devices, have been synthesized *via* transition-metal free polymerizations. Carbazole based polyazomethines have been synthesized *via* polycondensation reactions between di-substituted carbazoles, bearing amino and formyl functions in positions 3,6 or 2,7. Optical and electronical properties of such polymers have been studied depending of the linkage position. A comonomer EDOT has then been integrated into the polymer chain, and impact of such insertion has been studied.
Squaric and croconic acid base polymers have also been synthesized. By varying polymerization conditions, optoelectronic properties have been tuned, leading to the formation of polymers exhibiting a white emission. These polymers have then been integrated into OLED, as the active layer.
Finally, more original polymers have been synthesized, using more original reactions or monomers such as by forming *in situ* benzobisthiazole. Other polymers integrating more originals monomers, such a tetrazine or divanillin, have been synthesized. Optoelectronic properties of such materials have been studied for the purpose of their integration into devices.

Keywords : Squaric acid, Croconic acid, Carbazole, Imine, Azomethine, Tetrazine, Divanillin, OLED, Organic electronic, Polymer

Laboratoire de chimie des polymères organiques
UMR 5629, 16 avenue Pey-Berland, 33607 Pessac CEDEX France